



Department of Organic and Macromolecular Chemistry

Polymer Chemistry Research Group

# **Vitrimers based on vinylogous acyl exchange reactions**

Wim Denissen

Promotor: Prof. Dr. Filip Du Prez

Co-Promotor: Prof. Dr. Johan Winne

Ghent, 2016

Thesis submitted to obtain the degree of Doctor of Science: Chemistry



**Exam commision**

Prof. Dr. Richard Hoogenboom (Chair, Ghent University)

Prof. Dr. ir. Wim Van Paepegem (Ghent University)

Prof. Dr. ir. Dagmar D'hooge (Ghent University)

Prof. Dr. ir. Guy Van Assche (Vrije Universiteit Brussel)

Dr. François Tournilhac (ESPCI Paris)

Prof. Dr. Johan Winne (co-promotor, Ghent University)

Prof. Dr. Filip Du Prez (promotor, Ghent University)





**FLANDERS  
INNOVATION &  
ENTREPRENEURSHIP**



**Flanders**  
State of the Art

Research funded by the Agency for Innovation by Science and Technology in Flanders

Onderzoek gefinancierd door het Agentschap voor Innovatie door Wetenschap en Technologie



# Table of Contents

<b>Chapter 1</b>	<b>Introduction, aim and outline</b>	<b>1</b>
1.1	Introduction and aim	1
1.2	Outline	5
1.3	References	6
<b>Chapter 2</b>	<b>Introduction to Vitrimers</b>	<b>9</b>
2.1	The two classes of polymer materials	9
2.2	Non-covalent approaches for processable polymer networks	11
2.3	Covalent adaptable networks (CANs)	13
2.3.1	Dissociative CANs	14
2.3.2	Associative CANs	17
2.4	The concept of vitrimers	18
2.5	Vitrimer chemistries	21
2.5.1	Catalysed Carboxylate Transesterification	22
2.5.2	Transalkylation of triazolium salts	24
2.5.3	Siloxane silanol exchange reaction	26
2.5.4	Olefin metathesis exchange reaction	27
2.5.5	Disulfide exchange chemistry	28
2.5.6	Imine amine exchange chemistry	30
2.5.7	Transesterification of boronic esters	31
2.5.8	Transcarbamoylation of polyhydroxyurethane networks	32
2.5.9	Supramolecular bonds and associative exchange	34
2.6	Vitrimer applications	35
2.6.1	Network processing, welding and recycling	35
2.6.2	Processable composites	37
2.6.3	Liquid crystalline actuators	39
2.7	References	40
<b>Chapter 3</b>	<b>Vinylogous Transamination Chemistry</b>	<b>47</b>
3.1	Introduction	47
3.1.1	Alternatives for transesterification	48
3.1.2	Amine exchange of vinylogous acyls as alternative?	50
3.1.3	Literature amine exchange of vinylogous acyls	51
3.1.4	Enaminones in polymer chemistry	52
3.1.5	Synthetic approaches towards enaminones	54
3.2	Kinetic study of amine exchange of enaminones	55
3.2.1	Vinylogous urethanes	56

3.2.2	Vinylogous urea .....	59
3.2.3	Vinylogous amides .....	61
3.3	Rationalisation of the difference in exchange rate for enaminones .....	62
3.4	Conclusion .....	66
3.5	Experimental .....	67
3.5.1	Synthesis of N,N'-(ethane-1,2-diyl)bis(3-(butylamino)but-2-enamide and N,N'-(ethane-1,2-diyl)bis(3-(benzylamino)but-2-enamide) .....	67
3.5.2	Kinetics exchange reaction N,N'-(ethane-1,2-diyl)bis(3-(butylamino)but-2-enamide and benzylamine.....	68
3.5.3	Synthesis of 1-(3-oxobutanoyl) piperidine .....	68
3.5.4	Synthesis of 3-(butylamino)-1-(piperidin-1-yl)but-2-en-1-one and 3-(benzylamino)-1-(piperidin-1-yl)but-2-en-1-one .....	69
3.5.5	Synthesis of propyl acetoacetate .....	69
3.5.6	Synthesis of propyl-3-(butylamino)but-2-enoate and propyl-3-(benzylamino)but-2-enoate.....	70
3.5.7	N-benzyl-3-(benzylamino)but-2-enamide .....	71
3.5.8	Synthesis of 3-(benzylamino)-1-phenylbut-2-en-1-one and 3-(butylamino)-1-phenylbut-2-en-1-one .....	71
3.5.9	Kinetics exchange reaction 3-(butylamino)-1-phenylbut-2-en-1-one and benzylamine .....	72
3.5.10	Synthesis of 1,1'-(1,4-phenylene)bis(3-phenylprop-2-yn-1-one) .....	73
3.5.11	Synthesis of (2Z,2'Z)-1,1'-(1,4phenylene)bis(3(butylamino)-3-phenylprop-2-en-1-one) (R=butyl) and (2Z,2'Z)-1,1'-(1,4phenylene)bis(3(benzylamino)-3-phenylprop-2-en-1-one) (R = benzyl) .....	74
3.1.	References .....	75
<b>Chapter 4</b>	<b>Vinylogous urethane vitrimers.....</b>	<b>79</b>
4.1	Introduction.....	79
4.2	Method 1: Cross-linking amine-functional polymers.....	80
4.3	Method 2: low-MW monomer approach .....	82
4.3.1	Network preparation.....	82
4.3.2	Thermal analysis.....	86
4.3.3	Rheological study .....	87
4.3.4	Recycling study .....	91
4.3.5	Control of the glass transition temperature of Vurethane vitrimers.....	93
4.3.6	Non-condensation vinylogous urethane networks .....	96
4.4	Conclusion and perspectives .....	101
4.5	Experimental .....	103
4.5.1	Materials.....	103
4.5.2	Instrumentation .....	103
4.5.3	Synthesis of the copolymers of styrene and acrylonitrile .....	104
4.5.4	Reduction of styrene-acrylonitrile copolymer .....	104
4.5.5	Synthesis of acetoacetate monomers.....	105

4.5.6	Synthesis of methyl 1-acetylcyclopropane-1-carboxylate 16.....	107
4.5.7	Synthesis of methyl 2-(cyanomethyl)-3-oxobutanoate 18.....	108
4.5.8	Urethane network synthesis .....	108
4.5.9	Solubility experiments .....	109
4.6	References .....	109
<b>Chapter 5</b>	<b>Chemical control of vinylogous urethane amine exchange .....</b>	<b>113</b>
5.1	Introduction.....	113
5.2	Model compound study .....	114
5.3	Synthesis and characterisation of low Tg materials .....	119
5.4	Rheological study .....	121
5.4.1	Stress-relaxation experiments at elevated temperature .....	121
5.4.2	Comparison mechanical and molecular relaxation.....	123
5.4.3	Room-temperature stress-relaxation.....	124
5.4.4	What would be the preferred catalyst? .....	126
5.4.5	Triggered release of a base? .....	127
5.4.6	Catalysed poly VU networks with high Tg.....	128
5.5	Conclusions and perspectives.....	129
5.6	Experimental .....	130
5.6.1	Materials.....	130
5.6.2	Instrumentation .....	130
5.6.3	Synthesis of Methyl-3-(octylamino)but-2-enoate and methyl-3-((2-ethylhexyl)amino)but-2-enoate .....	131
5.6.4	Acetoacetylation of pripol2033 .....	132
5.6.5	Model compound study .....	132
5.6.6	Synthesis soft vitrimer networks.....	133
5.6.7	Synthesis photobase 8.....	134
5.6.8	Synthesis of hard vitrimer networks .....	135
5.6.9	Compression set experiments.....	136
5.7	References .....	136
<b>Chapter 6</b>	<b>Vinylogous urea vitrimers.....</b>	<b>139</b>
6.1	Introduction.....	139
6.2	First exploratory experiments on Vinylogous urea polymers.....	140
6.1	Thermal stability of different Vinylogous urea .....	142
	Mechanical properties of Vurea-3 with and without added catalyst.....	145
6.2	Frequency sweep experiments.....	147
6.3	Melt-flow index and extrusion .....	149
6.4	Vinylogous urea composites.....	151
6.4.1	Matrix adaptations and characterisation.....	152
6.4.2	Multi-layer composite preparation and characterisation.....	154
6.4.3	Proof of concept – composite processing and fiber recuperation .....	158
6.5	Conclusions and perspectives.....	160
6.6	Experimental .....	161

6.6.1	Materials.....	161
6.6.2	Instrumentation .....	161
6.6.3	Synthesis of N,N'-(1,4-phenylene)bis(3-oxobutanamide) 6 .....	162
6.6.4	Synthesis of 1,4-(piperazine)bis(acetoacetamide) 7.....	163
6.6.5	Representative synthesis of the Vurea networks .....	164
6.6.6	Preparation of a single-layer Vurea composite.....	165
6.7	References.....	166
<b>Chapter 7 - Conclusion and perspectives .....</b>		<b>167</b>
7.1	Aim of the work.....	167
7.2	Overview of the results .....	168
7.3	Perspectives .....	172
7.4	References.....	173
<b>Chapter 8 - Nederlandstalige samenvatting.....</b>		<b>175</b>
8.1	Inleiding.....	175
8.2	Doelstelling .....	176
8.3	Overzicht van de resultaten .....	177
8.4	Perspectieven .....	181
8.5	Referenties .....	182

## Abbreviations

2-EHA	2-Ethyl hexyl amine
CAN	Covalent Adaptable Network
DCE	Dichloroethane
DFT	Density functional theory
DMA	Dynamic mechanical analysis
DSC	Dynamic scanning calorimetry
EtOH	Ethanol
FRPC	Fiber reinforced polymer composites
FT-IR	Fourier transform infrared spectroscopy
LCE	Liquid crystalline Elastomers
Low-MW	Low molecular weight
MeOH	Methanol
PDMS	Poly(dimethylsiloxane)
ROMP	Ring opening metathesis polymerisation
$T_g$	Glass transition temperature
TGA	Thermogravimetric analysis
THF	Tetrahydrofuran
$T_m$	Melting point temperature
TPE	Thermoplastic elastomer
TREN	Tris(2-aminoethyl)amine
$T_v$	Topology freezing temperature
Vamide	Vinylogous amide
Vurea	Vinylogous urea
Vurethane	Vinylogous urethane





# Chapter 1

## Introduction, aim and outline

### 1.1 Introduction and aim

A world without polymers is nowadays almost impossible to imagine as these materials found their way to all kind of applications we could think of such as clothes, construction materials and cosmetics. Due to their versatility, the properties of polymers can be tailored to meet the specific demands of an application. In addition, they offer often ecological and economic benefits when compared to non-synthetic materials because of their light weight, low carbon footprint, straightforward processability and useful lifetime.

This great diversity of polymers can be classified in many ways, for example natural versus synthetic, organic versus inorganic and oil-resistant versus non-oil-resistant. But, when talking with a materials scientist about a particular material, one of the first questions that arise, would be:

“Is it a thermoplastic or a thermoset?”

Indeed, the most widespread classification is based on the way polymers respond to heat. According to this classification, polymers are divided in two kinds, thermoplastics and thermosets. The first group, thermoplastics, consist of long linear chains that upon heating, can freely move along each other and thus flow. As a results, thermoplastics are easily processed through fast processing techniques such as extrusion<sup>1</sup> and injection moulding and can be recycled in many cases as well.<sup>2</sup>

The other class, thermosets, are three-dimensional networks with all the chains interconnected to each other via so-called cross-links. These materials form thus one covalently bonded molecule after its preparation. Due to this network architecture, thermosets possess superior dimensional stability, creep/chemical

resistance and mechanical properties compared to thermoplastics. Therefore, they are the materials of choice for many high-demanding applications such as tyres, composites and sealants. However, because of its architecture, the shape in which they are prepared is also permanent and thermosets cannot be processed or recycled after full chemical cross-linking or ‘curing’. The combination of the superior mechanical properties of traditional thermosets with the ‘plastic’ properties that facilitate processing and recycling, is therefore a challenge that is attracting great interest from the academic community nowadays.

An attractive strategy, pursued to achieve the combination of plastic and thermosetting properties in a synthetic material, is the introduction of *exchangeable chemical bonds* into a polymer network, leading to dynamic cross-links. If chemical cross-links can be efficiently and reliably exchanged between different locations on the polymer chains, a molecular mechanism is provided for macroscopic flow without risking structural damage or permanent loss of material properties. Polymer networks containing such exchangeable bonds are also known as *covalent adaptable networks*, further referred to as *CANs* (Figure 1.1).<sup>3-5</sup>

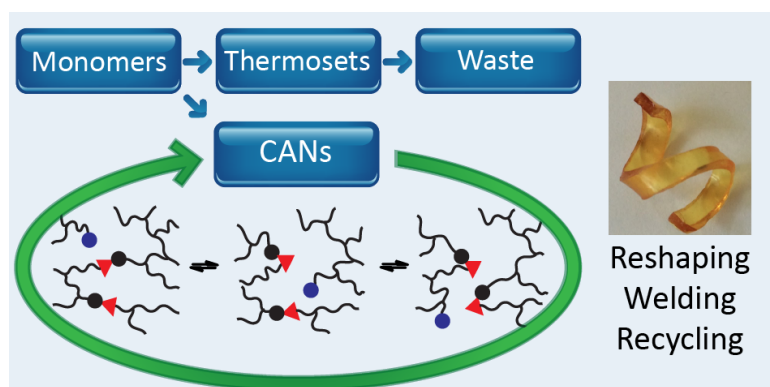


Figure 1.1: Classical thermosetting materials are fixed molecular networks that cannot be recycled or reshaped. By introducing exchangeable covalent bonds, covalent adaptable networks (CANs) become versatile materials with a high intrinsic value.

Today, most of the fundamental research on CANs has focused on so-called dissociative exchange mechanisms, based on reversible chemical cross-links such as the Diels-Alder reaction between furans and maleimides.<sup>6</sup> In these systems, heating displaces the equilibrium toward depolymerisation, which gives rise to a sudden viscosity drop, as is normally observed for thermoplastic materials.<sup>7</sup> Upon cooling, the cross-links are formed again, usually to the same extent as in the starting material, thus preserving or re-installing the desirable thermosetting properties (stiffness and insolubility). These reversible links thus allow for

thermal (re)processing of polymeric networks. The disadvantages of most dissociative CANs are the fundamental difficulty of finding chemical cross-links that are both strong and inert at the temperature of use, but kinetically reversible. In addition, the reformation of the cross-links could conflict with the vitrification of the polymer network, preventing full restoration of properties especially when targeting materials with a high glass-transition temperature. These drawbacks often lead to very limited useful temperature windows.

A second class of CANs, studied since the breakthrough invention of Leibler and co-workers that was published in *Science* in 2011,<sup>8</sup> exploit an *associative exchange mechanism*. This mechanism is based on a dynamic exchange reaction between polymer chains with bonds that are formed simultaneously or before other bonds are broken. As a result of this group exchange mechanism, often involving an addition/elimination type two step mechanism, associative CANs can change their network topology without loss of connectivity during the dynamic cross-link reorganization process (Figure 1.2). Thus, such networks are effectively permanent and insoluble, even at very fast exchange rates and/or high temperatures. Nevertheless, swift chemical exchange reactions can result in a liquid-like behaviour of the polymer network, useful for reshaping and reprocessing of the material with full recovery of mechanical properties.

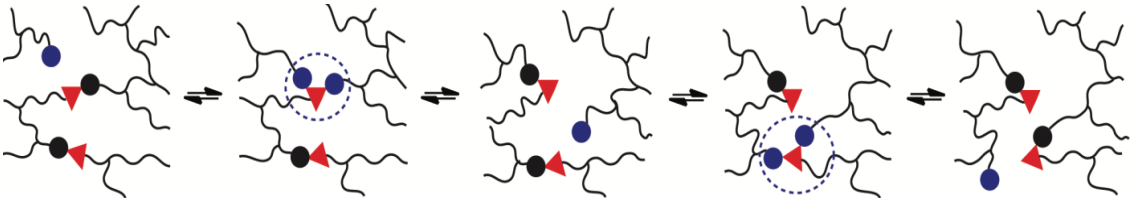


Figure 1.2: Associative exchange reactions enable network reorganisation without losing connectivity during exchange.

Interestingly, as with all chemical reactions, the rate of this associative exchange reaction increases gradually with temperature leading to an Arrhenius-like viscosity dependence, rather than a sudden and marked viscosity drop at the sol/gel transition. Thus, thermally triggered associative CANs have been coined vitrimers<sup>9</sup> because of their unique combination of insolubility and gradual thermal viscosity behaviour, in analogy with the thermal behaviour of traditional glass.

Due to the unique combination of features that vitrimers possess, *i.e.* mechanical properties of thermosets combined with a glass-like fluidity, vitrimers show great

promise to have a considerable impact on industries that rely on elastomers, thermosets and composites. Especially in this latter field, the enhanced processability could serve as a breakthrough technology for mass-production in the automotive industry. Nevertheless, before these materials can find their way to industry, major challenges remain. In the pioneering work, catalysed transesterification was used as exchangeable reaction. As the transesterification reaction is intrinsically rather slow, high catalyst loadings were required and even then, processability remains slow. Moreover, high glass-transition temperatures are not possible due to the limited solubility of these catalysts in aromatic monomers.

In this thesis, we aim to explore an alternative exchange reaction, namely the amine exchange of vinylogous acyls (Figure 1.3), for the development of catalyst-free vitrimers that have a high-glass transition temperature ( $T_g$ ) and enable fast processing.

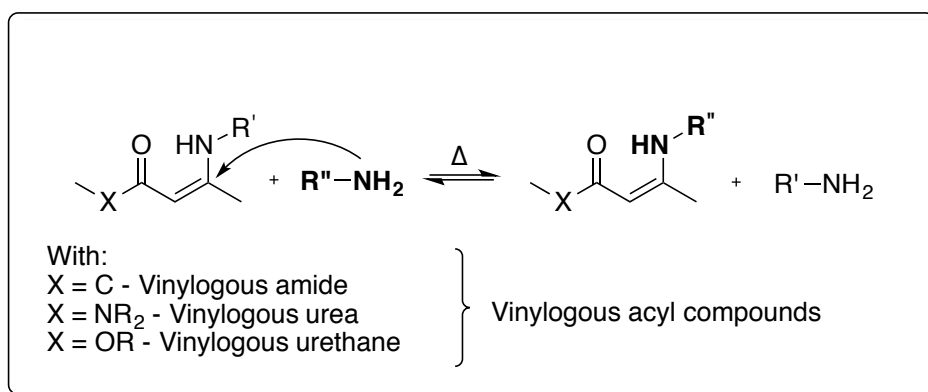


Figure 1.3: amine exchange of a vinylogous acyl motif.

The ultimate goal of the project would be to demonstrate the potential of the envisaged materials for high-end applications such as a matrix for composites, recyclable and *in situ* repairable polymer resins or rubbers in other structural components. Furthermore, we hope to make a significant contribution to the development of this new kind of materials so that in the future the answer on the aforementioned question would sometimes be:

“it’s a vitrimer!”

## 1.2 Outline

**Chapter 2** situates vitrimers in the world of polymers. First, the two classes of polymers, thermosets and thermoplastics, will be discussed shortly together with their virtues and limitations. Next, approaches to combine the assets of both classes are reviewed. Among them, vitrimers are a promising candidate as they show some unique features. The properties and thermal behaviour of vitrimers will be discussed together with all vitrimer chemistries that are currently known. Finally, some of the possible applications of vitrimers are presented.

**Chapter 3** gives an introduction to the proposed vinylogous acyl exchange chemistry followed by kinetic studies on model compounds of vinylogous urethanes, urea and amides. The results of this chapter have strongly focussed and guided our design of vitrimer materials described in the following chapters.

**Chapter 4** reports vitrimers using *the amine exchange of vinylogous urethanes*. In a first approach, the preparation of an amine-functional polymer was aimed for, which could be cross-linked using bis-acetoacetates. As this approach did not rapidly lead to useful materials, poly(vinylogous urethane) networks with an unprecedented polymer backbone were prepared from low-MW monomer mixtures and were characterised in detail with emphasis on the viscoelastic behaviour as a function of time and temperature. Furthermore, also some alternatives to the previously used condensation chemistry were examined. The unsuccessful synthesis of a monomer that would enable a ring-opening polymerisation is discussed together with a poly-addition approach. Although these experiments did not afford very useful results, they may be of interest for future research and design of novel enaminone-based vitrimer materials.

**Chapter 5** explores the ability to control the amine exchange kinetics of vinylogous urethanes via addition of simple additives. First, kinetic studies on low-MW compounds were performed in a model system that proved to closely mimic the conditions found in a polymer network. Next, poly(vinylogous urethane) elastomers were prepared, loaded with different additives. The viscoelastic properties were investigated and showed that they dramatically change depending on the used additive in a predictable way. Finally, this approach was also extended to a rigid vinylogous urethane network and showed that also for these networks, stress-relaxation could be further enhanced or fine-tuned by addition of catalysts.

**Chapter 6** addresses the *amine exchange of vinylogous urea* (rather than vinylogous urethanes) as novel dynamic covalent bonds for vitrimer materials. In chapter 3, vinylogous urea were found to exhibit the fastest exchange kinetics among all investigated vinylogous acyl motifs in this work. Following the successful polymer network syntheses based on vinylogous urethanes, also some materials incorporating the vinylogous urea bond could be prepared. From a processing point of view, these are highly interesting because such fast stress-relaxation (low viscosity) was achieved that extrusion would be feasible. Furthermore, with the ultimate goal to use vitrimers as matrix of composites, efforts were done to prepare composites with a vinylogous urea matrix together with initial characterisation and proof-of-concept experiments for composite processing.

**Chapter 7** will give a general conclusion and address some perspectives.

**Chapter 8** provides a summary of this thesis in Dutch.

## 1.3 References

- (1) Gaylord, N. G.; Van Wazer, J. R. *Journal of Polymer Science* **1961**, *51*, S77.
- (2) Biron, M. *Thermoplastics and Thermoplastic Composites: Technical Information for Plastics Users*; Elsevier Science, **2007**.
- (3) Kloxin, C. J.; Scott, T. F.; Adzima, B. J.; Bowman, C. N. *Macromolecules* **2010**, *43*, 2643.
- (4) Bowman, C. N.; Kloxin, C. J. *Angew. Chem., Int. Ed.* **2012**, *51*, 4272.
- (5) Kloxin, C. J.; Bowman, C. N. *Chem. Soc. Rev.* **2013**, *42*, 7161.
- (6) Cash, J. J.; Kubo, T.; Bapat, A. P.; Sumerlin, B. S. *Macromolecules* **2015**, *48*, 2098.
- (7) Zhang, Y.; Broekhuis, A. A.; Picchioni, F. *Macromolecules* **2009**, *42*, 1906.
- (8) Montarnal, D.; Capelot, M.; Tournilhac, F.; Leibler, L. *Science* **2011**, *334*, 965.
- (9) Capelot, M.; Montarnal, D.; Tournilhac, F.; Leibler, L. *J. Am. Chem. Soc.* **2012**, *134*, 7664.



## **Abstract**

In this chapter, the novel class of vitrimer materials will be situated in the wider polymer landscape. First, the two classes of polymers, thermosets and thermoplastics, will be briefly discussed together with their virtues and limitations. Next, recent approaches to combine the assets of both classes are reviewed. Among them, vitrimers are a promising candidate as they show some unique features. The specific properties and thermal behaviour of vitrimers will be discussed together with all vitrimer chemistries that are currently known. Finally, some of the possible applications of vitrimers will be discussed.

## **Published in:**

Denissen, W.; Winne, J. M.; Du Prez, F. E. *Chem. Sci.* **2016**, 7 (1), 30–38.



## Chapter 2

### Introduction to Vitrimers

#### 2.1 The two classes of polymer materials

Organic polymer materials are classically subdivided in two main classes, thermosets and thermoplastics, according to their thermal behaviour. Thermoplastics are long linear macromolecules that acquire their visco-elastic properties through entanglements of the long chains (Figure 2.1a). At low temperatures, only vibrational motions are enabled and these materials are hard and glassy with typical moduli in the order of GPa. Upon heating, large scale molecular motion becomes possible and the polymer transforms from a hard glassy material to a rubbery material with a typical modulus in the order of MPa (Figure 2.1b). At a short timescale, thermoplastics show an elastic behaviour due to the entanglements, which results in the rubbery plateau depending on the molecular weight. At a longer timescale or higher temperatures, however, the polymer chains can move alongside of each other (reptation) because this movement of polymer chains is only hindered by relatively weak effects such as intermolecular interactions, entanglements and occupied volume.<sup>1</sup> Consequently, at high temperatures or long time-scales, thermoplastics show a liquid behaviour. This ability of thermoplastics to flow upon heating is industrially highly desired as it enables multiple and easy processing such as extrusion, as well as simple recycling in many cases.

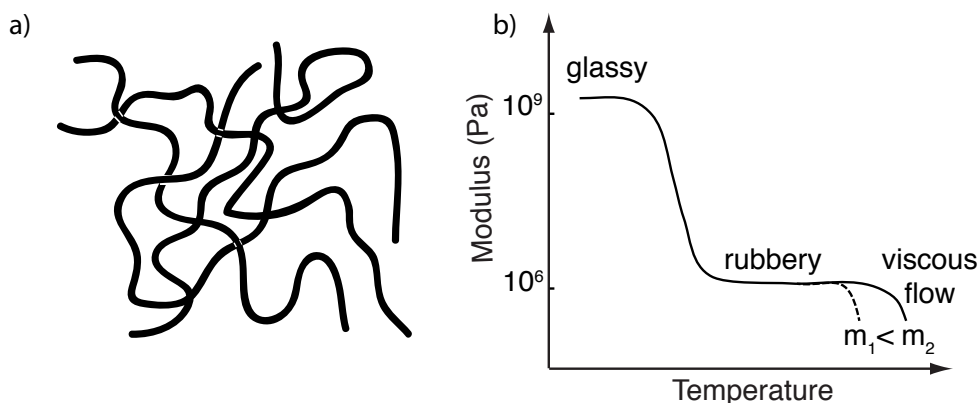


Figure 2.1. a) Representation of a thermoplastic material b) Typical mechanical properties at a timescale in the order of seconds of an amorphous thermoplastic material.

The second class of polymer materials, *thermosets*, can be regarded as thermoplastic polymers, which have been reinforced at a molecular level by the implementation of chemical cross-links, resulting in polymer networks that acquire a permanent shape, and become stiff and insoluble (Figure 2.2a). These materials are characterized by a threshold rubbery plateau where further heating does not lead to a liquid state before the onset of thermal degradation (Figure 2.2b). Today, thermosets are preferred over thermoplastics for various high temperature and structural applications such as adhesives, rubbers, coatings and composites because of their dimensional stability, creep resistance, chemical resistance and mechanical properties. However, due to their permanent molecular architecture, thermosets cannot be reshaped, processed or recycled after full cross-linking or curing. Indeed, thermosets such as epoxy resins or methacrylic networks are typically prepared via injection moulding, immediately in their definitive shape, and once cured, their shape cannot be changed.

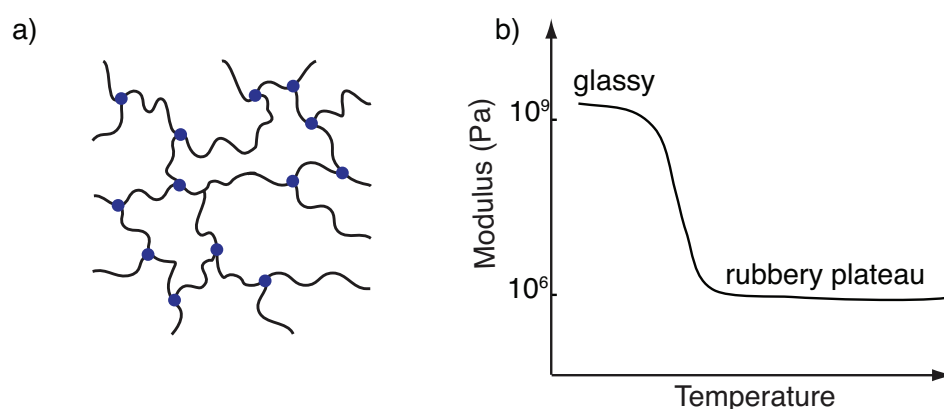


Figure 2.2. a) Representation of a thermosetting material. b) Typical mechanical properties at a timescale in the order of seconds of an amorphous thermoset.

Polymers that are able to combine the superior mechanical properties of thermosets with the “plastic” properties of thermoplastics to facilitate processing remain a challenge that has already attracted great interest in polymer chemistry for many decades (Figure 2.3). In the following sections, the different approaches towards materials that combine the properties of both thermosets and thermoplastics are discussed. Among these approaches, vitrimers are a very promising candidate to fulfil all the requirements.

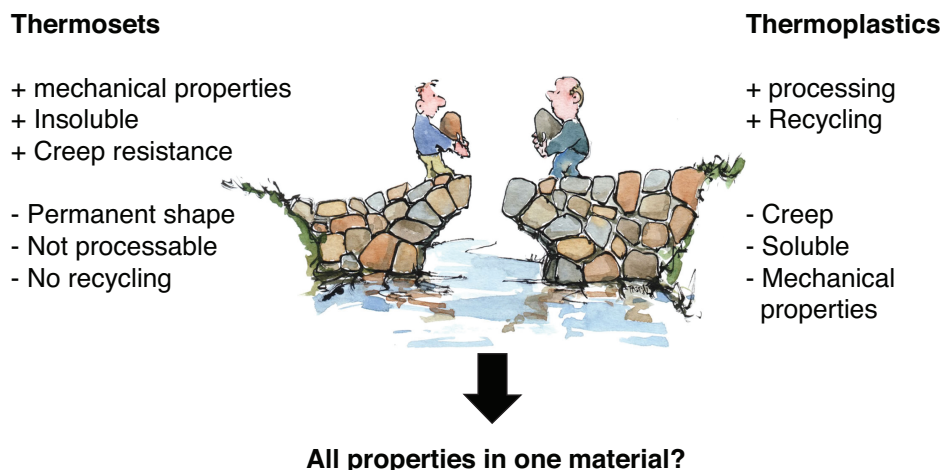


Figure 2.3: Can one material combine the most desirable attributes of both thermosets and thermoplastics?

## 2.2 Non-covalent approaches for processable polymer networks

One of the oldest strategies to combine the mechanical properties of cross-linked structures, in particular the elasticity of classical thermosetting elastomers, with the processability of thermoplastics, relies on phase-separated or crystalline zones in an amorphous thermoplastic material. These materials are also known as thermoplastic elastomers (TPEs).<sup>2</sup> The crystalline or phase-separated zones form hard domains serving as physical cross-links that are reversible in contrast to permanent chemical cross-links of thermosets (Figure 2.4). The obtained materials are thus rubbery or leathery in the application temperature window depending on the amount of hard domains. Some industrial examples of these materials are Kraton's Styrene-Butadiene-Styrene rubbers (SBS) used for shoe soles and BASF's Elastollan® thermoplastic urethanes (TPU) used for automotive applications.

The properties and application temperature of TPEs are highly dependent on the used soft and hard domains. The low temperature limit is defined by the glass transition temperature of the soft phase, as below this temperature TPEs become brittle. The upper boundary is defined by the melting temperature ( $T_m$ ) or  $T_g$  of the hard phase because the physical cross-links are eliminated and the material starts to flow and creep. Furthermore, when the amount of hard phase is larger than the soft phase, the polymer is essentially a toughened thermoplastic and not an elastomer. Consequently, thermoplastic elastomers can be used to replace

cross-linked materials with low  $T_g$ 's (*i.e.*  $T_g < \text{application temperature}$ ), but typical glassy thermosetting materials used for demanding applications cannot be targeted. In addition, when creep resistance and heat resistance are a crucial factor for applications, chemically cross-linked polymers remain irreplaceable.

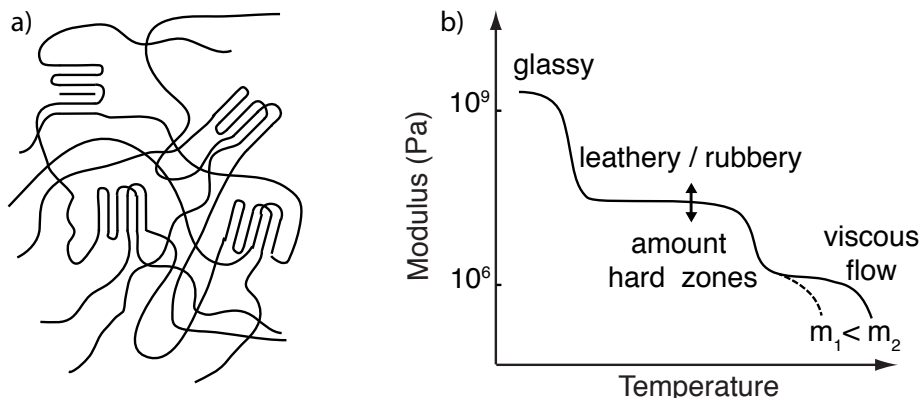


Figure 2.4: a) Representation of a thermoplastic elastomer. b) Typical mechanical properties at a timescale in the order of seconds of an amorphous thermoplastic material.

As an alternative to crystalline and phase-separated hard domains as reversible physical cross-links, also non-covalent networks can be formed using supramolecular interactions such as hydrogen bonds,<sup>3</sup>  $\pi$ - $\pi$  interactions<sup>4</sup> and metal complexes.<sup>5</sup> These bonds are readily and reversibly dissociated upon heating and thus allow for easy processing. At the same time, associating groups can introduce rubber-like elasticity,<sup>3</sup> self-healing properties<sup>6</sup> and increased toughness<sup>7</sup> in polymers. In contrast to permanent chemical bonds found in thermosets or the hard domains of TPEs below their  $T_g$  or  $T_m$ , the supramolecular motifs are characterized by a finite lifetime on experimental timescales as they constantly break and reform. This property is rather undesired for cross-linked structures because it makes supramolecular networks prone to creep and stress-relaxation, albeit at longer timescales when compared with polymers without associating groups.<sup>8</sup> In addition, solvents can induce an equilibrium shift to a dissociated state making supramolecular networks sensitive to solvents. Thus, although supramolecular networks are very promising as they show some unique features such as intrinsic self-healing, they lack dimensional stability and solvent resistance in comparison with covalently cross-linked networks.

## 2.3 Covalent adaptable networks (CANs)

Another attractive chemical strategy to achieve the combination of plastic and thermosetting properties in a synthetic material is offered by the introduction of exchangeable covalent bonds into a polymer network, leading to *dynamic cross-links*. If chemical cross-links can be efficiently and reliably exchanged between different positions of the organic polymer chains, a molecular mechanism is provided for macroscopic flow without risking structural damage or permanent loss of material properties. Polymer networks containing such exchangeable bonds are also known as covalent adaptable networks or CANs.<sup>9-11</sup> These CANs may be further classified based on the nature of their exchange mechanism, *i.e.* those relying on *dissociative or associative exchanges*.

The first group of CANs makes use of a dissociative cross-link exchange mechanism. During exchange, chemical bonds are first broken and then formed again at another or the same place (Figure 2.5a). The second group of CANs makes use of associative bond exchanges between polymer chains, in which the original cross-link between polymer chains is only broken when a covalent bond to another (part of the) polymer chain has been formed (Figure 2.5b). Due to the different kind of bond reshuffling, dissociative and associative CANs behave differently when network rearrangements are triggered.

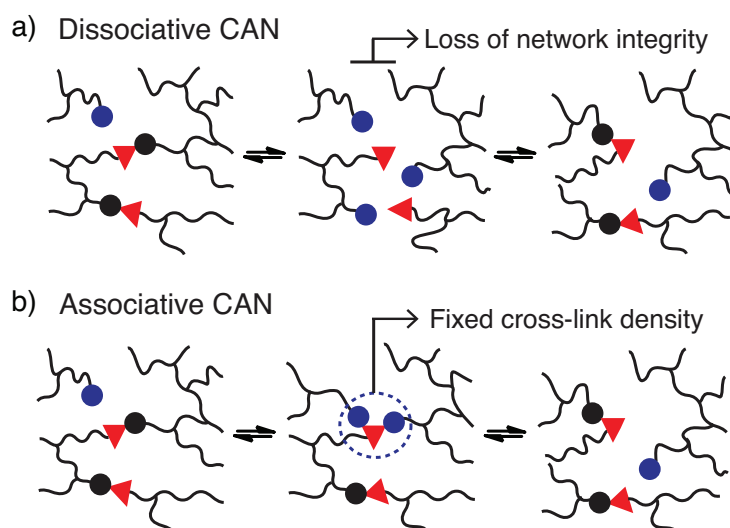


Figure 2.5. a) Dissociative exchange: bonds are first broken and then formed again. b) Associative exchange: bonds are only broken after new bonds are formed.

In the following subsections, first dissociative CANs will be discussed. Next, associative CANs will be reviewed followed by vitrimers as they can be categorized within this latter group of CANs.

### 2.3.1 Dissociative CANs

The most common “dissociative” group of CANs relies on a triggered displacement of an associating equilibrium towards the dissociated state. In these systems, application of a trigger such as UV-light or heat results in an increased rate of bond breaking/reforming and also in a net bond dissociation because the chemical equilibrium shifts to endothermic side. Upon cooling, the cross-links are formed again, usually to the same extent as in the starting material, thus preserving or re-installing the desirable thermosetting properties such as stiffness and insolubility. In this way, these dynamic cross-links allow for thermal (re-) processing of polymeric networks.

The mechanical properties and viscosity profile of dissociative CANs is highly dependent on the design of the polymer network, of which the two extreme situations at both sides of the continuum will be discussed here to illustrate the difference. The first extreme case comprises networks that are formed by an intrinsically reversible polymerisation of multifunctional low MW monomers. This approach results in networks with a very high density of reversible cross-links (Figure 2.6a). At low temperatures and at high enough conversion, the material will be well above its gel point, which means that the network is actually one molecule (disregarding network defects) and will behave like a solid. Upon heating, the equilibrium will be displaced towards the dissociated state and the material will undergo a gel-to-sol transition. In this way, the network will depolymerize to an oligomeric melt that behaves like a viscous liquid as the short chains and monomers can move freely alongside of each other. Consequently, this transformation is also associated with a narrow and strong viscosity drop<sup>12</sup> and the material will become soluble in the presence of a good solvent.<sup>13,14</sup>

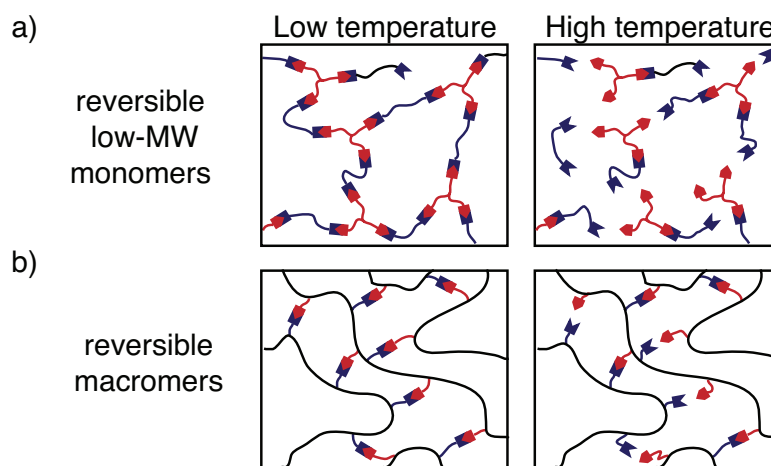


Figure 2.6. Reversible networks prepared from: upper) small multifunctional monomers resulting in network that undergoes a fast gel-to-sol transition upon heating. lower) a macromer with multiple reversible pending groups, which gives rise to a network that only undergoes a gel-to-sol transition upon close to full dissociation.

The second extreme case consists in a network formed by long linear molecules with interspersed or pending functional groups along the backbone that can be interconnected via a reversible reaction (Figure 2.6b). As these long chains can possess many pending groups along their backbone, they can also be considered as macromers with a high functionality. This high functionality of the macromer results in a gel point that can be easily reached even at low conversions (Figure 2.7). Consequently, such networks will also not undergo a gel-to-sol transition as easily as the former extreme case. For example, macromers with a functionality of 30 will require a dissociation of more than 80% of the reversible bonds.<sup>15,16</sup> Thus, for these macromer-based dissociative CANs, with increasing temperature the viscosity will partly be controlled by the rate of the reversible exchange reactions and the modulus will drop gradually due to the increasing net dissociation of the cross-links (giving a tilted rubbery plateau). Only when the equilibrium is shifted enough to induce a gel-to-sol transition (at high dissociation degrees, *i.e.* at low ‘forward’ conversion), the network is transformed to a thermoplastic melt and can flow freely.

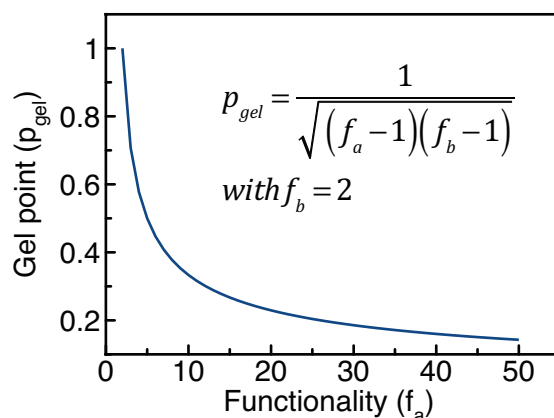


Figure 2.7. Calculated gel point according to the Flory-Stockmayer equation<sup>15,16</sup> as a function of the multifunctionality of a monomer combined with a bisfunctional monomer in a stoichiometric ratio of 1.

In the above discussion, the mobility limitations due to the glass transition were not considered. Nonetheless, the lack of segmental motions that can arise due to vitrification puts some important constraints on dissociative CANs that have a high  $T_g$ . Normally, when polymerisation of a network proceeds, there is an increase in the cross-linking density, which is accompanied with an increase in  $T_g$ . Thus, when the  $T_g$  of the curing CAN has risen to the applied curing temperature, segmental motions are arrested and the cross-linking rate will be strongly reduced.<sup>17</sup> In classical thermosets, a simple solution is to raise the curing temperature to temperatures above the material's final  $T_g$ , to avoid premature vitrification and allow the polymerisation reaction to reach completion. However, for dissociative CANS, increasing the curing temperature also means that the equilibrium will be shifted relatively more towards the dissociated state. The synthesis of high  $T_g$  dissociative CANs can thus be very challenging, as ideally the equilibrium should not significantly shift below the target  $T_g$ , while still a fast exchange is required at temperatures not too far above  $T_g$  (to avoid polymer degradation).

The most representative, and probably the most studied, example of a thermally triggered dissociative CAN relies on the well-known reversible Diels–Alder reaction between furans and maleimides (Figure 2.8).<sup>18,19</sup> Many other chemistries are also explored for the same purpose such as the reversible reaction between isocyanates and imidazoles<sup>20</sup> or anthracene dimerisation.<sup>21</sup> A more extensive list of used reversible chemistries and its properties can be found in a review of Bowman *et al.*<sup>11</sup>



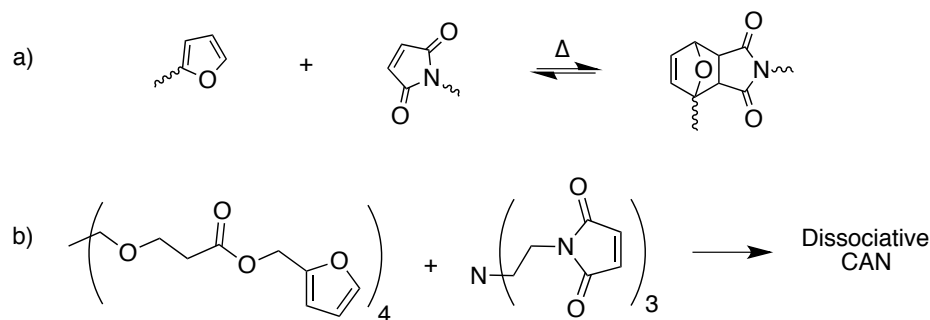


Figure 2.8. a) Reversible reaction between furans and maleimides. b) Used monomers by the pioneering work of Chen et al. for dissociative CANs.

### 2.3.2 Associative CANs

The second group of CANs that is distinguished in this work, are governed by exchange reactions that rely on associative exchange mechanisms: covalent bonds are released only after new ones have first been formed. These CANs do not depolymerise upon heating, but are characterized by a fixed cross-link density, making these networks permanent as well as dynamic. Inspired by controlled radical polymerization processes, the first purposely designed associative CANs (2005) were based on photo-mediated free radical addition fragmentation chain transfer reactions, by use of allyl sulphides as photo-labile moieties (Figure 2.9).<sup>22,23</sup>

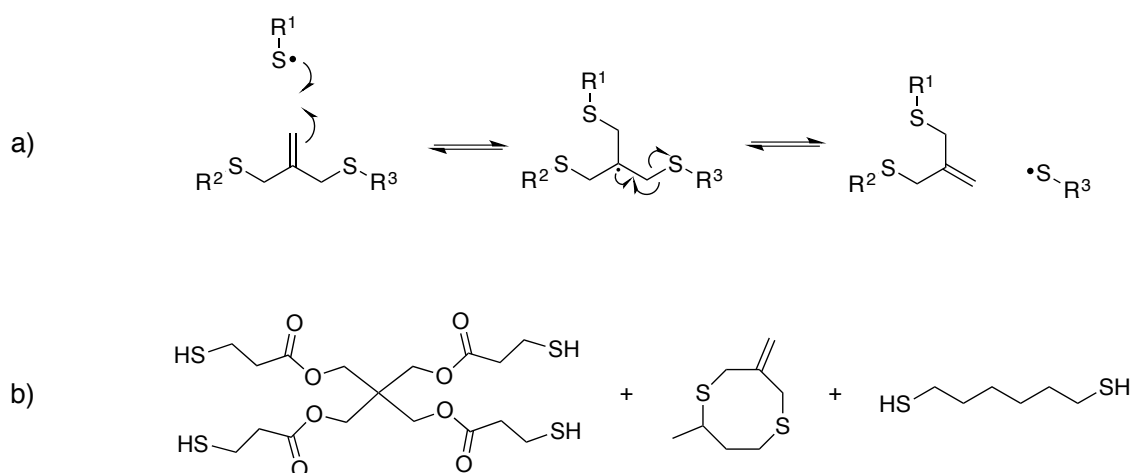


Figure 2.9. a) Addition-fragmentation chain transfer reaction of allyl sulfides. b) used monomers for the synthesis of networks containing allyl sulfides.

These networks exhibited stress- and strain-relaxation without change in material properties upon exposure to light. Later, a similar exchange mechanism was

introduced in CANs using alternative radical generators with trithiocarbonates<sup>24,25</sup> and thiurames.<sup>26</sup> Despite showing interesting flow and stress-relaxation, the ultimate adaptability or dynamic lifetime of these systems is limited due to the radical nature of the involved reactions, which gives rise to unavoidable termination reactions.

In 2011, Leibler and co-workers extended the realm of associative CANs by simply adding a suitable transesterification catalyst to epoxy/acid or epoxy/anhydride polyester-based networks.<sup>27</sup> The resulting networks underwent thermally triggered catalytic transesterification reactions, giving permanent polyester/polyol networks that show a gradual viscosity decrease upon heating. Such a viscosity profile is a distinctive feature of vitreous silica, which had never been observed in organic polymer materials. Hence, the authors introduced the name vitrimers for those materials.

## 2.4 The concept of vitrimers

Based on the pioneering work of Leibler *et al.*,<sup>28-32</sup> the vitrimer class of materials can be defined by some criteria. First, vitrimers are made of covalently bound chains forming an organic network. This network is furthermore able to change its topology via exchange reactions that are associative in nature and thermally triggered, resulting in the thermal malleability of the network. At higher temperatures, the viscosity of vitrimers is essentially controlled by chemical exchange reactions, giving a thermal viscosity decrease that follows the Arrhenius law, as is observed in typical inorganic silica materials. This latter property distinguishes vitrimers from dissociative CANs and thermoplastic materials because these materials evolve from a solid to a liquid state in a much more abrupt way, following the Williams-Landel-Ferry model (WLF) for thermoplastic polymer melts (Figure 2.10 and Figure 2.11a).

As vitrimers are permanent networks with a permanent connectivity at all temperatures (excluding degradation), these materials swell but do not dissolve in chemically inert solvents, even when heated. In contrast to classical polymer networks, swelling ratios can be expected to be higher since the elastic retractive forces, opposing the increase in entropy and heat of mixing associated with polymer swelling, can be relaxed due to topology rearrangements.

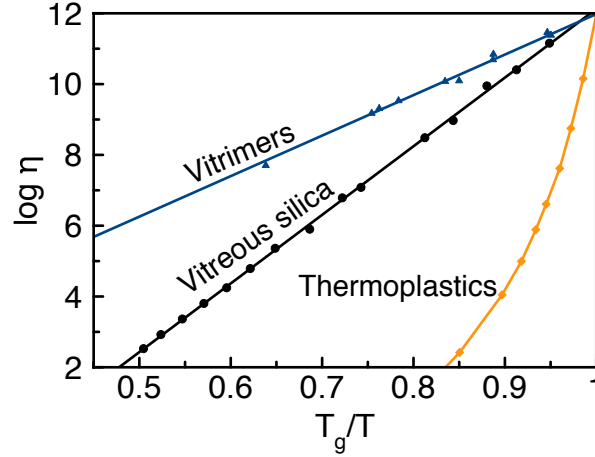


Figure 2.10. Angell fragility plot, showing the viscosity as a function of the inverse temperature, scaled with  $T_g$  (or  $T_v$  for vitrimers when  $T_v > T_g$ ). Thermoplastics<sup>33</sup> are characterised with a narrow glass transition temperature and thus a very fast decrease in viscosity near  $T_g$ . In contrast, vitrimers (epoxy-anhydride and epoxy-acid based<sup>32</sup>) show an Arrhenius-like dependence of the viscosity, which results in a gradual viscosity decrease similar to vitreous silica.<sup>34</sup>

The viscoelastic behaviour of vitrimers can be described using two transition temperatures. The first one is the usual glass transition temperature,  $T_g$ , between the glassy and rubbery state of polymer networks, correlated to the onset of long-range, coordinated molecular motion. The second transition temperature derives from the dynamic network cross-link exchange reactions. When the timescale of bond exchange reactions becomes shorter than the timescale of material deformation, the network can rearrange its topology, resulting in flow. Hence, a transition from viscoelastic solid to viscoelastic liquid occurs at a temperature denoted as the *topology freezing transition temperature*,  $T_v$ , by Leibler *et al.* This transition is conventionally chosen at the point where a viscosity of  $10^{12}$  Pa.s is reached.<sup>27,35</sup>  $T_v$  can also be observed experimentally by dilatometry, since a reorganising network has a higher expansion coefficient than a static network.

The two transition temperatures, characteristic for vitrimer materials, and their relevance, can best be clarified using two distinct examples. In the first example, the vitrimeric system has a  $T_g$  lower than  $T_v$  (Figure 2.11b). Upon heating from a temperature below  $T_g$  to a temperature between  $T_g$  and  $T_v$ , the glassy solid will first undergo a transition to the rubbery state and will behave as an elastomer since the exchange reaction is so slow that the network structure is essentially fixed. Only on further heating, the exchange reaction speeds up and becomes relevant at temperatures above  $T_v$ , transforming the elastomer to a viscoelastic

liquid of which the flow is mainly controlled by the cross-link exchange kinetics, giving the typical Arrhenian viscosity decrease.

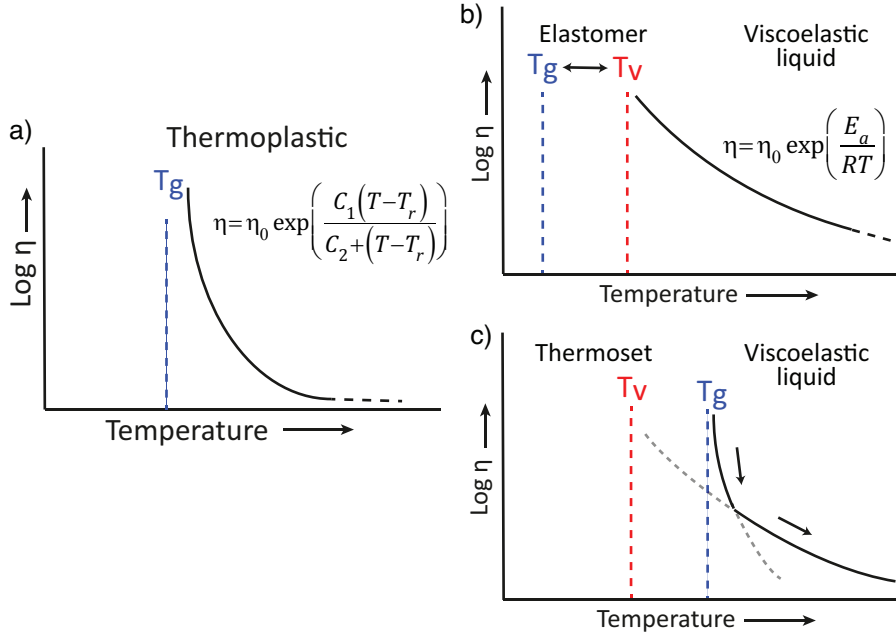



Figure 2.11. Representation of the viscoelastic behavior of a) Thermoplastics, described by the WLF-law. b) Vitrimers with a glass transition,  $T_g$ , lower than the topology freezing transition temperature,  $T_v$ . Upon heating, the vitrimer evolves from a glassy solid ( $T < T_g$ ) to an elastomer ( $T_g < T < T_v$ ) to a viscoelastic liquid ( $T > T_v$ ) that follows the Arrhenius law. c) Vitrimers with a hypothetical  $T_v$ , which is situated well below  $T_g$ . Upon heating, the vitrimer evolves from a glassy solid to a viscoelastic liquid with a viscosity that is first controlled through diffusion and then by the exchange kinetics (Arrhenius).

In the second example, an intrinsically fast exchange reaction is embedded in a rigid polymer matrix with a  $T_g$  that is higher than the expected  $T_v$  (Figure 2.11c). In such cases, where  $T_v$  can be calculated via extrapolation of stress-relaxation or creep experiments, this transition is hypothetical since the network is not ultimately frozen by the reaction kinetics, but by the lack of segmental motions associated with  $T_g$ . At temperatures below  $T_g$  no segmental motion occurs, consequently no exchange reactions can occur and the network is fixed (*cf.* diffusion limit). Upon heating above the glass transition region of the material, segmental motion is gradually initiated while the exchange reactions are already fast. In this initial situation, network rearrangement kinetics is diffusion-controlled and network topology rearrangements are dominated by segmental motions, which result in a WLF viscosity behaviour. When heating further, the

## 2.5 Vitrimer chemistries

Table 2.1: Overview of the exchange chemistries exploited for vitrimers.

Name	Reaction	Section
Transesterification	$\text{wavy line}-\text{C}(=\text{O})-\text{OR}^1 + \text{R}^2\text{OH} \rightleftharpoons \text{wavy line}-\text{C}(=\text{O})-\text{OR}^2 + \text{R}^1\text{OH}$	2.5.1, p.22
Transalkylation of triazolium salts	$\text{R}^1\text{-N}=\text{N}-\text{C}(\text{R}^2)=\text{N}-\text{CH}_2\text{R}^3\text{X}^- + \text{R}^4\text{-N}_4\text{R}^5 \rightleftharpoons \text{R}^1\text{-N}=\text{N}-\text{C}(\text{R}^2)=\text{N}-\text{R}^5 + \text{R}^4\text{-N}_4=\text{N}-\text{CH}_2\text{R}^3\text{X}^-$	2.5.2, p.24
Siloxane/silanol	$\text{wavy line}-\text{Si}^1-\text{O}-\text{Si}^2-\text{wavy line} + \text{X}^- \text{O}^-\text{Si}^3\text{wavy line} \rightleftharpoons \text{wavy line}-\text{Si}^1-\text{O}^-\text{X}^- + \text{wavy line}-\text{Si}^2-\text{O}-\text{Si}^3-\text{wavy line}$	2.5.3, p.26
Olefin metathesis	$[\text{Ru}]=\text{CH}-\text{R}^2 + \text{R}^3-\text{CH}=\text{CH}-\text{R}^4 \rightleftharpoons [\text{Ru}]=\text{CH}-\text{R}^3 + \text{R}^2-\text{CH}=\text{CH}-\text{R}^4$	2.5.4, p.27

Disulfide exchange	$R^1-S-S-R^2 + R^3-S-S-R^4 \rightleftharpoons R^1-S-S-R^3 + R^2-S-S-R^4$	2.5.5, p.28
Imine/amine	$Ar-CH=N-R^1 + H_2N-R^2 \rightleftharpoons Ar-CH=N-R^2 + H_2N-R^1$	2.5.6, p.30
Transesterification of boronic esters		2.5.7, p.31
Transcarbamoylation polyhydroxyurethanes	$\begin{array}{c} X \\   \\ \sim N \\   \\ C=O \\   \\ O-R^1 \end{array} + HO-R^2 \rightleftharpoons \begin{array}{c} X \\   \\ \sim N \\   \\ C=O \\   \\ O-R^2 \end{array} + HO-R^1$	2.5.8, p.31

---

### 2.5.1 Catalysed Carboxylate Transesterification

Leibler and co-workers initially demonstrated the concept of vitrimers by using simple carboxylic acid-based transesterification reactions, promoted by a catalyst (Figure 2.12b). In classical epoxy/acid polymer networks, the abundance of both free hydroxyl functions and carboxylic esters is guaranteed by simply mixing stoichiometric amounts of bi- and poly-functional monomers (Figure 2.12a). For epoxy/anhydride networks on the other hand, the polymerisation is more complex and the stoichiometry is carefully chosen, so that free hydroxyls are available throughout the network.<sup>30</sup>

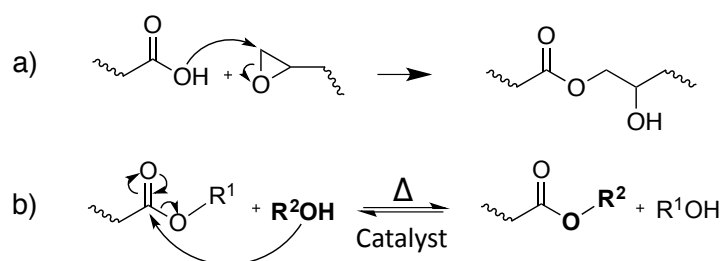


Figure 2.12. a) The reaction between epoxides and carboxylic acids results in a repeating unit, containing both an ester and a hydroxyl function. b) The catalytic transesterification reaction that can occur at elevated temperatures.

Interestingly, the rate of the catalysed transesterification reaction at room temperature is insignificant. Hence, typical soft epoxy/acid networks ( $T_g$  below room temperature) perform like conventional elastomers at room temperature, without creep. However, upon heating, rapid exchange reactions allow the rearrangement of the network structure, enabling the material to be deformed, processed and recycled (*cf.* Figure 3a).<sup>36</sup>

One of the features of the transesterification-based vitrimers is the relatively straightforward control of the exchange reaction kinetics through catalysis. By changing the amount and nature of catalyst, the activation energy and  $T_v$  can be tuned with minimal perturbation of material properties. For example, activation energies for 1,5,7-triazabicyclo[4.4.0]dec-5-ene (TBD), zinc(II)acetate ( $\text{Zn}(\text{OAc})_2$ ), and triphenylphosphine ( $\text{PPh}_3$ ) are 106, 86 and 43  $\text{kJ mol}^{-1}$  respectively.

In more recent work, Ji *et al.* demonstrated that also light can be used to process epoxy/acid-based transesterification vitrimers by dispersing 1 w/w% of carbon nanotubes (CNTs) into the polymer matrix.<sup>37</sup> Carbon nanotubes absorb light of almost all wavelengths and transform the energy to heat, resulting in fast and precise local heating. CNT-impregnated vitrimers were successfully reshaped, healed and even welded with non-CNT-vitrimers via irradiation with an infrared laser.

Another variant on epoxy-based transesterification vitrimers was reported by Williams and co-workers using epoxidized soybean oil and citric acid in the presence of water. Chemically, the system is very similar to Leibler's original system but with only renewable feedstock chemicals. Remarkably, these materials were found to relax stresses and are healable, even without the addition of any catalyst.<sup>38</sup> We believe that this uncatalysed transesterification occurs due to neighbouring group participation of the proximal carboxylic ester. The citric acid has three carboxyl acid moieties in close proximity whose central carboxylic acid is much less reactive and thus less likely to react with an epoxide to form an ester bond (Figure 2.13). As this free carboxylic acid is in close proximity, it could exert a rate-enhancing effect on the transesterification. A similar effect is also observed in the unusually rapid hydrolysis of monomethylphthalate<sup>39</sup> and phthalamic acid.<sup>40</sup>

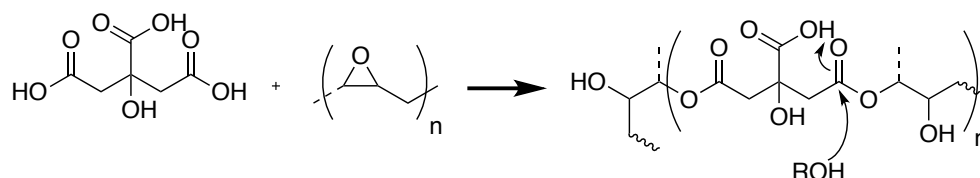


Figure 2.13. Reaction of epoxides with the terminal carboxylic acids of citric acid. The central carboxylic acid remains available for internally catalysing the transesterification reaction.

Relaxation times of these catalyst-free epoxy materials are considerably higher, 5.5h versus 2.4h for epoxy/acid resins with 5%  $\text{Zn}(\text{OAc})_2$  at  $150^\circ\text{C}$ . However, full

stress-relaxation could not be achieved in these epoxy/acid resins, probably due to the formation of irreversible cross-links upon prolonged heating.

As an alternative to epoxy-based transesterification vitrimers, Hillmyer et al. reported transesterification vitrimers prepared with isocyanate chemistry,<sup>41</sup> using hydroxyl-terminated four-arm shaped polylactide and methylenediphenyl diisocyanate (MDI) monomers. A dioctyltin catalyst ( $\text{Sn}(\text{oct})_2$ ) was used for both the polymerisation and the transesterification reaction. Compared to epoxy vitrimers, remarkably short relaxation times (50 s at 140°C) were observed at all isocyanate/alcohol ratios, even when only a small amount of free hydroxyl groups is present in the network. These short relaxation times can be attributed to the high abundance of ester groups in the network (polylactide backbone) and possibly to a higher catalyst activity. These results indicate that besides the amount of free hydroxyl groups, also the relative concentration or abundance of ester functions throughout the network matrix can influence the relaxation times tremendously.

Although all esterification-based vitrimers show good processability, long-term stability of the materials can be an issue through catalyst ageing or leaching, and ester hydrolysis. Especially the hydrophilic polylactide/urethane networks could have limited applications, as urethanes are known to absorb water.<sup>42</sup>

In summary, transesterification vitrimers, and especially epoxy-based ones, excel in availability of monomers and ease of synthesis, which makes them readily upscalable and applicable in an industrial context. On the other hand, fast processing is only achieved with high catalyst loadings and high temperatures. Moreover, catalyst (in)solubility becomes an issue, especially when rigid monomers are used for high  $T_g$  materials ( $>75^\circ\text{C}$ ).<sup>31</sup>

In addition to the experimental work on transesterification vitrimers, theoretical models were also developed for these pioneering systems, leading to further insights in the remarkable dynamic behaviour of these materials.<sup>43,44</sup>

### 2.5.2 Transalkylation of triazolium salts

Drockenmuller and co-workers reported new vitrimers based on transalkylation reactions in networks containing 1,2,3-triazolium salts, triazolines and pendant alkylhalide chains.<sup>45</sup> Such polyionic networks were synthesized via a one-pot



process through a polyaddition of  $\alpha$ -azide- $\omega$ -alkyne monomers involving a thermal ‘non-click’ azide-alkyne Huisgen 1,3-dipolar cycloaddition and a simultaneous cross-linking step, using a bifunctional alkylating agent such as dibromo and diiodo alkanes or alkylmesylates (Figure 2.14). The resulting networks showed typical Arrhenian stress-relaxation with an experimental activation energy of 140 kJ mol<sup>-1</sup> for the species with a bromide counter-ion. Short relaxation times ranging from 30 minutes at 130°C to a few seconds at 200°C were observed. Interestingly, flow properties in these systems can be controlled via the choice of counter-ion, as these can result in faster stress-relaxation (Br<sup>-</sup> >> I<sup>-</sup> > MsO<sup>-</sup>).

The origin of the stress-relaxation is assigned to transalkylation reactions in the network and confirmed via model compound studies. Mechanistically, the exchange reaction is still unclear at this time, although two realistic pathways can be imagined. In one scenario, suggested by the authors, a group transfer can be mediated by the nucleophilic attack of a counterion (halide or mesylate) on an alkyltriazolium species (Figure 2.14, arrow 1), which can then react with a different alkyl halide chain. This is a dissociative mechanism that should result in depolymerisation. However, this is not observed but might also be explained by substitution reactions that only happen within ‘pockets’ of ionic liquid-like ion pairs, preventing free diffusion of the new alkyl halide. In the other scenario, substitutions could also directly occur between alkyl triazolium salts and nucleophilic unalkylated triazoles, expelling a triazole and making a new triazolium species in a concerted S<sub>N</sub>2-type substitution (Figure 2.14, arrow 2). As iodides are more nucleophilic than bromides, but triazolium bromides give faster exchange reactions, this associative exchange mechanism seems more likely and also more readily explains the observed vitrimer properties. However, more work will need to be performed on these intriguing systems in order to clarify the exact chemical mechanisms.

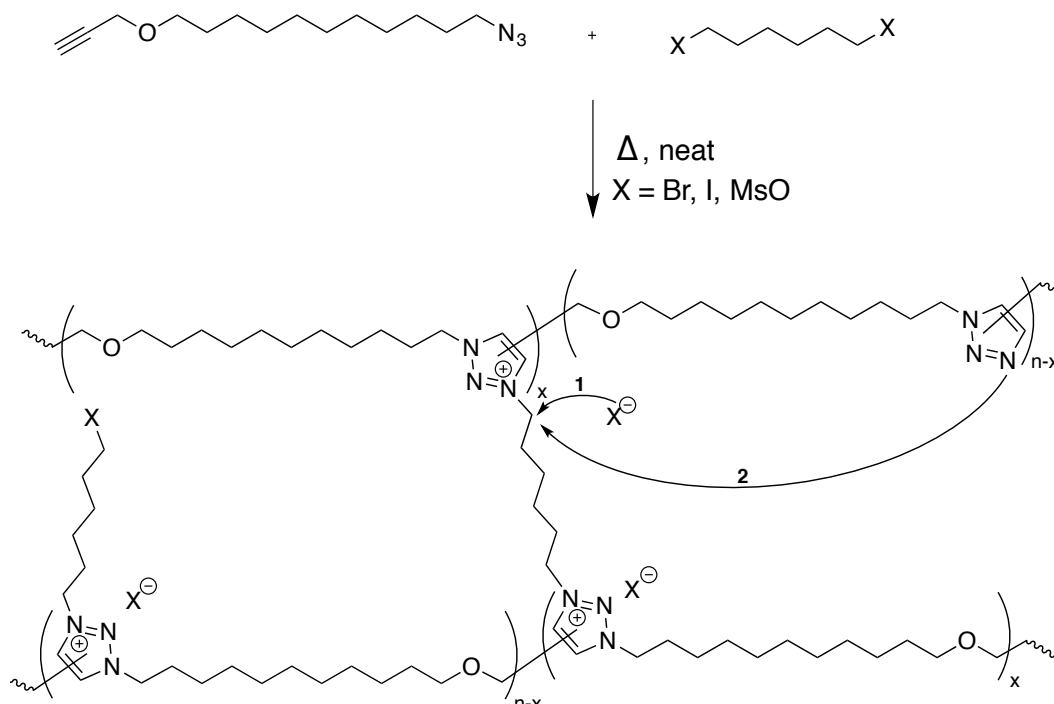


Figure 2.14. Polymerisation of  $\alpha$ -azide- $\omega$ -alkyne monomers with bisfunctional alkylating agents results in polymer networks via the formation of 1,2,3-triazoles followed by the cross-linking process through alkylation to 1,2,3-triazoliums. The resulting networks can rearrange their topology through exchange between 1,2,3-triazoles and 1,2,3-triazoliums.

Despite the straightforward polymerization of triazolium salt polyionic networks, which is an easy, solvent- and catalyst-free one-pot process, the transalkylation vitrimers compare unfavourably to the former two systems in terms of scalability and cost, requiring hazardous and more expensive chemicals (azides and alkylating reagents). On the other hand, these polyionic materials offer an interesting functionality by their conducting properties, which can be quite useful for certain niche applications.

### 2.5.3 Siloxane silanol exchange reaction

In 2012, McCarthy et al. drew attention to the addition/elimination of silanols or silanolate on siloxane moieties as a ‘forgotten’ dynamic covalent bond forming reaction, and demonstrated quantitative healing and stress-relaxation in polydimethylsiloxane (PDMS) networks.<sup>46</sup> In fact, these results were already suggested in the 1950s<sup>47-49</sup> and are also patented.<sup>50</sup> In this report, qualitative stress-relaxation experiments showed that PDMS elastomers undergo siloxane rearrangements (Figure 2.15), catalysed by the presence of either acids or bases. While the exchange kinetics can be enhanced via these catalysts,<sup>51</sup> degradation

through hydrolysis and thermal cyclisation-depolymerisation becomes an issue.<sup>52</sup> An interesting approach to avoid this degradation is the thermal decatalysation using a silanolate tetramethylammonium salt.<sup>47</sup> The silanolate anion induces rapid exchange reactions even below 130°C, but can be decomposed via thermal treatment at 150°C, thus transforming the living polymer to a permanent elastomer. Although the vitrimeric properties of such ‘living’ polysiloxane networks remain to be explored, and thermal degradation seems to be an important issue in known systems, the associative nature of the covalent bond exchange reaction should allow for the design of new siloxane-based vitrimer materials.

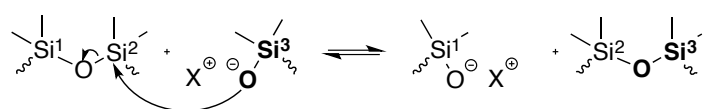


Figure 2.15. Siloxane silanol exchange reaction through addition and elimination of a silanolate anion.

#### 2.5.4 Olefin metathesis exchange reaction

While the olefin metathesis reaction is a very powerful tool for the formation of C-C bonds,<sup>53-56</sup> and has found wide use in ring opening metathesis polymerisation (ROMP), cross-metathesis is much less used in polymer synthesis, as it lacks an internal driving force. For topology rearrangements *via* group exchange equilibria in networks, however, cross-metathesis should be a good method as no driving force is required. Indeed, Guan and co-workers demonstrated the possibilities of the olefin metathesis reaction in cross-linked polybutadiene networks containing second-generation Grubbs catalyst (Figure 2.16).<sup>57-59</sup> This catalyst was used because of its superior stability towards air and moisture and its good functional group compatibility, as compared to more classical metathesis catalysts.<sup>60</sup> Networks were first prepared through free radical cross-linking of polybutadiene initiated by benzoyl peroxide.

As the 2<sup>nd</sup> generation Grubbs catalyst is not compatible with these cross-linking conditions, the catalyst needed to be introduced via a swelling experiment, which covalently incorporates the ruthenium catalyst by breaking some chains, also incorporating the original styrene-derived carbene ligand as a new chain end (*cf.* Figure 2.16a). The obtained elastomeric ruthenium-bonded networks already showed significant stress-relaxation and creep at ambient temperatures, due to

the highly effective exchange reaction. As expected, flow properties could be controlled via the catalyst concentration. For possible self-healing materials applications, this ambient exchange reaction is interesting since quantitative healing can be obtained, even at room temperature. For applications in typical vitrimer processing of rigid networks, the creep is highly undesirable for most applications where elastomers are typically used. Freezing the topology via the glass transition could be a solution to avoid creep, but may not be straightforward to implement. Furthermore, the sensitivity of the catalyst can also be used to ‘deactivate’ the catalyst after processing resulting in a permanent thermosetting elastomer.

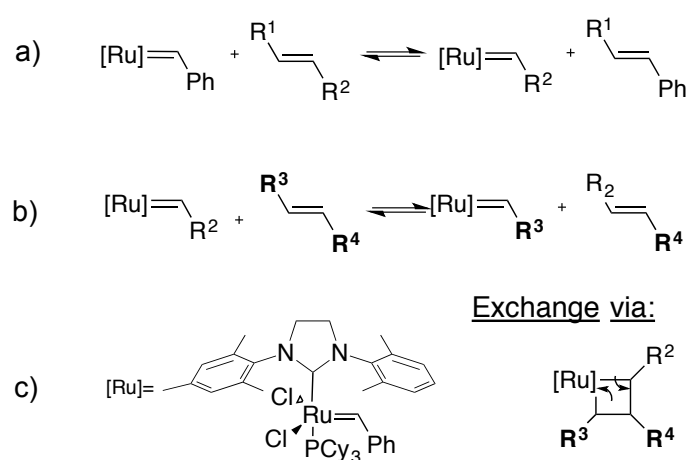


Figure 2.16. Olefin metathesis exchange reaction, a) Insertion of the Grubbs’ second generation catalyst into an alkyl chain b) Exchange of two alkene bonds. c) Left: structure of 2<sup>nd</sup> generation Grubbs’ catalyst; Right: the associative exchange mechanism of a metathesis reaction.

### 2.5.5 Disulfide exchange chemistry

The dynamic nature of sulfur-sulfur linkages and of disulfides<sup>61-74</sup> in particular has been extensively studied because of the great interest for vulcanized rubbers in the chemical industry.<sup>70,71</sup> Recent reports show that the behaviour of covalently exchanging disulfide bonds is a rather complex process, and involves several mechanisms that also depend on the used conditions and substitution patterns of the disulfides. In the most simple form, disulfides can be reduced to two thiols and then oxidized again via a clearly dissociative stepwise pathway (Figure 2.17a).<sup>65-67</sup> Alternatively, disulfides can be homolytically but reversibly opened to stabilised thiyl radicals under action of UV,<sup>74</sup> shear and/or heat,<sup>68-70</sup> another dissociative but more direct pathway (Figure 2.17b). An associative exchange is, in

principle, possible by an addition/elimination substitution with free thiols or possibly free thiyl radicals (Figure 2.17c).<sup>64,72,75</sup>

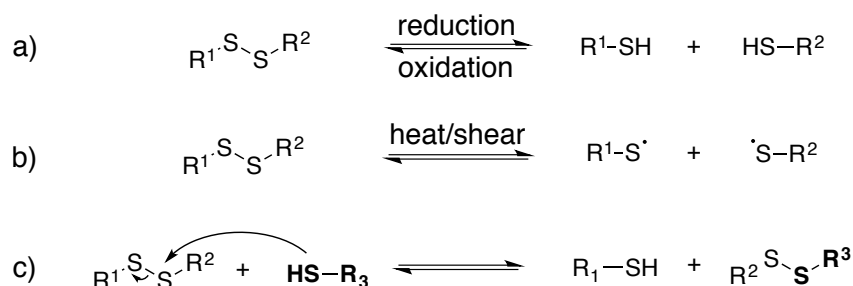


Figure 2.17. a) Reversible reduction and oxidation of disulfides b) Homolytical cleavage of disulfides into two thiyl radicals and reformation c) addition/elimination substitution of free thiols with disulfides.

Recently, Goossens and Klumperman *et al.*<sup>54</sup> reported dynamic networks based on base-catalysed thiol-disulfide exchange reactions and could correlate the mechanical relaxation times with those of the model compounds, showing properties reminiscent of vitrimers, probably related to an associative exchange mechanism of the type shown in Fig 8c. However, as oxidation of free thiols readily occurs under air and free thiols are required for the exchange reaction, these materials show a marked deterioration of dynamic properties over time. The same exchange reaction has also been used by Klumperman,<sup>46</sup> and by Zhang<sup>75</sup> in previous studies on self-healing materials.

Based on a different exchange mechanism, recently proposed to proceed via a radical mediated [2+1] mechanism,<sup>76</sup> Odriozola et al. demonstrated processable elastomers using aromatic disulfide metathesis<sup>61,62</sup> in poly(urea-urethane) networks. These networks showed quantitative self-healing at room temperature due to both dynamic hydrogen bond formation and network reshuffling (Figure 2.18). Interestingly, while these disulfide exchange reactions are known to occur rapidly at room temperature, little stress-relaxation is actually observed for deformations within the linear range of these materials at room temperature, as hydrogen bonds prevent the network to flow at low temperatures (TPE-like property). The viscoelastic properties of these networks are thus more complex compared to vitrimers relying on a single relaxation process, since these two relaxation effects are superposed on each other.

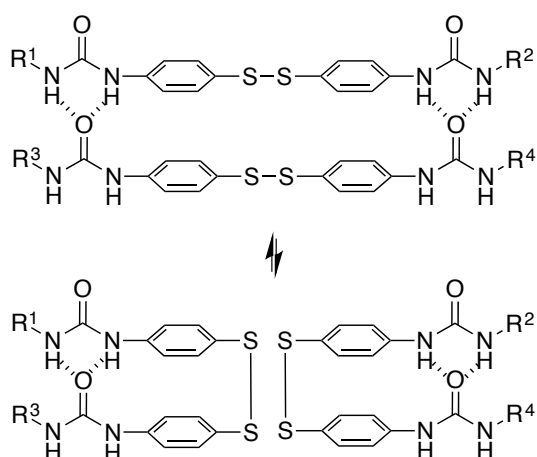


Figure 2.18. Aromatic disulfide metathesis proceeds at room temperature without any catalyst. The quadruple H-bonds of the urea groups prevent the network to flow at low temperatures.

### 2.5.6 Imine amine exchange chemistry

While the dynamic nature of imines in polymer chemistry is mainly exploited using its dissociative pathway involving reversible formation/hydrolysis of imines<sup>77-79</sup> (Figure 2.19a), associative pathways in absence of water via either amine exchange<sup>80</sup> (Figure 2.19b) or imine metathesis (Figure 2.19c) could also result in a dynamic behaviour.<sup>81</sup> Recently, Zhang and co-workers exploited associative imine chemistry for the design of malleable and recyclable polymer networks.<sup>82</sup> These cross-linked polyimine networks were prepared via the condensation of commercially available aldehydes and a mixture of di- and triamines in a solvent combination that further drives the reversible imine-forming condensation, which only has a very small intrinsic thermodynamic driving force. The stress-relaxation behaviour of the dried polyimine networks exhibited Arrhenius-like temperature dependence together with water-induced stress-relaxation at room temperature, indicating vitrimer-like properties. While this malleability was assigned by the authors to a direct imine metathesis reaction (Figure 2.19c), the fast stress-relaxation (30 min for 90% relaxation at 80°C) can be more readily explained by a fast imine addition-elimination exchange through intermediate aminal formation with abundant free amines (Figure 2.19b). Indeed, Di Stefano and co-workers have shown that even a minute amount of primary amines, which are highly likely to be present in the polyimine network, induce a very fast addition-elimination exchange reaction with imines.<sup>80</sup> In addition, this swift transimination can also explain the fast water-induced stress-relaxation as the dissociative hydrolysis, (Figure 2.19a) acting together

with transimination induced by free amines, allows for very efficient network rearrangements. Despite the interesting possibilities of the room temperature water-induced malleability of these networks, the mechanical properties and useful applications of these polyimines networks are limited by this unavoidable sensitivity towards hydrolysis. Furthermore, in very recent work, Zhang *et al.* reported a free radical metathesis-like exchange reaction of aromatic imine bonds for remoldable cross-linked polymers.<sup>83</sup>

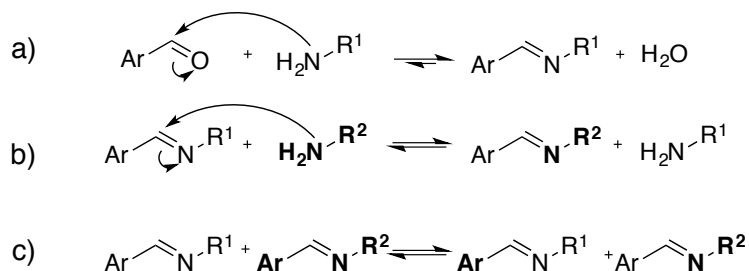


Figure 2.19. Reversible processes associated with imine chemistry. a) equilibrium of imine formation, via intermediate hemi-aminal formation; b) transimination between imines and amines via intermediate aminal formation; c) imine metathesis.

### 2.5.7 Transesterification of boronic esters

Until recently, boronic acids were mainly exploited in polymer chemistry due to their ability to condensate from boronic acid and 1,2-diols or 1,3-diols and reversibly dissociate (Figure 2.20a). This reversibility in combination with the ability to control the equilibrium via pH and pKa of the particular boronic esters, makes them very suitable for applications in aqueous media such as sugar sensing<sup>84-86</sup> and self-healing hydrogels.<sup>87-89</sup> Sumerlin and co-workers showed that this reversibility can also be used for self-healing bulk materials via intentional wetting of the broken surface and thus inducing local hydrolysis of the boronic acids.<sup>90</sup> Only very recently, Guan *et al.* reported dynamic and self-healing bulk materials that rely on the associative transesterification of boronic esters and 1,2-diols<sup>91</sup> (Figure 2.20b). These materials were prepared via a ROMP polymerisation of a 1,2-diol cyclooctene monomer followed by the curing of the resulting prepolymers with a bisfunctional boronic acid cross-linker in toluene, yielding semi-crystalline elastomers with a melting point between 10 and 50°C (Figure 2.20c). Furthermore, the rate of exchange and thus also stress-relaxation behaviour could be controlled via small modifications of the boronic acid cross-linker as a neighbouring tertiary amine enhances the exchange kinetics. The resulting polymers showed partial stress-relaxation at room temperature and full-

stress relaxation at elevated temperature, probably due to the crystallinity and a strong difference between the cross-linkers. Although boronic esters seem a promising chemistry for vitrimers because they combine high thermodynamic stability and kinetic tunability, the current system is limited not only due to the restrictions in monomer choice and thus materials properties but also the multiple steps needed to obtain the final polymer. The inherent hydrolytic lability of boronic esters may also be an issue.

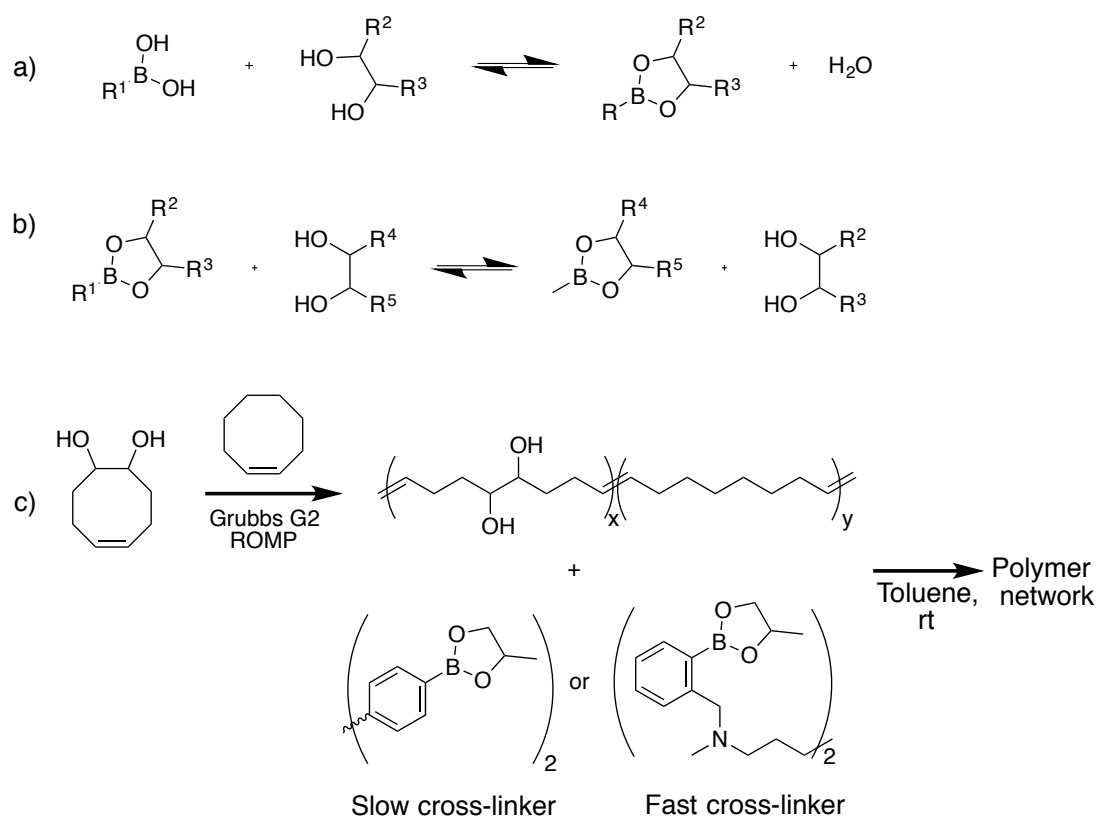


Figure 2.20: a) Reversible formation and dissociation of boronic acid with a 1,2-diol in presence of water. b) transesterification of boronic esters c) Synthesis of dynamic networks containing 1,2-diols and boronic esters via first ROMP polymerisation of diol-containing monomer followed by the cross-linking with boronic ester cross-linkers.

### 2.5.8 Transcarbamylation of polyhydroxyurethane networks

Inspired by the long-known stress-relaxation behavior of hydroxyurethanes,<sup>92,93</sup> Fortman et al. reported in 2015 polyurethane (PU)-based vitrimers prepared from 6-membered cyclic carbonates and trifunctional amines<sup>94</sup> (Figure 2.21a). The vitrimer nature of these networks, evidenced by their insolubility and Arrhenian stress-relaxation behaviour, was ascribed to addition/elimination-type



transcarbamoylation of the hydroxyurethanes present in the network (Figure 2.21b). Another pathway that could result in stress-relaxation behaviour involves the reversible dissociation towards the isocyanate and alcohol (Figure 2.21c). The temperature window of this dissociation is highly dependent on the used substituents (exploited for blocked isocyanates<sup>95</sup>) and in this case, *i.e.* for aliphatic urethanes, known to be around 250°C.<sup>96</sup> As the stress-relaxation behaviour occurred already between 170 and 190°C and no difference in activation energy was observed between the urethane (X = H) and the N-methyl urethane (X = CH<sub>3</sub>), which is not capable to form a neutral isocyanate upon dissociation, associative transcarbamoylation was appointed as the dominant pathway.

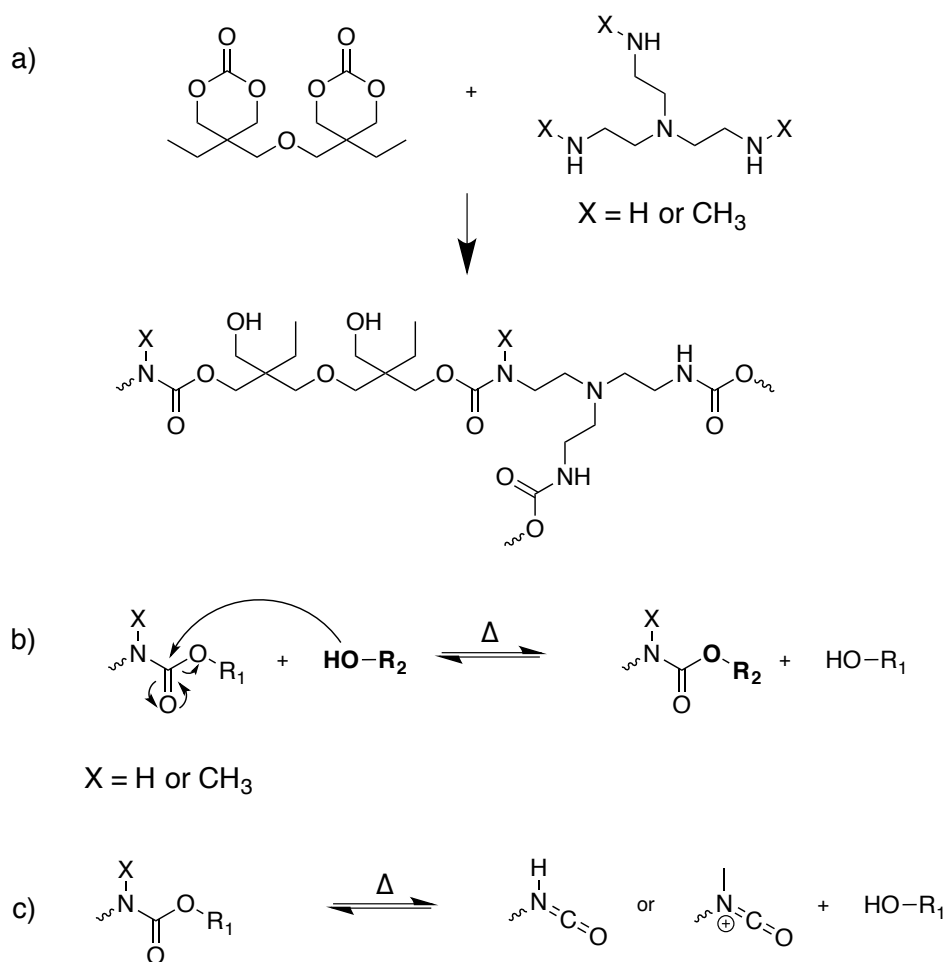


Figure 2.21: a) Synthesis of polyhydroxyurethane networks by reaction of a triamine monomer with a bis(cyclic carbamate) b) associative transcarbamoylation of alcohols and urethanes c) reversible dissociation of a urethane to an isocyanate and alcohol.

Although Fortman's polyhydroxyurethane networks showed good material properties comparable to those of conventional thermosets, the very slow

exchange kinetics is a limiting factor for these materials resulting in relaxation times of 80 minutes at 170°C. These long relaxation times in combination with high temperatures also induce minor degradation resulting in reduced mechanical properties over time. Indeed, original mechanical properties of pristine samples could not be obtained after grinding and compression moulding and also pristine samples subjected to the same thermal treatment showed a similar loss in materials properties. Fortman has also put forward a mechanochemical explanation of the transcarbamoylation reaction (supported by DFT calculations), which is markedly slower in model compounds.

### 2.5.9 Supramolecular bonds and associative exchange

Although supramolecular bonds are by definition dissociative, as they constantly break and reform, Sciortino *et al.* proposed a theoretical approach for a supramolecular gel based on DNA that is capable of rearranging its topology without losing overall connectivity via a “toe-hold mediated displacement”.<sup>97</sup> This ‘toe-hold mediated displacement’ takes place between a DNA array of two strands neighboured with some free base pairs, the so-called “toe-hold” (P-E1). First, an incoming free bridge (E2) attaches to the toe-hold. Next, the original strand of the DNA is displaced by the incoming free bridge via breakage of the adjacent base pair followed by formation with the base pair of the free bridge via a dynamic equilibrium through a series of low barrier base pair exchange events. As a base pair breaks and a new is formed afterwards, the enthalpy penalty is only limited and the process can proceed within the temperature range that the system is fully associated.

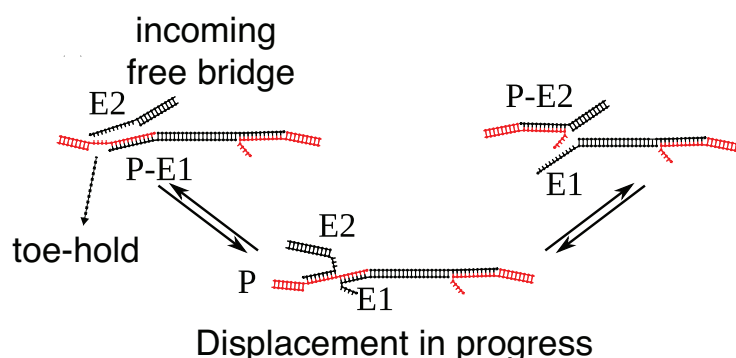


Figure 2.22: toe-hold mediated displacement of a two DNA strands via first binding to the toe-hold of an incoming free bridge followed by a sequential displacement of the adjacent base pairs. Figure adopted from (94).

A similar process could also be found in other systems where a segmental connection is made up via multiple small connections capable of dissociative exchange such as hydrogels based on clays and dendritic binders<sup>98</sup> as well as dissociative CANs made from macromers (*Cfr.* Figure 2.6). However, all these systems will only behave vitrimeric in a limited temperature window since full dissociation will occur at a certain temperature. Moreover, these systems are not characterized by a constant cross-link density. As a consequence, it is very questionable to label these theoretical systems as vitrimers.

## 2.6 Vitrimer applications

As vitrimers were only reported in 2011 for the first time, no large-scale industrial applications are known to the best of our knowledge. However, due to their unique features, they are most likely currently subject of research for several industrial applications including in our own research group. In this section, we will discuss some of the applications where vitrimers could provide added value. First, we will discuss more in general some important features of vitrimers. Next, we will discuss two particular applications, namely composites and liquid crystalline elastomers. Probably, many more applications that are not mentioned here will be reported in the future.

### 2.6.1 Network processing, welding and recycling

The most straightforward application of vitrimers would be as a replacement of conventional thermosetting materials where the vitrimer's ability to be processed and reshaped after complete curing could be exploited for manifold purposes. Reshaping could be very interesting for objects that can or need to be customised. These are currently expensive since a costly mould is to be prepared for each single object. When a basic shape could be prepared from a vitrimer and afterwards be shaped and formed to the desired dimensions, cost reductions could be achieved. For example, orthoses and prostheses for children are currently often replaced by another expensive one when the child grows. Using a vitrimer's ability to be formed upon heating, the object of interest could be made to 'grow' with the child.

A second feature of vitrimers that could be exploited is the ability to form joints between two parts. As vitrimers can rearrange their molecular structure upon

heating and form connections over the two parts, they can be welded together with a junction that is as strong as the bulk of the rest of the two objects. Currently, when complex objects are required, different moulded parts must be combined with either adhesives or bolts. As the use of bolts could be avoided, weight reductions can be achieved. Similar to welding, also repairing of cross-linked polymers becomes possible and thus allows to extend the lifetime of synthetic objects. Since the viscosity drop of vitrimers is very gradual, no precise temperature control is needed and simple tools such as a heat gun or an IR light beam, and some clamps to apply pressure could be used.

Vitrimers may also impact the end-of-life issues related to thermosets. Up-to-date, full recycling of thermosets is not possible. At most, thermosets are grinded and used as a filler to reduce cost of other materials or used as a source of energy by controlled combustion. Literature examples already showed that vitrimers can achieve the same mechanical properties after several grinding and compression moulding cycles. In this way, vitrimers could transform common cross-linked polymers from low value, fit-for-purpose discardable materials, into versatile raw materials with a high intrinsic value.

The processability of vitrimers may also address some of the safety and health issues that are now related to classical thermosets. Thermosets are mostly prepared from low molecular weight compounds via a very effective chemical reaction that needs to reach high conversions. The required building blocks are thus often hazardous chemicals because they are quite reactive. As a consequence, companies that prepare thermosetting materials must transport, store and handle these reactive compounds in their processes (*e.g.* isocyanates). When vitrimers could reach a processability that allows very fast cycle times for part production as required in industry, vitrimers could be prepared and fully cured in one central well-controlled place. The obtained materials are inert and can be stored, transported and processed to the final shape safely and without risks.

As discussed above, a free-flowing but fully cross-linked structure enables many possibilities for synthetic materials. However, the biggest challenge to compete with the current used bulk thermoset materials will be the cost. Only when the added value of the post-curing processability is large enough, vitrimer materials would become industrially feasible. Two such applications where the proof-of-concept is already demonstrated, are composites and liquid crystalline actuators (LCEs).

## 2.6.2 Processable composites

Fiber-reinforced polymer composites (FRPCs) are materials that are formed by combination of reinforcing materials, such as glass-fibres or carbon-fibres, with a polymer matrix that surrounds and binds the fibres together. This combination results in heterogeneous materials that are very strong and stiff and at the same time light-weight (Figure 2.23). Thus, FRPCs are often used as a light-weight alternative to metals, further driven by global trends towards cutting energy consumption and resource efficiency. Currently the aerospace industry is one of the biggest users of composites, but the automotive industry is massively increasing its light weighting efforts. While composites are already exploited for Formula One and luxury cars, it is expected that composites will find their way into other automotive segments in the near future, especially in electrically powered vehicles.

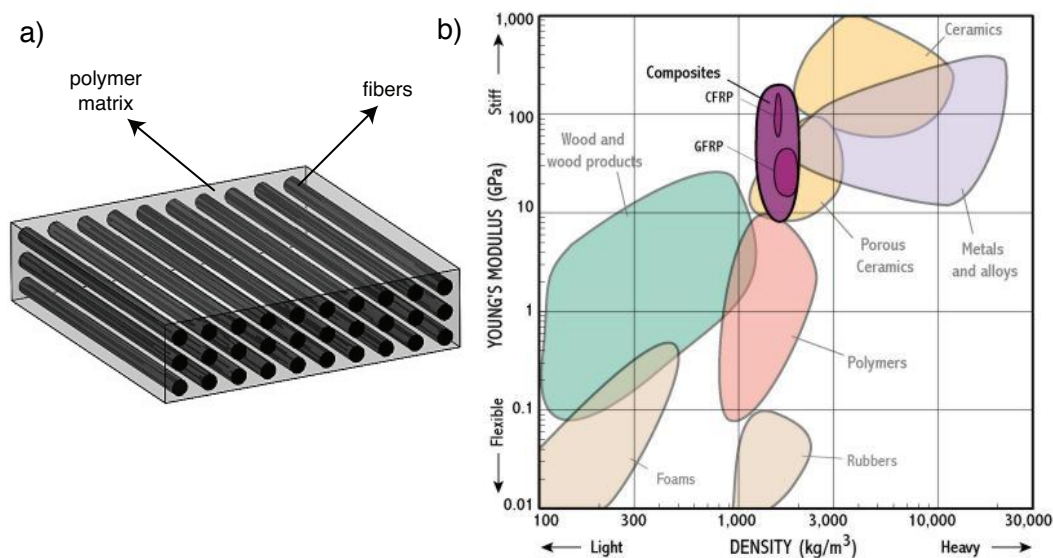


Figure 2.23: a) Schematic representation of a composite material. b) Stiffness as a function of specific weight for different materials.<sup>99</sup> Composites are very stiff for their specific weight compared to other materials.

For the polymer matrix in composites, both thermosets and thermoplastics can be used. For a long time, thermosets were used predominantly as they allow for easy fiber impregnation from a low viscous monomer mixture that can be reacted or fully cured *in situ*. Moreover, the resulting composites have excellent fatigue strength and creep resistance due to the cross-linked structure. As discussed before, however, thermosets have to be prepared in their final shape due to their permanent structure after full curing. A common practice to address this problem exists in partially curing the resin to a so-called B-stage or ‘*prepreg*’, which is

then shaped and fully cured. While this approach allows for a one-time processing, the curing of the prepregs should be stopped before gelation, which results in a limited shelf-life, careful storage and transport at low temperatures and the use of special foils as the prepregs are often tacky.

Due to the limitations of thermosetting composites, thermoplastic composites are nowadays more and more used. As the thermoplastic matrix can flow upon heating, thermoplastic composites can be easily thermoformed and the cycle time is only controlled by the time needed to heat and cool in contrast to the curing time. Therefore, they lend themselves more towards high volume mass production. However, to achieve good mechanical properties with a thermoplastic matrix, molecular weights should be high enough. This increase in molecular weight leads to a strong increase in viscosity and technically complicates the impregnation of the fibres. Moreover, rather expensive engineering plastics, such as polyether-etherketone (PEEK, 80 €/Kg) and polyethersulfone (PES), are often required to ensure good thermal and mechanical properties. Thermoplastic composites are often claimed to be more recyclable than their thermosetting counterparts. Nevertheless, removing the thermoplastic matrix from fibres is rather difficult (if not impossible in a cost effective manner) and mechanical grinding of composites and reusing them as short-fiber composites results in strongly decreased mechanical properties.

Very recently, also vitrimers were exploited as a matrix for composites.<sup>100-102</sup> As expected and already anticipated in the pioneering work,<sup>28</sup> FRPC using a vitrimer matrix showed some unique features that cannot be found in thermosets or thermoplastics FPRC's. For example, Leibler and co-workers showed with their transesterification chemistry that multiple welding of long-fiber epoxy vitrimer composites can be achieved without adhesives or mechanical fasteners. The welded parts showed a force at break up to 2800 N when welded for 25 minutes at 180°C, which is comparable to current used adhesives with a force at break in the 2500-5000 N range with the same experimental set-up.

Odriozola and co-workers exploited their aromatic disulfide chemistry in epoxy resins combined with carbon fibres and showed that these vitrimer FRPC's could be used to prepare enduring prepregs, which do not require cold storage and are not tacky. These prepregs could be pressed to a multi-layered composite and afterwards processed to a zig-zag shape (Figure 2.24). Furthermore, also repair of a delaminated composite and recycling of the carbon fibres via scission of the

aromatic disulfide bond was presented. Taynton et al. published similar results using their amine-imine exchange chemistry.<sup>102</sup>

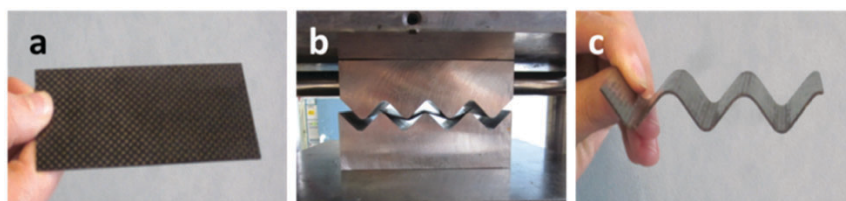


Figure 2.24: Thermoforming of a fully cured composite laminate. Figure reproduced from reference 102 with permission from The Royal Society of Chemistry.

The above three recent literature examples that exploit vitrimers as a matrix for FRPC's, have probably only scratched the surface of vitrimer applications in composites. In addition, the belief in their industrial relevance becomes clear as all vitrimer chemistries used for composites are patented.<sup>103,104</sup> Vitrimers based on imine/amine chemistry are currently (2016) explored to be marketed by the start-up Mallinda,<sup>105</sup> which targets tailored sport protection as only mild temperatures are needed for thermoforming.

### 2.6.3 Liquid crystalline actuators

One field where vitrimers have already shown to introduce added value is in the field of liquid-crystalline elastomers (LCEs).<sup>106,107</sup> These materials combine liquid crystal orientational order with the elastic properties of a polymer network into a single material. This coupling results in a material where the orientation of the liquid crystals results in an anisotropic environment for the polymer chains, which make the polymer chains deviate from a random orientation towards chains that are different parallel and perpendicular to the LC direction (Figure 2.25). When the liquid-crystal order is changed due to a trigger such as heating, also the polymer chains adopt a random conformation and the sample will undergo a dramatic yet reversible change in dimension.<sup>108,109</sup> Due to this feature of LCEs to adopt their shape upon heating, they show much promise as materials for actuators and artificial muscles in a wide range of areas such as robotics<sup>110</sup>, tissue engineering<sup>111</sup> and devices in aerospace.

The biggest issue of LCEs is the macroscopic orientation of the liquid-crystal order required for the reversible actuation, which is hard to realise. Currently, the most common method is a two-step process starting with weak cross-linking of

the crystalline polymer, which is then uniaxially stretched to align the mesogens, followed by the second cross-linking step to achieve permanent alignment.

By using vitrimers, Wei and Ji overcame this bottleneck, and polymer networks containing these mesogens can be made in a one-step fashion, followed by alignment of the crystals through elevation of the temperature combined with uniaxial tension which results in the alignment of the mesogens.<sup>107</sup> Very recently, the same authors showed that by use of the photothermal effect of dispersed carbon nanotubes in LCEs, actuation can be triggered very locally by shining light on the desired spot, even at temperatures of  $-130^{\circ}\text{C}$ .<sup>107</sup>

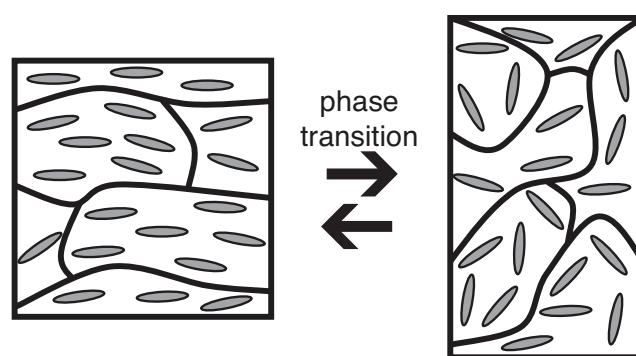


Figure 2.25: Liquid crystalline elastomers can undergo a reversible macroscopic deformation by a triggered change from isotropic to an anisotropic state due to the liquid crystal orientation. Figure adopted from ref.<sup>108</sup>

## 2.7 References

- (1) Sperling, L. H. *Introduction to Physical Polymer Science*; 4 ed.; Wiley-Interscience, 2005.
- (2) Drobný, J. G. In *Handbook of Thermoplastic Elastomers*; William Andrew Publishing: Norwich, NY, 2007, p 1.
- (3) Cordier, P.; Tournilhac, F.; Soulie-Ziakovic, C.; Leibler, L. *Nature* **2008**, *451*, 977.
- (4) Burattini, S.; Greenland, B. W.; Merino, D. H.; Weng, W.; Seppala, J.; Colquhoun, H. M.; Hayes, W.; Mackay, M. E.; Hamley, I. W.; Rowan, S. J. *J. Am. Chem. Soc.* **2010**, *132*, 12051.
- (5) Burnworth, M.; Tang, L.; Kumpfer, J. R.; Duncan, A. J.; Beyer, F. L.; Fiore, G. L.; Rowan, S. J.; Weder, C. *Nature* **2011**, *472*, 334.
- (6) van Gemert, G. M. L.; Peeters, J. W.; Söntjens, S. H. M.; Janssen, H. M.; Bosman, A. W. *Macromol. Chem. Phys.* **2012**, *213*, 234.
- (7) Ducrot, E.; Chen, Y.; Bulters, M.; Sijbesma, R. P.; Creton, C. *Science* **2014**, *344*, 186.
- (8) Leibler, L.; Rubinstein, M.; Colby, R. H. *Macromolecules* **1991**, *24*, 4701.
- (9) Bowman, C. N.; Kloxin, C. J. *Angew. Chem., Int. Ed.* **2012**, *51*, 4272.
- (10) Kloxin, C. J.; Bowman, C. N. *Chem. Soc. Rev.* **2013**, *42*, 7161.



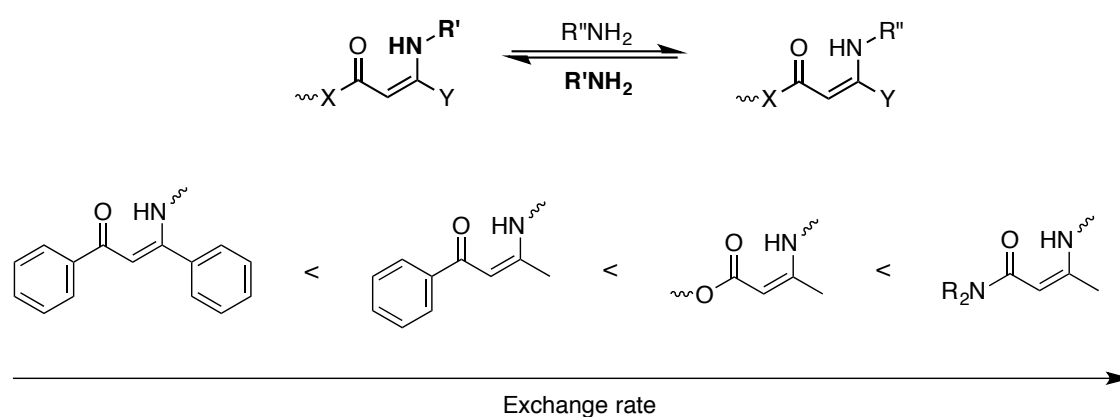
- (11) Kloxin, C. J.; Scott, T. F.; Adzima, B. J.; Bowman, C. N. *Macromolecules* **2010**, *43*, 2643.
- (12) Adzima, B. J.; Aguirre, H. A.; Kloxin, C. J.; Scott, T. F.; Bowman, C. N. *Macromolecules* **2008**, *41*, 9112.
- (13) Canary, S. A.; Stevens, M. P. *Journal of Polymer Science Part a-Polymer Chemistry* **1992**, *30*, 1755.
- (14) McElhanon, J. R.; Russick, E. M.; Wheeler, D. R.; Loy, D. A.; Aubert, J. H. *J. Appl. Polym. Sci.* **2002**, *85*, 1496.
- (15) Stockmayer, W. H. *The Journal of Chemical Physics* **1943**, *11*, 45.
- (16) Flory, P. J. *J. Am. Chem. Soc.* **1941**, *63*, 3083.
- (17) Enns, J. B.; Gillham, J. K. *J. Appl. Polym. Sci.* **1983**, *28*, 2567.
- (18) Chen, X.; Wudl, F.; Mal, A. K.; Shen, H.; Nutt, S. R. *Macromolecules* **2003**, *36*, 1802.
- (19) Chen, X. *Science* **2002**, *295*, 1698.
- (20) Chang, J. Y.; Do, S. K.; Han, M. J. *Polymer* **2001**, *42*, 7589.
- (21) Van Damme, J.; Vlamincx, L.; Van Assche, G.; Van Mele, B.; van den Berg, O.; Du Prez, F. *Tetrahedron* **2016**, *72*, 4303.
- (22) Scott, T. F.; Bowman, C. N.; Wayne, C. D.; Schneider, A. D. *Science* **2005**, *308*, 1615.
- (23) Kloxin, C. J.; Scott, T. F.; Park, H. Y.; Bowman, C. N. *Adv. Mater.* **2011**, *23*, 1977.
- (24) Nicolaÿ, R.; Kamada, J.; Van Wassen, A.; Matyjaszewski, K. *Macromolecules* **2010**, *43*, 4355.
- (25) Amamoto, Y.; Kamada, J.; Otsuka, H.; Takahara, A.; Matyjaszewski, K. *Angew. Chem., Int. Ed.* **2011**, *50*, 1660.
- (26) Amamoto, Y.; Otsuka, H.; Takahara, A.; Matyjaszewski, K. *Adv. Mater.* **2012**, *24*, 3975.
- (27) Angell, C. A. *Science* **1995**, *267*, 1924.
- (28) Montarnal, D.; Capelot, M.; Tournilhac, F.; Leibler, L. *Science* **2011**, *334*, 965.
- (29) Capelot, M.; Unterlass, M. M.; Tournilhac, F.; Leibler, L. *ACS Macro Lett.* **2012**, *1*, 789.
- (30) Capelot, M.; Montarnal, D.; Tournilhac, F.; Leibler, L. *J. Am. Chem. Soc.* **2012**, *134*, 7664.
- (31) Montarnal, D. Use of reversible covalent and non-covalent bonds in new recyclable and reprocessable polymer materials, PhD Thesis, Université Pierre et Marie Curie, 2011.
- (32) Capelot, M. Chimie de polycondensation, Polymères Supramoléculaires et vitrimères, PhD Thesis, Université Pierre et Marie Curie, 2013.
- (33) Plazek, D. J.; O'Rourke, M. V. *J. Polym. Sci., Part B: Polym. Phys.*, *9*, 209
- (34) Urbain, G.; Bottinga, Y.; Richet, P. *Geochemica et Cosmochimica Acta*, *46*, 1061.
- (35) Dyre, J. C. *Rev. Mod. Phys.* **2006**, *78*, 953.
- (36) Yu, K.; Taynton, P.; Zhang, W.; Dunn, M. L.; Qi, H. J. *RSC Adv.* **2014**, *4*, 10108.
- (37) Yang, Y.; Pei, Z.; Zhang, X.; Tao, L.; Wei, Y.; Ji, Y. *Chem. Sci* **2014**, *5*, 3486.
- (38) Altuna, F. I.; Pettarin, V.; Williams, R. *Green Chem.* **2013**, *15*, 3360.
- (39) Bender, M. L.; Chloupek, F.; Neveu, M. C. *J. Am. Chem. Soc.* **1958**, *80*, 5384.
- (40) Bender, M. L.; Chow, Y.-L.; Chloupek, F. *J. Am. Chem. Soc.* **1958**, *80*, 5380.

- (41) Brutman, J. P.; Delgado, P. A.; Hillmyer, M. A. *ACS Macro Lett.* **2014**, *3*, 607.
- (42) Oertel, G.; Abele, L. *Polyurethane Handbook: Chemistry, Raw Materials, Processing, Application, Properties*; Hanser, 1994.
- (43) Long, K. N. *J. Mech. Phys. Solids* **2014**, *63*, 386.
- (44) Smallenburg, F.; Leibler, L.; Sciortino, F. *Phys. Rev. Lett.* **2013**, *111*, 188002.
- (45) Obadia, M. M.; Mudraboyina, B. P.; Serghei, A.; Montarnal, D.; Drockenmuller, E. *J. Am. Chem. Soc.* **2015**, *137*, 6078.
- (46) Zheng, P.; McCarthy, T. J. *J. Am. Chem. Soc.* **2012**, *134*, 2024.
- (47) Gilbert, A. R.; Kantor, S. W. *J. Polym. Sci.* **1959**, *40*, 35.
- (48) Osthoff, R. C.; Bueche, A. M.; Grubb, W. T. *J. Am. Chem. Soc.* **1954**, *76*, 4659.
- (49) Kantor, S. W.; Grubb, W. T.; Osthoff, R. C. *J. Am. Chem. Soc.* **1954**, *76*, 5190.
- (50) Buese, M. A.; Chang, P. S. 5,347,028, 1994
- (51) Schmolke, W.; Perner, N.; Seiffert, S. *Macromolecules* **2015**, *48*, 8781.
- (52) Lee, T. C. P.; Sperling, L. H.; Tobolsky, A. V. *J. Appl. Polym. Sci.* **1966**, *10*, 1831.
- (53) Vougioukalakis, G. C.; Grubbs, R. H. *Chem. Rev. (Washington, DC, U. S.)* **2010**, *110*, 1746.
- (54) Nicolaou, K. C.; Bulger, P. G.; Sarlah, D. *Angew. Chem., Int. Ed.* **2005**, *44*, 4490.
- (55) Grubbs, R. H. *Tetrahedron* **2004**, *60*, 7117.
- (56) Chatterjee, A. K.; Choi, T.-L.; Sanders, D. P.; Grubbs, R. H. *J. Am. Chem. Soc.* **2003**, *125*, 11360.
- (57) Lu, Y.-X.; Tournilhac, F.; Leibler, L.; Guan, Z. *J. Am. Chem. Soc.* **2012**, *134*, 8424.
- (58) Lu, Y.-X.; Guan, Z. *J. Am. Chem. Soc.* **2012**, *134*, 14226.
- (59) Neal, J. A.; Mozhdehi, D.; Guan, Z. *J. Am. Chem. Soc.* **2015**, *137*, 4846.
- (60) Scholl, M.; Ding, S.; Lee, C. W.; Grubbs, R. H. *Org. Lett.* **1999**, *1*, 953.
- (61) Martin, R.; Rekondo, A.; Ruiz de Luzuriaga, A.; Cabañero, G.; Grande, H. J.; Odriozola, I. *J. Mater. Chem. A* **2014**, *2*, 5710.
- (62) Rekondo, A.; Martin, R.; Luzuriaga, A. R. d.; Cabañero, G.; Grande, H. J.; Odriozola, I. *Mater. Horiz.* **2013**, *1*, 237.
- (63) Lafont, U.; van Zeijl, H.; van der Zwaag, S. *ACS Appl. Mater. Interfaces* **2012**, *4*, 6280.
- (64) Canadell, J.; Goossens, H.; Klumperman, B. *Macromolecules* **2011**, *44*, 2536.
- (65) Tsarevsky, N. V.; Matyjaszewski, K. *Macromolecules* **2002**, *35*, 9009.
- (66) Tesoro, G. C.; Sastri, V. *J. Appl. Polym. Sci.* **1990**, *39*, 1425.
- (67) Sastri, V. R.; Tesoro, G. C. *J. Appl. Polym. Sci.* **1990**, *39*, 1439.
- (68) Takahashi, Y.; Tobolsky, A. V. *Polym. J. (Tokyo, Jpn.)* **1971**, *2*, 457.
- (69) Tobolsky, A. V.; Takahashi, M.; Macknight, W. J. *J. Phys. Chem.* **1964**, *68*, 787.
- (70) Rajan, V. V.; Dierkes, W. K.; Joseph, R.; Noordermeer, J. W. M. *Prog. Polym. Sci.* **2006**, *31*, 811.

- (71) Adhikari, B.; De, D.; Maiti, S. *Prog. Polym. Sci.* **2000**, *25*, 909.
- (72) Pepels, M.; Filot, I.; Klumperman, B.; Goossens, H. *Polym. Chem.* **2013**, *4*, 4955.
- (73) Imbernon, L.; Oikonomou, E. K.; Norvez, S.; Leibler, L. *Polym. Chem.* **2015**, *6*, 4271.
- (74) Michal, B. T.; Jaye, C. A.; Spencer, E. J.; Rowan, S. J. *ACS Macro Lett.* **2013**, *2*, 694.
- (75) Lei, Z. Q.; Xiang, H. P.; Yuan, Y. J.; Rong, M. Z.; Zhang, M. Q. *Chem. Mater.* **2014**, *26*, 2038.
- (76) Matxain, J. M.; Asua, J. M.; Ruiperez, F. *Phys. Chem. Chem. Phys.* **2016**, *18*, 1758.
- (77) Deng, G.; Li, F.; Yu, H.; Liu, F.; Liu, C.; Sun, W.; Jiang, H.; Chen, Y. *ACS Macro Lett.* **2012**, *1*, 275.
- (78) Deng, G.; Tang, C.; Li, F.; Jiang, H.; Chen, Y. *Macromolecules* **2010**, *43*, 1191.
- (79) Yang, B.; Zhang, Y.; Zhang, X.; Tao, L.; Li, S.; Wei, Y. *Polym. Chem.* **2012**, *3*.
- (80) Ciaccia, M.; Cacciapaglia, R.; Mencarelli, P.; Mandolini, L.; Di Stefano, S. *Chem. Sci* **2013**, *4*, 2253.
- (81) Belowich, M. E.; Stoddart, J. F. *Chem. Soc. Rev.* **2012**, *41*, 2003.
- (82) Taynton, P.; Yu, K.; Shoemaker, R. K.; Jin, Y.; Qi, H. J.; Zhang, W. *Adv. Mater.* **2014**, *26*, 3938.
- (83) Lei, Z. Q.; Xie, P.; Rong, M. Z.; Zhang, M. Q. *J. Mater. Chem. A* **2015**.
- (84) Jakle, F. *Chem. Rev. (Washington, DC, U. S.)* **2010**, *110*, 3985.
- (85) James, T. D.; Sandanayake, K.; Shinkai, S. *Angewandte Chemie-International Edition* **1996**, *35*, 1910.
- (86) Edwards, N. Y.; Sager, T. W.; McDevitt, J. T.; Anslyn, E. V. *J. Am. Chem. Soc.* **2007**, *129*, 13575.
- (87) He, L. H.; Fullenkamp, D. E.; Rivera, J. G.; Messersmith, P. B. *Chem. Commun. (Cambridge, U. K.)* **2011**, *47*, 7497.
- (88) Meng, H.; Xiao, P.; Gu, J. C.; Wen, X. F.; Xu, J.; Zhao, C. Z.; Zhang, J. W.; Chen, T. *Chem. Commun. (Cambridge, U. K.)* **2014**, *50*, 12277.
- (89) Deng, C. C.; Brooks, W. L. A.; Abboud, K. A.; Sumerlin, B. S. *ACS Macro Lett.* **2015**, *4*, 220.
- (90) Cash, J. J.; Kubo, T.; Bapat, A. P.; Sumerlin, B. S. *Macromolecules* **2015**, *48*, 2098.
- (91) Cromwell, O. R.; Chung, J.; Guan, Z. *J. Am. Chem. Soc.* **2015**, *137*, 6492.
- (92) Colodny, P. C.; Tobolsky, A. V. *J. Am. Chem. Soc.* **1957**, *79*, 4320.
- (93) Offenbach, J.; Tobolsky, A. V. *J. Colloid. Sci.* **1956**, *11*, 39.
- (94) Fortman, D. J.; Brutman, J. P.; Cramer, C. J.; Hillmyer, M. A.; Dichtel, W. R. *J. Am. Chem. Soc.* **2015**, *137*, 14019.
- (95) Delebecq, E.; Pascault, J.-P.; Boutevin, B.; Ganachaud, F. *Chem. Rev. (Washington, DC, U. S.)* **2013**, *113*, 80.
- (96) Simon, J.; Barla, F.; Kelemen-Haller, A.; Farkas, F.; Kraxner, M. *Chromatographia*, *25*, 99.
- (97) Romano, F.; Sciortino, F. *Phys. Rev. Lett.* **2015**, *114*, 078104.

- (98) Wang, Q.; Mynar, J. L.; Yoshida, M.; Lee, E.; Lee, M.; Okuro, K.; Kinbara, K.; Aida, T. *Nature* **2010**, *463*, 339.
- (99) <http://www-materials.eng.cam.ac.uk/>, Accessed on: 09/10/2016
- (100) Chabert, E.; Vial, J.; Cauchois, J.-P.; Mihaluta, M.; Tournilhac, F. *Soft Matter* **2016**, *12*, 4838.
- (101) Ruiz de Luzuriaga, A.; Martin, R.; Markaide, N.; Rekondo, A.; Cabanero, G.; Rodriguez, J.; Odriozola, I. *Mater. Horiz.* **2016**, *3*, 241.
- (102) Taynton, P.; Ni, H.; Zhu, C.; Yu, K.; Loob, S.; Jin, Y.; Qi, H. J.; Zhang, W. *Adv. Mater.* **2016**, *28*, 2904.
- (103) Odriozola, I.; Ruiz de Luzuriaga, A.; Rekondo, A.; Martin, R.; Markaide, N.; Cabañero, G.; Grande, H. J. Thermomechanically reprocessable epoxy composites and their manufacturing. 2015
- (104) Leibler, L.; Montarnal, D.; Tournilhac, F.; Capelot, M. Acid-hardening epoxy thermoset resins and composites that can be hot-processed and recycled. WO2011FR51231 20110530, 2013
- (105) <http://www.mallinda.com/>, Accessed on: 09/10/16
- (106) Pei, Z.; Yang, Y.; Chen, Q.; Terentjev, E. M.; Wei, Y.; Ji, Y. *Nat. Mater.* **2014**, *13*, 36.
- (107) Yang, Y.; Pei, Z.; Li, Z.; Wei, Y.; Ji, Y. *J. Am. Chem. Soc.* **2016**, *138*, 2118.
- (108) Ohm, C.; Brehmer, M.; Zentel, R. In *Liquid Crystal Elastomers: Materials and Applications*; DeJeu, W. H., Ed. 2012; Vol. 250, p 49.
- (109) Ohm, C.; Brehmer, M.; Zentel, R. *Adv. Mater.* **2010**, *22*, 3366.
- (110) McEvoy, M. A.; Correll, N. *Science* **2015**, *347*, 9.
- (111) Villar, G.; Graham, A. D.; Bayley, H. *Science* **2013**, *340*, 48.





## Abstract

In this chapter, an introduction to the chemistry of enaminones is presented, starting with a short discussion on their synthesis and use in polymer chemistry. Next, model compound studies on different enaminones are described to assess the kinetics of the amine exchange. This qualitative and quantitative study showed that the vinylogous transamination of enaminones spans over a very wide practical temperature window depending on their structure, ranging from rapid room temperature to temperatures as high as 170°C. Therefore, this chapter served and guided our design for vitrimer materials and will also help to predict and understand the results in following chapters.

## Published in:

Denissen, W.; Rivero, G.; Nicolaÿ, R.; Leibler, L.; Winne, J. M.; Du Prez, F. E. *Advanced Functional Materials* **2015**, 25 (16), 2451–2457.

Denissen, W. Winne, J. M.; Du Prez, F.E., Nicolaÿ, R.; Leibler, L.; Composition comprising a polymer network. WO/2016/097169

## Chapter 3

# Vinylogous Transamination Chemistry

### 3.1 Introduction

In 2011, vitrimers were reported for the first time and their unique features immediately showed great promise to affect many industries that rely on elastomers, thermosets and composites. In essence, vitrimers combine the mechanical properties of cross-linked materials with a glass-like malleability when heated. The foundation of this invention consists in exchange reactions that allow the rearrangement of network structures, while keeping a constant cross-link density during the exchange process, which was achieved using catalysed transesterification in epoxy networks.<sup>1-3</sup> As described in detail in chapter two, in recent years several other exchange chemistries have been reported with mixed success for vitrimer synthesis, but at the start of this project (end 2012), transesterification was the reference system. Although it was the first exchange chemistry used to demonstrate the concept of vitrimers, it provided already a high-level benchmark. Transesterification is a very simple and well-understood chemistry that can be easily implemented in materials with good properties, via the addition of a transesterification catalyst to known epoxy-acid and epoxy-anhydride formulations.

The pioneering polyester-type vitrimer systems also showed some limitations. As transesterification is a rather slow exchange reaction, considerable amounts of metal catalyst need to be used to achieve fast network rearrangements. For example, the epoxy-anhydride vitrimers consisted of 4-5% by weight of  $\text{Zn}(\text{Acac})_2$  catalyst to obtain the required processability. As a consequence, these high catalyst-loadings start to influence the materials properties and probably also enhances degradation at high temperatures. Moreover, epoxy-acid vitrimers with a high  $T_g$  could not be achieved since the solubility of the metal catalyst in aromatic media (rigid monomers) is too limited. Furthermore, transesterification catalysts also catalyse hydrolysis reactions, narrowing the application scope of polyester vitrimers. Thus, although the epoxy-vitrimers showed already great prospects, there was still room for improvement.

The goal of this PhD project consisted in the design and exploration of an alternative exchange reactions that could tackle some of the aforementioned limitations. Ideally, this envisaged exchange chemistry should be intrinsically fast and not require a catalyst. The dynamic covalent bond should be stable towards hydrolysis and to harsh high temperature conditions used during processing. The chemistry should also be easily implementable in polymer networks and enable high  $T_g$  materials with good mechanical properties. Furthermore, the chemistry should be easily scalable and preferentially be as simple as possible.

### 3.1.1 Alternatives for transesterification

As a first alternative to the use of the transesterification reactions in vitrimers, transamidation of polyamide networks was considered (Figure 3.1). On the one hand, the amide group is thermodynamically much more robust in comparison to the ester group. This aspect facilitates polyamide synthesis (high intrinsic driving force) and also makes the resulting polymer less susceptible to hydrolysis. On the other hand, amides are also much less reactive (less electrophilic) than esters, and transamidation can typically only be effected by air- and moisture-sensitive catalysts that are incompatible with many other functional groups<sup>4,5</sup> or by temperatures above 200°C that are incompatible with many polymer matrices.<sup>6</sup>

The increased chemical stability of amides versus esters arises from the conjugation effects between the lone electron pair on the nitrogen atom and the electron-withdrawing carbonyl group. One way to weaken this C-N bond and to enhance transamidation could be achieved by (very) bulky alkyl substituents on the amide nitrogen, which will disturb the co-planarity of the amide bond and thus the conjugation effect.<sup>7</sup> While this indeed weakens the C-N bond and allows for faster exchange reactions, the attack of a bulky free amine is also hindered, resulting in the dissociation of the amide towards an amine and very reactive ketene prone to many side reactions. For this reason, we did not explore substituted amides as dynamic bond as it progresses via a dissociative rather than an associative pathway, which is needed for vitrimers.



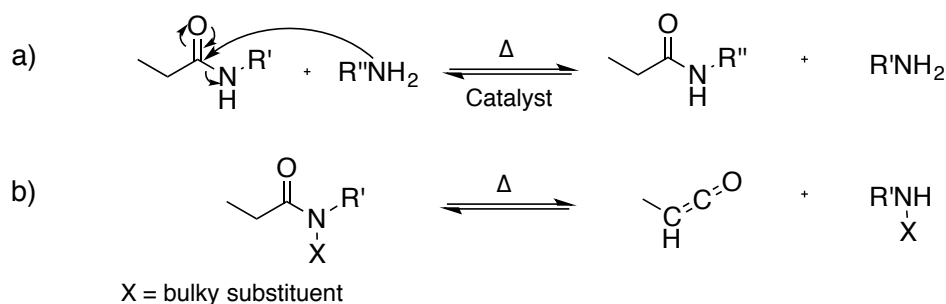


Figure 3.1. a) Catalytic transamidation of amides. b) Dissociation of a hindered amide towards a ketene and amine.

Related to amides, also urea and urethanes could be considered. While simple ureas do not undergo exchange reactions, sterically hindered ureas undergo a similar dissociation reaction as amides towards the corresponding amine and isocyanate (Figure 3.2). Such hindered urea are reported for the design of reversible and self-healing polymers.<sup>8</sup> However, their ultimate reversibility will be limited as upon heating, the formed isocyanates can react with water, which is known to be absorbed over time in polyurea networks, resulting in the formation of amines and CO<sub>2</sub>.

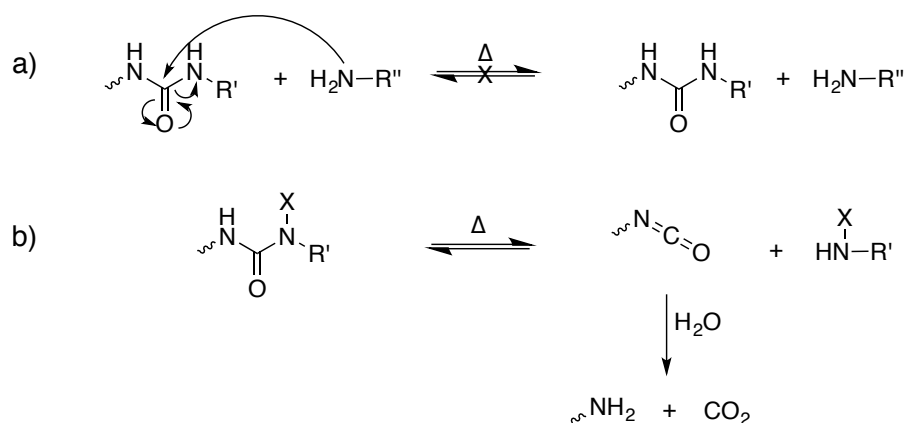


Figure 3.2: a) Simple urea do not undergo exchange reactions with amines. b) Sterically hindered urea can dissociate towards amines and isocyanates, which can react further with water present in the bulk of the material.

Urethanes on the other hand, are capable of trans-reactions in the presence of Lewis acid catalysts (Figure 3.3a).<sup>9</sup> However, this exchange reaction is also rather slow and at higher temperatures, the competing dissociation reaction towards isocyanates and alcohols can occur,<sup>10</sup> limiting again the ultimate reversibility of such systems and their practical use for vitrimers (Figure 3.3b).

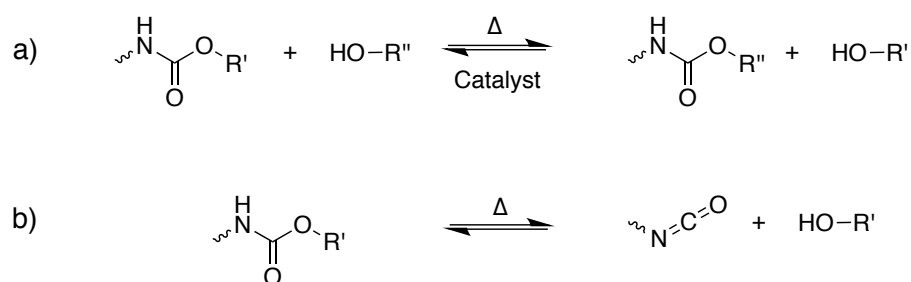


Figure 3.3. a) Transcarbamoylation of urethanes and alcohols. b) Dissociation of a carbamate to an alcohol and isocyanate.

### 3.1.2 Amine exchange of vinylogous acyls as alternative?

Another carbonyl-derived functional group related to amide bonds are vinylogous acyl moieties or enaminoxones. These chemical moieties ( $\text{N}=\text{C}=\text{C}(\text{=O})-\text{X}$ ) can be regarded as amides ( $\text{X} = \text{C}$ ), urethanes ( $\text{X} = \text{O}$ ) or ureas ( $\text{X} = \text{N}$ ) with a vinylic bond inserted in between the carbonyl carbon and its nitrogen atom (Figure 3.4). As the mesomeric ( $\pi$ -conjugative) electron withdrawing effect of the carbonyl is efficiently transmitted to the electron releasing effect of the amine lone pair (classical organic chemistry principle of vinylogy<sup>11-13</sup>), enaminoxones show striking chemical similarities compared to their non-vinyl interrupted counterparts.<sup>14,15</sup> On the one hand, these building blocks show a similar thermodynamic stability as urea, urethanes and esters because of efficient N to C  $\pi$ -bonding. On the other hand, enaminoxones are also Michael acceptors that are expected to readily undergo conjugated addition reactions with free amines. Indeed, compared to addition reactions to normal amides, Michael-type addition can proceed without disruption of the strong carbon-to-oxygen  $\pi$ -bond, but rather via the disruption of the much weaker carbon-to-carbon  $\pi$ -bond. This results in a much less endergonic addition step, and thus a much swifter exchange reaction.

The key question and hypothesis of this project comprises whether vinylogous transamination of enaminoxones could serve as a catalyst-free exchange reaction that enables the preparation of high  $T_g$  vitrimers (Figure 3.4).

For the nomenclature of enaminoxones, we will use the short hand terms vinylogous urea/urethane/amide depending on the atom besides the carbonyl function as indicated in Figure 3.4. Enaminoxones or vinylogous acyls will be used as collective name for all three compounds.

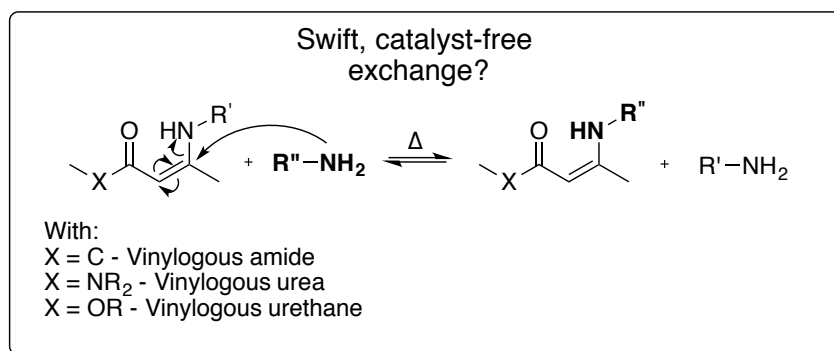


Figure 3.4: Can the amine exchange of vinylogous acyls be used as a dynamic bond for vitrimers?

### 3.1.3 Literature amine exchange of vinylogous acyls

Although amine exchange of vinylogous acyls have been examined to a much lesser extent than simple transamidation or transesterification reactions, many examples can be found in the organic chemistry literature with different substrates, amines and various reaction conditions, illustrating the feasibility and robustness of this exchange reaction.<sup>16-19</sup> For example, Abdullah et al. used both an intermolecular as intramolecular transamination of a vinylogous amide for the synthesis of pyridone (Figure 3.5a). The exchange reaction progressed in refluxing ethanol using the hydrochloric salt of methylamine. In another example by Friary et al., transamination was performed in bulk conditions with an aromatic amine such as aniline (Figure 3.5b). Many more examples exist, illustrating the feasibility of the amine exchange of enaminones, which have mostly been overlooked as a dynamic covalent bond in modern polymer chemistry applications.

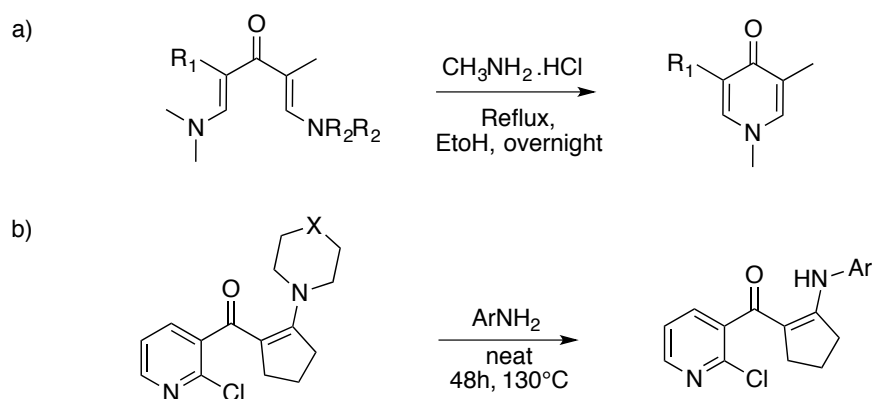


Figure 3.5. a) Inter- and intramolecular transamination for the synthesis of a pyridone.  
b) Example of a vinylogous transamination reaction.

### 3.1.4 Enaminones in polymer chemistry

In polymer chemistry, previous interest in enaminones arose mainly for one of two possible reasons.

Firstly, enaminones are of special interest since they form a near-planar six-membered ring via an intramolecular H-bond (Figure 3.6a). Due to this feature, enaminones have been used as rigid structures to replace aromatic hydrocarbon rings (pseudo-aromatics) to obtain polymers with a high strength, high glass transition temperature and thermal stability without compromising too much on solubility and processability,<sup>20-25</sup> which becomes an issue when the backbone consist of many aromatic rings. One illustrative examples is the polymerisation of di-ynones with aromatic diamines, yielding polymers with a  $T_g$  up to 235°C (Figure 3.6b).

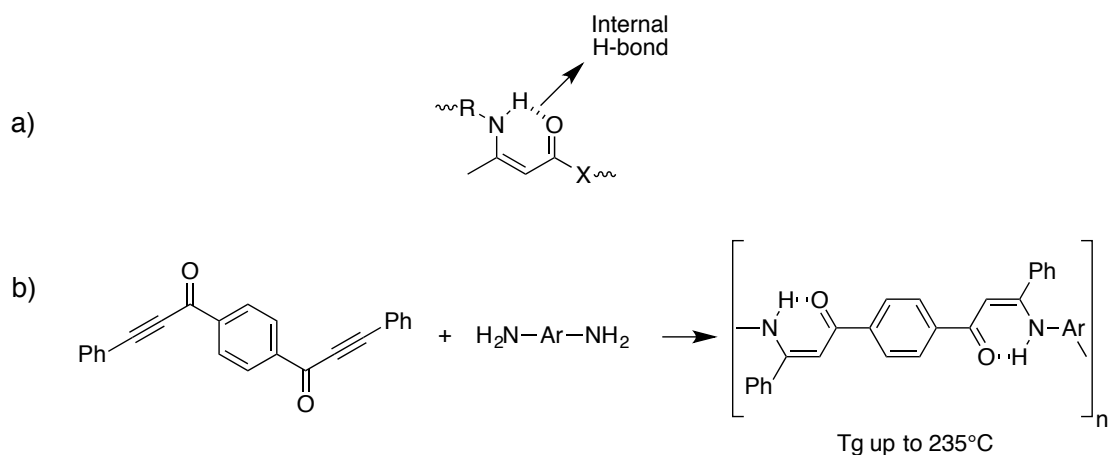


Figure 3.6. a) Enaminones form rigid 6-membered rings due to the intramolecular hydrogen bond. b) polymerisation of an ynone monomer with an aromatic diamine yields polymers with very high  $T_g$ 's.

A second interest in enaminones or more precisely vinylogous urethanes arises from their very straightforward assembly from amines and acetoacetates at room temperature, even in the presence of water. Applications can be found in the field of water-borne coatings,<sup>26</sup> adhesives<sup>27</sup> and paint formulations.<sup>28</sup> Vinylogous urethanes made from acetoacetate functions are especially useful when an increased non-volatile content and a non-isocyanate-based room temperature cure is required. In general, two approaches are used (Figure 3.7). The first way consists in the functionalisation of alcohol-bearing polymers such as polyvinyl alcohol towards the corresponding acetoacetate functional polymer, which can be cross-linked via amines.<sup>26</sup>

A second approach uses a copolymerisation of the commercially available acetoacetoxyethyl methacrylate with other acrylates yielding again an acetoacetate functionalized polymer.<sup>29-31</sup>

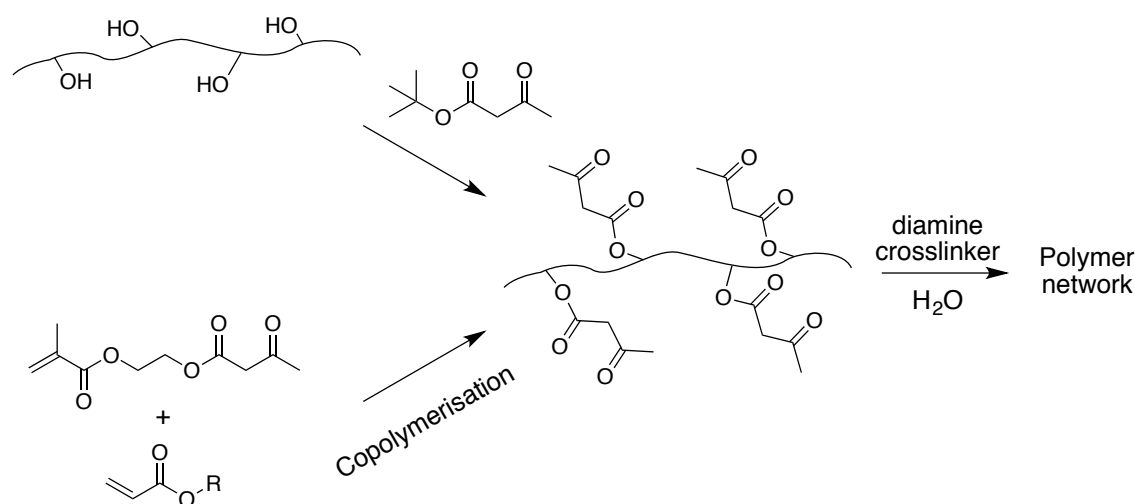


Figure 3.7: Preparation of vinylogous urethane polymer networks via reaction of amines and acetoacetate-functional polymer from either conversion of hydroxyl groups to acetoacetates (top) or via copolymerisation of acetoacetoxyethyl methacrylate and other (meth-)acrylates.

Interestingly, none of the materials described above have been designed for (*i.e.* slight excess amine) or tested on their ability for network rearrangements through covalent bond exchanges.

### 3.1.5 Synthetic approaches towards enaminoxones

While enaminoxones can be obtained via many synthetic routes as reviewed by Elassar et al.<sup>14</sup>, mainly three methods are used in polymer chemistry (Figure 3.8). The most used approach consist in the condensation of 1,3-diketones and amines (Figure 3.8a). This condensation reaction with release of water occurs spontaneously at room temperature.<sup>32</sup> Furthermore, the precursors are easily prepared in a one-step fashion from alcohols or amines in the case vinylogous urethanes and amides respectively.<sup>33,34</sup> A second approach uses a nucleophilic vinylogous substitution of 1-alkoxy-3-ones with amines with the release of an alcohol, which is reported to occur also at room temperature with near quantitative yields (Figure 3.8b).<sup>35</sup> Disadvantageous for this method is the preparation of these 1-alkoxy-3-ones, which can be yielded from 1,3-diketones and thus require an additional synthesis step. As an alternative to the previous two methods, which use a condensation reaction, a conjugated addition of amines to ynones has also been exploited for the synthesis of enaminoxones, with the feature that no low MW condensate is released (Figure 3.8c). Nevertheless, synthesis of these reactive ynones involves either expensive precursors such as propiolic acid<sup>36</sup>

or less scalable methods using for example organolithium compounds.<sup>37</sup> For this reason, the main focus of this PhD research exploited mostly the simple polycondensation of amines and 1,3-diones (Fig 8a).

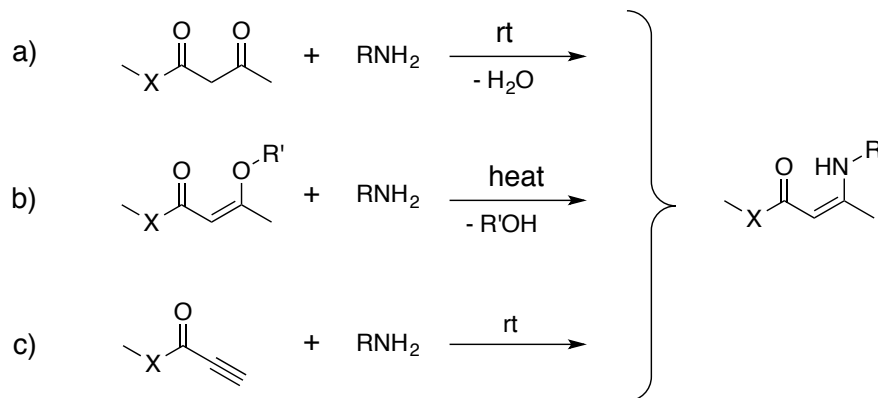


Figure 3.8: three possible synthetic approaches for enaminones. a) condensation of amines and 1,3-diones, b) vinylogous nucleophilic substitution of 1-alkoxy-3-ones with amines. c) conjugated addition of amines to ynones.

### 3.2 Kinetic study of amine exchange of enaminones

Before applying the amine exchange of enaminones for the synthesis of vitrimer materials, model studies on low molecular weight compounds were conducted to obtain a better understanding of the kinetics of the known – but hitherto not well-characterised - exchange reaction. In the absence of systematic kinetic data from the literature, this study will thus serve to focus and guide our design and understanding of enaminone vitrimers in the coming chapters.

In order to assess the kinetics of the amine exchange of enaminones, two model compounds of each class (*i.e.* vinylogous urea/urethanes/amides) were prepared in a fashion that they can be distinguished and quantified by either GC-FID or <sup>1</sup>H-NMR. This objective was achieved by preparing a butyl- and benzyl amine enaminone compounds. Due to the difference of the inductive effect between the alkyl and the phenyl group, a difference in chemical shift was expected, in particular of the protons besides the enaminone-NH (indicated with \* in Figure 3.9).

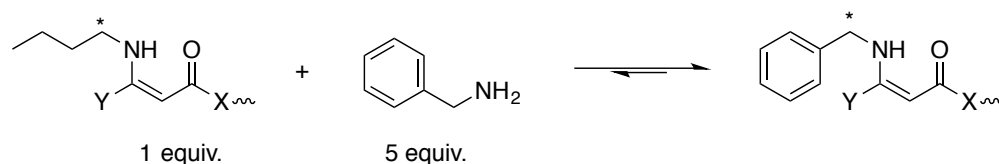


Figure 3.9: General approach used to assess the vinylogous transamination exchange kinetics.

In a typical experiment, the butyl compounds were mixed with a fivefold excess of benzyl amine to obtain a pseudo-first order reaction. In this manner, the backwards reaction of the released amine as well as the relative decrease in concentration of the reaction partner becomes negligible at low conversions. Furthermore, concentrations were chosen so that they were optimal for <sup>1</sup>H-NMR characterisation (approximately 10 mg in 0.65 mL) and aprotic apolar solvents such as benzene, toluene and xylene were used in order to mimic an apolar polymer matrix. For sake of comparison, the same concentrations were used for the different enamminones.

### 3.2.1 Vinylogous urethanes

N-butyl vinylogous urethane **1** and N-benzyl vinylogous urethane **3** were first prepared by simple condensation of propyl acetoacetate with butylamine and benzylamine, respectively (for the syntetic procedures, see section 3.5.6 p.70). Next, the butyl model compound **1** was mixed with five equivalents of benzylamine **2** in deuterated benzene (Figure 3.10). Aliquots of the resulting mixture were heated to 100, 120, and 140 °C, respectively and <sup>1</sup>H-NMR spectra were recorded at different time intervals for each sample. In this way, the amine exchange reaction could be easily followed by monitoring the well resolved signals of compounds **1** and **3**.



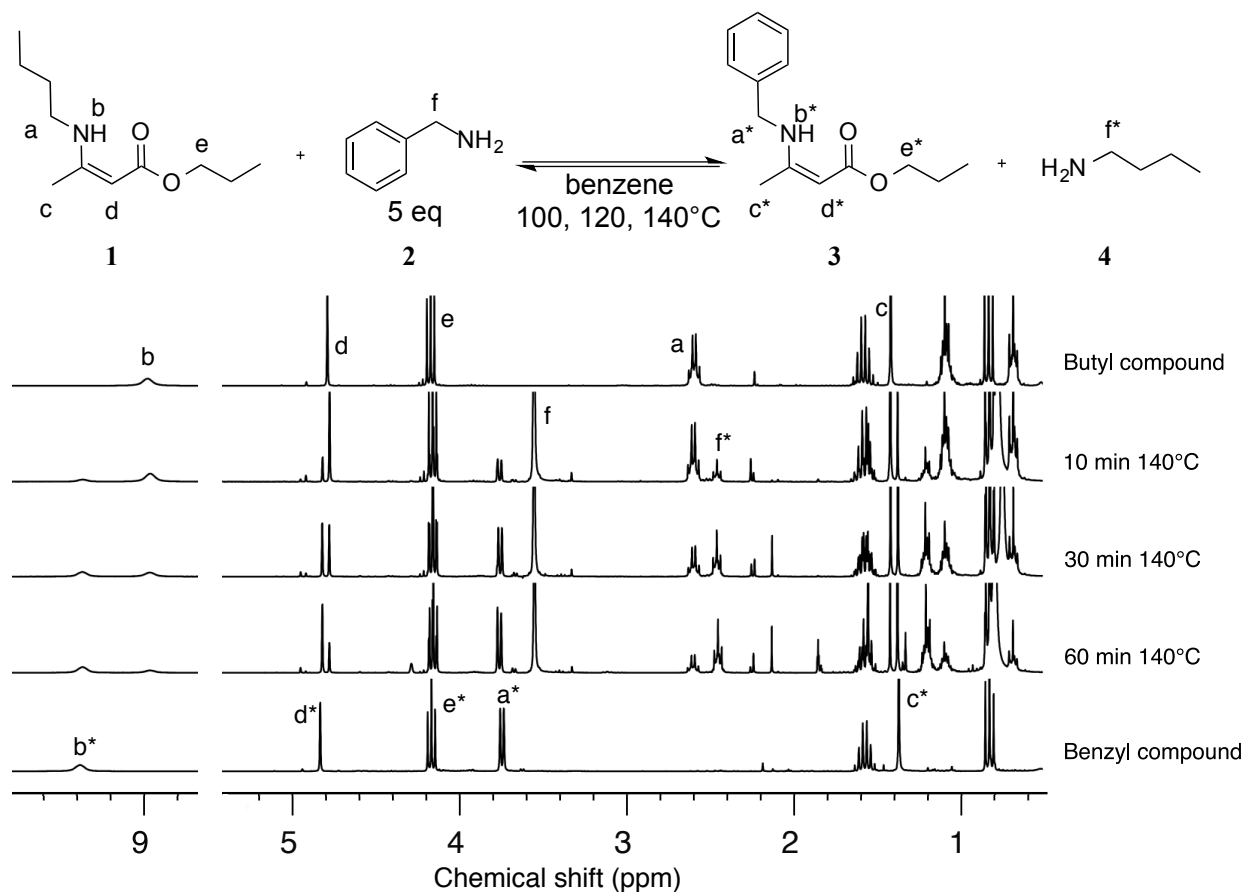


Figure 3.10. a) the butyl vinylogous urethane was mixed with five equivalents of benzylamine in deuterated benzene to examine the exchange kinetics. b) <sup>1</sup>H-NMR allows to follow the exchange reaction via the appearance of the well resolved signals of the benzyl-compound.

In Figure 3.11a, the remaining fraction of compound **1** is plotted against the reaction time. At low conversions, *i.e.* under pseudo-first order conditions, a linear decay is observed. At higher conversions, the reaction evolves slowly to a chemical equilibrium, as the backward reaction becomes more important. At 100°C, the reaction is rather slow with only 50% conversion observed after 175 minutes while the reaction becomes reasonably fast at 140°C as the equilibrium concentration is almost reached after 90 minutes.

To fit the decrease of the reactant as a function of time, equation 3.1 was used, which was designed to describe pseudo-first order reactions of isotope exchange reactions.<sup>38</sup> This equation takes the backward reaction at higher conversions into account and allows to obtain the rate constant via fitting.

$$[Reactant] = 1 - (x_{\infty} - \exp\left(\frac{-kt}{x_{\infty}}\right)) \quad (\text{Eq. 3.1})$$

When the obtained rate constants at different temperatures are plotted in an Arrhenius plot, an activation energy of  $(59 \pm 6)$  kJ mol<sup>-1</sup> was obtained via the slope of the fit. For comparison, this value is approximately 20 kJ mol<sup>-1</sup> lower than that of transesterification reactions catalysed by Zn(OAc)<sub>2</sub> or Sn(Oct)<sub>2</sub>.<sup>3,39</sup>

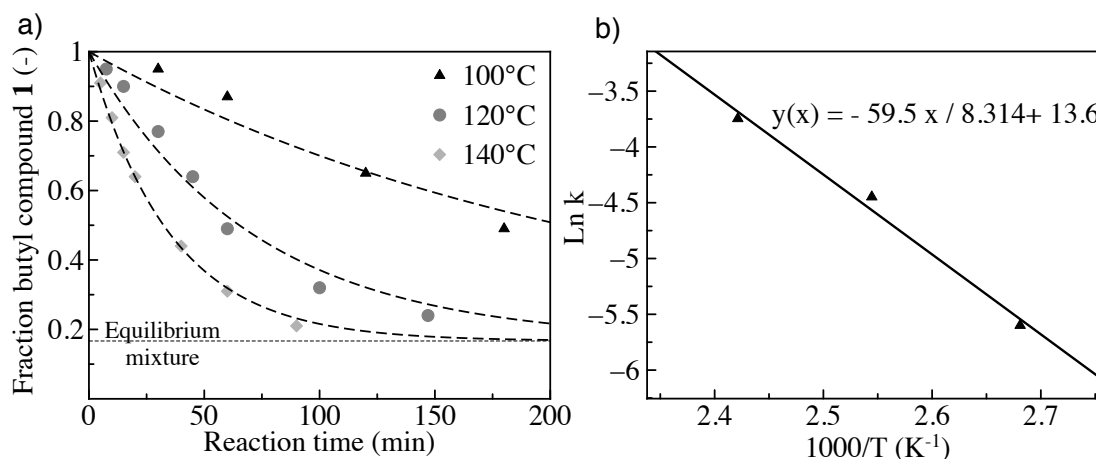


Figure 3.11. a) Disappearance, through exchange reactions, of the butyl compound 1 as a function of time for different temperatures. b) Calculation of the activation energy via determination of the slope in the Arrhenius plot.

The low-MW model *vinyllogous urethanes* (Vurethanes) were also used to verify the thermal stability of these groups under conditions that would mimic thermal treatment of a bulk material. Side reactions such as decomposition or the nucleophilic attack of an amine on the carbonyl group could result in deterioration of the material or irreversible cross-links, which would be detrimental for the envisaged material properties. Therefore, compound **3** was heated for 14h at 150°C in the presence of five equivalents benzylamine (Figure 3.12a). <sup>1</sup>H-NMR spectra of the initial mixture, the mixture after thermal treatment and the vinyllogous urea compound **5** that would be formed in case of the side reaction, were compared and showed no significant changes (Figure 3.12b). This observation indicates that the delocalisation of the free electron pair of the amino-group through the double bond, inhibits strongly the otherwise expected nucleophilic attack of amines on the ester subfunction present in a vinyllogous amine.<sup>40</sup>

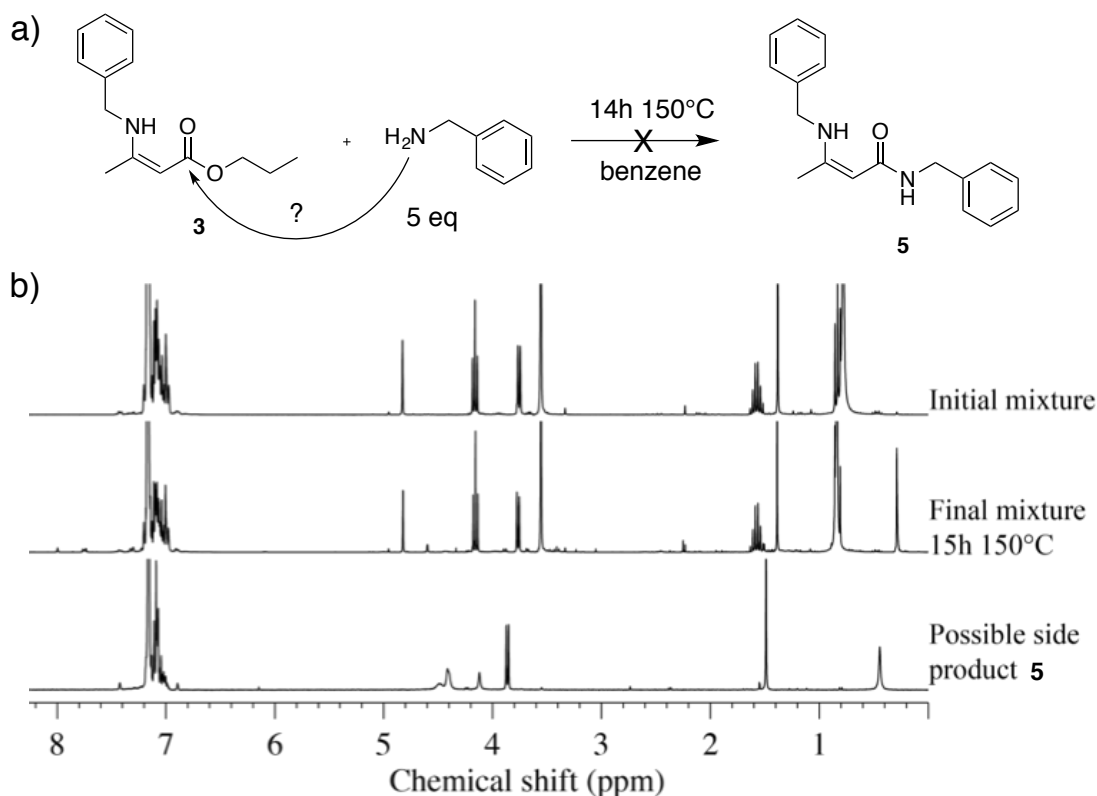


Figure 3.12. a) Control experiments to discard the occurrence of side reactions. b) <sup>1</sup>H-NMR spectra before and after thermal treatment and reference compound **5** for comparison.

### 3.2.2 Vinylogous urea

The amine exchange reactions on *vinylogous urea* (Vurea) bonds were examined using the same method as described above for vinylogous urethanes. Two different vinylogous urea bonds were examined (for the synthetic procedures, see section 3.5.1 starting at p.67) and they were later also found to show a markedly different thermal stability (*Cfr.* Chapter 6). Those two are Vurea prepared from primary amines and secondary amines, which we will refer to as respectively a primary Vurea and secondary Vurea. In stark contrast to Vurethanes, Vurea were found to show already fast exchange kinetics, even at room temperature. For example, primary Vurea reached exchange equilibrium after 30 minutes at 30°C (Figure 3.13a and b). Interestingly, the exchange kinetics of the primary Vurea were significantly faster than those of the secondary Vurea (Figure 3.13c and d). For instance, the amine exchange reaction at 20°C of the primary Vurea proceeded at about the same rate as the corresponding reaction of the secondary Vurea at 45°C. The activation energies of both Vureas were calculated as 54 (±6)

$\text{kJ mol}^{-1}$  and  $49 (\pm 1) \text{ kJ mol}^{-1}$  for the primary and secondary Vurea respectively. Remarkably, the activation energy of the faster primary Vureas is higher (albeit not significantly different), than those of the secondary Vurea. This observation indicates that some other factors should be included, which will be discussed in greater detail in section 3.3.

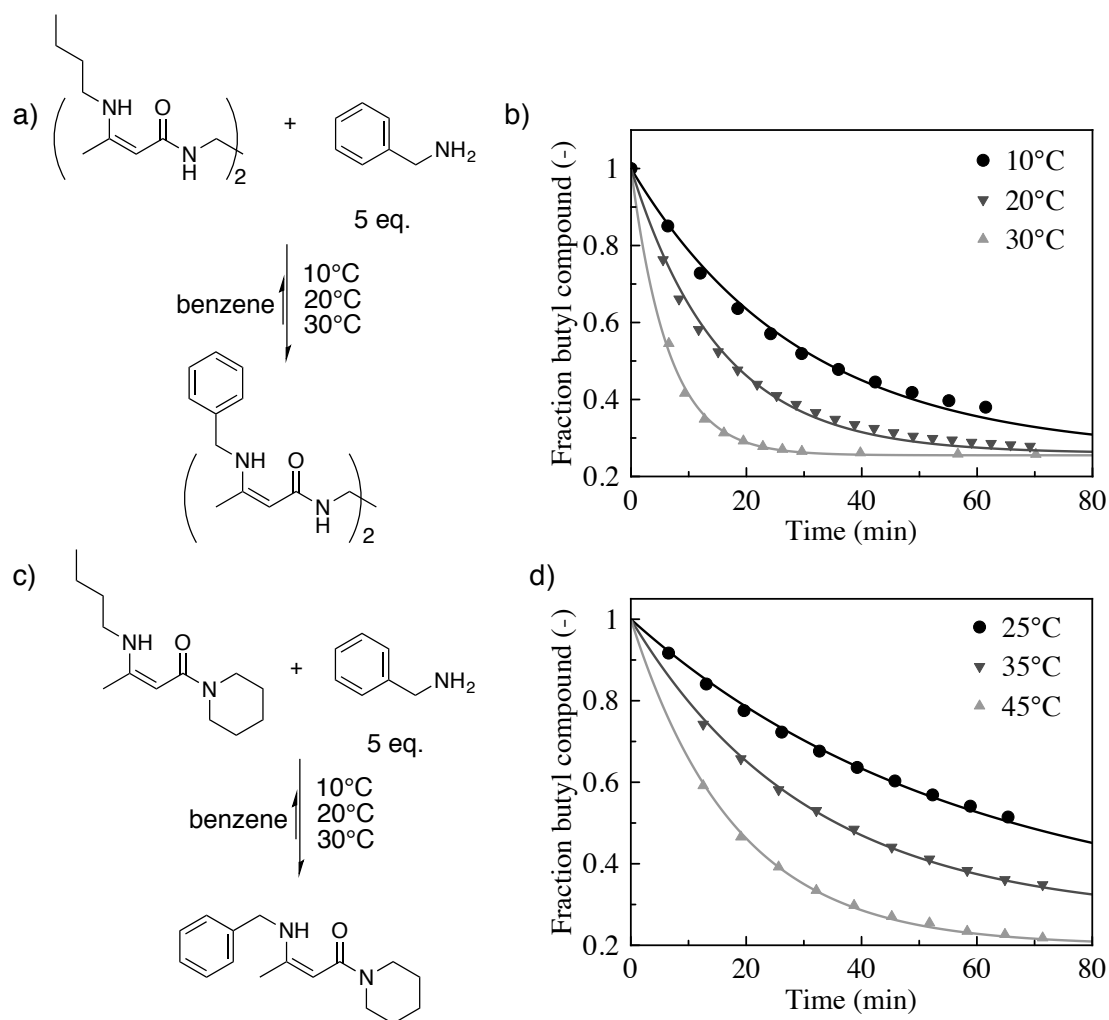


Figure 3.13. Model reaction and exchange kinetics for a and b) primary Vurea. c and d) secondary Vurea.

Nevertheless, the fast exchange, combined with the additional rigidity of urea-alike bonds, and possibility to form H-bonds for the primary Vurea makes these Vurea very interesting for vitrimer materials with high  $T_g$ 's.

### 3.2.3 Vinylogous amides

Next, vinylogous amides (Vamides) were examined (for the synthetic procedures, see section 3.5.8 p.71). These moieties showed much slower exchange kinetics compared to the former two classes, even at much higher temperatures. Although the experimental activation energy of  $(38 \pm 3) \text{ kJ mol}^{-1}$  was found to be significant lower, the macroscopic relaxation times were found to be considerably longer and the exchange reaction requires much higher temperatures. This difference is indicative of a very different reactivity of Vamides compared to Vurethanes and Vureas. These results imply that a change in temperature has a lower impact on the exchange kinetics and that this exchange could progress via another pathway.

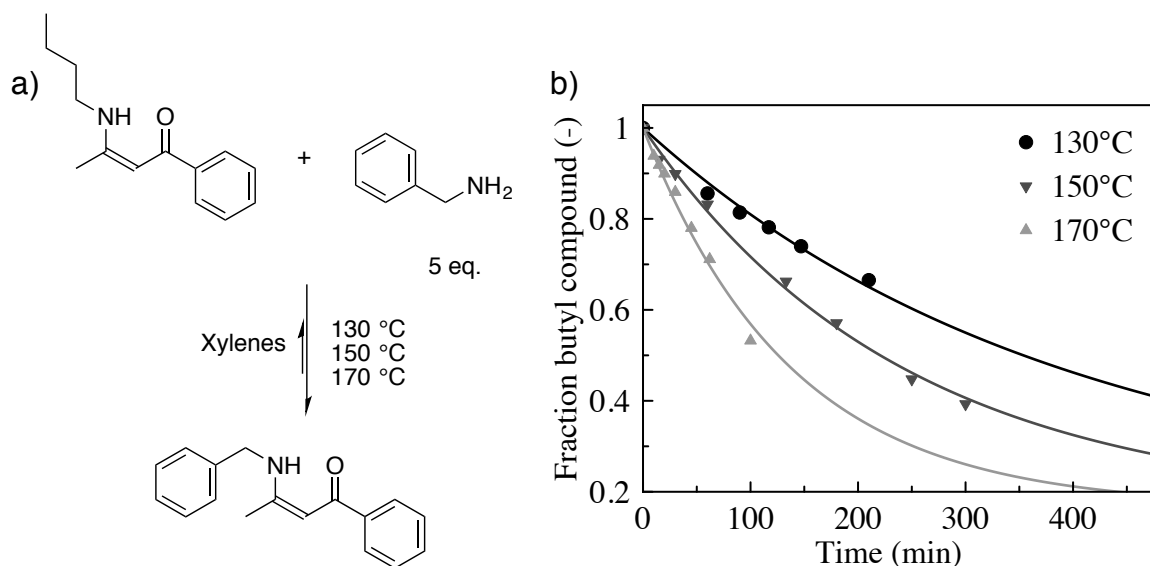


Figure 3.14. a) model compounds used for vinylogous amides. b) exchange kinetics of vinylogous amides.

Finally, also the kinetics of a differently substituted Vamide (Figure 3.15) was explored. These alternative substrates resulted from our efforts to prepare enaminoxones from conjugated ynones through direct addition of amines rather than condensation of diketones. As can be expected from the stabilisation of these substrates through conjugation with the additional phenyl ring, the amine exchange reaction turned out to be even slower, with only a 6% observed conversion after 120 minutes at 170 °C. Hence no kinetic study was performed in greater detail.

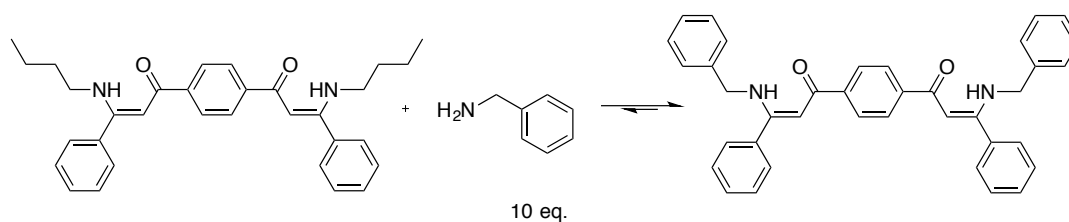


Figure 3.15: Model reaction for the examination of vinylogous amide transamination

### 3.3 Rationalisation of the difference in exchange rate for enaminones

From the kinetic studies above, it can be concluded that vinylogous transamination rates of enaminones vary strongly with the nature of the X-group bonded directly to the carbonyl group. The relative order of the exchange rate of the different enaminones is shown in Figure 3.16. While Vurea showed already fast exchange at room temperature, Vurethanes needed heating and only became fast from 100°C on. Vamides on the other hand required even higher temperatures up to 170°C to undergo transamination reactions in a reasonable timeframe.

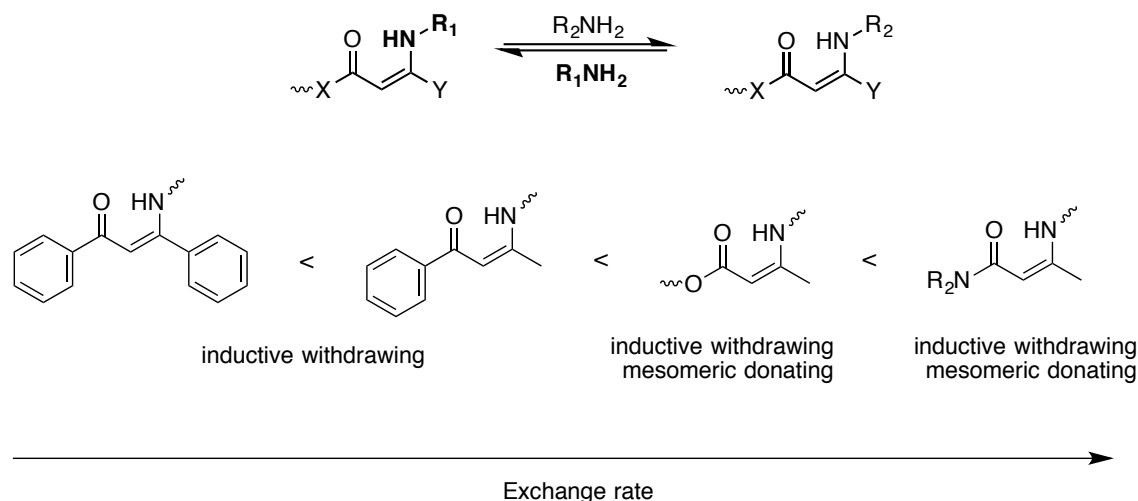


Figure 3.16: relative order of the exchange rate for the different enaminones.

To explain these marked differences in exchange rates, a hypothesis can be postulated based on the most probable exchange mechanisms. Outlined in Figure 3.17, two possible scenarios are proposed.

In the first pathway (Figure 3.17a), also our hypothesis used for the design of the kinetics experiments, a direct Michael addition of an amine occurs with the formation of a zwitterionic intermediate, which can be directly stabilized to an enol form through an internal proton shift. This mechanism should be hindered by the more electron donating X-groups as they destabilise the oxyanion in the intermediate, leading to a prediction of reactivity opposite to that observed experimentally.

Due to this discrepancy, a second pathway was considered (Figure 3.17b), in which the enaminone is in equilibrium with its protonated iminium form in an acid-base equilibrium. The relative basicity of the enaminone moiety will critically depend on the electron withdrawing nature of the carbonyl. The source of the acidic proton can be either from residual water or from another enaminone NH. Given the strong electrophilic nature of this iminium intermediate, the attack of the amine should take place very rapidly, with the formation of a protonated aminal. After proton exchange, the other amine is expelled and the reaction progresses back to its enaminone form. The protonation of the enaminone is probably strongly endothermic (and a major contributor in the activation energy) and there is indeed a clear correlation between the expected basicity of the enaminone and its observed amine exchange rate.

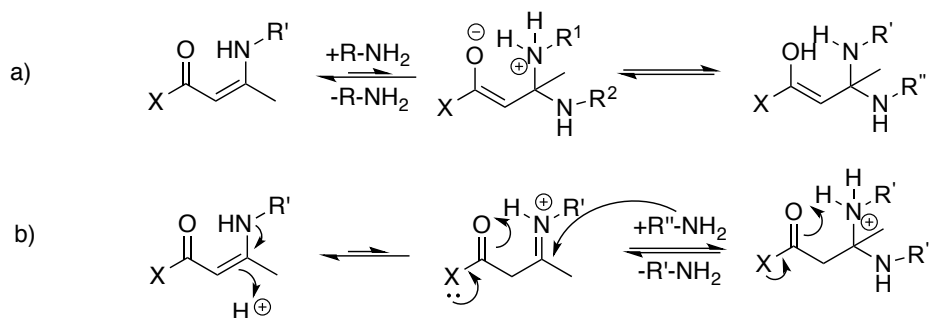
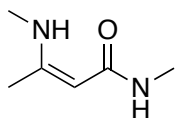
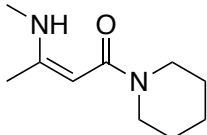
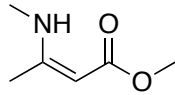
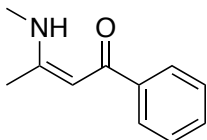
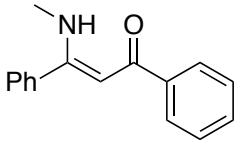


Figure 3.17: Transamination mechanism via a) direct Michael Addition resulting in a zwitter-ionic intermediate. b) attack of the amine on an iminium intermediate.

In Table 3.1, the different enaminones are listed from fast exchange to slow exchange together with their kinetic parameters. It can be observed that the activation energies do not follow the expected trend. In particular, for the much slower Vamides, a lower activation energy was obtained in our experimental set-up. In light of the above discussion and the hypothesis that VU amine exchange progresses via an iminium intermediate rather than via direct Michael addition, these observations are not so surprising. The equilibrium between the enaminone and the iminium intermediate will have a large influence on the activation energy,

which depends on the basicity of the enaminone-moiety and the concentration of protons from other sources such as traces of water. As these influences were not accounted for in the present kinetic studies, additional experiments were conducted.

Table 3.1: Kinetic parameters for the different enamines

Structure	$E_a$ (kJ mol <sup>-1</sup> )	Rate constant $k / T$ (s <sup>-1</sup> ) / °C	T range (°C)
 1° Vurea	54 ± 6	4.2 x 10 <sup>-4</sup> / 10 8.0 x 10 <sup>-4</sup> / 20 2.0 x 10 <sup>-5</sup> / 30	10 - 30
 2° Vurea	49 ± 1	2.1 x 10 <sup>-4</sup> / 25 3.9 x 10 <sup>-4</sup> / 35 7.4 x 10 <sup>-4</sup> / 45	25 - 45
 Vurethane	59 ± 6	6.2 x 10 <sup>-5</sup> / 100 2.0 x 10 <sup>-4</sup> / 120 3.9 x 10 <sup>-4</sup> / 140	100 - 140
 Vamide	38 ± 3	3.6 x 10 <sup>-5</sup> / 130 5.8 x 10 <sup>-5</sup> / 150 1.0 x 10 <sup>-4</sup> / 170	130 - 170
 Vamide	/	1.4 x 10 <sup>-5</sup> / 170	170 and higher

In order to elaborate more on the hypothesis of the importance of protonated species and their influence on the activation energy, the amine exchange of Vurethanes and Vamides was studied in the presence of 5 mol% *p*-toluene sulfonic acid (Figure 3.18a). In this way, a constant concentration of protonated species was obtained, which should result in a better representation of the relative reactivity rather than one that possibly depends on small influences of the



environment. Vureas were not investigated in presence of acid as an even faster exchange rate would be hard to follow.

As depicted in Figure 3.18b, the rate of exchange of Vurethanes is increased strongly since the reaction rate at 60°C in presence of acid equals approximately the exchange rate at 100°C in absence of any added acid. Similarly, also Vamides exhibited faster exchange (Figure 18c). These results indicate that protonated species are indeed important during the amine exchange of enaminones. Similar to previous findings, the amine exchange of Vurethanes remains faster than Vamides, which is in agreement with the assumption that the reaction progresses via an iminium intermediate.

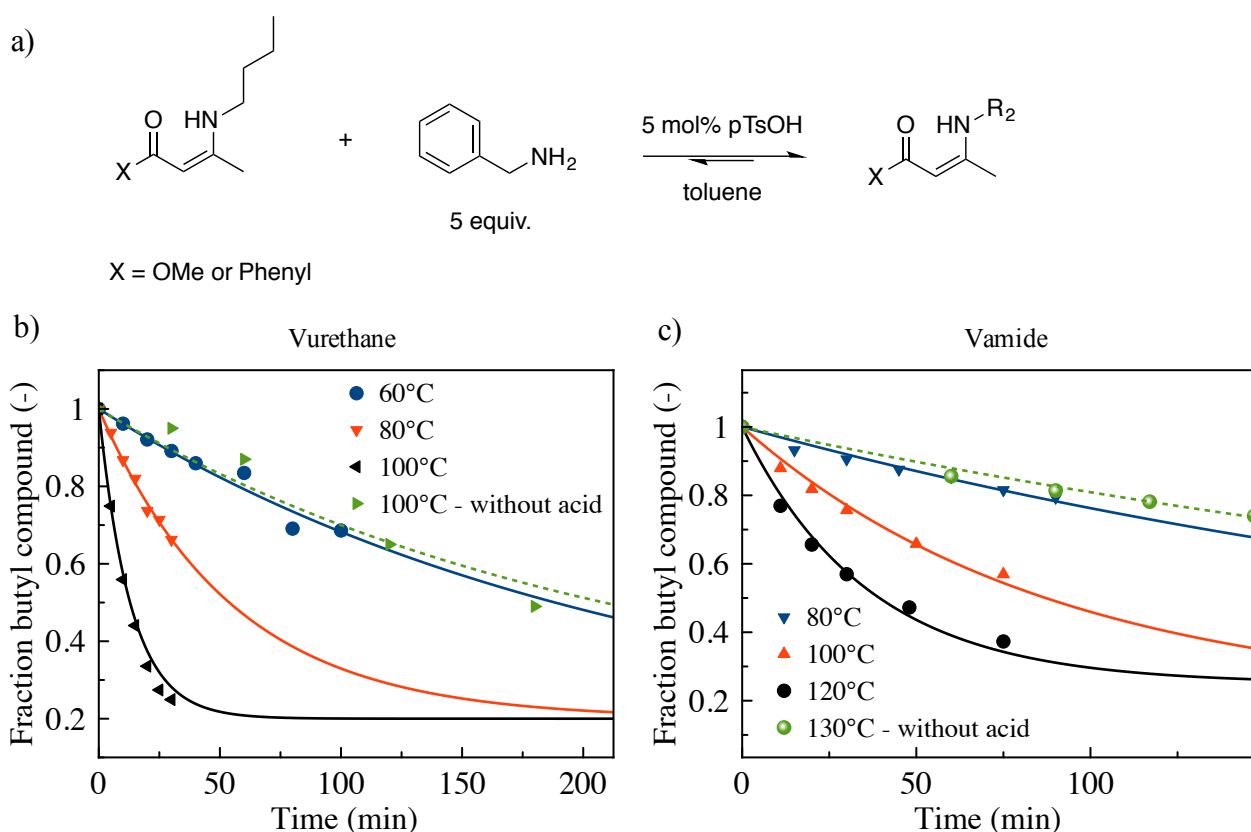
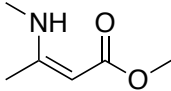
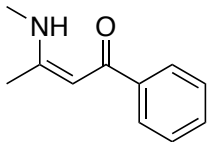


Figure 3.18: a) Model reaction in presence of acid and kinetics for b) Vurethanes and c) Vamides.

In Table 2, the calculated activation energies in the presence of acid are shown. Although the reaction goes faster, both values are higher albeit not significant for the Vurethanes. Most likely, the same mechanistic pathway is followed but due to the increased proton concentration, more iminium molecules are present resulting in a faster reaction. The reason why the Vamides are slower but do not show a higher activation energy than Vurea and Vurethanes remains unknown. As the

focus of this thesis was situated on the material level, no additional efforts were made.

Table 3.2: Activation energy and rate constants obtained for amine exchange of Vurethanes and Vamides in the presence of acid.

Structure	$E_a$ (kJ mol <sup>-1</sup> )	Rate constant $k / T$ (s <sup>-1</sup> ) / °C	T range (°C)
	$70 \pm 5$	$6.5 \times 10^{-5} / 60$ $2.4 \times 10^{-4} / 80$ $1.0 \times 10^{-3} / 100$	60 - 100
	$56 \pm 5$	$3.6 \times 10^{-5} / 80$ $5.8 \times 10^{-5} / 100$ $1.0 \times 10^{-4} / 120$	80 - 120

### 3.4 Conclusion

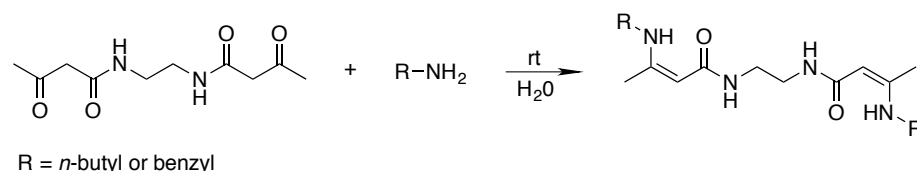
In this chapter, an introduction to the chemistry of enaminones was presented, starting with a short discussion on their synthesis and use in polymer chemistry. Next, model compound studies that were performed in this work on different enaminones are described to assess the kinetics of vinylogous transamination. This qualitative and quantitative study showed that the vinylogous transamination of enaminones spans over a very wide practical temperature window, ranging from rapid room temperature exchanges for Vurea to temperatures as high as 170°C for substituted Vamides. A rationalisation of these differences was presented and two possible exchange mechanism were provided. Activation energies were calculated from the available data, but these seem to imply a more complicated reaction mechanism that both depends on the nature of the X-group bonded to the enaminone moiety and the concentration of protonated species.

In general, based on these results, Vurea and Vurethanes are considered as most interesting since they show swift exchange kinetics at room temperature (Vurea) or around 100°C (Vurethanes) that would enable fast processing. In addition,

Vurea and Vurethane building blocks are readily prepared in a scalable manner. Therefore, this chapter served and guided our design for vitrimer materials and will also help to predict and understand the results in following chapters.

## 3.5 Experimental

### 3.5.1 Synthesis of N,N'-(ethane-1,2-diyl)bis(3-(butylamino)but-2-enamide) and N,N'-(ethane-1,2-diyl)bis(3-(benzylamino)but-2-enamide)



N,N'-(ethane-1,2-diyl)bis(3-oxobutanamide) (1 equiv., 1 g) and butylamine (2 equiv.) or benzylamine (2 equiv.) were mixed in 20 mL water and stirred for 6h at room temperature. The white precipitate was filtered, washed with water (3x10 mL) and dried *in vacuo* yielding N,N'-(ethane-1,2-diyl)bis(3-(butylamino)but-2-enamide) or the corresponding N,N'-(ethane-1,2-diyl)bis(3-(benzylamino)but-2-enamide) both as a white powder.

Yield N,N'-(ethane-1,2-diyl)bis(3-(butylamino)but-2-enamide): 95%

$^1\text{H}$  NMR (300 MHz, benzene- $\text{d}_6$ )  $\delta$  (ppm) = 9.55 (br s, 2H, 2x  $\text{NHCH=}$ ), 5.47 (br s, 2H, 2x  $\text{NHCO}$ ), 4.28 (s, 2H, 2x  $\text{CH=}$ ), 3.32 (4H, br s,  $-\text{NHCH}_2\text{CH}_2\text{NH}-$ ), 2.72 (4H, app. q,  $J \cong 6.4$  Hz, 2x  $-\text{CH}_2\text{CH}_2\text{NHC=}$ ), 1.52 (6H, s,  $\text{CH}_3\text{C=}$ ), 1.19 (band, 8H,  $-\text{CH}_2-$ ), 0.73 (t,  $J=7.2$  Hz, 6H,  $\text{CH}_3\text{-CH}_2-$ )

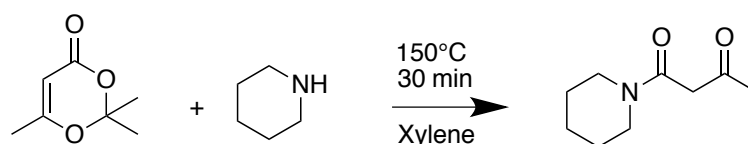
Yield N,N'-(ethane-1,2-diyl)bis(3-(benzylamino)but-2-enamide): 93%

$^1\text{H}$  NMR (300 MHz, benzene- $\text{d}_6$ ):  $\delta$  (ppm) = 10.00 (br s, 2H, 2x  $\text{NHCH=}$ ), 7.08-5.98 (band, 8H,  $\text{CH}_{\text{ar}}$ ), 5.23 (br s, 2H, 2x  $\text{NHCO}$ ), 4.24 (s, 2H, 2x  $\text{CH=}$ ), 3.86 (d,  $J=6.68$ , 4H,  $\text{PhCH}_2\text{NH}-$ ), 3.27 (br s, 4H,  $-\text{NHCH}_2\text{CH}_2\text{NH}-$ ), 1.44 (s, 6H,  $\text{CH}_3\text{C=}$ )

### 3.5.2 Kinetics exchange reaction N,N'-(ethane-1,2-diyl)bis(3-(butylamino)but-2-enamide and benzylamine

Benzylamine (0.25 mmol, 26 mg) was added to a solution of N,N'-(ethane-1,2-diyl)bis(3-(butylamino)but-2-enamide (0.05 mmol, 8.15 mg) *i.e.* the N-butyl vinylogous urea model compound in benzene-d<sub>6</sub> (0.79 mL). Five equivalents of benzylamine versus the vinylogous urea groups were used to obtain a pseudo-first order reaction at low conversions. The mixture was kept at 10°C, 20°C and 30°C in a NMR-tube and spectra were taken on-line at different time intervals. The reaction was followed by integration of the apparent quadruplet signal at 2.72 ppm of the butyl compound and the triplet signal at 3.86 ppm of the benzyl compound.

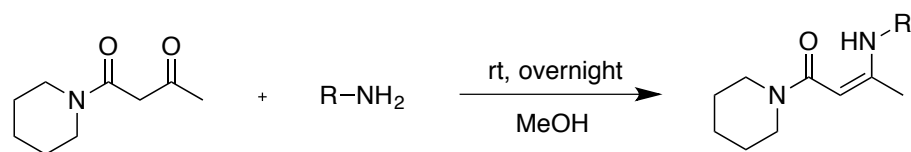
### 3.5.3 Synthesis of 1-(3-oxobutanoyl) piperidine



2,2,6-Trimethyl-4H-1,3-dioxin-4-one (1 equiv., 5.0 g) and piperidine (1.1 equiv., 3.29 g) were mixed in 7 mL xylene and heated for 30 min at 150°C in a preheated oil bath. The solvent, excess piperidine and released acetone were removed *in vacuo* yielding the desired product as a viscous oil (yield = 99%).

<sup>1</sup>H NMR (300MHz, CDCl<sub>3</sub>) δ (ppm) = 3.48–3.26 (band, 6 H), 2.4–2.75 (band, 6H), 2.19 (s, 3H). In accordance with the product prepared by Shridharan et al.<sup>41</sup>

### 3.5.4 Synthesis of 3-(butylamino)-1-(piperidin-1-yl)but-2-en-1-one and 3-(benzylamino)-1-(piperidin-1-yl)but-2-en-1-one



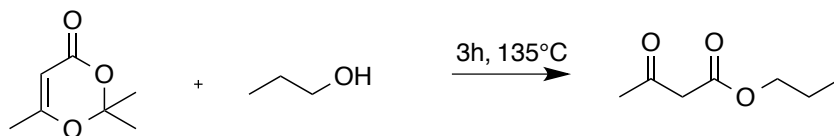
R = *n*-butyl or benzyl

Piperidine acetoacetamide (1 equiv., 1g) and butylamine (1.5 equiv., 0.646 g) or benzylamine (1 equiv., 0.633 g) were mixed in 5 mL MeOH and stirred overnight. The solvent was removed in vacuo and the mixture was extracted twice with DCM/water. The combined organic phases were dried with  $\text{MgSO}_4$ , filtered and the solvent was evaporated yielding the desired product as a viscous oil.

Yield 3-(butylamino)-1-(piperidin-1-yl)but-2-en-1-one: 93%.  $^1\text{H}$  NMR (300MHz,  $\text{CDCl}_3$ )  $\delta$  (ppm) = 9.52 (br s, 1H, NH), 4.50 (s, 1H, =CH), 3.45 (t,  $J=5.3$  Hz, 4H,  $\text{NCH}_2$ ), 3.18 (txd,  $J=7.0$  and 5.9 Hz, 2H,  $-\text{NH}-\text{CH}_2$ ), 1.92 (s, 3H,  $\text{CH}_3\text{C}=\text{CH}_2$ ), 1.60-1.51 (band, 8H, 2 x ring  $\text{CH}_2$  +  $\text{CH}_3\text{CH}_2\text{CH}_2\text{CH}_2\text{NH}$ ), 1.42 (m, 2H, ring  $\text{CH}_2$ ), 0.93 (t,  $J = 7.2$  Hz, 3H,  $\text{CH}_3\text{CH}_2$ ).  $^{13}\text{C}$  NMR (75Mhz,  $\text{CDCl}_3$ )  $\delta$  (ppm) = 169.9 (C), 159.6 (C), 80.6 (CH), 47.8 ( $\text{CH}_2$ ), 42.2 ( $\text{CH}_2$ ), 32.6 ( $\text{CH}_2$ ), 26.1 ( $\text{CH}_2$ ), 24.9 ( $\text{CH}_2$ ), 20.1 ( $\text{CH}_2$ ), 20.0 ( $\text{CH}_3$ ), 13.8 ( $\text{CH}_3$ ).  $\text{C}_{13}\text{H}_{25}\text{N}_2\text{O}^+$  (225.2 g/mol),  $m/z$ (ESI-MS): 225.3

Yield 3-(benzylamino)-1-(piperidin-1-yl)but-2-en-1-one: 91%.  $^1\text{H}$  NMR (300MHz,  $\text{CDCl}_3$ )  $\delta$ (ppm) = 9.95 (br s, 1H), 7.22-7.37 (5H, band), 4.72 (1H, d,  $J = 0.6$  Hz), 4.42 (d, 2H,  $J = 6.45$  Hz), 3.48 (t, 4H,  $J = 5.23$  Hz), 1.92 (d, 3H,  $J = 0.6$  Hz), 1.54 – 1.68 (band, 6H).

### 3.5.5 Synthesis of propyl acetoacetate

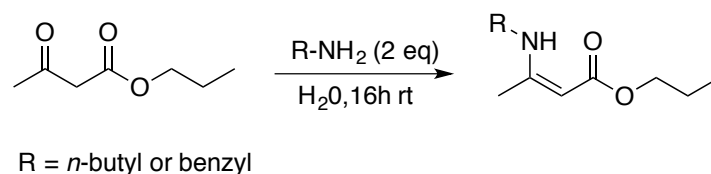


2,2,6-Trimethyl-4*H*-1,3-dioxin-4-one (5.38 g, 34 mmol) and 1-propanol (10 mL) were mixed in a pressure tube and heated for 3h at 135°C. After the reaction was

finished according to TLC, the excess of 1-propanol was removed *in vacuo* yielding pure propyl acetoacetate (yield: 98%).

$^1\text{H}$  NMR (300 MHz,  $\text{CDCl}_3$ ):  $\delta$  (ppm) = 4.10 (t,  $J = 6.5$  Hz, 2H), 3.45 (s, 2H), 2.27 (s, 3H), 1.63 (m, 2H), 0.94 (t,  $J = 6.5$  Hz, 3H). In accordance with <sup>42</sup>.

### 3.5.6 Synthesis of propyl-3-(butylamino)but-2-enoate and propyl-3-(benzylamino) but-2-enoate



Propyl acetoacetate (0.250 g, 1.73 mmol) and butyl- or benzylamine (2 eq, 3.47 mmol) were dissolved in 5 mL methanol and stirred overnight. When the enaminone formation was complete (TLC), the solvent was removed and the mixture was extracted twice with brine and  $\text{CH}_2\text{Cl}_2$ . The combined organic phases were dried with  $\text{MgSO}_4$  and evaporated, yielding the desired product. The obtained product was purified by flash chromatography using EtOAc/hexane (25/75).

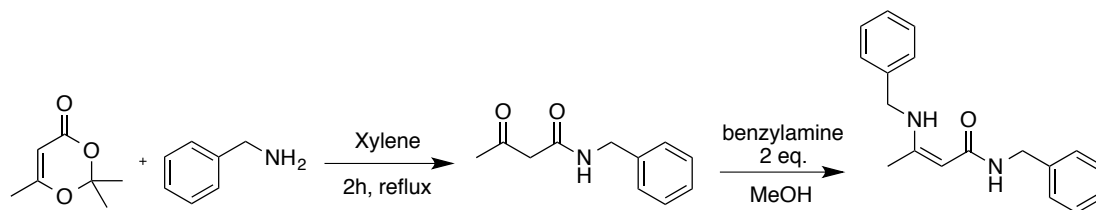
Yield propyl-3-(butylamino)but-2-enoate: 92%, 0.317 g

$^1\text{H}$  NMR (300 MHz,  $\text{CDCl}_3$ ):  $\delta$  (ppm) = 8.55 (s, 1H), 4.44 (s, 1H), 3.98 (t,  $J = 6.77$  Hz, 2H), 3.20 (q,  $J = 6.52$  Hz, 2H), 1.91 (s, 3H), 1.65 – 1.39 (band, 7H), 0.94 (t,  $J = 7.37$  Hz, 6H).  $^{13}\text{C}$  NMR(125Mhz,  $\text{CDCl}_3$ )  $\delta$  (ppm) = 170.8 (C), 161.9 (C), 81.7 (CH), 64.0 ( $\text{CH}_2$ ), 42.7 ( $\text{CH}_2$ ), 32.4 ( $\text{CH}_2$ ), 22.4 ( $\text{CH}_2$ ), 20.0 ( $\text{CH}_2$ ), 19.4 ( $\text{CH}_3$ ), 13.9 ( $\text{CH}_3$ ), 10.5 ( $\text{CH}_3$ ).  $\text{C}_{11}\text{H}_{22}\text{NO}_2^+$ (200.17 g/mol),  $m/z$ (ESI-MS): 200.2

Yield benzyl-3-(butylamino)but-2-enoate: 94%, 0.379 g

$^1\text{H}$  NMR (300 MHz,  $\text{CDCl}_3$ ):  $\delta$  (ppm) = 8.96 (s, 1H, NH), 7.39 – 7.27 (m, 5H, ArH), 4.56 (s, 1H,  $-\text{CO}-\text{CH}=\text{}$ ), 4.45 (d,  $J = 6.36$ , 2H,  $\text{PhCH}_2\text{NH}-$ ), 4.02 (t,  $J = 6.76$ , 2H,  $-\text{OCH}_2\text{CH}_2-$ ), 1.93 (s, 3H,  $\text{CH}_3\text{C}=\text{}$ ), 1.65 (m, 2H,  $\text{CH}_3\text{CH}_2-$ ), 0.96 (t,  $J=7.42$ , 3H,  $\text{CH}_3-\text{CH}_2-$ ).  $^{13}\text{C}$  NMR(125Mhz,  $\text{CDCl}_3$ )  $\delta$  (ppm) = 170.7 (C), 161.8 (C), 138.7 (C), 128.7 (CH), 127.3 (CH), 126.7 (CH), 83.2 (CH), 64.7 ( $\text{CH}_2$ ), 46.8 ( $\text{CH}_2$ ), 22.4 ( $\text{CH}_2$ ), 19.4 ( $\text{CH}_3$ ).  $\text{C}_{14}\text{H}_{20}\text{NO}_2^+$ (234.32 g/mol),  $m/z$ (ESI-MS): 234.2

### 3.5.7 N-benzyl-3-(benzylamino)but-2-enamide

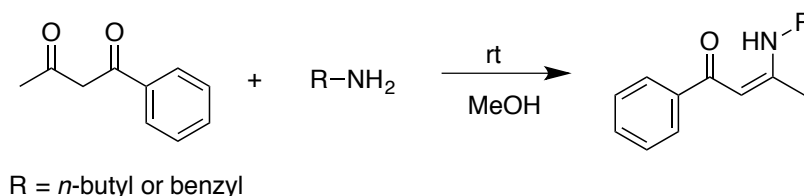


A solution of 2,2,6-trimethyl-4*H*-1,3-dioxin-4-one (0.5 g, 3.52 mmol) and benzylamine (1.13 g, 10.5 mmol) in 1.5 mL xylene was refluxed for 2h. When the conversion of the starting product was complete (TLC), the solvent was removed. The obtained mixture consists of mainly *N,N*-benzylacetamide and a small amount of *N*-benzyl-3-(benzylamino)but-2-enamide according to <sup>1</sup>H-NMR. This mixture was dissolved in 10 mL MeOH and benzylamine (0.75 g, 7.04 mmol) was added. The mixture was stirred at room temperature over the weekend resulting in a white suspension. This suspension was poured in 25 mL and the white precipitate was filtered off, washed with water and dried to obtain *N*-benzyl-3-(benzylamino)but-2-enamide.

Yield: 85%, 0.83 g

<sup>1</sup>H NMR (300 MHz, CDCl<sub>3</sub>): δ (ppm) = 9.53 (s, 1H), 7.38 – 7.24 (band, 10H), 4.47 – 4.39 (band, 5H), 1.89 (s, 3H). <sup>13</sup>C NMR (125 MHz, CDCl<sub>3</sub>): δ (ppm) = 139.4 (C), 128.7 (CH), 128.6 (CH), 127.1 (CH), 126.7 (CH), 85.5 (CH), 46.6 (CH<sub>2</sub>), 43.5 (CH<sub>2</sub>), 19.4 (CH<sub>3</sub>). C<sub>18</sub>H<sub>21</sub>N<sub>2</sub>O<sup>+</sup> (281.3 g/mol). *m/z*(ESI-MS): 281.2

### 3.5.8 Synthesis of 3-(benzylamino)-1-phenylbut-2-en-1-one and 3-(butylamino)-1-phenylbut-2-en-1-one



Benzoyl acetone (1.5 g, 9.25 mmol) and butylamine (1.83 mL, 18.5 mmol) or benzyl amine (2 mL, 18.5 mmol) were mixed in 10 mL MeOH and stirred overnight at room temperature after which full conversion was observed with TLC (rf = 0.36 EtOAc/hept 20/80). The solvent was removed *in vacuo* and filtered over a short column of silica to remove the excess of amine.

Yield 3-(benzylamino)-1-phenylbut-2-en-1-one: 81%

$^1\text{H}$  NMR (300 MHz,  $\text{CDCl}_3$ ):  $^1\text{H}$  NMR (400 MHz,  $\text{CDCl}_3$ ):  $\delta(\text{ppm}) = 11.75$  (s, 1H), 7.98 - 7.75 (m, 2H), 7.51-7.16 (m, 8H), 5.75 (s, 1H), 4.54 (d,  $J = 6.3$  Hz, 2H), 2.07 (s, 3H). In agreement with <sup>43</sup>.

Yield 3-(butylamino)-1-phenylbut-2-en-1-one: 83%

$^1\text{H}$  NMR (300 MHz,  $\text{CDCl}_3$ ):  $\delta$  (ppm) = 11.5 (br s, 1H), 7.90-7.86 (band, 2H), 7.43-7.40 (band, 3H), 5.58 (s, 1H), 3.34 (td,  $J=6.89$ ; 5.92 Hz), 2.09(s, 3H), 1.71-1.62 (m, 3H), 1.52-1.44 (m, 2H), 0.98 (t,  $J=7.27$  Hz, 3H). In agreement with <sup>43</sup>.

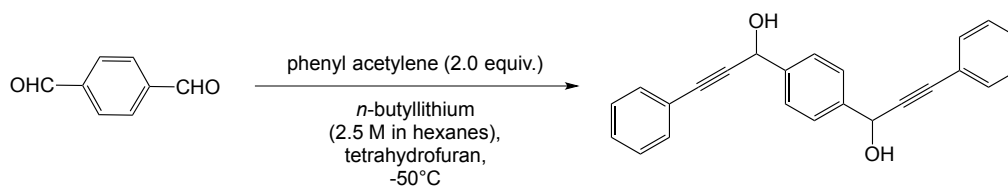
### 3.5.9 Kinetics exchange reaction 3-(butylamino)-1-phenylbut-2-en-1-one and benzylamine

Benzylamine (2.3 mmol, 246 mg) was added to a solution of 3-(butylamino)-1-phenylbut-2-en-1-one i.e. the *N*-butyl vinylogous amide model compound (0.46 mmol, 100 mg) in xylenes (7.54 mL). Five equivalents of benzylamine versus the vinylogous amide groups were used to obtain a pseudo-first order reaction at low conversions. The mixture was kept at 130°C, 150°C and 170°C in a pressure-tube and GC analysis was performed different time intervals. The reaction was followed by integration of the FID-signals at 6.7 min and at 7.45 min for the butyl- and benzyl model compound respectively. The integrated signals were corrected using a calibration curve for both compounds to take a different molar response factor in account. GC was performed on an Agilent 7890A system equipped with a VWR Carrier-160 hydrogen generator and an Agilent HP-5 column of 30 m length and 0.320 mm diameter. A FID detector was used and the inlet was set to 250°C with a split injection of ratio 25:1. Hydrogen was used as carrier gas at a flow rate of 2 mL/min. The oven temperature was increased with 20°C/min from 50°C to 120°C, followed by a ramp of 50°C/min. to 300°C and 5 min isothermal at 300°C.



### 3.5.10 Synthesis of 1,1'-(1,4-phenylene)bis(3-phenylprop-2-yn-1-one)

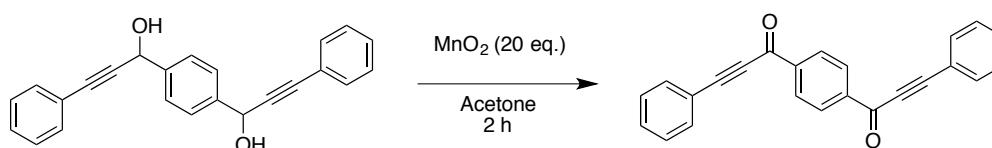
#### a) 1,1'-(1,4-phenylene)bis(3-phenylprop-2-yn-1-ol)



A solution of phenyl acetylene (11.2 mL, 100 mmol) in anhydrous tetrahydrofuran was first cooled down to  $-50^{\circ}\text{C}$  while maintaining under inert atmosphere. After 5 min, a solution of terephthalaldehyde (6.5 g, 47.6 mmol) in anhydrous tetrahydrofuran (100 mL) was added while keeping the solution temperature at  $-50^{\circ}\text{C}$ . Stirring was continued for 1 hour with the temperature steadily increasing to  $0^{\circ}\text{C}$ . After one hour the reaction was worked up with an aqueous saturated ammonium chloride solution (50 mL) dissolving again all solids. Then, the bulk tetrahydrofuran was removed *in vacuo* and the obtained aqueous phase was combined with diethylether (400 mL). The organic phase was separated, washed with brine (10 mL), dried over magnesium sulphate, filtered over a pad of cotton and concentrated under reduced pressure giving 1,1'-(1,4-phenylene)bis(3-phenylprop-2-yn-1-ol) as a white precipitate (13.82 g, 86%).

$^1\text{H-NMR}$  (300 MHz,  $\text{CDCl}_3$ )  $\delta$  (ppm) = 7.68 (s (br.), 4 H,  $\text{CH}_{\text{Ar, centre}}$ ), 7.52-7.47 (band, 4H,  $\text{CH}_{\text{Ar}}$ ), 7.37-7.32 (band, 6H,  $\text{CH}_{\text{Ar}}$ )

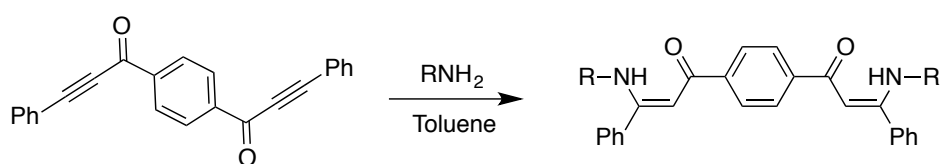
#### b) Oxidation with manganese(IV) oxide



To a solution of 1,1'-(1,4-phenylene)bis(3-phenylprop-2-yn-1-ol) (13.82 g, 40.9 mmol, 1.0 equiv.) in acetone (400 mL) was added all at once solid manganese(IV) oxide (57.6 g, 818 mmol, 20 equiv.) while maintaining room temperature. After full conversion, the solids were filtered off over a pad of magnesium sulphate (50 g) and rinsed thoroughly with boiling acetone (10 x 150 mL). This step was repeated until all product was extracted out of the magnesium cake. Then, the collected organic phase was evaporated *in vacuo* giving a pastel yellow precipitate (8.615 g, 63%).

$^1\text{H}$ -NMR (300 MHz,  $\text{CDCl}_3$ ):  $\delta$  (ppm) = 8.38 (s, 4 H,  $\text{CH}_{\text{Ar, centre}}$ ), 7.77-7.72 (band, 4 H,  $\text{CH}_{\text{Ar, meta}}$ ), 7.56-7.44 (band, 6 H,  $\text{CH}_{\text{Ar, ortho + para}}$ ) ppm.  $^{13}\text{C}$ -NMR (100 MHz,  $\text{CDCl}_3$ ):  $\delta$ (ppm) = 177.1 (C=O), 140.5 (C), 133.2 (CH), 131.2 (CH), 129.7. In agreement with <sup>37</sup>.

**3.5.11 Synthesis of (2Z,2'Z)-1,1'-(1,4phenylene)bis(3(butylamino)-3-phenylprop-2-en-1-one) (R=butyl) and (2Z,2'Z)-1,1'-(1,4phenylene)bis(3(benzylamino)-3-phenylprop-2-en-1-one) (R = benzyl)**



1,1'-(1,4-phenylene)bis(3-phenylprop-2-yn-1-one) (1 eq., 0.5 g) was mixed with butyl- or benzylamine (3 eq., 0.33 g butylamine or 0.48 g benzylamine) in 20 mL toluene for 2h at 60°C followed by overnight stirring at room temperature. Next, the solvent was evaporated *in vacuo* yielding the desired product without further purification. For the benzyl compound, residual benzylamine was present but did not formed a problem as the compound was only used to have an indication of thee chemical shift of the  $\text{NHCH}_2$ -signals to follow the exchange kinetics.

Yield (2Z,2'Z)-1,1'-(1,4phenylene)bis(3(butylamino)-3-phenylprop-2-en-1-one): 94%.  $^1\text{H}$ -NMR (300 MHz,  $\text{CDCl}_3$ ):  $\delta$  (ppm) = 11.5 (br s, 2H, NH), 7.92 (s, 4H,  $\text{CH}_{\text{ar, centre}}$ ), 7.42-7.63 (band, 10H,  $\text{CH}_{\text{ar}}$ ), 5.78 (s, 2H, 2x  $\text{CHC=}$ ), 3.24 (m, 4H, 2x- $\text{CH}_2\text{NH-}$ ), 1.59 (4H, m, 2x  $\text{CH}_3\text{-CH}_2\text{-CH}_2\text{-CH}_2\text{-NH-}$ ), 1.40 (4H, m, 2x  $\text{CH}_3\text{-CH}_2\text{-CH}_2\text{-CH}_2\text{-NH}$ ), 0.89 (6H, t,  $J=7.28$  Hz, 2x  $\text{CH}_3\text{-CH}_2\text{-}$ ).  $^{13}\text{C}$ -NMR (125 MHz,  $\text{CDCl}_3$ ):  $\delta$  (ppm) = 187.4 (C), 167.2 (C), 142.0 (CH), 135.6 (CH), 129.4 (CH), 128.5 (CH), 126.9 (CH), 93.5 (CH), 44.5 ( $\text{CH}_2$ ), 32.8 ( $\text{CH}_2$ ), 19.9 ( $\text{CH}_2$ ), 13.7 ( $\text{CH}_3$ ).  $\text{C}_{32}\text{H}_{37}\text{N}_2\text{O}_2^+$  (481.7 g/mol).  $m/z$ (ESI-MS): 549.2

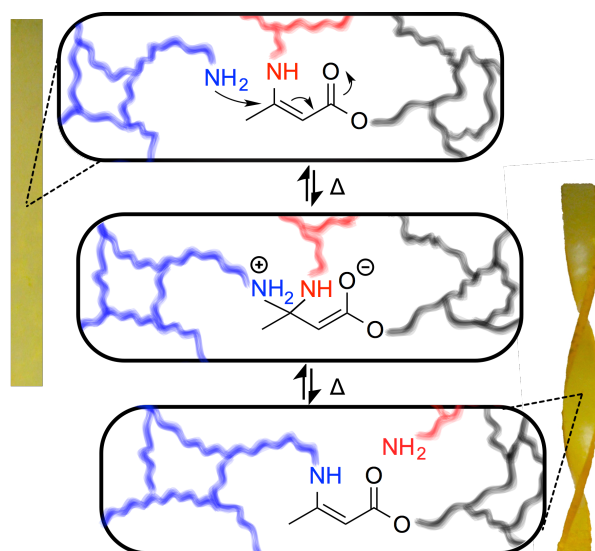
Yield (2Z,2'Z)-1,1'-(1,4phenylene)bis(3(benzylamino)-3-phenylprop-2-en-1-one)= 96%.  $^1\text{H}$ -NMR (300 MHz,  $\text{CDCl}_3$ ):  $\delta$  (ppm) = 11.8 (br s, 2H), 7.94 (s, 4H), 7.18-7.48 (band, 20H), 5.87 (s, 2H), 4.45 (d, 4H,  $J=6.48$  Hz), 3.90 (imp, benzylamine), 2.37 (s, 6H), 1.59 (imp, benzylamine).

### 3.1. References

- (1) Capelot, M.; Montarnal, D.; Tournilhac, F.; Leibler, L. *J. Am. Chem. Soc.* **2012**, *134*, 7664.
- (2) Montarnal, D. Use of reversible covalent and non-covalent bonds in new recyclable and reprocessable polymer materials, PhD Thesis, Université Pierre et Marie Curie, 2011.
- (3) Montarnal, D.; Capelot, M.; Tournilhac, F.; Leibler, L. *Science* **2011**, *334*, 965.
- (4) Eldred, S. E.; Stone, D. A.; Gellman, S. H.; Stahl, S. S. *J. Am. Chem. Soc.* **2003**, *125*, 3422.
- (5) Hoerter, J. M.; Otte, K. M.; Gellman, S. H.; Cui, Q.; Stahl, S. S. *J. Am. Chem. Soc.* **2008**, *130*, 647.
- (6) Miller, I. K. *Journal of Polymer Science Part a-Polymer Chemistry* **1976**, *14*, 1403.
- (7) Hutchby, M.; Houlden, C. E.; Haddow, M. F.; Tyler, S. N. G.; Lloyd-Jones, G. C.; Booker-Milburn, K. I. *Angewandte Chemie-International Edition* **2012**, *51*, 548.
- (8) Ying, H.; Zhang, Y.; Cheng, J. *Nature Communications* **2014**, *5*.
- (9) Jousseume, B.; Laporte, C.; Toupance, T.; Bernard, J. M. *Tetrahedron Lett.* **2002**, *43*, 6305.
- (10) Delebecq, E.; Pascault, J.-P.; Boutevin, B.; Ganachaud, F. *Chem. Rev. (Washington, DC, U. S.)* **2013**, *113*, 80.
- (11) Blatt, A. H. *The Journal of Organic Chemistry* **1936**, *1*, 154.
- (12) Fuson, R. C. *Chem. Rev. (Washington, DC, U. S.)* **1935**, *16*, 1.
- (13) Krishnamurthy, S. *J. Chem. Educ.* **1982**, *59*, 543.
- (14) Elassar, A.-Z. A.; El-Khair, A. A. *Tetrahedron* **2003**, *59*, 8463.
- (15) Michael, J. P.; De Koning, C. B.; Gravestock, D.; Hosken, G. D.; Howard, A. S.; Jungmann, C. M.; Krause, R. W. M.; Parsons, A. S.; Pelly, S. C.; Stanbury, T. V. *Pure Appl. Chem.* **1999**, *71*, 979.
- (16) Al-Saleh, B.; Al-Awadi, N.; Al-kandari, H.; Abdel-Khalik, M. M.; Elnagdi, M. H. *J. Chem. Res.* **2000**, 16.
- (17) Abdulla, R. F.; Emmick, T. L.; Taylor, H. M. *Synth. Commun.* **1977**, *7*, 305.
- (18) Ostrowska, K.; Ciechanowicz-Rutkowska, M.; Pilati, T.; Zzuchowski, G. *Monatshefte für Chemie/Chemical Monthly* **1999**, *130*, 555.
- (19) Friary, R. J.; Seidl, V.; Schwerdt, J. H.; Chan, T. M.; Cohen, M. P.; Conklin, E. R.; Duelfer, T.; Hou, D.; Nafissi, M.; Runkle, R. L. *Tetrahedron* **1993**, *49*, 7179.
- (20) Ueda, M.; Kino, K.; Hirono, T.; Imai, Y. *Journal of Polymer Science: Polymer Chemistry Edition* **1976**, *14*, 931.
- (21) Ueda, M.; Otaira, K.; Imai, Y. *Journal of Polymer Science: Polymer Chemistry Edition* **1978**, *16*, 2809.
- (22) Bass, R. G.; Sinsky, M. S.; Connell, J. W.; Waldbauer, R. O.; Hergenrother, P. M. *Journal of Polymer Science Part A: Polymer Chemistry* **1989**, *27*, 171.
- (23) Sinsky, M. S.; Bass, R. G.; Connell, J. W.; Hergenrother, P. M. *Journal of Polymer Science Part A: Polymer Chemistry* **1986**, *24*, 2279.

- (24) Wilbur, J. M.; Bonner, B. A. *Journal of Polymer Science Part A: Polymer Chemistry* **1990**, *28*, 3747.
- (25) Pavlisko, J. A.; Huang, S. J.; Benicewicz, B. C. *Journal of Polymer Science: Polymer Chemistry Edition* **1982**, *20*, 3079.
- (26) Mori, A.; Kitayama, T.; Takatani, M.; Okamoto, T. *J. Appl. Polym. Sci.* **2004**, *91*, 2966.
- (27) Lu, J.; Easteal, A. J.; Edmonds, N. R. *Pigm. Resin Technol.* **2011**, *40*, 161.
- (28) Witzeman, J. S.; Atkins, D. G. Stabilized non-polymeric acetoacetate esters that promote adhesion to metallic and oxidized substrates US6005146 A, 1998
- (29) Feng, J. R.; Pham, H.; Macdonald, P.; Winnik, M. A.; Geurts, J. M.; Zirkzee, H.; van Es, S.; German, A. L. *Journal of Coatings Technology* **1998**, *70*, 57.
- (30) Krajnik, J.; Lam, V.; Sabo, L.; Camerson, J.; Mittleman, M.; Wise, K. Waterborne coating composition.US 20020103278 A1, 2002
- (31) Lavoie, A. C.; Bors, D. A.; Brown, W. T. Functionalization of polymers via enamine of acetoacetate.US 5494975 A, 1996
- (32) Hélio A. Stefani, I. M. C. *Synthesis-stuttgart* **2000**, *2000*, 1526.
- (33) Clemens, R. J.; Hyatt, J. A. *The Journal of Organic Chemistry* **1985**, *50*, 2431.
- (34) Witzeman, J. S.; Nottingham, W. D. *The Journal of Organic Chemistry* **1991**, *56*, 1713.
- (35) Effenberger, F. *Chem. Ber.* **1965**, *98*, 2260.
- (36) Truong, V. X.; Dove, A. P. *Angewandte Chemie-International Edition* **2013**, *52*, 4132.
- (37) Hergenrother, P. M.; Bass, R. G.; Sinsky, M. S.; Connell, J. W. Polylenamines from aromatic diacetylenic diketones and diamines.1988
- (38) Logan, S. R. *J. Chem. Educ.* **1990**, *67*.
- (39) Brutman, J. P.; Delgado, P. A.; Hillmyer, M. A. *ACS Macro Lett.* **2014**, *3*, 607.
- (40) Higashi, F.; Tai, A.; Adachi, K. *Journal of Polymer Science Part a-1-Polymer Chemistry* **1970**, *8*, 2563.
- (41) Sridharan, V.; Ruiz, M.; Carlos Menendez, J. *Synthesis-Stuttgart* **2010**, 1053.
- (42) Zolfigol, M. A.; Kolvari, E.; Abdoli, A.; Shiri, M. *Mol. Diversity* **2010**, *14*, 809.
- (43) Rout, L.; Kumar, A.; Dhaka, R. S.; Dash, P. *RSC Adv.* **2016**, *6*, 49923.





## Abstract

In this chapter, two approaches were examined to prepare vinylogous urethane vitrimers, more precisely the cross-linking of amine functional prepolymers and the mixing of Low-MW multi-amines and multi-acetoacetates. This latter approach was successful and resulted in the first proof-of-concept vitrimers based on the amine exchange of enaminones. The resulting networks showed good mechanical properties ( $T_g = 87^\circ\text{C}$ ,  $E' \sim 2.4$  GPa) and a typical vitrimer behaviour as the materials were insoluble and at the same time dynamic as proven by stress-relaxation and creep experiments. Finally, a screening of monomers was performed showing that  $T_g$ 's as high as  $145^\circ\text{C}$  are possible and some attempts to find alternatives to the used condensation chemistry are presented.

## Published in:

Denissen, W.; Rivero, G.; Nicolaÿ, R.; Leibler, L.; Winne, J. M.; Du Prez, F. E. *Advanced Functional Materials* **2015**, 25 (16), 2451–2457.

Denissen, W. Winne, J. M.; Du Prez, F.E., Nicolaÿ, R.; Leibler, L.; Composition comprising a polymer network. WO/2016/097169

## Chapter 4

# Vinylogous urethane vitrimers

### 4.1 Introduction

In the previous chapter, we showed that vinylogous transamination of enaminones is feasible and depending on the used compounds, becomes fast in different temperature windows, ranging from room temperature to 150°C. As a first enaminone moiety to implement in materials for the preparation of vitrimers, we chose for vinylogous urethanes. These compounds showed fast exchange from 100°C on (Figure 4.1a) and were stable in the presence of amines, even after a rather harsh thermal treatment. Furthermore, vinylogous urethanes can be easily prepared on large scale by mixing amines and acetoacetyl esters, while these latter compounds can be produced by simple acetoacetylation of various polyol building blocks or materials, giving ready access to useful polyacetoacetate monomers and polymers (Figure 4.1b).

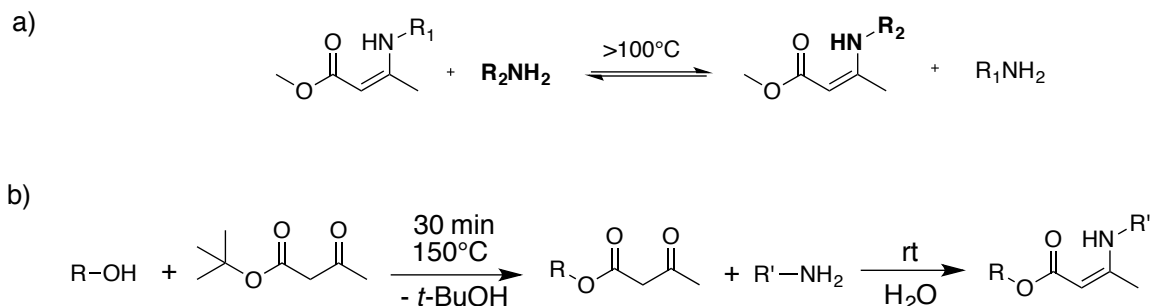


Figure 4.1: a) Transamination of vinylogous urethanes occurs swiftly at temperatures above 100°C. b) Synthesis of vinylogous urethanes through acetoacetylation of alcohols followed by a spontaneous condensation with amines.

To obtain vitrimer materials using vinylogous transamination chemistry, four requirements should be fulfilled:

1. The envisioned network composition should be well above its gel point.
2. Vurethanes must be present in the cross-links or backbone.
3. Free amines should be present to allow for network rearrangements upon heating.

4. Moieties that could give unwanted side-reactions with amines upon heating should be avoided, thus all backbones containing esters are excluded.

These four conditions can be achieved using two different approaches:

- a) The cross-linking of long linear chains bearing amine functions with bis-acetoacetates.
- b) An off-stoichiometric polymerisation of low-MW polyamines (in slight excess) and polyacetoacetate monomers.

## 4.2 Method 1: Cross-linking amine-functional polymers

As a first approach, pre-polymers with pending primary amines that will be cross-linked with bisacetoacetates were examined (Figure 4.2). As the functionality of the prepolymer is very high, only a little amount of bisacetoacetate cross-linker is required to reach the gel point. By using sub stoichiometric amounts of cross-linker, many free amines will also be available throughout the bulk of the material, and exchange is thus expected to occur rapidly, resulting in good processability. The main challenge of this approach exists in finding suitable amine-functional prepolymers. One of the only commercially available amine-functional prepolymers is polyallylamine, which is extremely hydrophilic and thus not practical for materials that should be heated above 100°C for processing. Furthermore, also amine-functionalised PDMS is available but is of no interest for rigid thermoset materials.

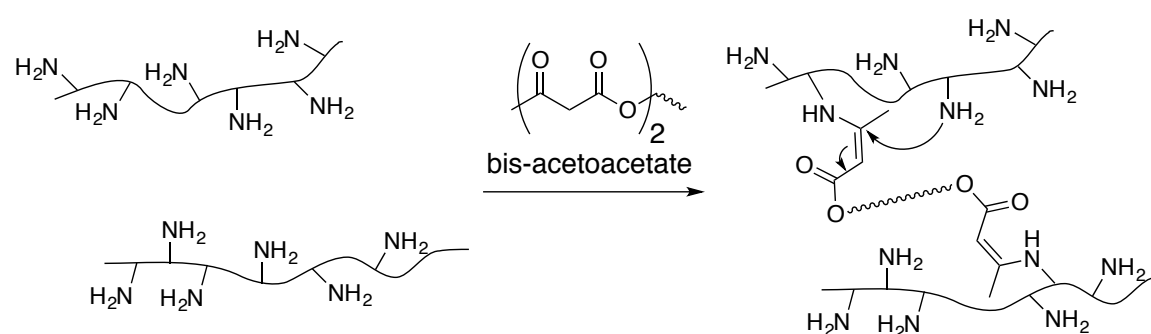


Figure 4.2: Cross-linking of amine-functional prepolymer with bisacetoacetates.

As an alternative to polyallylamine and amine-functionalised PDMS, a custom-made prepolymer was considered, which also allowed to fine-tune the desired backbone constitution in terms of molecular weight and amount of pending amines. A straightforward synthesis method was found in the hydride reduction of



acrylonitrile-styrene copolymers (SAN) (Figure 4.3). Other classical methods to introduce amines on polymer backbones via substitution reactions either require protection groups or hazardous azides, limiting scalability. Furthermore, the styrene-allyl amine backbone was expected to deliver materials with good mechanical properties and relatively high hydrophobicity as a results of the abundance of phenyl groups.

In a first step, styrene **1** and acrylonitrile **2** were polymerized in a controlled fashion via RAFT-polymerisation. This method allows for the synthesis of copolymers with a predetermined narrow-disperse molecular weight. The fraction of nitrile functions were ranged from 35% to 65% acrylonitrile and molecular weights up to 45 kDa were achieved<sup>1</sup>. However, the use of molecular weights higher than 10 kDa proved to be very problematic in the nitrile reduction step due to the increasing viscosity and poor solubility (immediate and irreversible precipitation). For the lower MW copolymers, the nitrile groups of the SAN-polymer could be converted to the corresponding primary amines with a four-fold excess of  $\text{LiAlH}_4$ , followed by aqueous work-up.

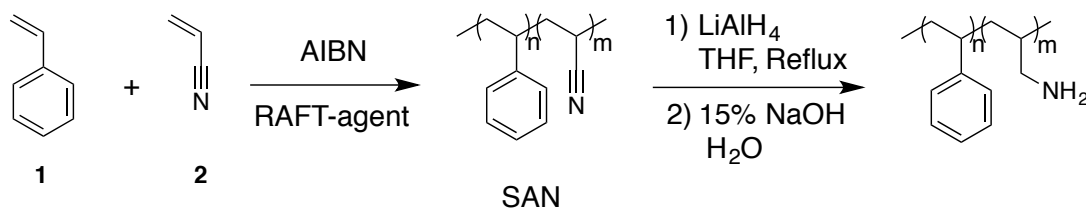
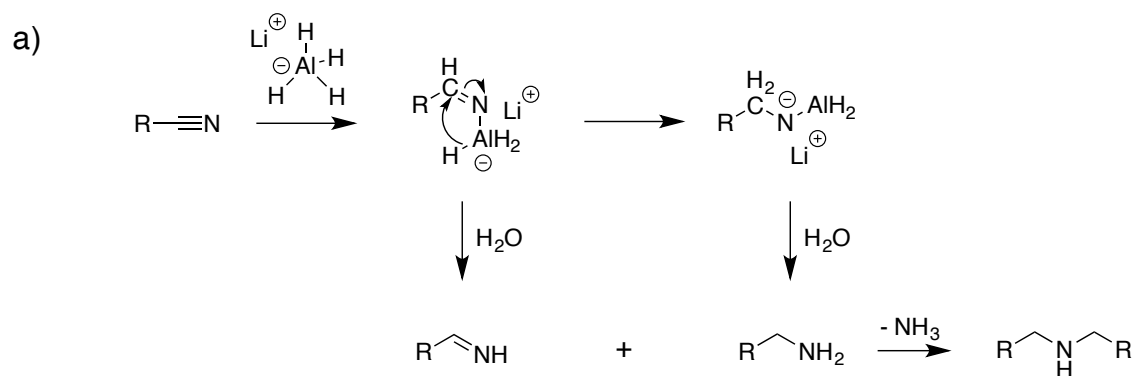


Figure 4.3: Copolymerisation of acrylonitrile and styrene followed by reduction of nitrile yielding an hydrophobic amine-functional prepolymer.

While the method shown in Figure 4.3 should give linear, amine-functional prepolymers, the obtained white powdery polymers in fact no longer dissolved even after prolonged heating in a good solvent such as THF, which might be an indication of the formation of cross-links. Indeed, the formation of secondary amines is a general problem that is also encountered during catalytic hydrogenations of nitriles.<sup>2,3</sup> This unwanted side-reaction is caused by a nucleophilic attack of primary amines on imines (reaction intermediates *en route* to the final amine) with the elimination of ammonia (Figure 4.4a). This hypothesis is further supported by FT-IR spectra before and after reduction. While the characteristic band of the nitrile-stretch ( $\text{C}\equiv\text{N}$ ) at  $2236\text{ cm}^{-1}$  disappeared, a new band matching the  $\text{C}=\text{N}$  stretch of imines at  $1653\text{ cm}^{-1}$  arose together with a broad amine band around  $3300\text{ cm}^{-1}$  (Figure 4.4b). Further optimisation of the polymer synthesis, including moving towards lower nitrile

contents to limit the side reactions, are certainly possible but in light of the priorities of this PhD project, this avenue was not further pursued in favour of alternative methods that did afford well-defined and scalable materials.



b)

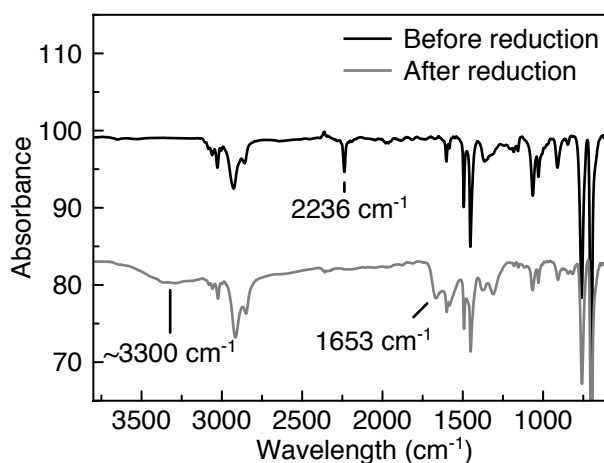


Figure 4.4: a) Side-reaction encountered during hydrogenation of nitriles. Secondary imines formed through partial hydrogenation react with amines to form secondary amines with the release of ammonia. b) FT-IR spectra before and after reduction show the disappearance of nitriles and the appearance of both amines and imines.

## 4.3 Method 2: low-MW monomer approach

### 4.3.1 Network preparation

As an alternative approach, polymer networks that contain both Vurethanes and free amines were targeted by mixing low-MW polyamines and polyacetoacetates. As a wide range of polyacetoacetate monomers can readily be prepared from

available alcohol monomers and combined with commercially available polyamine monomers, this approach should give access to various poly(vinylogous urethane) polymers, which can be tuned according to the targeted material properties by varying the monomers and the stoichiometry. This approach is more challenging because high conversions in the formation of enaminone links will be required to obtain good networks beyond the gel point. For our initial screening, a selection of monomers was made, with the aim to obtain materials with good mechanical properties, high glass transition temperature, easy preparation and good availability of monomers. The conformationally rigid cyclohexane dimethanol bisacetoacetate **3** (CDM-AA), which was synthesized with a one-step procedure from cyclohexane dimethanol, was selected as acetoacetate monomer. *m*-Xylylene diamine **4** and tris(2-aminoethyl)amine **5** (TREN) were identified as preferred amine monomers (Figure 4.5).

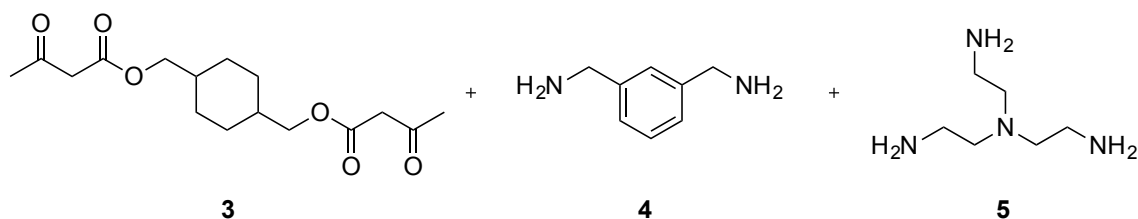


Figure 4.5: Monomers chosen for the Vurethane vitrimer preparation.

The condensation reaction between amines and acetoacetates readily occurs at room temperature but generates one equivalent of water that needs to be removed. This aspect complicates the synthesis of defect-free networks. After exploring a few approaches, a practical method was found wherein the networks were first slowly cured as a film (~1 mm thickness) at 90°C over a 24 h period and were then post-cured for 30 minutes at 150°C to ensure full curing and dryness. In this way, defect-free samples could be obtained as a film of 1 mm thick on a typical 5 to 25-gram scale and used for further characterisation. IR spectroscopic analysis confirmed the full conversion of acetoacetates to vinylogous urethanes with the disappearance of the ester and ketone bands at 1724 and 1700  $\text{cm}^{-1}$ , respectively, and the appearance of the C=C and C=O bands of the vinylogous urethane at the lower wave numbers 1604 and 1640  $\text{cm}^{-1}$ , respectively (Figure 4.6). A small shoulder remained visible around 1724  $\text{cm}^{-1}$ , which probably arises from remaining acetoacetate moieties present in imperfect networks (which is expected given the only very small excess of amine used). In any case, this shoulder does not decrease with additional heating.

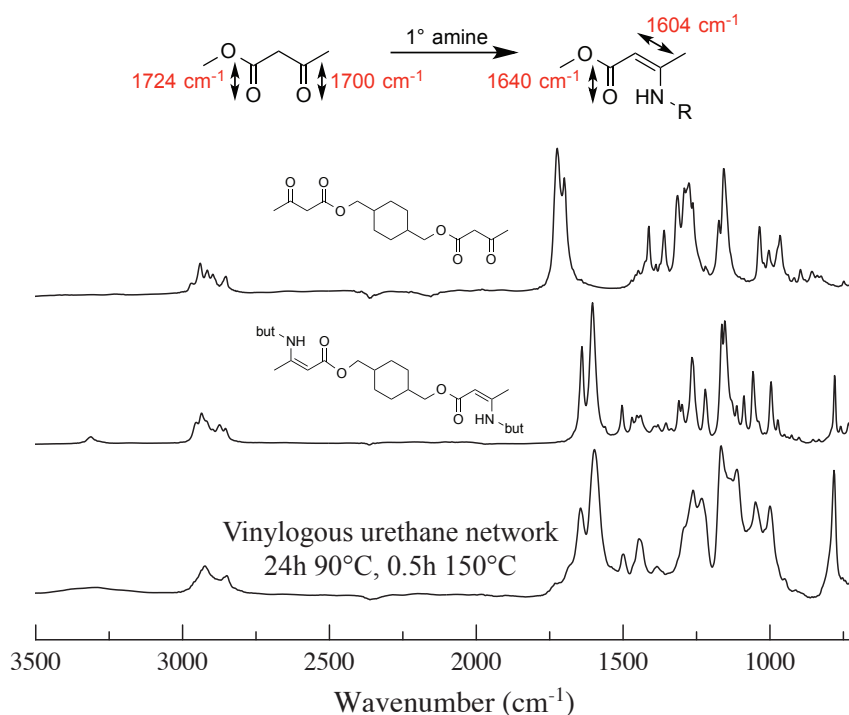


Figure 4.6: Conversion of the acetoacetate function to vinylogous urethanes monitored by FTIR. Almost full conversion was observed after curing.

In the prepared poly(vinylogous urethane) networks, the stoichiometry of the functional groups is a crucial factor, since the availability of sufficient free amines is absolutely essential for a fast reorganization process through the envisaged transamination reaction. In fact, any ‘stoichiometric’ network will always be imperfect and show some amount of free amines. However, preparing a network with a controlled and reliable amount of pending free amines could be better achieved by working under non-stoichiometric conditions. An excess of amine monomer will also affect the gel point conversion as well as the network topology. In order to find an optimal trade off, three compositions with a constant theoretical gel point of 0.83, calculated according to the formula of Flory-Stockmayer<sup>4</sup> and a stoichiometric ratio  $[R = (\text{equivalent acetoacetate}) / (\text{equivalent amine})]$  of 1, 0.95 and 0.90 were initially studied.

As expected, the obtained networks showed significant swelling but we were pleased to observe that they did not dissolve in a good solvent such as *N*-methylpyrrolidone (NMP), even when heated for 24h at 100°C (Table 4.1), well above the glass transition temperature of these materials (*vide infra*). No significant change in sol fraction was observed between 16h and 24h of heating (Figure 4.7a). Furthermore, a similar swelling experiment, but with an excess of

benzyl amine in the solvent, resulted in a complete dissolution of the material indicating amine exchange reactions and thus depolymerisation (Figure 4.7b). This experiment already indicates a quickly operating amine exchange reaction in these materials. As can be further clearly observed from Table 4.1, materials with more free amines also show a higher swelling ratio and soluble fraction, which is indeed expected for less densely cross-linked networks with more network defects.

Table 4.1: Swelling ratio and soluble fraction in NMP (100°C, 24h) for different stoichiometric ratios [ $R = (\text{equivalent acetoacetate}) / (\text{equivalent amine})$ ].

Ratio <b>3:4:5</b>	<b>R</b>	Swelling Ratio (%)	Soluble fraction (%)
0.90 : 0.40 : 0.40	0.90	750	25
0.95 : 0.46 : 0.36	0.95	590	7
1.00 : 0.52 : 0.32	1.00	390	4

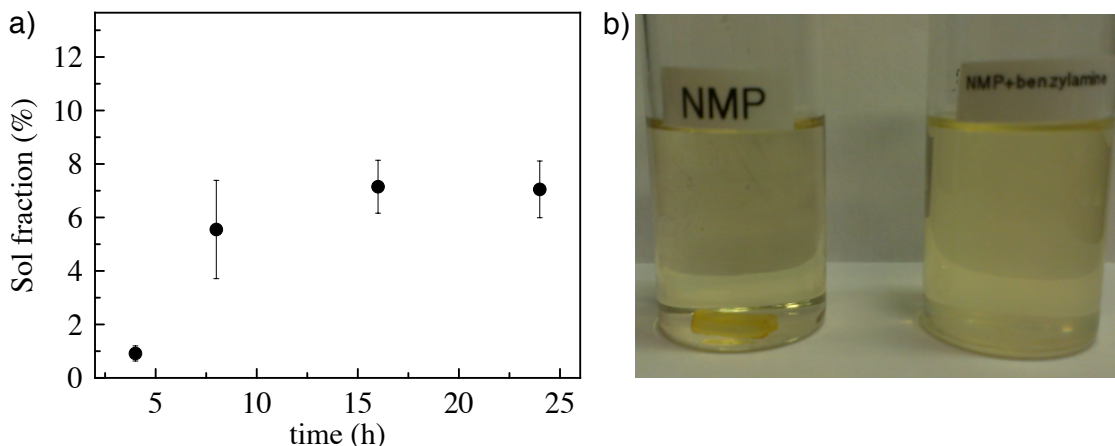


Figure 4.7: a) Sol fraction of a  $R=0.95$  network at 100°C in NMP as a function of time. b) Solubility test on the poly(vinyllogous urethane) network: the network is insoluble after 24h at 100°C in NMP (left). Upon addition of benzyl amine, the network dissolves as a result of exchange reactions (right).

The less densely cross-linked networks with larger amounts of free amines also showed an increased soluble fraction (Table 4.1). Without a significant excess of amines, however, only a very small amount of amines would be available for network reorganization. Therefore, a stoichiometric ratio of 0.95 was chosen as a good compromise for our initial studies, with ample free amines to facilitate exchange whilst having an acceptable soluble fraction ( $<10\%$ ). This somewhat off-stoichiometric ratio was also expected to result in a more reproducible amount of actual free amines in the bulk material. Indeed, a large variation in material

properties could result from small, unavoidable deviations of stoichiometry in a  $R = 1.00$  network, which would make our initial studies and characterisation of these novel materials unnecessarily difficult.

### 4.3.2 Thermal analysis

The bulk polymerization of CDM-AA, *m*-xylylene diamine and TREN as described above, yielded a glassy network with excellent mechanical properties, evidenced by a glass transition temperature of  $\sim 87^\circ\text{C}$  (Figure 4.8a), a storage modulus of  $\sim 2.4$  GPa (Figure 4.8b) and stress at break of  $\sim 90$  MPa (Figure 4.12b). Dynamic mechanical analysis (DMA) confirmed the presence of a network with a rubbery plateau situated at 10 MPa. By thermogravimetric analysis (TGA), the vinylogous urethane networks proved to have good thermal stability with a mass loss of 2.5 % at  $287^\circ\text{C}$  under air and  $295^\circ\text{C}$  under nitrogen atmosphere (Figure 4.8c) using a heating rate of  $10^\circ\text{C min}^{-1}$ .

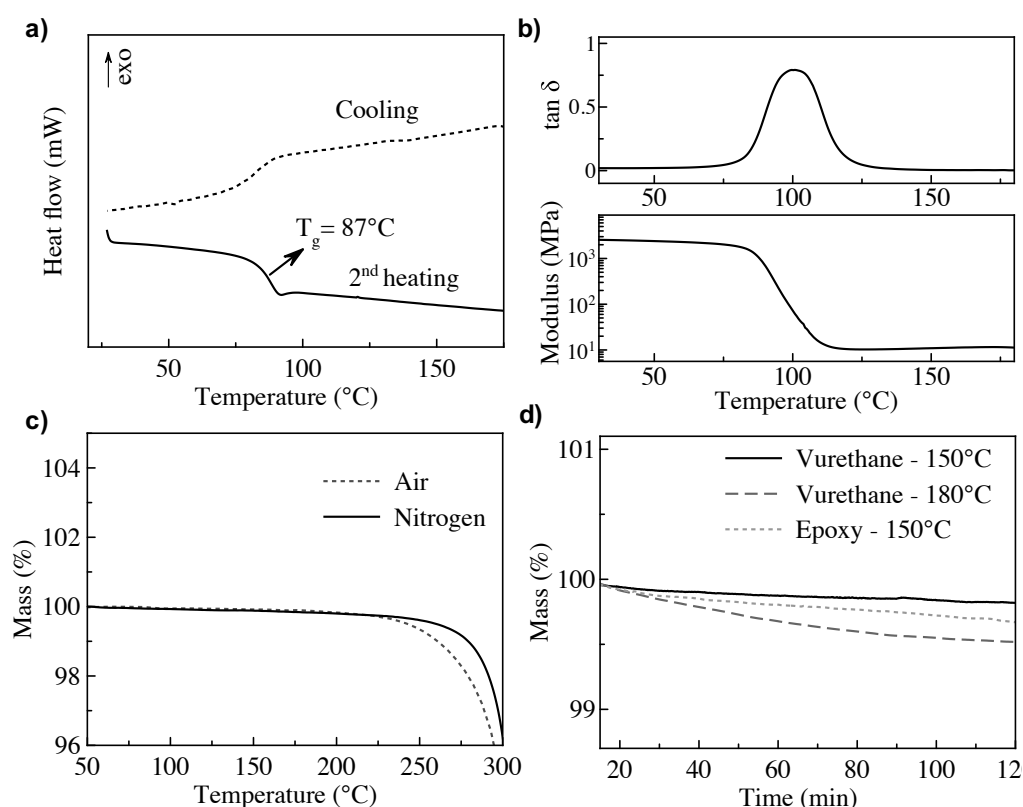


Figure 4.8: Thermal analysis of the poly(vinylogous urethane) network by means of a) DSC thermogram, b) DMTA, c) TGA, mass loss as a function of temperature with a heating rate of  $10^\circ\text{C min}^{-1}$ . d) isothermal TGA with mass loss as a function of time at a specified temperature (an epoxy/amine network is shown for comparison).

Since useful vitrimer materials are expected to withstand elevated temperatures for longer periods when being processed, isothermal TGA was also conducted at both 150°C and 180°C (Figure 4.8d). The weight loss after 2h at 150°C and 180°C is negligible (<0.5%) and comparable to that of a commercial epoxy (EPON 828 cured with DETA<sup>5]</sup>), indicating that the vinyllogous urethane networks are stable when heated within a reasonable timeframe.

### 4.3.3 Rheological study

The flow properties of the vinyllogous urethane networks were studied by stress-relaxation and creep experiments. For the stress-relaxation, measurements were performed in torsion rather than shear geometry to avoid slippage between the sample and the plate during the measurements.<sup>6</sup> Thus, rectangular samples were subjected to a torsional strain of 1% and the relaxation modulus was monitored as a function of time. As shown in Figure 4.9, full stress-relaxation was observed at all temperatures. This behaviour is in accordance with a viscoelastic fluid, further indicating that no non-exchangeable cross-links were introduced during the curing step or stress-relaxation experiment.

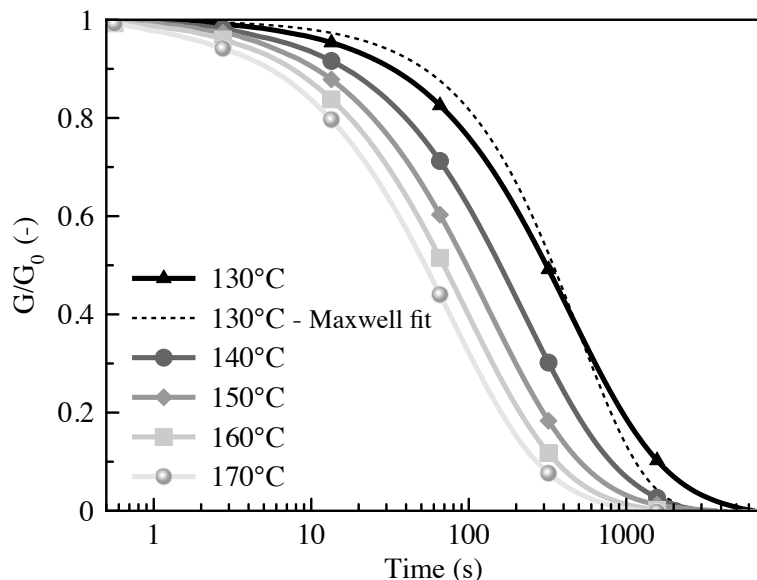


Figure 4.9: Normalized stress-relaxation curves at different temperatures. To the measurement of 130°C, a fit is made using the Maxwell equation.

As described by Leibler and co-workers,<sup>7</sup> the relaxation behaviour of vitrimers can be described by the equation for the Maxwell model:

$$\frac{G}{G_0} = e^{-t/\tau} \quad \text{Eq. 4-1}$$

Using this equation and the relaxation time  $\tau$  that is extracted from the data when  $G/G_0$  equals  $1/e$  (which corresponds to  $t=\tau$ ), a good fit of the measured relaxation modulus can be obtained, as shown in Figure 4.9. The relaxation times range from 550 s at 130°C to 85 s at 170°C (Table 4.2). Compared to other vitrimer systems and taking into account that no catalyst is used in this rather rigid polymer structure, these values are situated among the top-performing vitrimer systems and were a huge improvement to Leibler's pioneering epoxy-anhydride system with a relaxation time of 4117 s at 170°C with 10mol% catalyst.<sup>8</sup> Only very recently, Odriozola et al. showed that vitrimers from epoxy resins with exchangeable aromatic disulphides have similar relaxation times, *i.e.* 120s at 170°C for a polymer with a  $T_g$  of 130°C<sup>9</sup>. The short relaxation times achieved in our poly(vinylogous urethane) vitrimers likely reflects the very high density of vinylogous urethanes in the network and the low activation energy for exchange.

Table 4.2: Measured relaxation time at a specified temperature and the calculated viscosity using the relaxation time and shear modulus from DMTA-measurements.

Temperature (°C)	Relaxation time (s)	Viscosity (Pa.s)
130	496	$1.6 \times 10^9$
140	252	$8.3 \times 10^8$
150	155	$5.1 \times 10^8$
160	111	$3.6 \times 10^8$
170	85	$2.8 \times 10^8$

Furthermore, the viscosity at a certain temperature can be calculated from the measured relaxation times using Eq. 4.2 and 4.3 with the storage modulus  $E'$  from DMA and  $\nu=0.5$ , the Poisson ratio usually used for rubbers.

$$\eta = \tau \cdot G_0 \quad \text{Eq. 4-2}$$

$$\text{with } G_0 = \frac{E'}{2(1 + \nu)} \quad \text{Eq. 4-3}$$



As depicted in Figure 4.2, these viscosities are in the order of  $10^8$ - $10^9$  Pa.s, which is several orders of magnitude higher compared to typical thermoplastic melts used in extrusion conditions ( $<10^6$  Pa.s) and roughly in the range of asphalt ( $\sim 10^8$  Pa.s). This viscosity range also implies that very fast processing methods such as extrusion are excluded for these and other vitrimeric materials currently known. Other methods such as compression moulding are perfectly feasible and will be demonstrated later in this chapter.

One distinct feature of vitrimers is the dependence of the viscosity and thus also the relaxation times as a function of temperature. While the relaxation times of normal polymer melts is described by the WLF-equation (Eq. 4-4), vitrimers can be described by the Arrhenius law (Eq. 4-5) as the associative exchange reactions govern the viscosity.

$$\tau = \tau_{\text{ref}} \exp\left(\frac{C_1(T - T_{\text{ref}})}{C_2 + (T - T_{\text{ref}})}\right) \quad \text{Eq. 4-4}$$

$$\tau(T) = \tau_0 \exp\left(\frac{E_a}{RT}\right) \quad \text{Eq. 4-5}$$

As shown in Figure 4.10, the relaxation times indeed follow the Arrhenius law, and an activation energy of  $60 (\pm 5)$  kJ mol<sup>-1</sup> was calculated from the slope. This result is in quite good agreement with the activation energy of  $60 (\pm 6)$  kJ mol<sup>-1</sup> obtained for the model compounds. For further illustration, these data were also fitted to the WLF-equation using  $T_r = 130^\circ\text{C}$ ,  $\tau_{130^\circ\text{C}}$ ,  $C_1 = -8.86$  and  $C_2 = 101.6$ ,<sup>10</sup> showing a very clear and strong deviation from such a viscosity profile.

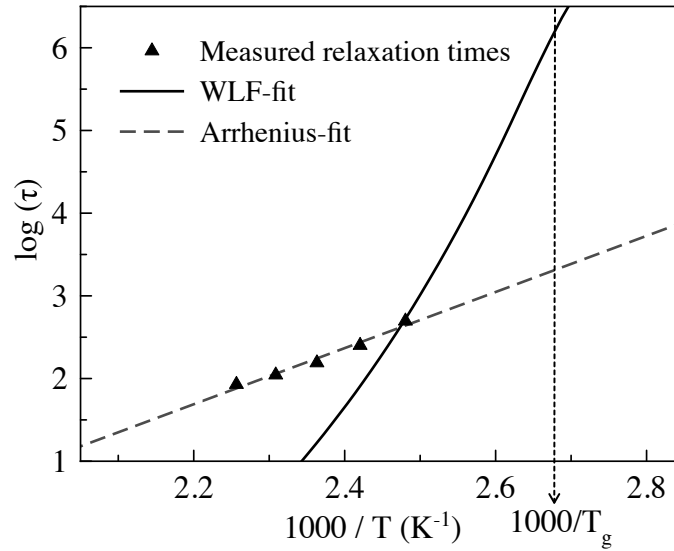


Figure 4.10: Fitting of the logarithm of the relaxation times as a function of the inverse temperature to the Arrhenius equation and WLF equation.

Another key characteristic of vitrimers is the topology freezing transition temperature,  $T_v$ , that corresponds to the transition from a solid to a liquid state, as a result of exchange reactions within the polymeric network.<sup>11</sup> This transition is conventionally chosen as the temperature where the viscosity reaches  $10^{12}$  Pa.s,<sup>12,13</sup> and for the material used in our rheology study, the value of  $T_v$  can be extrapolated from the Arrhenius fitted line to a relaxation time of  $3 \cdot 10^5$  s. This extrapolation results in a  $T_v$  of 29 °C for this material, which is below its  $T_g$  of 87°C and thus only a calculated value without real meaning. As discussed in chapter 2, in these cases where  $T_v < T_g$ , exchange reactions and also stress-relaxation will start as soon as the chains have enough mobility due to the change from the frozen glassy state to its rubbery state with increased chain mobility. Thus, these materials will evolve from its solid glassy state to a viscoelastic rubbery state.

In accordance with our stress-relaxation experiments, creep experiments also confirmed that the vinylogous urethane networks behave like a viscoelastic liquid at elevated temperatures. Figure 4.11 depicts the results of elongational creep experiments at different temperatures. Following the initial elastic response, primary creep with a rapid rate decrease is observed. Then, a steady state is reached, characterized by a constant creep rate. When the stress is released, the material recovers only its initial elastic response and a permanent deformation remains. The networks were easily deformed up to 45% elongation without rupture over a broad temperature range. These results clearly show that these

vinyllogous urethane-based vitrimers can be processed without a precise temperature control. This test provides an illustrative contrast to the stringent conditions necessary for processing thermoplastics in this way.

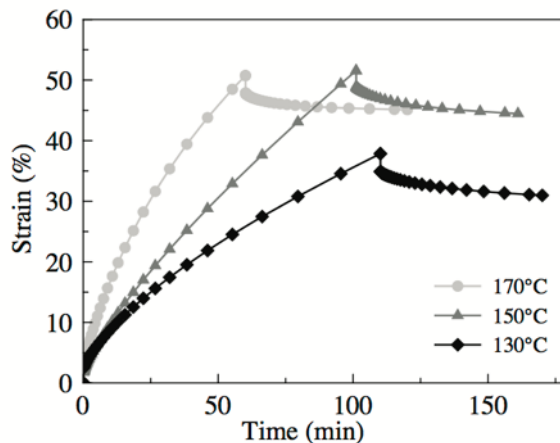


Figure 4.11: Elongational creep of the vinyllogous urethane network with an applied stress of 0.1 MPa at different temperatures.

#### 4.3.4 Recycling study

The recyclable nature of the networks was examined by first grinding the samples into particles that were used as raw substance for compression moulding (Figure 4.12a). To ensure the reversibility, the procedure was repeated four times and after every cycle, the samples were subjected to tensile tests, DMA, DSC, solubility experiments, and ATR-FTIR for characterization. Tensile tests revealed that the mechanical properties were fully recovered after being remoulded for 30 minutes at 150°C (Figure 4.12b). No change was observed in the Young's modulus and stress at break while the strain at break ranged between 5.5 and 7.5 %, independently of the recycling cycle.

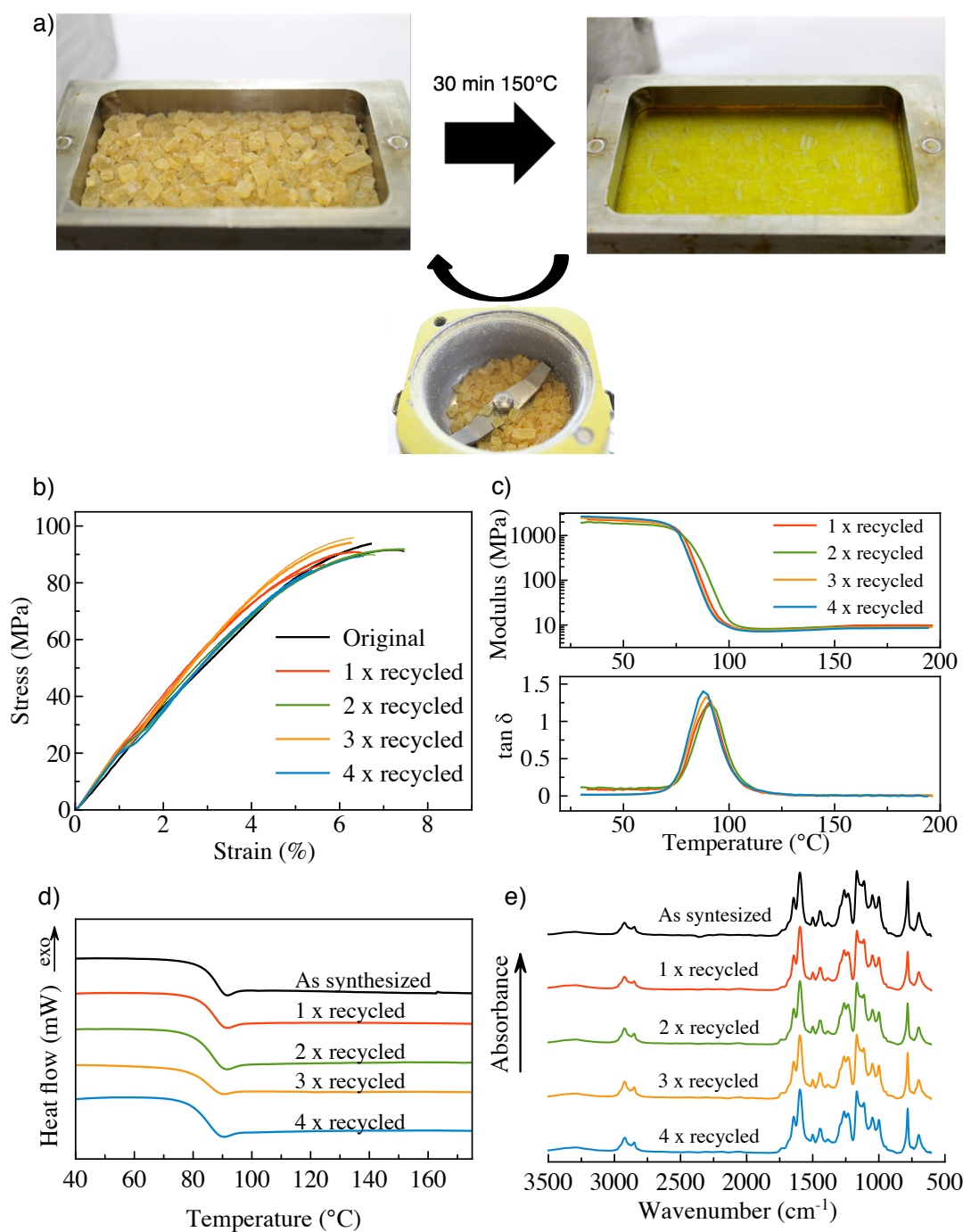


Figure 4.12: a) Recycling of the grinded polymer network by compression moulding. b, c, d and e) stress-strain curves, DMA, DSC and FT-IR of the recycled samples demonstrates full recovery of the mechanical properties.

In addition, DMA confirmed the recovery of the mechanical properties, as the observed rubbery plateau was constant within experimental error ( $\pm 5\%$ ), which indicates that also the cross-link density is not altered (Figure 4.12c). Since we observed a slight shift in the maximum value of  $\tan \delta$ , DSC was performed and

this showed that the  $T_g$  at the second heating changed by less than 1 °C (Figure 4.12c).

In further agreement with DMA results, solubility experiments for recycled networks showed that the soluble fraction varied from 7 to 14% without following a clear trend (Table 4.3), with the soluble fraction of the as-synthesized material being almost identical to that of the material recycled four times. Furthermore, no chemical degradation was visible on ATR-FTIR, *i.e.* the IR-spectra after subsequent cycles were almost identical (Figure 4.12e). In general, the vinylogous urethane networks exhibited excellent recycling properties over four recycling cycles without loss of mechanical properties or chemical changes.

Table 4.3: Soluble fraction in NMP of the original poly(vinylogous urethane) network and the recycled samples. The highest and lowest value of three measurements are shown.

Sample	Swelling Ratio (%)
As synthesised	9 – 13
1 x recycled	6 – 8
2 x recycled	9 – 11
3 x recycled	12 – 15
4 x recycled	8 - 12

#### 4.3.5 Control of the glass transition temperature of Vurethane vitrimers

In the experiments described above, we demonstrated that the amine exchange of vinylogous urethanes can be used to prepare vitrimers with mechanical properties that can compete with commercial resins, and show relaxation times that are among the fastest of the currently known vitrimers. A  $T_g$  of 87°C was obtained via the chosen monomer mixture, which would already be acceptable for a wide range of applications. While lowering the glass-transition is usually simple as more flexible building blocks are readily available (see Chapter 5), higher  $T_g$  materials are often desired for high-end applications. Therefore, a screening was performed to explore the upper-limits of the glass-transition and mechanical properties that could be obtained using the vinylogous urethane chemistry (using commercial

building blocks). Thus, a new selection of monomers was made aiming for increased glass transition temperatures (Figure 4.13).

Rather than sticking to the previously used quite flexible triamine cross-linker **5** (TREN), which is actually the only aliphatic primary triamine monomer that is commercially available at reasonable cost, the composition was changed and a trifunctional acetoacetate monomer (tris-AA) was used as cross-linker. Such cross-linkers can be easily obtained from commercially available triol monomers. Thus, two different acetoacetate cross-linkers **6** and **7** were selected and combined with bisfunctional acetoacetate **8** and a selection of four amines **9-12** with the same excess of amines ( $R = 0.95$ ) and similar cross-link density as previously used. Furthermore, in the selection of the acetoacetate monomers, no aromatic acetoacetates were used as they show poor stability. Since aromatic alcohols are better leaving groups compared to aliphatic alcohols, aromatic alcohol based acetoacetates are sensitive to nucleophilic attack on the carbonyl.

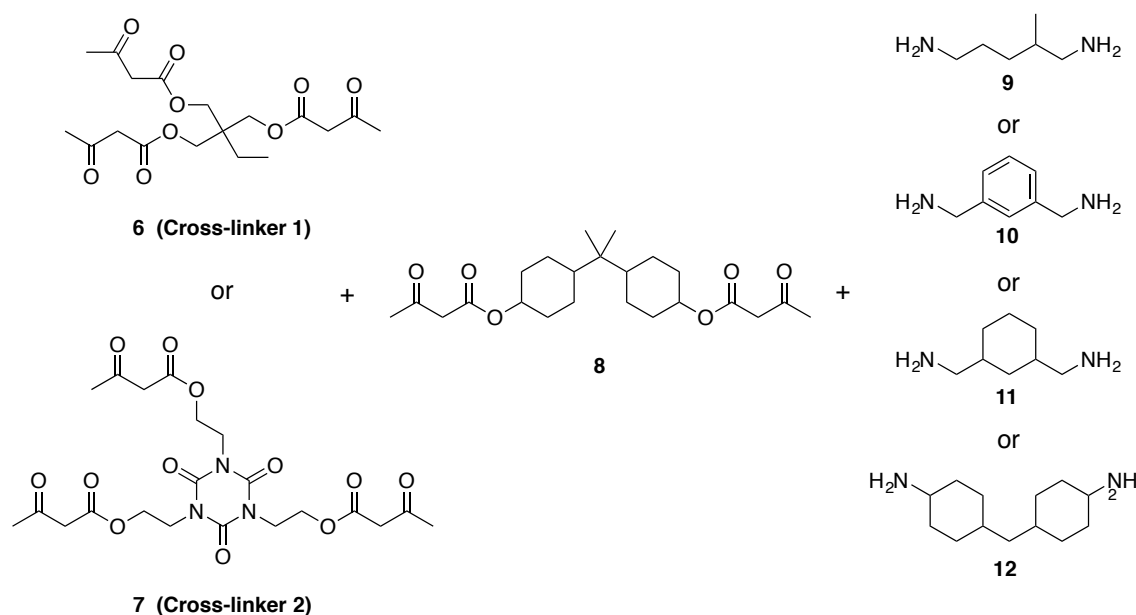
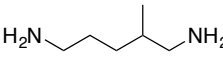
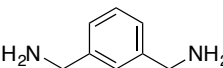
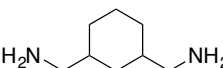
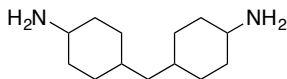
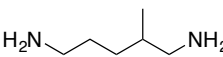
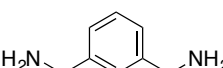
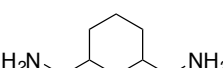
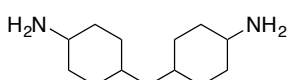


Figure 4.13: Selected monomers aimed for poly(vinylogous) urethane vitrimers with a  $T_g$  as high as possible.

As shown in Table 4.1, the  $T_g$ s of the prepared materials range from 70°C (entry 1) up to 145°C (entry 8). Although, Tris-AA **7** has a twice as much flexible methylenes ( $-\text{CH}_2-$ ), it has a markedly higher  $T_g$  than when tris-AA **6** was used (entry 6 versus entry 3). This difference is probably caused by the rigid isocyanurate centre. Somewhat unexpectedly, the cyclic aliphatic 1,3-cyclohexanebis(methylamine) **11** resulted in materials with a higher  $T_g$  compared

to materials with the aromatic *m*-xylylene diamine **10** (entry 2 vs 3 and entry 6 vs 7).

Table 4.4: Mechanical properties of poly(vinylogous urethane) vitrimers made using the monomers as shown in Figure 4.13 and the two types of cross-linkers.

Entry	cross-linker	Amine monomer	T <sub>g</sub> <sup>a</sup> (°C)	E <sup>b</sup> (Mpa)	Yield Strain (%)	Yield stress (MPa)
1	1		70	2467 ± 102	4.2 ± 1.2	62 ± 5
2	1		75	3180 ± 28	1.5 ± 0.2	48 ± 6
3	1		97	2130 ± 95	1.0 ± 0.1	20 ± 2
4	1		144	2056 ± 24	3.2 ± 0.3	36 ± 5
5	2		86	2413 ± 60	2.1 ± 0.1	48 ± 2
6	2		110	2830 ± 44	3.2 ± 0.3	70 ± 2
7	2		119	3180 ± 35	2.7 ± 0.3	39 ± 7
8	2		145	2123 ± 224	1.6 ± 0.4	31 ± 4

a) Determined via DSC. b) from tensile tests.

In terms of mechanical properties, all moduli range from 2 to 3 GPa, which is comparable to commercial used resins. The materials prepared with *m*-xylylene diamine **10** showed the highest moduli up to 3.2 GPa. All materials are rather brittle with low yield strains (<4.2%), which is not so uncommon for polymer networks. Yet, a high variance was observed (1 – 4.2%). This variation in yield strains is unexpected since the cross-link density should not significantly vary by changing the monomers but not their ratios. Furthermore, the yield strain of the model material discussed before in this chapter was 6%, which is again significantly higher. Most likely, these discrepancies can be explained via the

preparation method. To obtain defect-free samples with the used condensation chemistry, all materials were first cured, then grinded and pressed. This pressing procedure probably should be optimized for materials with a higher  $T_g$ . As a consequence, these yield strain and yield stress values can be considered as a lower boundary with room for improvement. Nonetheless, yield stresses up to 70 MPa (entry 6) were observed, which is again comparable to commercial resins.

#### 4.3.6 Non-condensation vinylogous urethane networks

In the work presented above, all Vurethane networks were prepared via the condensation reaction between amines and acetoacetates releasing water. Although it is possible to obtain defect free-samples via either a patient curing method that allows the slow evaporation of water without bubble-formation or through the vitrimer's intrinsic property to be processed after full curing, a method that easily yields defect-free samples without post-processing would be convenient.

Inspired by the ease in which epoxy-networks are prepared via the reaction of acids and epoxides through ring opening, an alternative polymerisation strategy was considered. In our attempt, we aimed for the cyclic vinylogous urethane **13**. This monomer could be susceptible to react with an amine and hereby form a linear Vurethane and another free amine that on its turn could react further to form a polymer (Figure 4.14a). Via combination of cyclic Vurethane **13** with a bis(cyclic Vurethane) and an primary amine that starts the ring-opening polymerisation, Vurethane networks could be formed (Figure 4.14b). As driving force, we surmised that the ring-tension combined with the gain of the internal hydrogen bond could be enough to overcome the loss in entropy caused by the polymerisation.



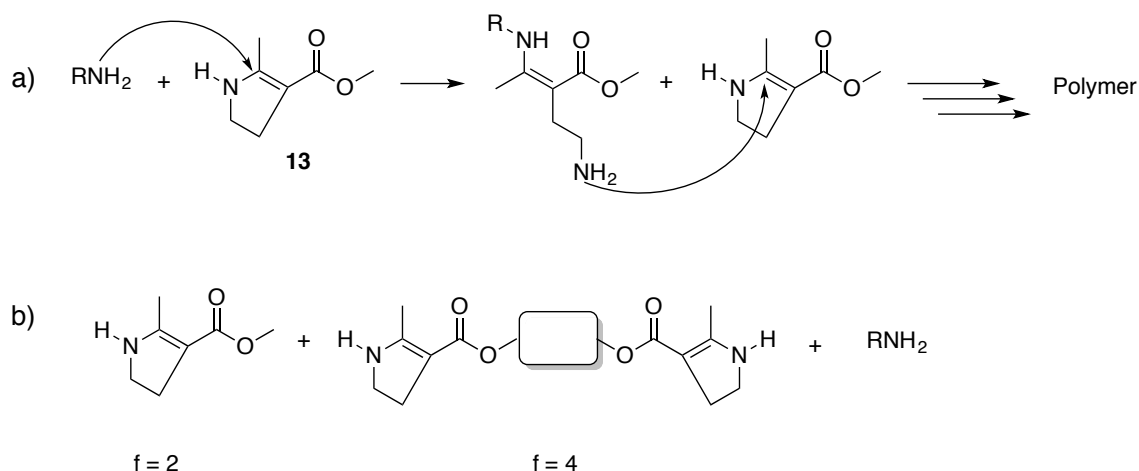


Figure 4.14: Principle of the envisaged cyclic Vurethane system.

In our first attempt, we aimed to prepare the cyclic Vurethane monomer **13** through reaction of ammonia on activated cyclopropane **16** as described by L'hommet and co-workers (Figure 4.15).<sup>14</sup> First, the activated cyclopropane **16** was prepared in a modest yield (68%) after purification by refluxing methyl acetoacetate **14** with 1,2-dibromoethane **15** in acetone in the presence of sodium carbonate. Next, the general procedure for the synthesis of **13** was tested, which was described as heating one equivalent of activated cyclopropane **16** with one equivalent amine in ethanol (EtOH) or methanol (MeOH) for eight hours. As indicated in Table 4.5, predominantly the starting product was observed in the <sup>1</sup>H-NMR of the crude mixture with no indications of the desired products (Entry 1 and 2). Next, heating the aforementioned mixture at 140°C in a pressure tube (conditions which were mentioned in an example) resulted in a complex mixture of different compounds and some remaining starting product (entry 3). Efforts to isolate the compounds only resulted in impure fractions (<5% yield). Finally, an alternative approach was examined using Ni(ClO<sub>4</sub>)<sub>2</sub>·6H<sub>2</sub>O.<sup>15</sup> Both refluxing in dichloromethane and dichloroethene (DCE) proved also to be unsuccessful as no conversion was observed.

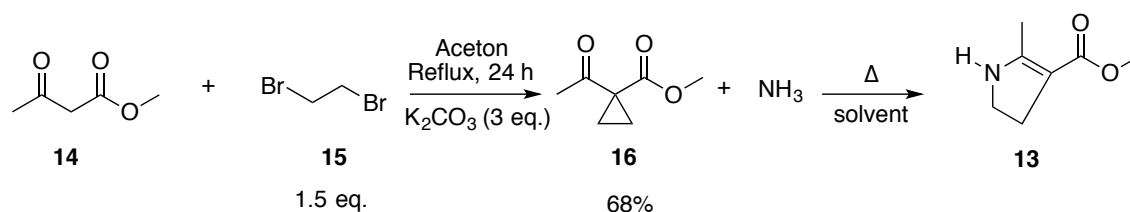


Figure 4.15: First examined synthetic path towards cyclic Vurethane **13**.

Table 4.5: Summary of used conditions and observations in the synthesis of **13**.

Entry	Conditions	Observation
1	MeOH, reflux, 8 h	Almost no conversion (NMR)
2	EtOH, reflux, 8 h	Almost no conversion (NMR)
3	EtOH, 140°C, 2 h	Mixture of multiple products (TLC). Low yield (<5%) and impure products (NMR)
4	DCM, 2 h, reflux (40°C) 20 mol% Ni(ClO <sub>4</sub> ) <sub>2</sub> ·6H <sub>2</sub> O	0% conversion (GC/NMR)
5	DCE, 2 h, reflux (84°C) 20 mol% Ni(ClO <sub>4</sub> ) <sub>2</sub> ·6H <sub>2</sub> O	0% conversion (GC/NMR)

Since efforts to prepare cyclic Vurethane **13** from **16** did not yield a trace of the desired product, we changed our strategy to the reduction of the nitrile-containing beta-ketoester **18**. This compound can form **13** upon ring-closure when the nitrile-functionality is reduced to the corresponding amine. First, the *in-situ* formed sodium salt of MeAA **14** was reacted with bromoacetonitrile **17** affording nitrile **18** in a modest yield (50%).<sup>16</sup> The crucial step is the reduction of the nitrile to the corresponding amine. For this reaction, several reduction methods were screened as summarised in Table 4.6. While hydrogen in presence of Pd/C did not result in any reaction (entry 1 and 2), the addition of two equivalents of acetic acid (AcOH) made the reduction of nitrile moiety successful. To our surprise, not the desired cyclic Vurethane **13** was isolated but pyrole **19** (entry 3 and 4). Since these attempts did not yield the desired product and a bis(cyclic Vurethane monomer), which would be even more challenging to synthesise, is also essential to obtain networks, the idea of using cyclic Vurethanes was not pursued further.

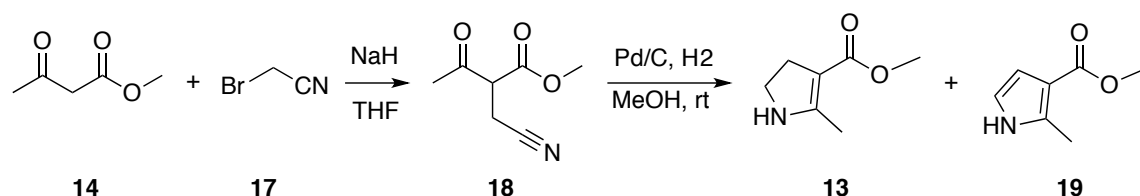
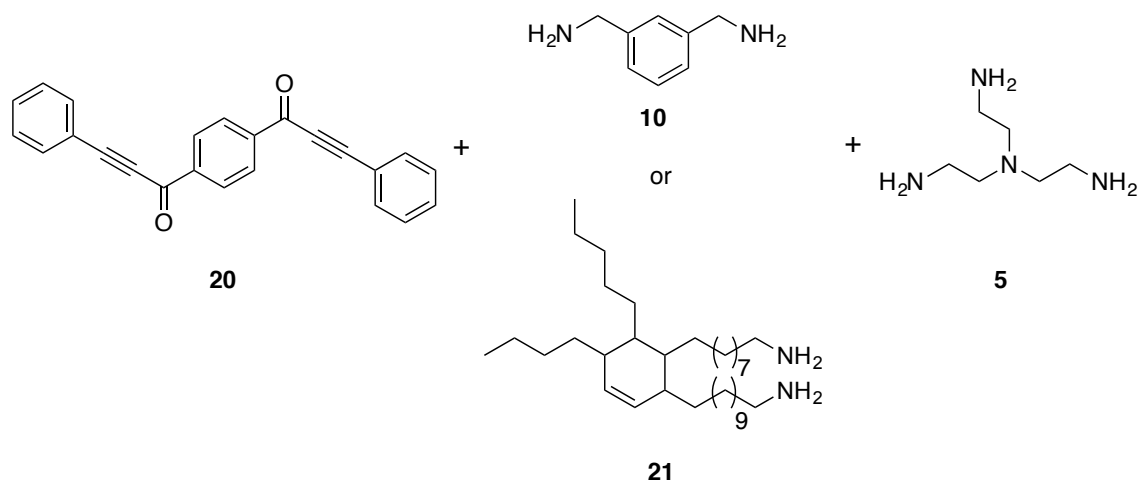
Figure 4.16: Second examined path towards cyclic Vurethane **13**

Table 4.6: Summary of conditions and results obtained in the reduction of **18**.

Entry	Conditions	Observation
1	5% Pd/C, balloon H <sub>2</sub> , overnight	No conversion (TLC)
2	10 % Pd/C, balloon H <sub>2</sub> , overnight	No conversion (TLC)
3	5% Pd/C + 2 equiv. AcOH double balloon H <sub>2</sub> , overnight	Partial conversion, formation of pyrole <b>19</b> (yield = 49%)
4	10% Pd/C + 2 equiv. AcOH double balloon H <sub>2</sub> , overnight	Low conversion, formation of pyrole <b>19</b> (not isolated)
5	40 bar H <sub>2</sub> , 10% Pd/C, overnight	Full conversion formation pyrole <b>19</b> (not isolated)

Finally, as an alternative to cyclic Vurethanes circumventing the condensation chemistry, the polymerisation of ynone **20** was examined. Although polymerisation of ynone **20** does not result in Vurethanes but in a Vamides, our interest in this monomer existed as thermoplastics with a Tg up to 235°C and good thermal stability were reported using this monomer.<sup>17</sup>

Unfortunately, ynone **20** turned out to be a troublesome monomer for network preparation as it mixes poorly with the amine monomers and only melts at 185°C. In the first trials, ynone **20**, *m*-xylylene diamine **10** and TREN **5** were selected and different mixing strategies were evaluated. For example, a first trial consisted in mixing all monomers in bulk, followed by compression moulding. This approach resulted in very heterogeneous materials. In a second attempt, the monomers were first dissolved in dichloromethane, which was then removed *in vacuo*. The obtained powder was compression moulded at 150°C, which resulted again in heterogeneous materials.



It became apparent that efficient mixing would be the all-determining step. Therefore, in order to achieve better mixing, *m*-xylylene diamine **10** was replaced by priamine 1071 **21**. Next, ynone **20** was dissolved with priamine **21** in DCM and stirred for 2h at room temperature, followed by removal of the solvent *in vacuo*, yielding a thick oily dark-greenish mixture. Then, TREN **5** was added followed by compression moulding for one hour at 150°C, which resulted in a dark brownish, visually homogeneous sample. IR-analysis indicated full conversion with the complete disappearance of the acetylenic C≡C band at 2187 cm<sup>-1</sup> (Figure 4.17a). A DSC measurement showed a subtle and broad shift of the baseline between 40 and 80°C, indicating the presence of a glass transition and based on the broadness also a rather inhomogeneous network structure (Figure 4.17). This hypothesis was further confirmed by DMTA. The Vamide-network exhibited at room temperature a storage modulus (E') of 2270 Mpa, a typical value for thermoset material below its T<sub>g</sub>. Upon heating, the storage modulus decreased very gradually from the GPa range at 70°C in two steps to 8 Mpa at 167°C (rubbery plateau value). This broad transition is again an indication of an inhomogeneous structure. More flexible zones that probably consist of mainly priamine, gain network mobility before the more rigid zones consisting of ynone **20** and TREN, resulting in a gradual decrease of the storage modulus.

The motivation to investigate these non-condensation chemistries existed in finding a simple polymerisation method that would yield defect-free samples. However, the evaluated methods for the polymerisation of ynone **20** proved to be even more complicated. In addition, the obtained sample turned out to be inhomogeneous. Therefore, no further efforts were made to improve our methods and investigate these materials in greater detail.

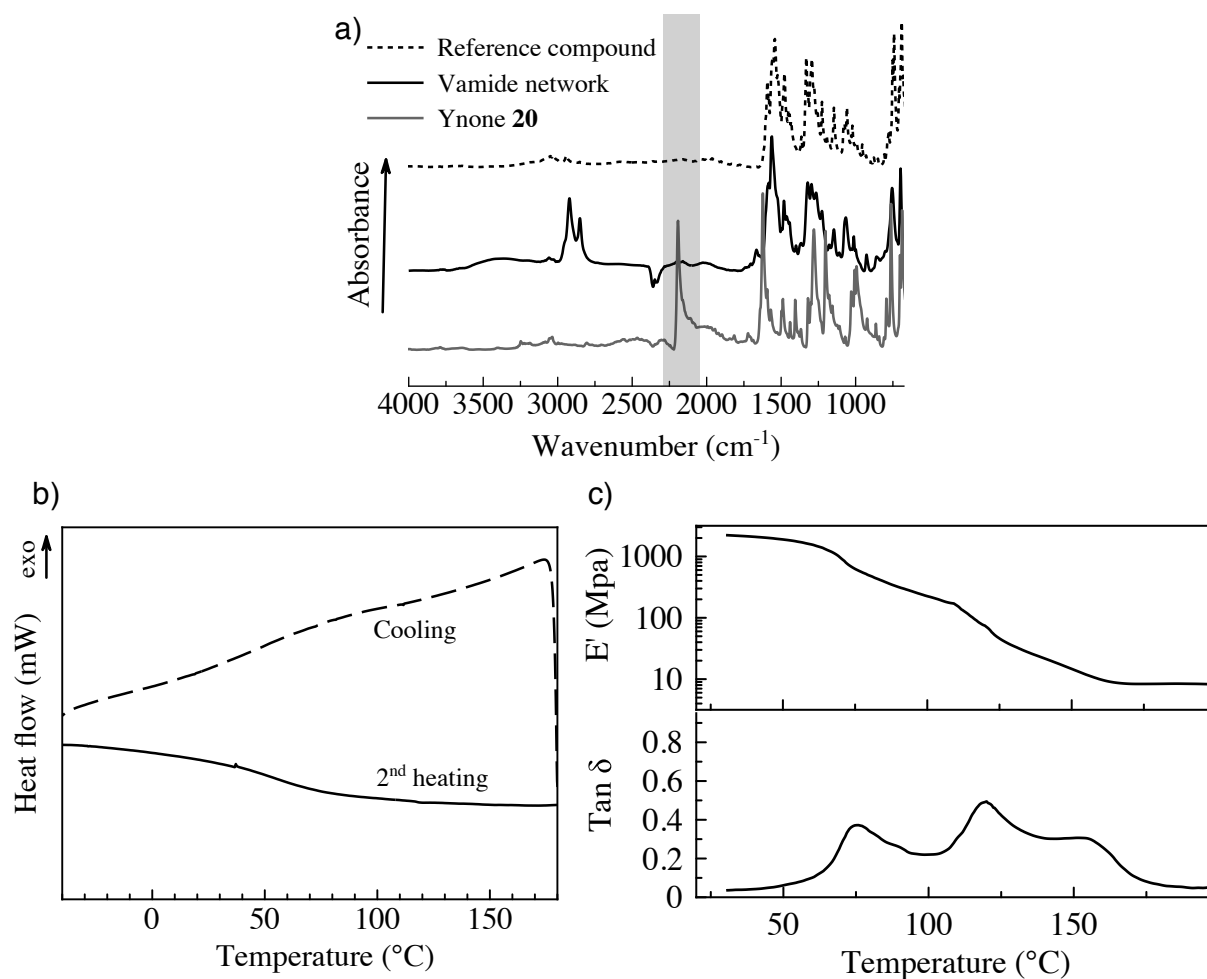


Figure 4.17: a) IR-spectra of ynone **20** (lower), Vamide polymer made from monomers **20**, **21** and **5** (middle) and a low-MW reference compound (upper curve). b) DSC-traces of the Vamide polymer. c) DMA of the Vamide polymer.

## 4.4 Conclusion and perspectives

In this chapter, three methods were examined to prepare vitrimers capable of stress relaxation through transamination of vinylogous urethanes. The first strategy, relying on amine-functional prepolymers, was abandoned as the synthesis of these prepolymers proved to be problematic due to a side-reaction, resulting in unwanted cross-linking.

The second approach, starting from low-MW amine and acetoacetate monomers, demonstrated the first proof-of-concept vitrimers based on vinylogous transamination. Poly(vinylogous urethane) networks with a glass transition temperature of 87°C and a storage modulus of ~2.4 GPa were obtained. As

expected for a polymer network, the samples were insoluble even at elevated temperature while a rubbery plateau was observed by DMA. Stress-relaxation and creep experiments showed a viscoelastic liquid behaviour. Due to the fast exchange reactions and high density of exchangeable bonds throughout the network, relaxation times as short as 85 s at 170°C were achieved without the use of any catalyst. Moreover, the poly(vinylogous urethane) networks can be recycled by grinding and without loss of mechanical properties. These properties position these materials among the top-performing vitrimers currently known.

Next, using the versatility of the vinylogous urethane chemistry, a screening of monomers was performed, materials with a  $T_g$  up to 145°C were feasible and properties are comparable with those of commercial resins.

In the third approach, alternatives for the used condensation chemistry were evaluated. On the one hand, cyclic monomers were considered but the synthesis of these monomers was unsuccessful. On the other hand, ynone monomers were exploited but due to the difficulties encountered to obtain homogeneous materials, also this approach was not investigated in great detail.

Although these results were promising, some challengers and questions remain such as:

- 1) The viscosities are still rather high and do not allow for fast processing necessary for industrial applications. Attempts to address this challenge were made in the next two chapters using either catalysts (Chapter 5) or vinylogous urea (Chapter 6).
- 2) On material level, full stress-relaxation is achieved within 15 minutes at 140°C while in the previous chapter, equilibrium of the model compounds is only reached after 90 minutes. This discrepancy probably arises from the dilution used in the model reactions. This hypothesis will be discussed in the next chapter.

## 4.5 Experimental

### 4.5.1 Materials

butylamine ( $\geq 99\%$ ), *m*-xylylene diamine ( $\geq 99\%$ ), tris(2-aminoethyl)amine (96%), cyclohexane dimethanol (mixture of *cis* and *trans*, 99%), 2,2,6-trimethyl-4*H*-1,3-dioxinon-4-one ( $\geq 93\%$ ), *tert*-butyl acetoacetate ( $\geq 98\%$ ), LiAlH<sub>4</sub> ( $>97\%$ ), styrene, hydrogenated bisphenol A (90%), 1,1,1-tris(hydroxymethyl)propane ( $>98\%$ ), 1,3,5-tris(2-hydroxyethyl)isocyanurate ( $>97\%$ ), methyl acetoacetate ( $>99\%$ ), dibromoethane (98%), 1,5-diamino-2-methylpentane (99%), 1,3-cyclohexanebis(methylamine) (mixture of isomers, 99%), 4,4'-methylenebis(cyclohexylamine) (95%), bromoacetonitrile (97%), were purchased from Sigma Aldrich. Acrylonitrile ( $>99\%$ ) was purchased from Acros Organics.

### 4.5.2 Instrumentation

Nuclear magnetic resonance spectra were recorded on a Bruker Avance 300 or a Bruker Avance II 700 spectrometer at room temperature. IR spectra were collected using a Perkin-Elmer Spectrum1000 FTIR infrared spectrometer with a diamond ATR probe. Thermogravimetric analyses were performed with a Mettler Toledo TGA/SDTA851e instrument under air or nitrogen atmosphere at a heating rate of  $10^{\circ}\text{C min}^{-1}$  from  $25^{\circ}\text{C}$  to  $500^{\circ}\text{C}$ . Differential scanning calorimetry (DSC) analyses were performed with a Mettler Toledo instrument 1/700 under nitrogen atmosphere at a heating rate of  $10^{\circ}\text{C min}^{-1}$ . Dynamic mechanical analysis (DMA) was performed on a SDTA861e DMA from Mettler Toledo. Stress-relaxation experiments were conducted on an Ares G2 rheometer from TA-instruments in torsion geometry with a samples dimension of  $(1.3 \times 14.5 \times 22) \text{ mm}^3$ . An axial force of -0.01 N and a deformation of 1% were applied. Creep experiments were performed on rectangular samples (5 mm x 1.4 mm x 10 mm) by using a TA-Q800 DMA; a constant stress of 0.1 MPa was applied. Tensile testing was performed on a Tinius-Olsen H10KT tensile tester, equipped with a 100 N load cell, using a flat dog bone type specimen with an effective gauge length of 13 mm, a width of 2 mm, and a thickness of 1.3 mm. The samples were cut out using a Ray-Ran dog bone cutter. The tensile tests were run at a speed of 10 mm/min.

### 4.5.3 Synthesis of the copolymers of styrene and acrylonitrile

Styrene and acrylonitrile were filtered over  $\text{Al}_2\text{O}_3$  to remove the stabilizers. AIBN, 2-(((butylthio)carbonothioyl)thio)propionic acid, styrene and acrylonitrile were mixed in a tube and subjected to three freeze-pump-thaw cycles. Next, the mixture was heated for the indicated time (see table). Next, the resulting mixture was diluted in a minimal amount THF and precipitated dropwise in a strongly stirred solution of ice cold MeOH (10x volume mixture). The precipitate was filtered, redissolved in THF and precipitated out in the same manner, this process was repeated two time. Finally, the resulting polymer was dried *in vacuo* to yield the desired copolymer.

Table 4.7: Experimental details for the synthesis of the different SAN-copolymers

AIBN/RAFT/ Styrene/Acrylonitrile (equiv.)	Styrene (%)	Acrylonitrile (%)	Polymerisation time (h:min)	MW (kDa)	DP
0.11/1.0/122.6/66.0	65	35	8:00	11.5	1.10
0.11/1.0/103.5/103.5	50	50	2:30	13.7	1.11
0.11/1.0/80.3/149.1	35	65	2:15	10.0	1.09

$^1\text{H-NMR}$  (300 MHz,  $\text{CDCl}_3$ ):  $\delta$  (ppm) =6.9-7.35 (m, 1H, ArH), 6.3-6.9 (m, 2H, ArH), 2.35-2.65 (m,  $\text{CH}_2\text{CH}(\text{CN})\text{CH}_2$ ), 2.15-2.35 (m,  $\text{CH}_2\text{CH}$  (Styrene,  $\text{CH}_2$ ), 1.2-1.8 (m,  $\text{CH}_2\text{CH}_2\text{CH}_2$ ).

IR (ATR,  $\text{cm}^{-1}$ ): 3028 (m), 2927 (m), 2238 (m), 2162 (w), 1966 (w), 1732 (w), 1602 (m), 1494 (s), 1452 (s), 1364 (br), 1156 (w), 1064 (m), 1028 (m), 912 (m), 760 (s), 703 (s), 620 (m)

### 4.5.4 Reduction of styrene-acrylonitrile copolymer

To a solution of  $\text{LiAlH}_4$  (0.35 g, 6.39 mmol, 3 equiv.) in anhydrous THF (10 mL) cooled in an ice-bath, 1 g of styrene-acrylonitrile in 5 mL THF was added dropwise using an addition funnel. The resulting mixture was refluxed for 2h under  $\text{N}_2$ -atmosphere. Next, the solution was cooled in an icebath and 0.5 mL

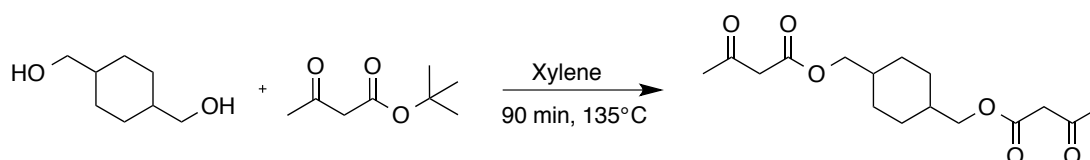


water, 0.5 mL 15% NaOH and 1.5 mL was slowly added (very exothermic!). The resulting mixture was stirred strongly until a loose, white precipitate was observed. The precipitate was filtered off and washed with THF. The filtrate, containing the polymer, was evaporated *in vacuo* yielding a white powder (0.689 g).

IR (ATR,  $\text{cm}^{-1}$ ): 3368 (br), 3028 (m), 2927 (m), 2850 (s), 2162 (w), 1982 (w), 1651 (br), 1600 (m), 1493 (s), 1451 (s), 1373 (br), 1313 (br), 1165 (m), 1029 (m), 814 (m), 758 (s), 703 (s)

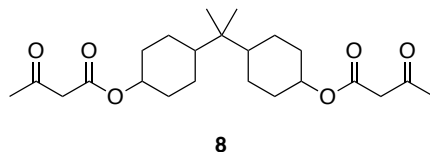
#### 4.5.5 Synthesis of acetoacetate monomers

##### 1,4-Bis(hydroxymethyl)cyclohexane bis-acetoacetate



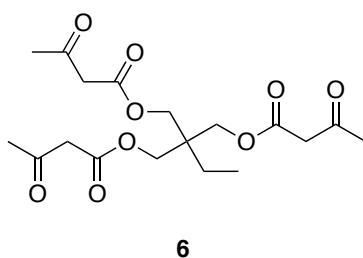
1,4 cyclohexane dimethanol (88.9 g, 0.61 mol) and *tert*-butyl acetoacetate (200 g, 1.26 mol) were dissolved in 120 mL of xylene in a 1 L flask equipped with a still head and cooler. The mixture was heated for 90 minutes at 135°C. The *tert*-butanol product was removed by distillation during the reaction and the temperature in the still head was typically between 75 and 90°C. When the temperature dropped to 50°C, the mixture was cooled and the solvent was removed *in vacuo*. The resulting crude product crystallized upon cooling with ice and consisted of a 28:72 mixture of the *cis*- and *trans* isomer, as indicated by the singlets at 4.08 ppm for the *cis*-isomer and 3.97 ppm for the *trans*-isomer. Recrystallization of the crude product in isopropanol yielded 72% of white crystals, which consisted of 92 % of the *trans*-acetoacetate.

$^1\text{H}$  NMR (300 MHz,  $\text{CDCl}_3$ )  $\delta$  (ppm)= 4.09 (d,  $J = 7.2\text{Hz}$ , 4H *cis*,  $-\text{CH}_2\text{O}-$ ), 3.97 (d, 6.48 Hz, 4H *trans*,  $2x-\text{CH}_2\text{O}-$ ), 3.47 (s, 4H,  $2x \text{C}=\text{OCH}_2\text{C}=\text{O}$ ), 2.28 (s, 3H,  $2x \text{CH}_3\text{C}=\text{O}$ ), 1.83–1.78 (m, 4H, CH ring), 1.68–1.62 (m, 2H, CH ring), 1.05–1.01 (m, 4H, CH ring). The obtained material was identical as the product obtained by Witzeman et al.<sup>18</sup>

**Propane-2,2-diylbis(cyclohexane-4,1-diyl) bis(3-oxobutanoate) (HBFA-AA) 8:**

Hydrogenated bisphenol A was acetoacetylated using the same procedure as the cyclohexane dimethanol described above. The obtained crude product was not recrystallized but thoroughly dried after which it crystallised spontaneously after several days. Completion of the reaction was verified via  $^1\text{H}$ -NMR through the conversion of the  $\text{CHOH}$  at 3.55 ppm to 4.71 ppm. The product consisted as a cis- and trans-mixture.

$^1\text{H}$  NMR (300 MHz,  $\text{CDCl}_3$ )  $\delta$  (ppm)=5.12 (m, 2H, cis  $\text{OCH}(\text{CH}_2)_2$ ), 4.71 (m, 2H trans,  $\text{OCH}(\text{CH}_2)_2$ ), 3.47 (s, 2H cis,  $\text{C}(=\text{O})\text{CH}_2$ ), 3.43 (s, 2H trans,  $\text{C}(=\text{O})\text{CH}_2$ ), 2.29 (s, 3H, cis  $\text{CH}_3\text{C}(=\text{O})$ ), 2.27 (s, 3H, trans  $\text{CH}_3\text{C}(=\text{O})$ ), 2.07-1.95 (band, 2H, CH ring), 1.77-1.70 (band, 4H, CH ring), 1.54-1.47 (band, 2H, CH ring), 1.34-1.12 (band, 6H, ring CH), 1.17-1.11 (band, 2H, CH ring), 0.75-0.72 (band, 6H, cis/trans/enol  $\text{CHCCH}_3$ ).  $^{13}\text{C}$ -NMR (75 MHz,  $\text{CDCl}_3$ )  $\delta$ = 200.7 (C), 166.7(C), 74.8, (CH<sub>2</sub>), 74.9 (CH<sub>2</sub>), 50.5 (CH<sub>2</sub>), 42.6 (CH<sub>3</sub>), 43.3 (CH<sub>3</sub>), 42.9 (CH<sub>3</sub>), 30.6 (CH<sub>2</sub>), 30.5 (CH<sub>2</sub>), 30.2 (CH<sub>3</sub>), 30.0 (CH<sub>3</sub>), 20.6 (CH<sub>3</sub>), 20.5 (CH<sub>3</sub>).  $\text{C}_{23}\text{H}_{36}\text{O}_6$  (408.5 g/mol). m/z(ESI-MS): 426.3 ( $\text{M}+\text{NH}_4^+$ ).

**2-Ethyl-2-(((3-oxobutanoyl)oxy)methyl)propane-1,3-diyl bis(3-oxobutanoate) 6**

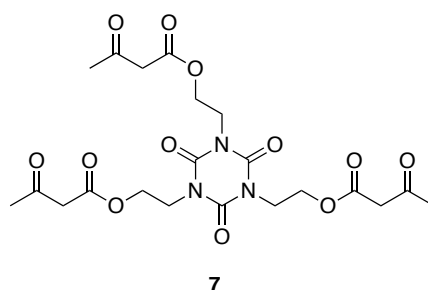
The round-bottomed flask or reactor was loaded with polyol (1 equiv.). Next, nitrogen was bubbled through the neat polyol for 5 minutes while stirring gently at room temperature (to ensure all oxygen was removed from the mixture). Afterwards, *tert*-butyl acetoacetate (3.2 equiv.) was added all at once at room temperature. The temperature was steadily increased to 140 °C where it was held constant for 2 hours (temperature probe). The formed *tert*-butanol and excess of *tert*-butyl acetoacetate were removed through nitrogen bubbling while keeping the

temperature fixed at 140 °C. Puring was continued until it was confirmed via NMR that all *t*-butanol was removed.

$^1\text{H}$  NMR (300 MHz,  $\text{CDCl}_3$ )  $\delta(\text{ppm})$ = 4.10 (s, 6H, 3x  $-\text{CH}_2\text{O}-$ ), 3.50 (s, 6H, 3x  $\text{C}=\text{OCH}_2\text{C}=\text{O}$ ), 2.27 (s, 9H, 3x  $\text{C}=\text{OCH}_3$ ), 1.49 (q,  $J$ =7.5 Hz, 2H,  $-\text{CH}_2\text{CH}_3$ ), 0.90 (t,  $J$ =7.5 Hz, 3H,  $-\text{CH}_2\text{CH}_3$ ). The obtained material was identical as the product obtained by Witzeman et al.<sup>18</sup>

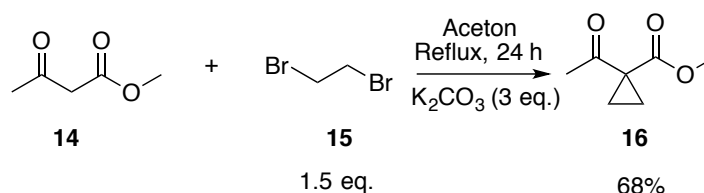
**(2,4,6-Trioxo-1,3,5-triazinane-1,3,5-triyl)tris(ethane-2,1-diyl) tris(3-oxobutanoate)**

The product was obtained using the same procedure for the synthesis of **6**.



$^1\text{H}$  NMR (300 MHz,  $\text{CDCl}_3$ )  $\delta(\text{ppm})$ = 4.35 (t,  $J$  = 5.23, 6H, 3x  $-\text{CH}_2\text{N}-$ ), 4.15 (t,  $J$ = 5.23, 6H,  $-\text{CH}_2\text{O}-$ ), 3.39 (s, 6H, 3x  $\text{C}=\text{OCH}_2\text{C}=\text{O}$ ), 2.20 (s, 9H, 3x  $\text{CH}_3\text{C}=\text{O}$ ).  $^{13}\text{C}$ -NMR (75 MHz,  $\text{CDCl}_3$ )  $\delta$  (ppm)=200.4 ( $\text{C}=\text{O}$ ), 167.0 ( $\text{C}=\text{O}$ ), 149.0 (C), 61.6 ( $\text{CH}_2$ ), 49.7 ( $\text{CH}_2$ ), 41.7 ( $\text{CH}_2$ ), 30.2 ( $\text{CH}_3$ ).  $\text{C}_{21}\text{H}_{27}\text{N}_3\text{O}_{12}$  (513.4 g/mol).  $m/z$ (ESI-MS): 531.2 ( $\text{M}+\text{NH}_4^+$ ).

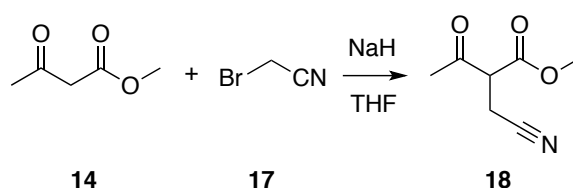
#### 4.5.6 Synthesis of methyl 1-acetylcyclopropane-1-carboxylate **16**



Methyl acetoacetate **14** (1 equiv., 42.96 g), 1,2-dibromoethane **15** (1.5 equiv., 104.45 g) and  $\text{K}_2\text{CO}_3$  (3 equiv., 76.8 g) were dissolved in 380 mL acetone and refluxed for 24h. The mixture was filtered and the solvent removed in vacuo. This mixture was resolved in diethylether and extracted twice with 5% NaOH solution

to remove the residual methyl acetoacetate. After removing the solvent *in vacuo*, the mixture was purified via vacuum distillation (30 torr, bp. 85-95°C) to give **16** as a colourless liquid. Yield: 67%, 34.45 g.  $^1\text{H}$  NMR (300 MHz,  $\text{CDCl}_3$ )  $\delta(\text{ppm})$ = 3.75 (s, 3H,  $\text{CH}_3\text{-O}$ ), 2.47 (s, 3H,  $\text{CH}_3\text{C=O-}$ ), 1.48 (s, 4H,  $\text{CH}_2$  cyclopropane). The obtained material was identical as the product obtained by L'homme et al.<sup>14</sup>

#### 4.5.7 Synthesis of methyl 2-(cyanomethyl)-3-oxobutanoate **18**



Methyl 2-(cyanomethyl)-3-oxobutanoate **18** was prepared using an adapted procedure described by Demir et al.<sup>16</sup>

To a stirred solution of MeAA **14** (0.5 g, 4.31 mmol, 1 equiv) in anhydrous THF (5 mL), 60% NaH on mineral oil (0.215 g, 5.38 mmol, 1.25 equiv.) was added slowly and stirred for 1h at room temperature. Then, a solution of bromoacetonitrile **17** (0.612m, 5.12 mol, 1.25 equiv.) in anhydrous THF (5 mL) was added dropwise using an addition funnel. After 4h, the reaction mixture was filtered and THF was removed *in vacuo*. The resulting mixture was extracted using water and ethyl acetate. The combined organic layers were collected, dried over  $\text{MgSO}_4$  and the solvent was removed under reduced pressure. The crude product was purified via flash chromatography (hexane-ethyl acetate (3/2)).

Yield: 50%.  $^1\text{H}$  NMR (300 MHz,  $\text{CDCl}_3$ )  $\delta(\text{ppm})$ =3.90 (t, 1H,  $J$ = 7.21 Hz,  $\text{C=OCHC=O}$ ), 3.84 (s, 3H,  $\text{CH}_3\text{O-}$ ), 2.85 (dd, 2H,  $J$ =7.21,  $J$ =4.42,  $\text{CH}_2\text{-CN}$ ) 2.38 (s, 3H,  $\text{CH}_3\text{CO-}$ ). The obtained material was identical as the product obtained by Demir et al.<sup>16</sup>

#### 4.5.8 Vurethane network synthesis

*m*-Xylylene diamine (2.111 g, 15.5 mmol), tris(2-aminoethyl)amine (1.774 g, 12.1 mmol) and 1,4-cyclohexanedimethanol bisacetoacetate (10 g, 32.0 mmol) were mixed in a vial and heated in an oil bath thermostated at 80°C. When a homogeneous liquid mixture was obtained, the mixture was taken out of the oil

bath while keeping mixing manually. After 2 minutes, the mixture turned white due to phase separation (water release of the condensation reaction). The resulting white paste was taken out of the vial and pressed into a film of 1.3 mm between two Teflon sheets using a pre-heated press at 90°C. After 30 minutes, the film was transferred into a convection oven and dried during 24h at 90°C, followed by a short post-cure process of 30 min at 150°C.

All other Vurethane networks were prepared using the same method and stoichiometric ratios and as presented above while the curing was performed for 3h at 150°C under vacuum. The resulting hard foamy samples were grinded and compression moulded to a defect-free sample for further analysis.

#### 4.5.9 Solubility experiments

Solubility tests were carried out with samples of a size of  $(10 \times 10 \times 1.3)$  mm<sup>3</sup> with a weight of around 170 mg and 25 mL of NMP as a solvent. The samples were heated for 24 h at 100°C. Then, the solvent was removed *in vacuo* and replaced twice by MeOH to remove NMP as much as possible. Finally, the samples were dried under vacuum, first overnight at 40°C and then at 120°C for 2 h to ensure a complete removal of the solvent from the material. The swelling ratio was calculated using equation Eq. 4-6.

$$\text{swelling ratio (\%)} = \frac{m_{\text{swollen}} - m_{\text{dry}}}{m_{\text{dry}}} \times 100\% \quad \text{Eq. 4-6}$$

## 4.6 References

- (1) Fan, D. Q.; He, J. P.; Xu, J. T.; Tang, W.; Liu, Y.; Yang, Y. L. *Journal of Polymer Science Part a-Polymer Chemistry* **2006**, *44*, 2260.
- (2) Khurana, J. M.; Kukreja, G. *Synth. Commun.* **2002**, *32*, 1265.
- (3) Hoyer, R. C. *J. Chem. Educ.* **1999**, *76*, 33.
- (4) Flory, P. J. *J. Am. Chem. Soc.* **1941**, *63*, 3083.
- (5) Hillewaere, X. K. D.; Teixeira, R. F. A.; Nguyen, L.-T. T.; Ramos, J. A.; Rahier, H.; Du Prez, F. E. *Adv. Funct. Mater.* **2014**, *24*, 5575.
- (6) Dessi, C.; Tsibidis, G. D.; Vlassopoulos, D.; De Corato, M.; Trofa, M.; apos; Avino, G.; Maffettone, P. L.; Coppola, S. *Journal of Rheology* **2016**, *60*, 275.
- (7) Montarnal, D.; Capelot, M.; Tournilhac, F.; Leibler, L. *Science* **2011**, *334*, 965.

- (8) Montarnal, D. Use of reversible covalent and non-covalent bonds in new recyclable and reprocessable polymer materials, PhD Thesis, Université Pierre et Marie Curie, 2011.
- (9) Ruiz de Luzuriaga, A.; Martin, R.; Markaide, N.; Rekondo, A.; Cabanero, G.; Rodriguez, J.; Odriozola, I. *Mater. Horiz.* **2016**, *3*, 241.
- (10) Sperling, L. H. *Introduction to Physical Polymer Science*; 4 ed.; Wiley-Interscience, 2005.
- (11) Capelot, M.; Unterlass, M. M.; Tournilhac, F.; Leibler, L. *ACS Macro Lett.* **2012**, *1*, 789.
- (12) Dyre, J. *Rev. Mod. Phys.* **2006**, *78*, 953.
- (13) Angell, C. A. *Science* **1995**, *267*, 1924.
- (14) Celerier, J. P.; Haddad, M.; Jacoby, D.; Lhomme, G. *Tetrahedron Lett.* **1987**, *28*, 6597.
- (15) Martin, M. C.; Patil, D. V.; France, S. *The Journal of Organic Chemistry* **2014**, *79*, 3030.
- (16) Demir, A. S.; Emrullahoglu, M. *Tetrahedron* **2005**, *61*, 10482.
- (17) Hergenrother, P. M.; Bass, R. G.; Sinsky, M. S.; Connell, J. W. Polylenamines from aromatic diacetylenic diketones and diamines.1988
- (18) Witzeman, J. S.; Nottingham, W. D. *The Journal of Organic Chemistry* **1991**, *56*, 1713.





## Abstract

In this chapter, we show that the amine exchange of vinylogous urethanes can be significantly influenced by simple additives. As anticipated, the transamination reactions can be further accelerated using either Brønsted or Lewis acid additives. Remarkably, however, a strong inhibitory effect is observed when a base is added. These effects have been mechanistically rationalised, guided by low molecular weight kinetic model experiments and applied on a vinylogous urethane elastomer. Thus, vitrimer elastomer materials can be rationally designed to display a wide range of viscoelastic properties. Finally, this approach was extended to rigid vinylogous urethane vitrimers resulting in strongly reduced relaxation times.

## References

Denissen, Droesbeke, M.; Nicolaÿ, R.; Leibler, L.; Winne, J. M.; Du Prez, F. E.; revised paper, Nature Communications.

Denissen, W. Winne, J. M.; Du Prez, F.E., Nicolaÿ, R.; Leibler, L.; Composition comprising a polymer network. WO/2016/097169



## Chapter 5

# Chemical control of vinylogous urethane amine exchange

### 5.1 Introduction

In the previous chapter, the amine exchange of vinylogous urethanes (Vurethanes) was found to be a very useful dynamic covalent reaction for the design of novel vitrimer materials that show good mechanical properties and fast stress-relaxation compared to existing vitrimers. Although relaxation times were already among the shortest measured in rigid vitrimer materials, the viscosity remains in the order of  $10^8$ - $10^9$  Pa.s, well above those of thermoplastic polymer melts. In this chapter, in an attempt to further lower the viscosity of the materials and thus also to enhance the processability, we aimed to accelerate the VU amine exchange reaction via addition of catalysts.

In our approach, a screening of catalysts was first performed on low-MW model compounds. Next, to facilitate the study of the influence of these catalysts on a materials level, we prepared low  $T_g$  materials in order to avoid interference of the glass transition on the exchange kinetics within the material. At the same time, catalytic control could also be a quite useful concept in the field of vitrimer elastomers because these dynamic low- $T_g$  materials can be very challenging. A precise control of the kinetics exchange is required to enable fast processing at elevated temperatures (high rate of exchange) and dimensional stability at service temperature (no or very low rate of exchange). Indeed, in some systems such as Leibler's pioneering transesterification-based vitrimer resins, the exchange reaction is intrinsically slow and high catalyst loadings and temperatures are required to enable processing in a reasonable timeframe.<sup>1-3</sup> Other systems have to rely on exchange reactions that are already fast at room temperature. While room temperature dynamic behaviour can lead to interesting self-healing properties for materials that are used below their glass transition,<sup>4,5</sup> the low temperature exchange reactions will also give deformation at service temperature, precluding many applications.

## 5.2 Model compound study

To establish and verify to what extent the VU amine exchange kinetics can be controlled by catalysts, and to gain further insight into the factors that govern the exchange dynamics, we first prepared and investigated low molecular weight compounds. In contrast to our previous studies (see Chapter 4),<sup>6</sup> the exchange experiments were designed in a way that mimics the VU polymer matrix as closely as possible, *i.e.* a vinylogous urethane functional group in each repeating unit and only a few reactive free amines as network defects. Thus, no solvent was used and a fivefold molar excess of (liquid) VUs versus amines was employed in the presence of small quantities of added catalysts (Figure 5.1). This excess was used to create a pseudo-first order reaction in which the backwards reaction is negligible at low conversions. This experimental set-up should also serve to confirm our previous hypothesis that the difference in relaxation times between the model compounds and stress-relaxation experiments observed in chapters 3 and 4, is due to the much stronger dilution of the model compounds in those earlier kinetic assays.

As described in detail in chapter 3 (see Figure 3.17 p.63), we surmised that proton transfers are essential steps during the exchange process and that protonated species are important reaction intermediates. Thus, the effect of acids and bases was tested on the exchange kinetics of two simple model compounds. While *p*-toluene sulfonic acid (*p*TsOH) and sulphuric acid (H<sub>2</sub>SO<sub>4</sub>) were selected as acids, triazabicyclodecene (TBD) was used as strong base that would minimise the equilibrium concentrations of protonated species. These additives should be able to quite effectively control the amount of protonated (ammonium-type) species present in the reaction medium (For structures, see Figure 5.1b). In addition, dibutyltin dilaurate (DBTL) was also examined as a potential Lewis acid catalyst for the carbonyl-mediated amine exchange reaction. Furthermore, these four different additives were all chosen to exhibit a boiling point far above the envisaged material processing temperatures, in order to avoid evaporative loss. For the used protic acids, it is important to emphasise that these will always be present in ionised form, combined with an amine in the form of an ammonium salt, further preventing evaporative catalyst-leaching. Simple carboxylic acids were considered less useful because – under the harsh thermal reprocessing conditions – they could irreversibly react with amines when heated (giving amides).

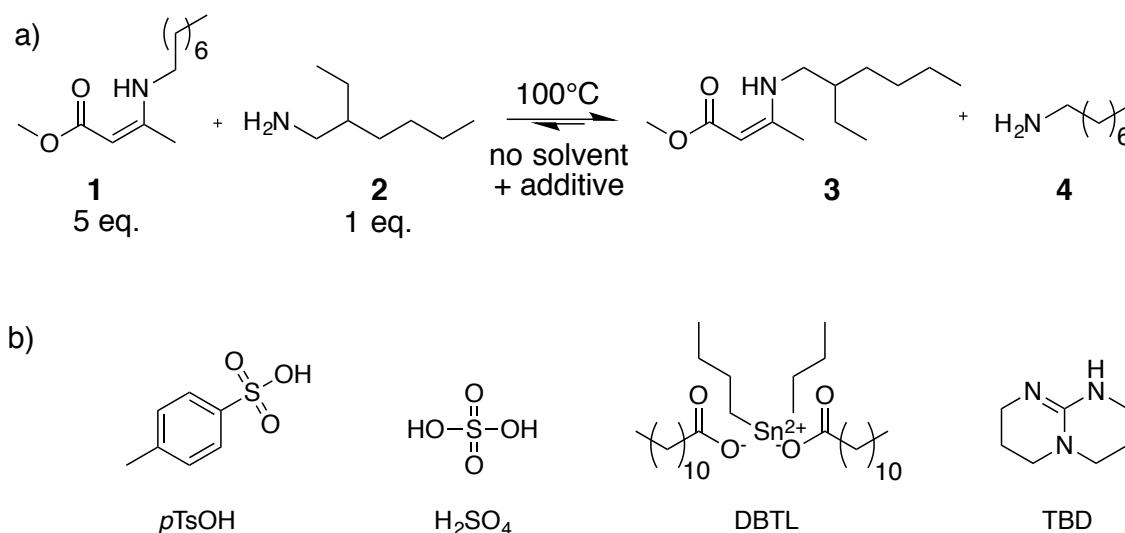


Figure 5.1: a) Model reaction and possible exchange pathways. b) Structure of used catalysts.

To prevent evaporative loss of amines, long alkyl chain amines were used in our kinetic assays. Reactions of 5 equivalents of *N*-octyl vinyllogous urethane model compound **1** with 1 equivalent of 2-ethyl hexyl amine (2-EHA) **2** were performed at 100°C under inert atmosphere and monitored by the disappearance of 2-EHA **2** and appearance of *n*-octyl amine **4** using GC with FID detection. A control experiment without any additives showed that more than one hour of heating is needed to reach the equilibrium, which is situated at a fraction of 0.17 for 2-EHA **2** due to the 5/1 ratio of **1** and **2** used (Figure 5.2). As expected, in the presence of both Lewis and Brønsted acids, the reaction rate is increased significantly. The addition of only 1 mol% *p*TsOH (compared to amine **2**) decreased the time to reach equilibrium to less than 10 minutes. Surprisingly, sulfuric acid was found to be a much less efficient catalyst under the same acidic proton concentrations (0.5 mol%), indicating a possible counterion-effect. The Lewis acid DBTL also catalyzes the reaction efficiently, although higher catalyst loadings are required. Finally, and most interestingly, only a very slow exchange reaction is observed at 100 °C when the amidine base TBD is added.

These model study results clearly indicate that the kinetics of VU amine exchange can be readily controlled, using only small amounts of acids and bases.

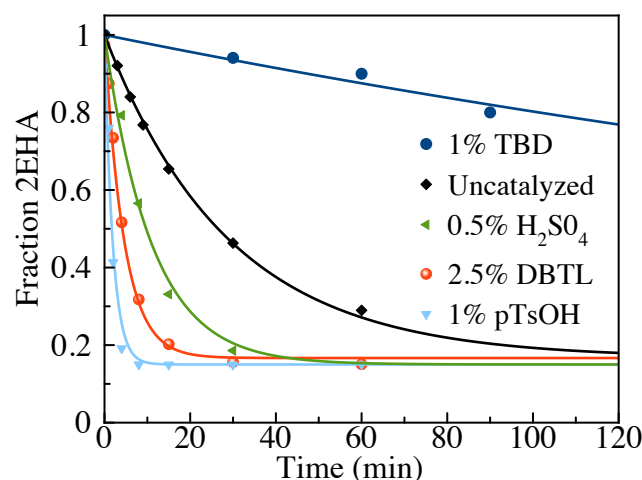


Figure 5.2: Decrease of 2-ethylhexyl amine as a function of time at 100°C in the presence of different additives. The amount of catalyst was calculated as mol% versus 2-ethylhexyl amine.

In order to investigate the kinetics of the exchange reaction in more detail and to distinguish between different possible mechanistic models, further model studies were conducted under a slightly different set-up. For this, 1 equivalent of the vinylogous urethane **1** was dissolved in 5 molar equivalents of benzyl amine. This allowed a simple monitoring of the progress of the amine exchange reaction by  $^1\text{H}$  NMR. Under these pseudo-first order conditions, amine exchange reactions were monitored at different temperatures (80°C, 100°C and 120°C) in the presence of various additives. For the fastest catalyst systems (pTsOH and DBTL), longer measurements were done for exchange reactions at lower temperatures (down to 60°C). In an initial assay conducted at 120°C (Figure 5.3), we also included additional Brønsted acidic and basic additives.

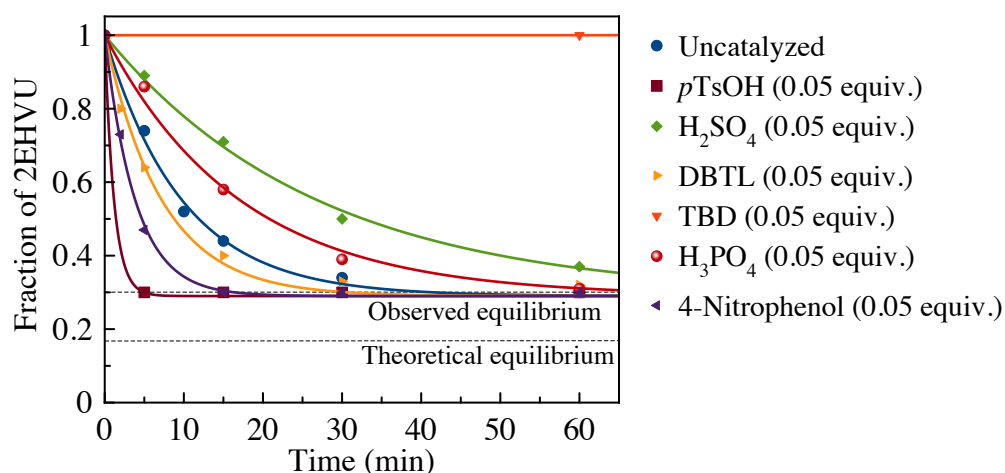


Figure 5.3: Decrease of the fraction of 2-ethyl hexyl Vurethane due to amine VU exchange reactions as a function of time.

In the series of Brønsted acids, *para*-toluene sulfonic acid, *para*-nitro phenol, sulfuric acid and phosphoric acid, a remarkable trend manifested itself. Whereas the organic monobasic acids have a comparable accelerating effect on the amine exchange (as expected), the multibasic inorganic acids actually have an inhibitory effect on the rate of exchange. This can be rationalised by the tendency of the poorly soluble inorganic anions to form clusters or complexes with the ammonium ions. Thus, acidic protons actually become less available for these reactions, and the addition of these acids do not increase the equilibrium concentration of the protonated reaction intermediates. Indeed, the protonated VU intermediates are likely much worse (sterically encumbered) ligands for the sulphate and phosphate anions, shifting protons away from them under these conditions. On the other hand, the organic counter ions are equally suited for both alkyl ammonium species as well as protonated reaction intermediates. The earlier observed difference between *p*TsOH and sulfuric acid can also be understood in this way. In any case, the sulphate anion seems to be a special case.

In the series of base additives, the strong guanidine base TBD was found to completely shut down amine exchange at 120°C, while the secondary amine dihexylamine (DHA) significantly slowed down the exchange reactions. Finally, the Sn(IV)-based Lewis acid DBTL slightly accelerated the amine exchange reaction.

We next investigated the most promising additives *p*TsOH and DBTL as additives at different temperatures, allowing Arrhenius plots and calculation of the activation energies (Figure 5.4). The activation energy of the uncatalysed and *p*TsOH-catalysed reactions were within experimental error (~74 kJ/mol) while a markedly different temperature dependence was observed for the DBTL-catalysed reactions, giving a much lower activation energy of only 51 (±7) kJ/mol.

From a mechanistic viewpoint, the only small difference in activation energy between the not catalysed and acid-catalysed samples indicates that most likely the same reaction pathway is followed in both the catalysed and ‘uncatalysed’ process and that the faster reaction rates in the presence of a protic acid is the consequence of the higher concentration of active protonated species, as compared to the reference material (Figure 5.5a). This explains the markedly faster exchange without a different temperature dependence.

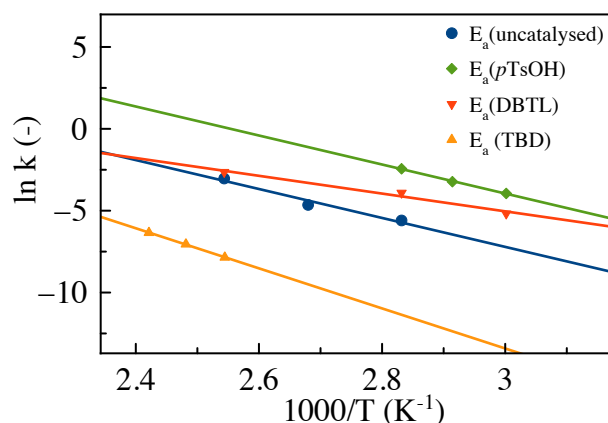


Figure 5.4: Arrhenius plot of the kinetic study.

On the other hand, the DBTL-loaded samples showed a strong decrease in activation energy to  $51 (\pm 7)$  kJ mol<sup>-1</sup>. These observations point to a different reaction mechanism, such as carbonyl activation of the vinylogous urethane by Lewis acid complexation (Figure 5.5b). Because of the decreased slope in the Arrhenius plot, exchange reactions could become more significant at lower temperatures with this catalyst. Conversely, the samples inhibited with TBD showed an increased slope and a significantly elevated activation energy of  $102 (\pm 3)$  kJ mol<sup>-1</sup>, again pointing to a different mechanism, involving addition/elimination reactions without cationic protonated intermediates (through zwitterionic intermediates) as shown in Figure 5.5c.

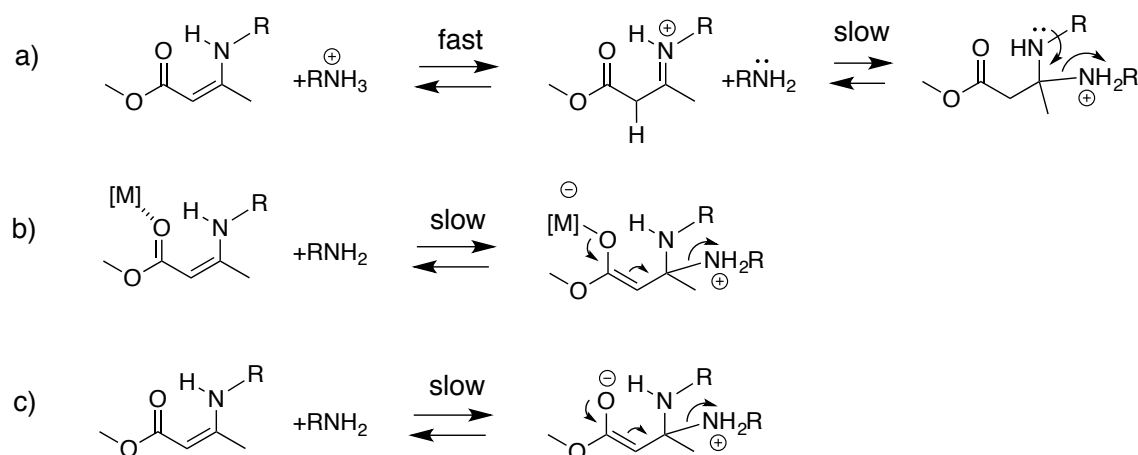


Figure 5.5: Proposed mechanism of VU amine exchange. a) in neutral and acidic conditions via the formation of an iminium intermediate. b) in presence of a Lewis Acid, which activates the carbonyl via coordination and stabilizes the zwitter-ionic intermediate. c) in basic conditions via a direct conjugated addition and an unstabilised zwitter-ionic intermediate.

### 5.3 Synthesis and characterisation of low $T_g$ materials

Having established the effects of various additives on low MW model reactions, the influence of additives on the viscoelastic behaviour of vinylogous urethane based polymer networks was examined. Thus, low  $T_g$  vinylogous urethane networks were prepared by mixing priamine 1074 **5**, tris(2-aminoethyl)amine **6**, acetoacetylated pripol **7** and one of the selected additives from our initial screening study. These soft materials allow stress relaxation experiments at lower temperatures.

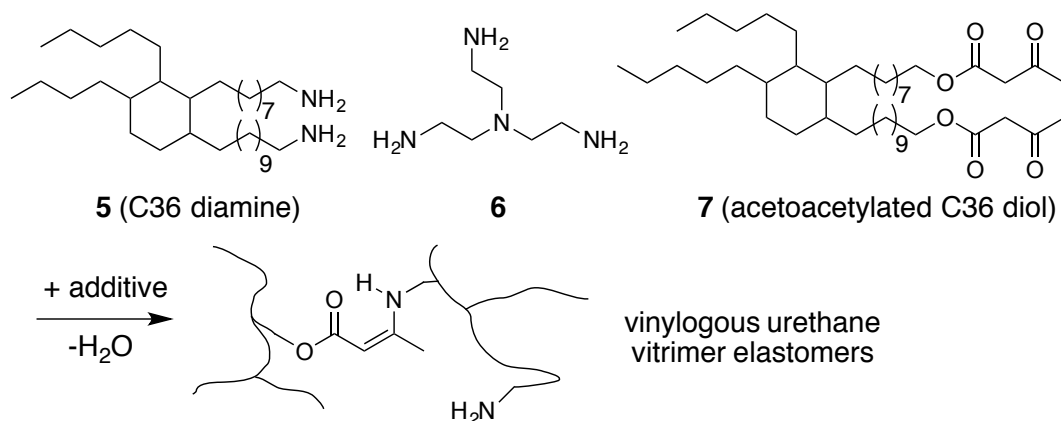


Figure 5.6: Used monomers (priamine **1**, tris(2-aminoethyl)amine **2** and acetoacetylated pripol **3**) for the synthesis of elastomeric vitrimers.

As before, poly VU networks were prepared by the spontaneous condensation reaction between acetoacetates and amines (Figure 5.6), using a small excess of amines versus acetoacetates (a ratio of 100:95) in order to ensure that free amines, required for the exchange reaction, would be available throughout the polymer network. After curing for 6h at 90°C, full conversion of the acetoacetates to the vinylogous urethanes was confirmed by infrared spectroscopy (Figure 5.7a). Moreover, these curing conditions appeared also sufficient to remove all the water released during the condensation reaction as no more mass loss was observed by thermogravimetric analysis (TGA) after 4h (Figure 5.7b). This is in contrast with the higher  $T_g$  networks prepared earlier in chapter 4, where a post curing step at 150°C was required to achieve full curing and complete dryness. The higher chain mobility and more apolar backbone in these flexible elastomer networks is indeed expected to facilitate the loss of water.

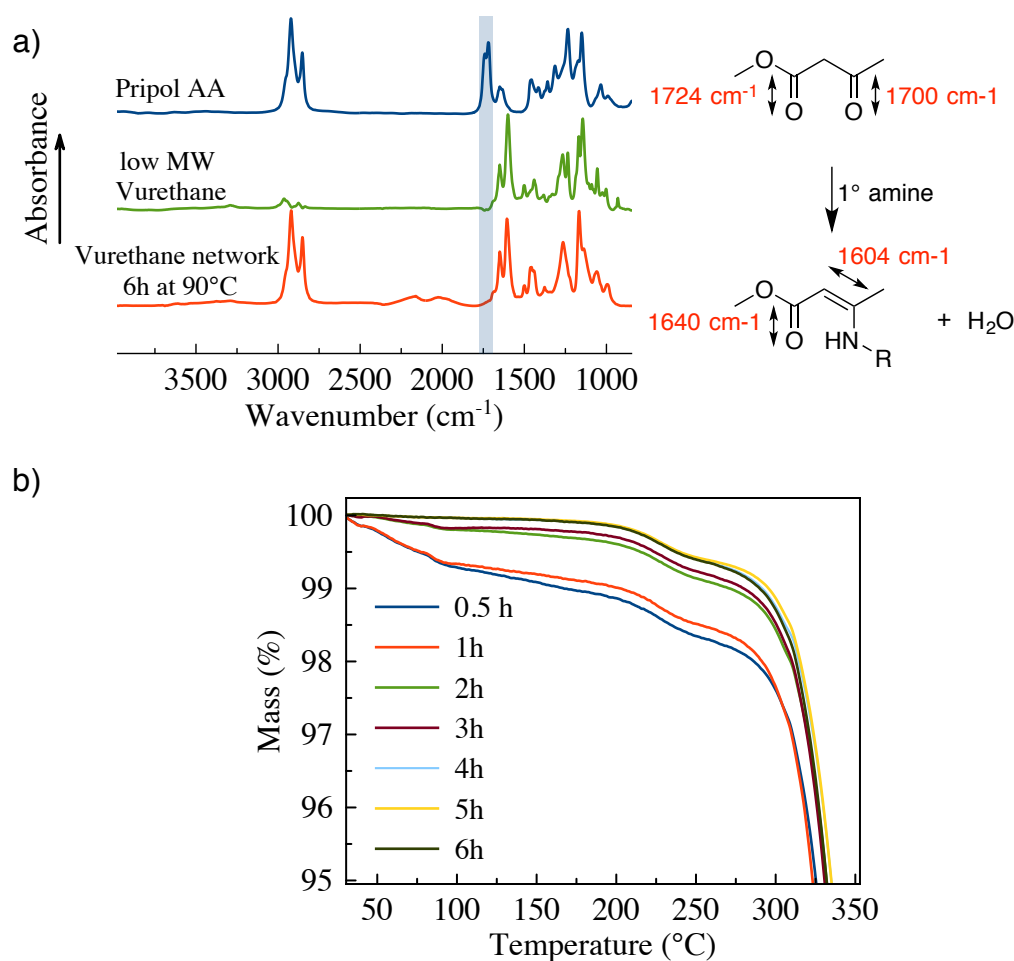


Figure 5.7: a) FT-IR spectra showing the full conversion of pripol-AA **7** to Vurethanes in the network. A low MW Vurethane (N-octyl vinylogous urethane) is shown as reference. b) TGA curves of the polymer as a function of curing time to verify the complete removal of water. After 5h, no more mass loss is observed.

Different monomer stoichiometric ratios were explored to obtain poly-VU networks (Table 5.1). The mechanical properties of the vitrimers prepared according to the above procedure can be tuned over a wide range by simply changing the monomer ratios. With decreasing cross-link density, the glass-transition ranged from  $-9^\circ\text{C}$  to  $-33^\circ\text{C}$ , also modulus and yield stress decreased in the same trend, while the yield elongation increased from 46% up to 255 %. Using a monomer ratio of 0.40:0.40:0.95 of **5:6:7**, a network with a  $T_g$  of  $-25^\circ\text{C}$ , a Young modulus of 2.0 MPa, an elongation at break of 140% and a yield stress of 1.2 MPa was obtained. This intermediate composition was selected for the rheological study with the addition of different catalysts. Next to the ‘uncatalysed’ reference material, four more materials were prepared by simply adding a fixed mol% of the catalyst in relation to the total amount of amine monomer. In order to avoid complete protonation or complexation of all the free amines in the resulting networks, these catalyst loadings were kept well below 5 mol%. For example, 0.5



mol% of *p*TsOH catalyst should result in the protonation of 10% of all the free amines in the final network.

Table 5.1: : Properties of soft VU networks with different compositions.

Equivalents of 5 : 6 : 7	$T_g$ (°C)	$E'$ (MPa) <sup>a</sup>	Young modulus $E$ (MPa) <sup>b</sup>	Yield Elongation (%) <sup>b</sup>	Yield Stress (MPa) <sup>b</sup>
0.00 : 0.67 : 0.95	- 9	3.9	$3.35 \pm 0.01$	$46 \pm 5$	$2.22 \pm 0.25$
0.20 : 0.53 : 0.95	- 20	3.3	$2.34 \pm 0.02$	$65 \pm 7$	$1.74 \pm 0.27$
0.40 : 0.40 : 0.95	- 25	2.2	$1.99 \pm 0.05$	$119 \pm 9$	$1.20 \pm 0.06$
0.60 : 0.27 : 0.95	- 30	1.5	$1.13 \pm 0.02$	$140 \pm 6$	$0.81 \pm 0.05$
0.80 : 0.13 : 0.95	- 33	1.1	$0.64 \pm 0.05$	$255 \pm 35$	$0.55 \pm 0.03$

a) Measured *via* DMA at 50°C. b) Measured *via* tensile testing, average of 4 measurements.

## 5.4 Rheological study

### 5.4.1 Stress-relaxation experiments at elevated temperature

The obtained networks were subjected to stress-relaxation experiments in a rheometer (plate-plate geometry), wherein a deformation of 5% was applied and the decrease of stress was measured over time. This deformation is well within the linear viscoelastic region of the materials according to a strain-sweep experiment. Since the stress-relaxation behaviour of vitrimers can be described by the Maxwell law  $G(t)/G_0 = \exp(-t/\tau)$ , relaxation times were taken when the normalized stress decreased to a value of 0.37 (1/e). The uncatalysed reference network showed a relaxation time of approximately 10 minutes at 120 °C. Addition of 0.5 mol% *p*TsOH versus the total quantity of initial amines in the used monomers (~10 % protonation of the excess amines), shortened the relaxation time to only 2 minutes. As in the low MW model experiments, the influence of 0.25% of H<sub>2</sub>SO<sub>4</sub> and 1.90% DBTL was also significant but less pronounced (Figure 5.8a).

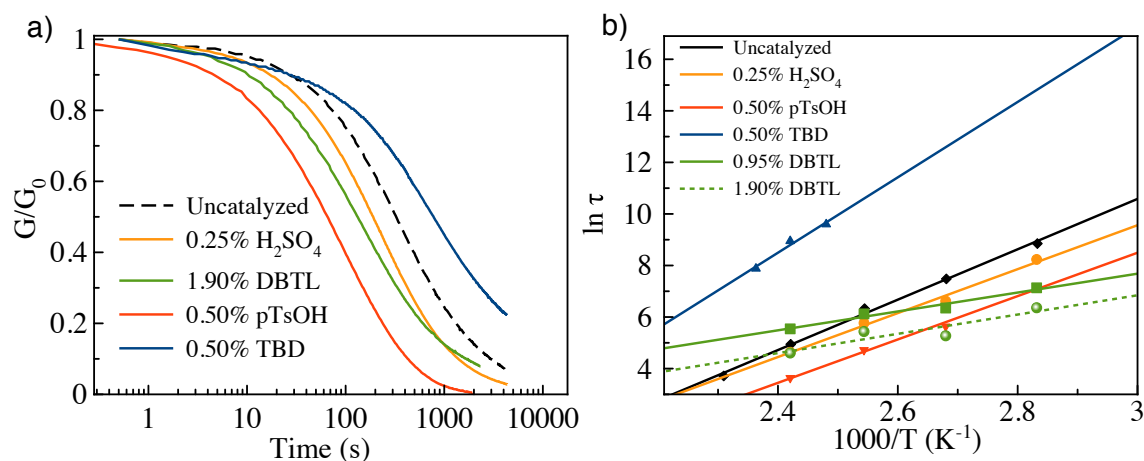


Figure 5.8: a) Stress-relaxation experiment for networks with acid and base additives at 120°C and a deformation of  $\gamma=5\%$ ; b) Arrhenius plot for samples loaded with catalysts. The amount of catalyst was calculated as mol% versus the amine functionalities in the initial monomer mixture.

When the relaxation times measured at different temperatures are examined in an Arrhenius plot, a linear relationship can be observed, which is characteristic for vitrimer materials.<sup>2</sup> The samples containing 0.5% pTsOH exhibit a clear downward shift compared to the uncatalysed samples and again only a small distinction between the activation energies can be observed. They were measured as  $(81 \pm 3)$  for the uncatalysed and  $(70 \pm 4)$  kJ mol<sup>-1</sup> for the sample with 0.5% pTsOH from the slopes of the curves in Figure 5.8b. These values are comparable to those measured for the model compound exchange reactions ( $73 \pm 11$  kJ/mol) and slightly higher than those for the high  $T_g$  vinylogous urethane networks from previous chapter ( $60 \pm 5$  kJ/mol). Possibly, this rise in activation energy is caused by the more hydrophobic matrix wherein long aliphatic chains of priamine **5** and acetoacetylated pripol **7** selectively destabilise the cationic reaction intermediates and transition states.

As in the low MW model study, these results indicate that the same reaction pathway is followed in both the catalysed and ‘uncatalysed’ networks, implicating protonated species as crucial reaction intermediates (see Figure 5.5). The faster reaction rates in the presence of a protic acid is thus the consequence of the higher concentration of active protonated species, as compared to the reference material (Figure 5.5a). On the other hand, the DBTL-loaded samples show a strong decrease in activation energy to  $30 (\pm 4)$  kJ mol<sup>-1</sup>. These observations are again in line with a very different reaction mechanism, such as carbonyl activation of the vinylogous urethane by Lewis acid complexation (Figure 5.5b), wherein the

concentration of protonated species is inconsequential. Remarkably, the DBTL catalyst also acts as an inhibitor of the ‘protic’ pathway, as above a certain temperature the relaxation becomes slower than in the uncatalysed version. Carboxylate anions can indeed act as proton scavenger for ammonium species in non-aqueous media, giving lower concentrations of alkyl ammonium species.

Because of the decreased slope in the Arrhenius plot, the DBTL-catalysed exchange reaction remains more significant at lower temperatures with this catalyst (lower  $T_v$ ). Conversely, the samples inhibited with the guanidine base TBD showed an increased slope and a significantly elevated activation energy of  $(122 \pm 19)$  kJ mol<sup>-1</sup>, again pointing to a very different mechanism, not involving addition/elimination reactions to protonated intermediates, but rather going through a direct addition pathway of a neutral amine to a neutral VU (Michael addition). This zwitterionic pathway is much slower but can become fast at higher temperatures (Cfr. Figure 5.5c).

#### 5.4.2 Comparison mechanical and molecular relaxation

At the end of chapter 4, we made the observation that the vinylogous urethane vitrimers prepared there achieved full-stress relaxation after only 15 minutes at 140°C, while the model compound study in chapter 3 required 90 minutes at the same temperature before an equilibrium state was obtained. This difference in mechanical and chemical relaxation times was rationalised by the much lower concentration of VU used in the model compounds. Since no dilution was used in the model compound study presented above and a Vurethane to amine ratio of 5:1 was used, which matches the 19:1 ratio used in the materials already better compared to the 1:5 ratio used previously, an improved correlation is expected. Indeed, as depicted in Figure 5.9, a good quantitative and qualitative agreement is observed between the mechanical and molecular relaxation. Obviously, the remark can be made that the catalyst loadings of model compounds and materials are not identical and the correlations could be a coincidence. Nevertheless, the observed timescales are in good agreement and are another proof that the dynamic behaviour is caused by the exchange reactions within the network. In light of the now revealed role of protonated species in the reaction mechanism of uncatalysed networks, it is also not surprising that the exchange reaction proceeds much slower in a hydrophobic solvent (benzene) as compared to bulk conditions of VU/amine with a lot of hydrogen bond acceptors.

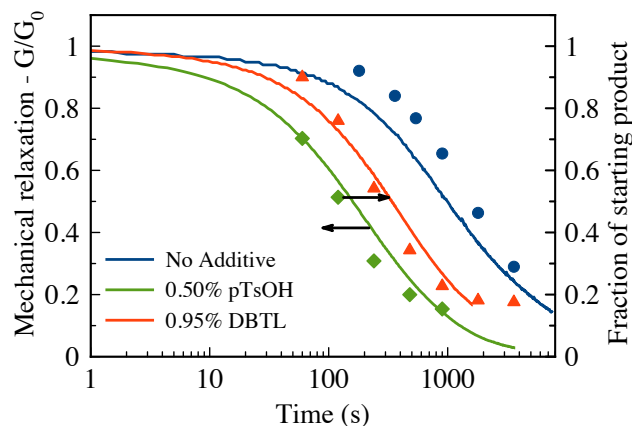


Figure 5.9: Comparison of the conversion of the model compound (dots, right axis) with the mechanical stress-relaxation (full line, left axis) caused by the uncatalysed, *p*TsOH and DBTL catalysed exchange reactions at 100°C, both in the case of model reactions and VU vitrimer samples.

### 5.4.3 Room-temperature stress-relaxation

In order to investigate the possibility of exchange reactions at room temperature and thus the resistance or susceptibility to creep in these elastomers, further stress-relaxation experiments (small deformation,  $\gamma=5\%$ ) and compression set experiments (large deformation, 25% compression) were conducted at 30°C. In the stress-relaxation tests, the uncatalysed reference sample, together with the 0.50% *p*TsOH and 0.50% TBD-catalysed sample, relaxed approximately 10% of the initial stress after six hours (Figure 5.10). Such partial relaxation is not uncommon, even for classical elastomers,<sup>7</sup> in particular when considering the intentionally installed network defects in these materials.<sup>7</sup> Looking back to this experiment, a recovery step at the end of the creep-experiment would be interesting to assess the real permanent deformation.

Thus, while *p*TsOH significantly enhances network rearrangements at elevated temperature, it does not lead to increased stress relaxation at 30°C. On the other hand, vitrimer elastomers loaded with DBTL exhibited a strong stress-relaxation, indicating significant network rearrangements at room temperature. Indeed, as anticipated, due to the low activation energy, the reaction is not sufficiently decelerated at 30°C in order to effectively freeze the network topology, making this catalyst less interesting to use in elastomeric vitrimers (cf. Figure 5.8b).

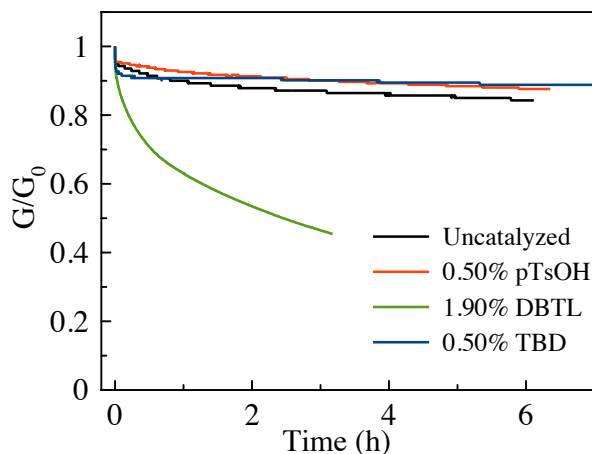


Figure 5.10: Room temperature stress-relaxation experiments.

In the compression set experiments, samples were compressed to 75% of their initial thickness for 24h at 30°C. After removal of the applied deformation and recovery time of 30 minutes, samples were measured again and compared to the initial thickness. The samples without additive and with 0.5% pTsOH had a medium and largely comparable compression set resistance with a permanent deformation of 38 and 43% respectively (Figure 5.11).

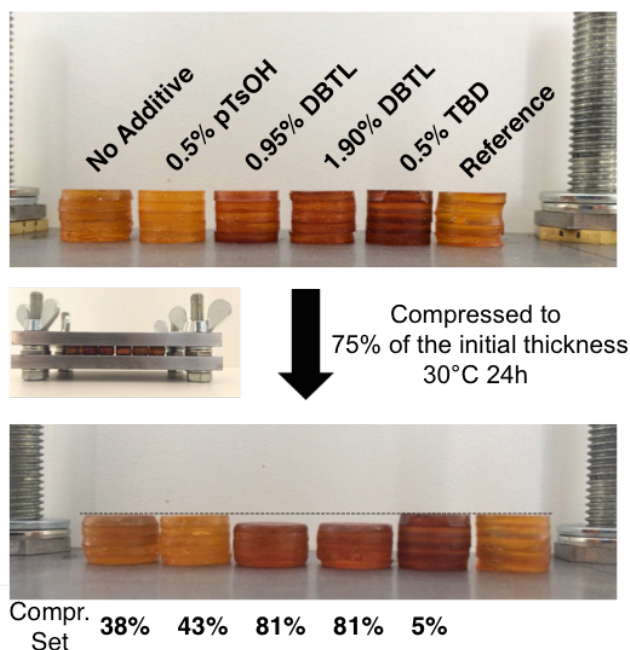


Figure 5.11: Compression set experiment of elastomer vitrimers with different catalysts.

In agreement with the stress-relaxation experiments, the samples with DBTL showed a much larger permanent deformation of 81%, indicating a very extensive

stress-relaxation. Interestingly, TBD-loaded samples showed excellent resistance towards compression as they almost completely returned to their initial position and performed like a true elastomer (only 5% permanent deformation), which can nevertheless be processed at elevated temperatures albeit over a longer time.

#### 5.4.4 What would be the preferred catalyst?

After the rheology and creep measurements presented above, one could wonder which catalyst would be the best choice for these vitrimer elastomer materials. Ideally, fast processing should be achieved at temperatures above 100°C while the exchange reaction should slow down upon cooling to room temperature to a negligible rate, making the material essentially a fixed network. This latter condition can also be quantified with the vitrification temperature  $T_v$  that indicates the temperature at which a viscosity of  $10^{12}$  Pa.s is reached, and is also conventionally used in vitrimers as the transition between a solid and liquid state.<sup>2</sup>

From the data in Figure 5.8, for different catalysts in a VU elastomer, the activation energies and  $T_v$ 's can be calculated and are tabulated in table 1. From these, it can be concluded that the  $T_v$  of the same vitrimer network can be varied over a huge temperature range of 150°C by simply changing the added catalyst. As observed experimentally, DBTL has the lowest resistance to creep, corresponding with its (calculated)  $T_v$  of -63 and -70°C for a catalyst loading of respectively 0.95% and 1.90%. Thus, at service temperature, this elastomer behaves as a viscous liquid. On the other hand, the protic acid catalysed Vurethane vitrimers exhibit a higher activation energy (similar to the uncatalysed sample) but a much faster exchange reaction. Thus, in this system the improved processability only has a relatively small trade-off in creep-resistance. In any case, while this moderate creep-resistance is rather undesired for most elastomer applications, the improved processability (faster stress relaxation) is interesting for high  $T_g$  vitrimer thermoset materials (*vide infra*). Finally, the samples loaded with TBD showed excellent creep-resistance but also have a poor processability. In an ideal scenario, the  $T_v$  of the material could be lowered somewhat to allow processing at a reasonable temperature while preventing room temperature creep.

Table 5.2: Summary of the obtained activation energies and calculated  $T_v$ 's of the Vurethane vitrimers..

Catalyst	$E_a$ (Kj mol <sup>-1</sup> )	$T_v$ (°C)
Uncatalysed	81 ± 3	27
0.50% pTsOH	70 ± 4	-1
0.25% H <sub>2</sub> SO <sub>4</sub>	70 ± 5	10
0.95% DBTL	30 ± 4	-63
1.90% DBTL	31 ± 10	-70
0.50% TBD	122 ± 19	87

#### 5.4.5 Triggered release of a base?

One practical way to combine a fast processability with good creep resistance would be offered via the incorporation of a photobase in the Vurethane polymer. Such a photobase is a compound that is transformed to a base after irradiation. In this fashion, fast processing would be possible until irradiation with UV, which would liberate a base that sequesters all ammonium species and thus slows down the exchange reaction to a non-cationic pathway, effectively fixing the network topology at room temperature. We briefly explored this possibility, in which photobase **8** was selected (For synthetic procedure, see 5.6.7 p.134), a photolabile precursor of the strong amidine base DBN ( $pK_a=13.5$  of  $BH^+$ ). The intrinsically weak C-N bond in an alkylated aminal **8** (Figure 5.12a) can undergo homolytic cleavage followed by hydrogen abstraction of the stabilized radical resulting in 1,5-diazabicyclo[4.3.0]non-5-ene **9** (DBN) and 2-(1-methyl ethenyl) naphthalene **10**.<sup>8</sup>

While this approach was considered and the photobase was synthesised, it was observed that also Vurethanes show a strong UV absorption. Unfortunately, the absorption of Vurethanes is not only in the same region of the photobase, but also even stronger (Figure 5.12b). Realising that the photobase would be present in small quantities surrounded by a Vurethane matrix, this approach was considered not feasible for bulk samples and thus not pursued any further. For thin samples/coatings and more UV-transparent matrices such as polydimethylsiloxanes (PDMS) cross-linked with Vurethanes, this approach could remain interesting.

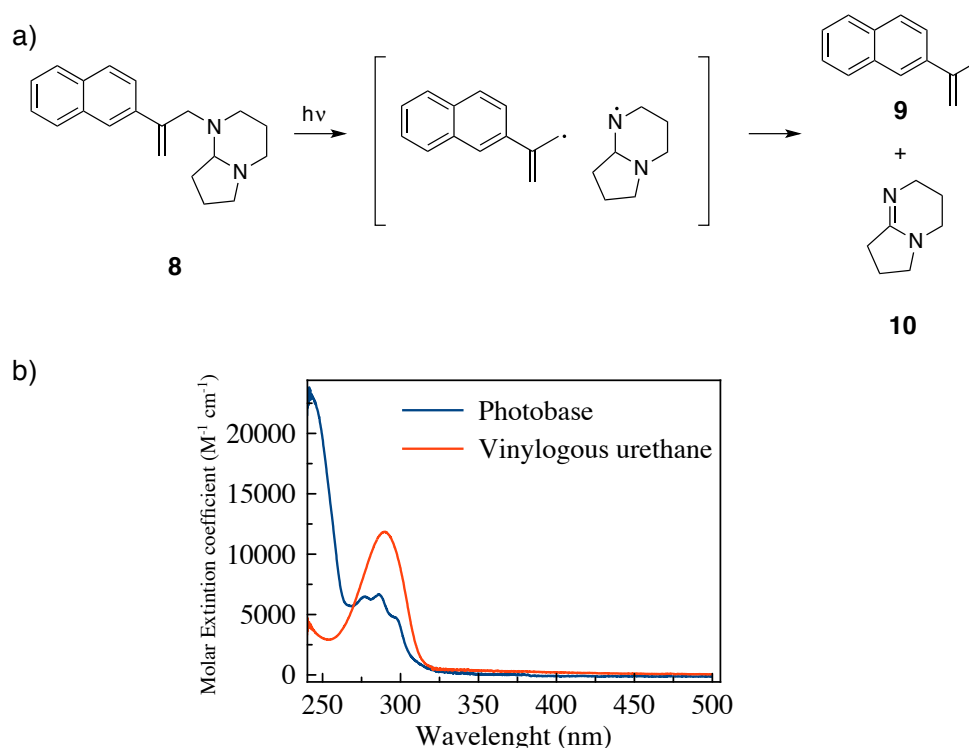


Figure 5.12. a) Irradiation of photobase **8** results in a decomposition with the release of DBN **10**, a strong base. b) Extinction coefficient as a function of the wavelength for Vurethanes and photobase **8** reveals an overlapping UV-absorption of both compounds.

#### 5.4.6 Catalysed vinylogous urethane networks with high $T_g$

Finally, to demonstrate that the catalytic control of VU vitrimers is not limited to elastomeric networks and that also faster stress-relaxations can be achieved in high  $T_g$  VU networks using catalysts, the same rigid VU networks as discussed in chapter 4 were prepared with addition of 0.5 % *p*TsOH ( $T_g = 87\text{ }^\circ\text{C}$ ,  $E' = 2.4\text{ GPa}$  at  $30\text{ }^\circ\text{C}$ ). Stress-relaxation experiments were conducted in torsion geometry<sup>9</sup> with a deformation of 1 % and compared to the uncatalysed samples. Similar to the elastomeric networks, a much faster stress-relaxation can be observed, again without a significant change in activation energy (Figure 5.13a and b). Interestingly, relaxation times as short as 10 seconds at  $160\text{ }^\circ\text{C}$  were measured for the acid catalysed samples. Such fast stress-relaxation enables processing similar to vitreous glass. For example, analogous to making capillary tubes from a pipette in a flame, fusilli shaped samples were prepared from a flat bar in approximately



one minute, via uncontrolled heating with a heat gun ( $100^{\circ}\text{C} < T < 150^{\circ}\text{C}$ ) and a couple of clamps (Figure 5.13c).

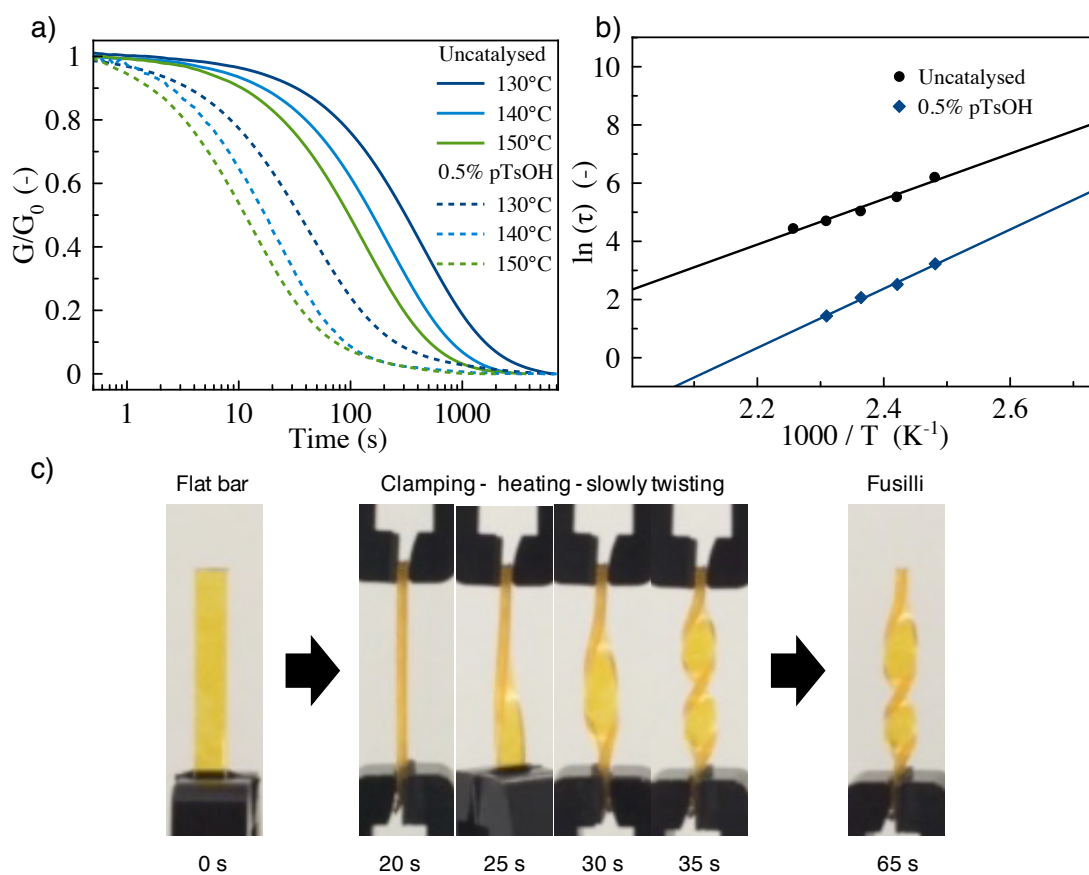


Figure 5.13: a) Stress-relaxation experiments of an uncatalysed and catalysed hard Vurethane sample. b) Arrhenius plot of the relaxation times. c) Twisting of a flat bar to a fusilli-shape using a heat-gun and clamps with an indication of the time needed to perform the actions below the pictures.

Although relaxation times are shortened significantly and a large enhancement in terms of processability is achieved, the lowest viscosity reached is  $3.1 \cdot 10^7$  Pa.s at  $160^{\circ}\text{C}$ . While this already comes close to the viscosity range of thermoplastics, it remains an order of magnitude too high to process these materials with typical thermoplastic methods such as extrusion.

## 5.5 Conclusions and perspectives

In summary, we showed that VU amine exchange could be easily controlled using acid and base additives on both low-MW compounds and polymer networks. A close correlation between model reactions and mechanical relaxations was

observed, confirming that simple model experiments enable the rational design of vitrimers with predictable and tunable viscoelastic behaviour.<sup>2</sup>

Addition of acids increased the exchange rate and allowed for faster processing while a strong base such as TBD decreases the exchange rate. Furthermore, addition of a Lewis acid also increased the exchange rate but resulted in a significant decrease of the activation energy, which is unwanted as it also introduces creep at service temperature. *p*TsOH proved to be the best performing catalyst as it shortened the relaxation times strongly at elevated temperature and performed only slightly worse than an uncatalysed sample at room temperature. In an attempt to combine fast processing with complete dimensional stability at room temperature after trigger, an approach using a photobase was evaluated. Unfortunately, the maximal UV-absorption of the Vurethane and the photobase appeared to be in the same region, rendering this approach not feasible for this kind of materials.

Finally, this approach was extended to hard Vurethane vitrimer samples and resulted in strongly reduced relaxation times, as short as 10 s at 160°C. These short relaxation times enabled fast processing similar to glass but remains an order of magnitude too high for extrusion.

## 5.6 Experimental

### 5.6.1 Materials

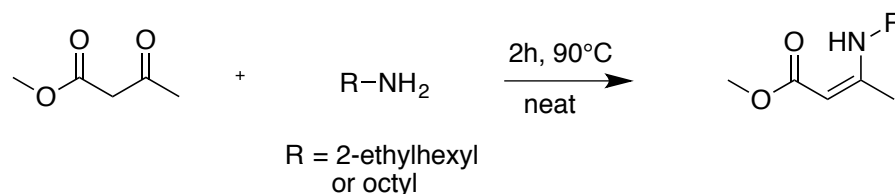
2-Ethyl hexylamine (98%), methylacetoacetate (99%), octylamine (99%), tert-butyl acetoacetate (98%), triazabicyclodecene (98%), tris(2-aminoethyl)amine (96%), sulfuric acid (95-98 %) and *p*-toluene sulfonic acid (98%) were purchased from Sigma Aldrich. Pripol 2044 and priamine 1074 were kindly provided by Croda.

### 5.6.2 Instrumentation

Nuclear magnetic resonance spectra were recorded on a Bruker Avance 300 at room temperature. IR spectra were collected using a Perkin-Elmer Spectrum1000 FTIR infrared spectrometer with a diamond ATR probe. Thermogravimetric

analyses were performed with a Mettler Toledo TGA/SDTA851e instrument under air or nitrogen atmosphere at a heating rate of 10 °C min<sup>-1</sup> from 25 °C to 500 °C. Differential scanning calorimetry (DSC) analyses were performed with a Mettler Toledo instrument 1/700 system under nitrogen at a heating rate of 10 °C min<sup>-1</sup>. Dynamic mechanical analysis (DMA) was performed on a SDTA861e DMA from Mettler Toledo. For the low  $T_g$  samples, stress-relaxation experiments were conducted on a Anton-Paar physica MRC 301 rheometer with a plate-plate geometry of 25 mm and a strain of 5%. Rheology-experiments of the hard samples were performed on a Ares G2 rheometer from TA-instruments (used from the MMC-group, EPSCI) in torsion geometry with samples of dimension (1.3 x 14.5 x 22)<sup>3</sup> using an axial force of -0.01 N and a deformation of 1 %. GC-FID was performed on an Agilent 7890A system equipped with a VWR Carrier-160 hydrogen generator and an Agilent HP-5 column of 30 m length and 0.320 mm diameter. A FID detector was used and the inlet was set to 250°C with a split injection of ratio 25:1. Hydrogen was used as carrier gas at a flow rate of 2 mL/min. The oven temperature was increased with 20°C/min from 50°C to 120°C, followed by a ramp of 50°C/min. to 300°C.

### 5.6.3 Synthesis of methyl-3-(octylamino)but-2-enoate and methyl-3-((2-ethylhexyl)amino)but-2-enoate

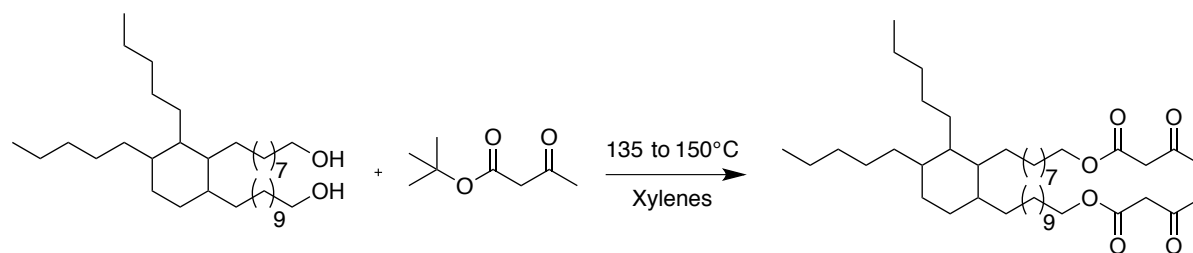


Methyl acetoacetate (1.0 equiv.) and 2-ethyl hexylamine or octylamine (1.1 equiv.) were mixed in bulk and heated for 2h at 90°C while purging with N<sub>2</sub> to remove H<sub>2</sub>O. The excess of amine was removed by passing the mixture over a short silica column using ethyl acetate as an eluent.

Yield methyl-3-(octylamino)but-2-enoate: 99%. <sup>1</sup>H NMR (300 MHz, CDCl<sub>3</sub>): δ (ppm) = 0.88 (t, 3H,  $J$  = 7.3 Hz, CH<sub>3</sub>CH<sub>2</sub>-), 1.26-1.38 (m, 9zH, -CH<sub>2</sub>-), 1.51-1.59 (m, 2H, -NHCH<sub>2</sub>CH<sub>2</sub>CH<sub>2</sub>-), 1.91 (s, 3H, CH<sub>3</sub>C=), 3.19 (td,  $J$ =7.00 and 5.87, 2H, -NHCH<sub>2</sub>CH<sub>2</sub>-), 3.60 (s, 3H, CH<sub>3</sub>O-), 4.44 (s, 1H, -COCH=), 8.55 (br s, 1H, NH) ppm. HR-MS(ESI): calculated for C<sub>13</sub>H<sub>26</sub>NO<sub>2</sub><sup>+</sup> [M+H]<sup>+</sup> 228.1958; found 228.1966.

Yield methyl-3-((2-ethylhexyl)amino)but-2-enoate: 99%  $^1\text{H}$  NMR (300 MHz,  $\text{CDCl}_3$ ):  $\delta$  (ppm) = 0.72 (t,  $J=7.2$ , 3H,  $\text{CH}_3\text{CH}_2-$ ), 0.85 (t, 3H,  $\text{CH}_3\text{CH}_2-$ ), 1.17 (m, 9H, 4x $\text{CH}_2$ , 1x $\text{CH}$ ), 1.47 (s, 3H,  $\text{CH}_3\text{C}-$ ), 2.70 (t, 2H,  $-\text{NHCH}_2\text{CH}-$ ), 3.56 (s, 3H,  $\text{CH}_3\text{O}-$ ), 4.76 (s, 1H,  $-\text{COCH=}$ ), 9.08 (br s, 1H,  $-\text{NH}-$ ). HR-MS(ESI): calculated for  $\text{C}_{13}\text{H}_{26}\text{NO}_2^+$   $[\text{M}+\text{H}]^+$  228.1958; found 228.1968.

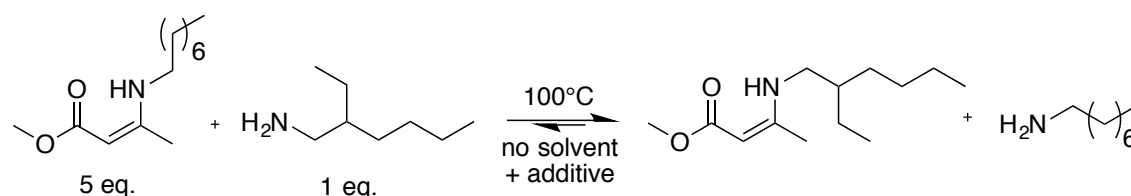
#### 5.6.4 Acetoacetylation of pripol2033



Pripol 2033 (10.0 g, 1 equiv.) and tert-butylacetoacetate (6.71 g, 2.3 equiv.) were dissolved in 8.5 mL xylene and 5.5 mL hexane. The mixture was heated to 135°C in a distillate set-up until the temperature of the vapor dropped below 63°C. Then the heat was turned up to 150°C until no more solvent was transferred into the receiving flask. The remainder of the solvent was removed under high vacuum at 80°C raised until 100°C, yielding the desired product. No further purification was required.

Yield: 98%.  $^1\text{H}$  NMR (300 MHz,  $\text{CDCl}_3$ ):  $\delta$ (ppm) = 0.79 (m, 6H,  $\text{CH}_3\text{CH}_2-$ ), 1.19 (m,  $\text{CH}_2$ ), 1.57 (m, 4H,  $\text{CH}$  ring), 2.20 (s, 6H,  $\text{CH}_3(\text{CO})-$ ), 3.38 (s, 6H,  $-(\text{CO})\text{CH}_2(\text{CO})-$ ), 4.06 (t, 4H,  $-\text{CH}_2\text{CH}_2\text{O}-$ )

#### 5.6.5 Model compound study



The *N*-octyl vinylogous urethane (5 equiv.) was mixed together with 2-ethyl hexylamine (1 equiv.), dodecane (Internal standard, 0.5 equiv.) and the catalyst (see table 1) in a test tube. The resulting mixture was heated at 100°C. At

specified time intervals, samples (~10 mg) were taken and immediately diluted in dichloromethane. The ratio of 2-ethylhexyl amine (3.41 min) and octyl amine (3.67 min) was analysed using GC-FID.

Table 5.3: Used equivalents of catalyst for the model compound study

Catalyst	Equivalents
No additive	/
<i>p</i> -Toluene sulfonic acid	0.01
Triazabicyclodecene	0.01
Dibutyl tin dilaureate	0.025
Sulfuric acid	0.005

### 5.6.6 Synthesis of soft vitrimer networks

Priamine 1074, TREN and acetoacetylated pripol were weighed in this given sequence in a vial. The resulting biphasic system was then manually mixed until a homogeneous mixture was obtained. The mixture was poured on a Teflon sheet and manually spread to thickness of around 1 mm and heated for 6 h at 90 °C. The obtained films were compression moulded for 30 minutes at 150°C to get fully homogeneous, defect-free samples (Figure 5.14).

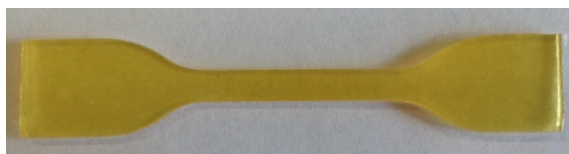


Figure 5.14: dog-bone sample that was cut out from a press-moulded sample.

Table 5.4: Equivalents and amounts used to prepare samples for the rheological measurements.

Reagents	Eq	N (mol)	MW (g/mol)	m (g)
Pripol AA	0.95	0.0211	710.00	15.00
TREN	0.40	0.0089	146.23	1.30
Priamine	0.40	0.0089	547.00	4.86

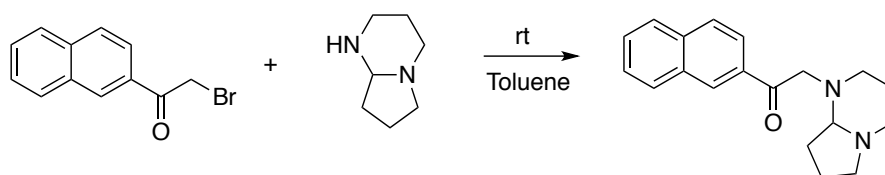
For the catalysts, equivalents were calculated as mol% versus the amines of the monomer mixture: pTsOH (0.5%, 0.18 m%): 0.038 g, H<sub>2</sub>SO<sub>4</sub> (0.25%, 0.05 m%): 0.011 g, DBTL (0.95%, 1.2m%): 0.267 g, DBTL (1.9%, 2.4 m%): 0.534 g

TBD was incorporated *via* swelling. The samples were swollen during 15 minutes in DCM in which 14.6 mg/mL TBD was dissolved. The solvent was removed *in vacuo* overnight.

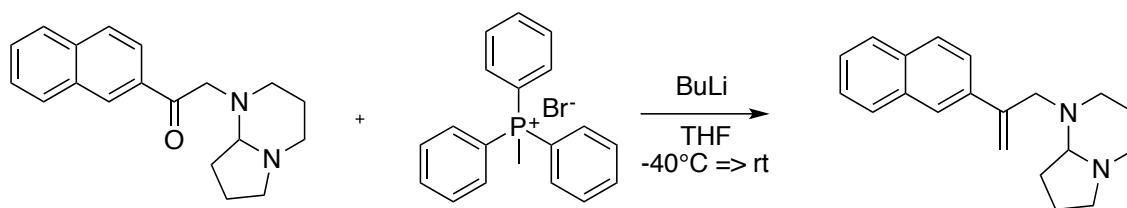
### 5.6.7 Synthesis photobase 8

This compound was prepared using an adapted procedure reported by Turner *et al.*<sup>10</sup>

#### Step 1



2-Bromo-1-(naphthalen-2-yl)ethan-1-one (1.00 g, 4.0 mmol) was dissolved in 5 mL dry THF and added to a solution of 1,5-diazabicyclo[4.3.0]nonane (1.00 g, 8.0 mmol) in 5 mL dry THF. The mixture was stirred overnight at room temperature, filtered, washed with demineralized water and dried over MgSO<sub>4</sub>. The resulting mixture is further purified via column chromatography using DCM/petroleumether/TEA (50:49:1) as eluent, yielding the desired  $\alpha$ -amine ketone as an oil (yield = 80 %).

**Step 2**

A solution of methyl triphenylphosphonium bromide (2.42 g, 6.79 mmol) in tetrahydrofuran (5 mL) was cooled to  $-30^{\circ}\text{C}$  and then a solution of *n*-butyllithium in *n*-hexane (2.5 M, 2.7 mL, 6.79 mmol) was added drop wise to the reaction mixture at  $-30^{\circ}\text{C}$ . The resulting bright yellow suspension was gradually warmed to  $-10^{\circ}\text{C}$  over 30 minutes. The reaction mixture was then cooled again to  $-30^{\circ}\text{C}$  before a solution of  $\alpha$ -amine ketone from previous step (1.00 g, 3.42 mmol) in tetrahydrofuran (6 mL) was added dropwise. The resulting mixture was gradually warmed to room temperature over 1 hour and stirred overnight at room temperature. The resulting mixture was purified via column chromatography using DCM/petroleumether/TEA (50:49:1) as eluent yielding the desired product as a brown oil (0.313 g, 31%) in accordance with literature.<sup>10</sup>

Yield: 31%, 0.313 g.  $^1\text{H}$  NMR (300 MHz,  $\text{CDCl}_3$ ):  $\delta$  = 7.97 (s, 1H, ArH), 7.85-7.65 (4H, m, ArH), 7.45-7.35 (2H, m, ArH), 5.59 (s, 1H, =CH), 5.41 (s, 1H, =CH), 3.88 (1H, d,  $J$ =13.6,  $\text{NCH}_2\text{CH}_2\text{CH}_2$ ), 3.07 (3H, m,  $-\text{NCH}_2$ ), 2.97 (1H, d,  $J$  = 13.7 Hz,  $\text{NCH}_2\text{C}(\text{CH})\text{Ph}$ ), 2.44-1.45 (10H, m, ring  $\text{CH}_2$ ),

**5.6.8 Synthesis of hard vitrimer networks**

*m*-Xylylene diamine (2.111 g, 15.5 mmol), tris(2-aminoethyl)amine (1.774 g, 12.1 mmol), and 1,4-cyclohexanedimethanol bisacetoacetate (10.000 g, 32.0 mmol) and pTsOH (0.5 mol% versus amines) were mixed in a vial and heated in an oil bath thermostated at  $80^{\circ}\text{C}$ . When a homogeneous liquid mixture was obtained, the mixture was taken out of the oil bath while keeping mixing manually. After 2 min, the mixture turned white due to phase separation (water release of the condensation reaction). The resulting white paste was taken out of the vial and pressed into a film of 1.3 mm between two Teflon sheets using a press preheated at  $90^{\circ}\text{C}$ . After 30 min, the film was transferred into a convection oven and dried during 24 h at  $90^{\circ}\text{C}$ , followed by a short post-curing process of 30 min at  $150^{\circ}\text{C}$ .

### 5.6.9 Compression set experiments

Compression set experiments were conducted according to ASTM D395. Disk shape samples with a diameter of 12 mm were cut out and five of these samples were stacked together. These samples were all compressed to exactly the same thickness of 9.21 mm and heated for 2h at 140°C, resulting in samples with exactly the same height. Next, the samples were compressed to 6.9 mm using a spacer (i.e. 76% of its initial thickness) and are put into an air-circulated oven for 24h at 30°C. After this period, the specimens are removed from the fixture and after 30 minutes, their heights are measured. Compression set was calculated using the formula: Compression Set =  $\{(\text{orig. thickness} - \text{final thickness}) / (\text{orig. thickness} - \text{spacer thickness})\} * 100\%$ .

## 5.7 References

- (1) Capelot, M.; Montarnal, D.; Tournilhac, F.; Leibler, L. *J. Am. Chem. Soc.* **2012**, *134*, 7664.
- (2) Montarnal, D.; Capelot, M.; Tournilhac, F.; Leibler, L. *Science* **2011**, *334*, 965.
- (3) Capelot, M.; Unterlass, M. M.; Tournilhac, F.; Leibler, L. *ACS Macro Lett.* **2012**, *1*, 789.
- (4) Lei, Z. Q.; Xiang, H. P.; Yuan, Y. J.; Rong, M. Z.; Zhang, M. Q. *Chem. Mater.* **2014**, *26*, 2038.
- (5) Cash, J. J.; Kubo, T.; Bapat, A. P.; Sumerlin, B. S. *Macromolecules* **2015**, *48*, 2098.
- (6) Denissen, W.; Rivero, G.; Nicolaÿ, R.; Leibler, L.; Winne, J. M.; Du Prez, F. E. *Adv. Funct. Mater.* **2015**, *25*, 2451.
- (7) Imbernon, L.; Norvez, S.; Leibler, L. *Macromolecules* **2016**, *49*, 2172.
- (8) Suyama, K.; Shirai, M. *Prog. Polym. Sci.* **2009**, *34*, 194.
- (9) Dessi, C.; Tsibidis, G. D.; Vlassopoulos, D.; De Corato, M.; Trofa, M.; apos; Avino, G.; Maffettone, P. L.; Coppola, S. *Journal of Rheology* **2016**, *60*, 275.
- (10) Turner, S. C.; Baudin, G. Photoactivatable nitrogen-containing bases based on alpha-amino alkenes. *CA 2 283 446*, 1998





## **Abstract**

In this chapter, Vurea were examined for their potential in vitrimer materials. An initial assessment of thermal stability of different Vurea moieties indicated that Vurea prepared by acetoacetylation of secondary amines have superior thermal stability. Based on these results, Vurea networks were prepared by mixing piperazine acetoacetamide **7**, 1,6-hexane diamine and TREN and were characterised in detail. Simultaneously, the effect of an acid catalyst (0.5 mol% pTsOH) was evaluated. The properties of both networks proved to be good ( $T_g \sim 110^\circ\text{C}$ ,  $E \sim 2.2$  Gpa) and the acid catalysed-networks showed very short relaxation times, in the order of seconds. In a final part of this chapter, Vurea based composites were prepared in collaboration with the MMS-research group (Ughent) and evaluated as enduring preregs. Furthermore, also a proof-of-concept of thermoforming and fibre-recuperation was provided.

## **Published in:**

Denissen, W. Winne, J. M.; Du Prez, F.E., Nicolaÿ, R.; Leibler, L.; Composition comprising a polymer network. WO/2016/097169

## Chapter 6

# Vinylogous urea vitrimers

### 6.1 Introduction

In chapter 3, the transamination of three different classes of enaminones was examined via a model compound study. These studies indicated that vinylogous urea (Vurea) exhibited the fastest transamination kinetics of these enaminones. When a Vurea compound was mixed with an amine, full exchange equilibrium was typically reached after 90 minutes at 25°C, even under strongly diluted conditions. This fast exchange is a remarkable contrast with the vinylogous urethanes that needed temperatures above 100°C to undergo fast exchange as discussed in the previous two chapters.

With the purpose to obtain vitrimers with mechanical properties comparable to conventional thermosets, and a processability that could compete with those of thermoplastics, a very fast exchange reaction is required. In fact, the low-MW studies suggested that Vurea would be the most interesting of all enaminones, at least in high T<sub>g</sub> materials where exchange reactions are blocked by topological freezing below a certain temperature. The critical reader might thus question why the more slowly exchanging vinylogous urethanes (Vurethanes) were first examined or at least discussed in this text. Actually, Vurea were the first enaminone moieties explored on a polymer level in this doctoral research, but due to thermal stability problems observed in the initially obtained materials, the focus of our research efforts shifted to Vurethanes, which did not show thermal stability issues in similar materials. Following our in-depth study of Vurethanes, gaining valuable insights and experiences, we remained intrigued by the fast kinetics of Vurea and their potential for the processability of vitrimers. Our focus then returned to the limited thermal stability with the aim to find a solution. Consequently, this chapter will first discuss the exploratory experiments that revealed the limited thermal stability of Vurea and compare this to Vurethanes, followed by a more detailed discussion of our efforts to increase the thermal stability of Vurea materials.

Finally, as mentioned in the introduction, one of the envisaged applications of vitrimers is situated in the field of composites. At the end of this chapter, some Vurea composites will also be reported, providing a proof-of-concept for such applications.

## 6.2 First exploratory experiments on Vinylogous urea polymers

In our approach to prepare Vurea networks, 1,6-hexane diamine **1** and tris(2-amineoethyl)amine **2** (TREN) were mixed with the commercially available *N,N*-(ethylenediamine)bis-(acetoacetamide) **3** (Figure 6.1a). This mixture was heated to 100°C, together with a minimal amount of water as a solvent to achieve a homogeneous mixture, which transformed rapidly to a white ‘mozzarella’-like substance due to phase-separation of the formed polymer and the released water of the condensation reaction. After curing 3h at 150°C under vacuum, a hard, light yellow, foamy sample was obtained. As a reference material, also a similar Vurethane network was prepared by mixing *m*-xylylene diamine **4**, TREN **2** and ethyleneglycol-bis(acetoacetate) **5**, which are all liquid and did not require the addition of solvent to achieve good mixing. The flexible 1,6-diamino hexane **1** was purposely replaced by the more rigid *m*-xylylene diamine **4** to compensate for the loss of hydrogen-bonds that would result in a decrease of the  $T_g$ .

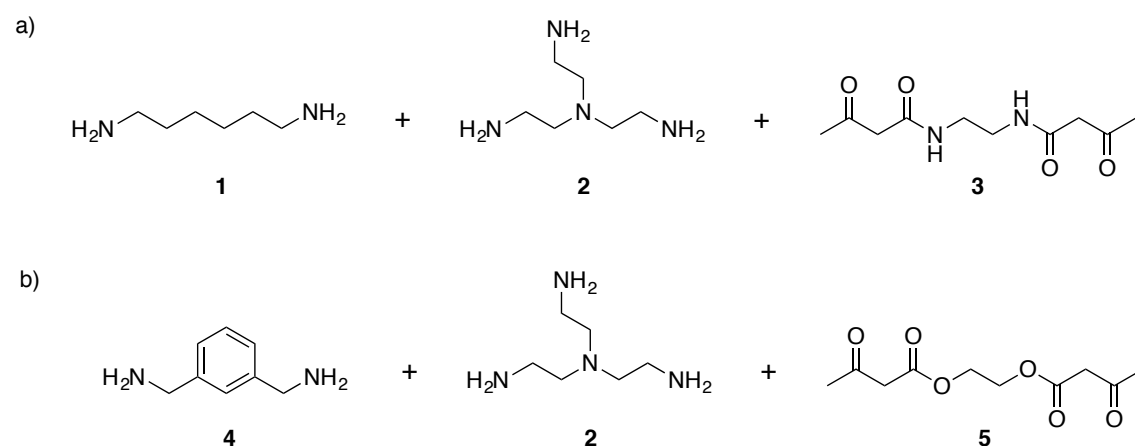


Figure 6.1: a) Used monomers for the preliminary examination of Vurea networks. b) Monomers used for Vurethane networks as a reference.

According to IR-analysis, full conversion of the acetoacetamides to the corresponding Vurea functionality was achieved after curing 3h at 150°C under vacuum. Indeed, the C=O ketone band at 1709 cm<sup>-1</sup> completely disappeared and a

good match between the Vurea polymer and a Low-MW Vurea-reference compound could be observed (Figure 6.2).

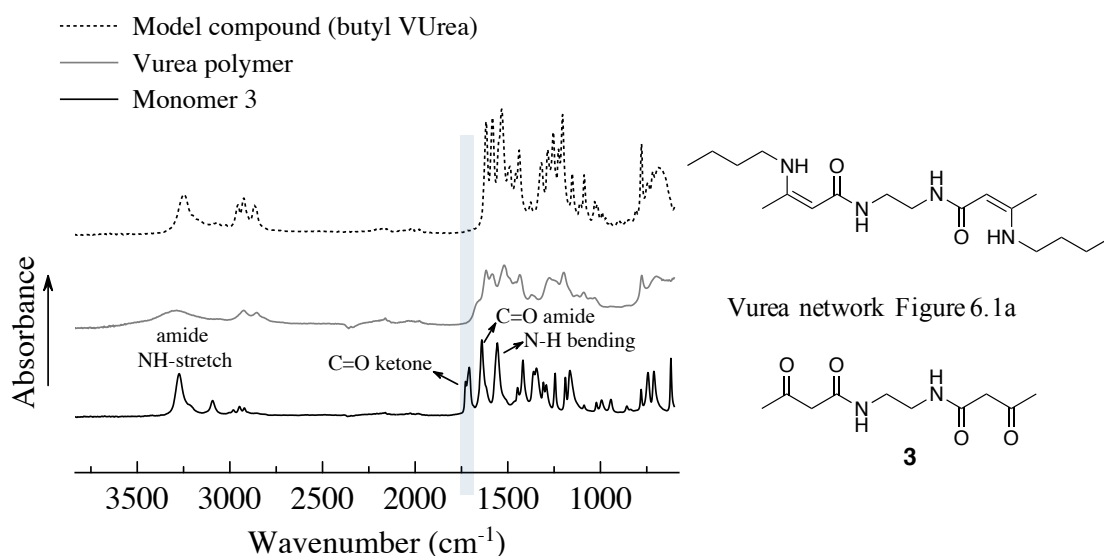


Figure 6.2: IR-spectra of the start product (red), Vurea polymer after curing (blue) and a low MW Vurea model compound.

Next, DSC-measurements were performed with four consecutive heating/cooling cycles from 25°C to 180°C. In the DSC traces of the subsequent heating steps, a clear decrease in  $T_g$  from 128°C for the second heating to 114°C for the fourth heating was observed for the Vurea network (Figure 6.3a). This decrease of  $T_g$  can be an indication of thermal degradation reactions. Indeed, when bonds are broken, also the cross-link density decreases, which can be correlated with a material's  $T_g$ . On the other hand, the Vurethane reference network showed a constant glass-transition, indicating the integrity of the cross-linked network throughout the thermal cycles.

To further check the thermal degradation hypothesis, an isothermal TGA at 160°C for 120 minutes was performed on both materials. Again, a significant difference between Vurea and Vurethanes was observed (Figure 6.3b). The Vurea network showed an initial weight loss of approximately 0.5% in the heating step to 160°C, followed by a continuous weight loss during the isothermal step. This continuous weight loss is another clear indication of thermal degradation reactions. The Vurethane, which was prepared in the same way, exhibited a small initial weight loss of less than 0.25%, followed by a constant plateau, as would be expected for a thermally stable polymer network.

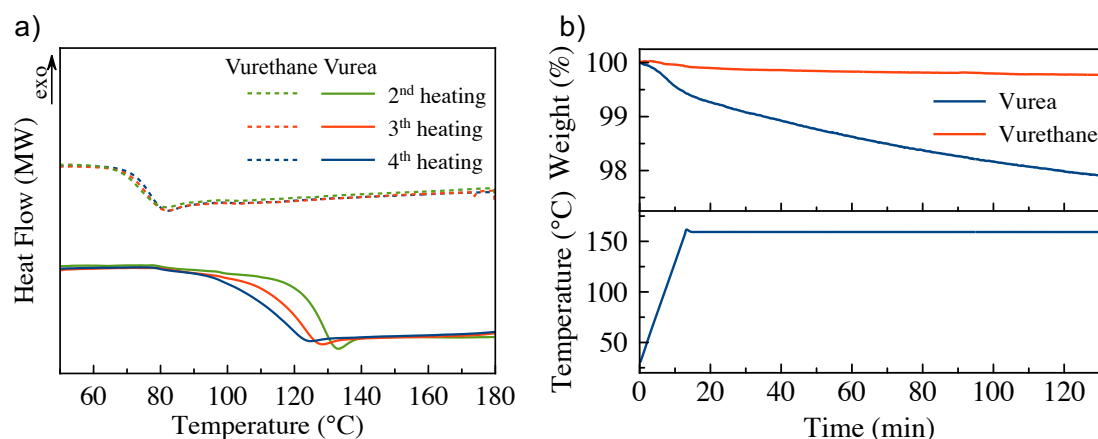


Figure 6.3: a) DSC-thermogram with four cycles. b) Isothermal TGA-analysis at 160°C with the mass loss as a function of time shown in the upper box and the used temperature program in the lower box.

Due to a clearly superior thermal stability of vinylogous urethanes compared to this Vurea-moiety, our focus was shifted to Vurethanes, and the results of this study were presented in the previous two chapters. However, in order to exploit the fast exchange kinetics, vinylogous urea polymers were later revisited in a more extensive study of a variety of Vurea materials using different monomers that could give more robust materials. This work will be presented in the next section of this chapter.

## 6.1 Thermal stability of different Vinylogous urea

To tackle the limited thermal stability of Vurea, alternative acetoacetamide monomers were considered and used to prepare Vurea networks. As depicted in Figure 6.4, 1,4-(phenylene)bis(acetoacetamide) **6** and 1,4-(piperazine)bis(acetoacetamide) **7** were selected as acetoacetamide monomers, easily obtained in one step from respectively primary aromatic amines and secondary aliphatic amines. The reactivity of the resulting Vurea polymers is indeed expected to be significantly altered by these modifications. In a similar manner as described before, Vurea networks were prepared by mixing the selected acetoacetamides **6** or **7** with amine monomers **1** and **2** followed by a curing step of 3h at 150°C in the vacuum oven to ensure full dryness and complete conversion and prevent oxidative degradation. The materials obtained from monomers **3**, **6** and **7** were named Vurea-1, Vurea-2 and Vurea-3, respectively.

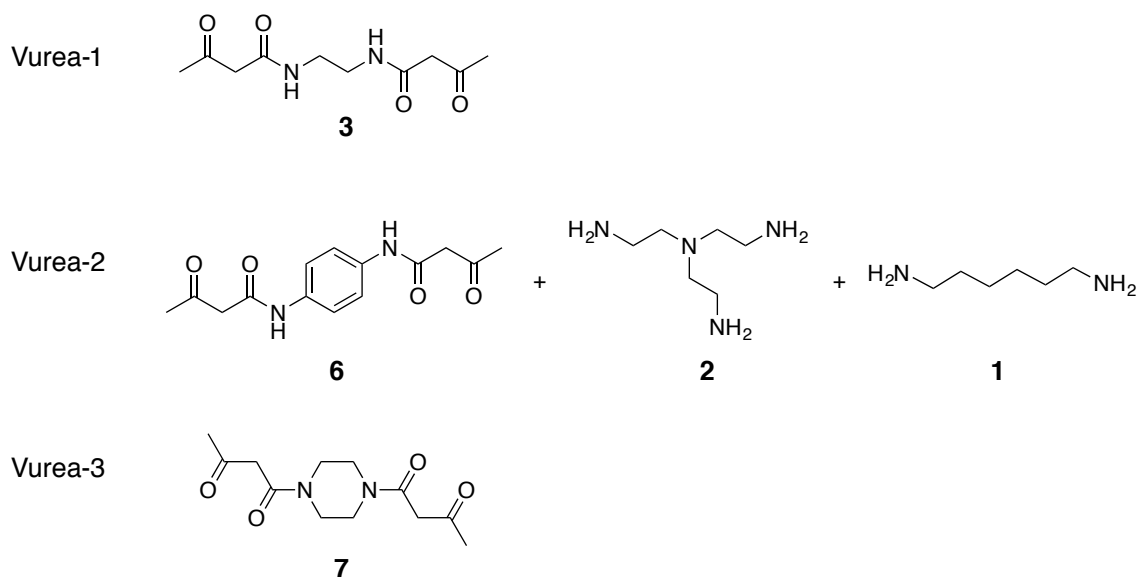


Figure 6.4: Three different Vurea networks prepared by mixing acetoacetamide(**3-6-7**):triamine **2**:diamine **1** in a ratio of 0.95:0.40:0.40.

IR-analysis of the newly prepared materials Vurea-2 and Vurea-3 (Figure 6.5) showed similar to Vurea-1 a complete disappearance of the C=O stretch of the ketone around  $1700\text{ cm}^{-1}$ , indicating full conversion (see Figure 6.5a and b).

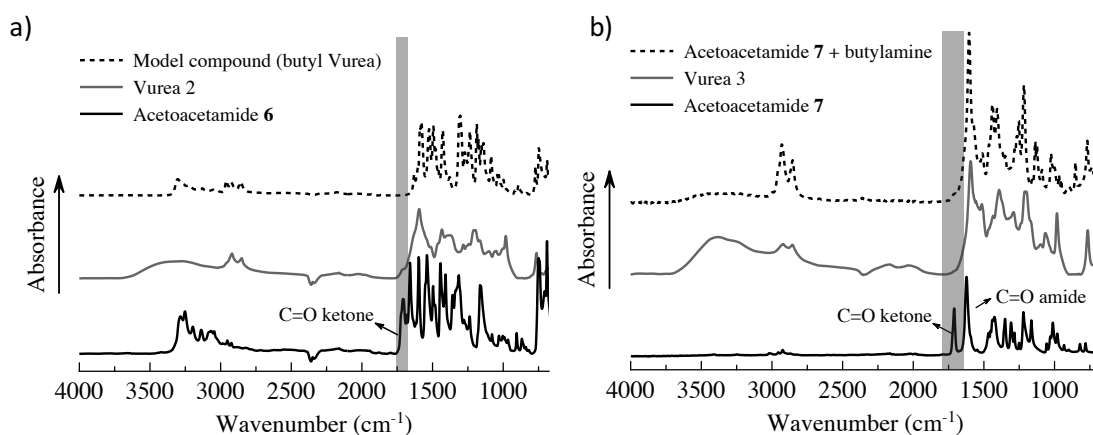


Figure 6.5: IR-spectra of the starting product (bottom curve), Vurea polymer after curing for 3h at  $150^{\circ}\text{C}$  under vacuum (middle curve) and a low MW Vurea model compound (top curve) of Vurea 2 (a) and Vurea 3 (b).

Next, TGA-measurements were carried out to assess the thermal stability of the different Vurea networks. In polymer literature, these measurements are typically performed with a heating rate of  $10^{\circ}\text{C min}^{-1}$ . Nevertheless, we observed that these experimental conditions actually did not reveal the limited thermostability of the Vurea-1 since a significant mass loss was only noticed at temperatures above

225°C (Figure 6.6a). Therefore, we reasoned that TGA-measurements with a heating rate of  $1\text{ }^{\circ}\text{C min}^{-1}$  would be a much better assessment of its real thermal stability, as it approaches more the situation of an isothermal TGA which does show significant degradation for Vurea-1 (see Figure 6.3). Indeed, a slower heating rate reduces thermal lag although this is expected to be small with the small sample sizes of  $\sim 5\text{ mg}$ . Moreover, a slower heating rate also subjects the samples to a thermal treatment that is similar to that in vitrimer processing (*i.e.* several minutes at a certain temperature range, rather than seconds). For clarity, also the first derivative (DTGA) was examined as it more clearly marks the temperature point of initial mass loss.

As can be seen in Figure 6.6a, a difference of approximately 25-50°C was observed for the onset and progress of mass loss between the TGA-thermograms with a heating rate of  $10^{\circ}\text{C min}^{-1}$  and  $1^{\circ}\text{C min}^{-1}$ . Furthermore, the DTG-curve (first derivative of TGA) showed that the onset of degradation actually occurs already around 160°C, which is in agreement with the isothermal TGA displayed in Figure 6.3b.

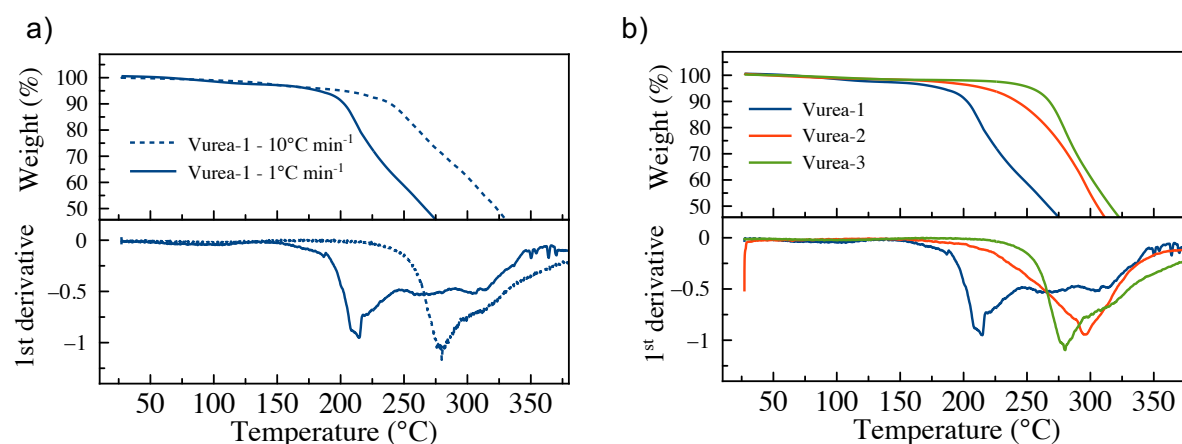


Figure 6.6:a) TGA-curve (top) and its first derivative (bottom) of Vurea-1 at a heating rate of  $1^{\circ}\text{C min}^{-1}$  and  $10^{\circ}\text{C min}^{-1}$ . b) TGA-curve (top) and its first derivative (bottom) of different Vureas at  $1^{\circ}\text{C min}^{-1}$ .

As expected from the stiffer building block structure (secondary amides), Vurea-3 exhibited a significantly different thermal stability profile, with a much later onset and progress of degradation shifted by over 50°C to  $\sim 220^{\circ}\text{C}$  (determined visually from the DTG-trace with a heating rate of  $1^{\circ}\text{C min}^{-1}$ ). This measurement shows that before significant mass loss occurs, the samples survived more than an hour without mass loss at temperatures above  $150^{\circ}\text{C}$ . On the other hand, the



degradation of Vurea-2 appears to start only slightly later than Vurea-1, at  $\sim 155^\circ\text{C}$  on the DTG albeit at a slower rate.

Because of the superior thermal stability of Vurea-3, this composition was chosen for further in-depth characterisation. In parallel, samples with 0.5 mol% pTsOH catalyst were also investigated. Although the model compound study of chapter 3 already revealed intrinsic fast exchange at room temperature, we presumed that the presence of acidic protons could enhance the exchange reactions of Vurea even more. In this way, we aimed to explore the boundaries in terms of processability of Vurea vitrimers.

In light of the observation that secondary amide-derived Vurea show a decreased sensitivity towards thermal decomposition, a possible mechanism for this degradation can be thought to involve the N-H proton. Its abstraction from a protonated Vurea moiety (a postulated intermediate in the thermal exchange reaction itself) can indeed result in a fragmentation process that would not be a viable pathway in a secondary amide-derived Vurea. Most likely the same mechanism is operating in Vurea-2, albeit at higher temperatures.

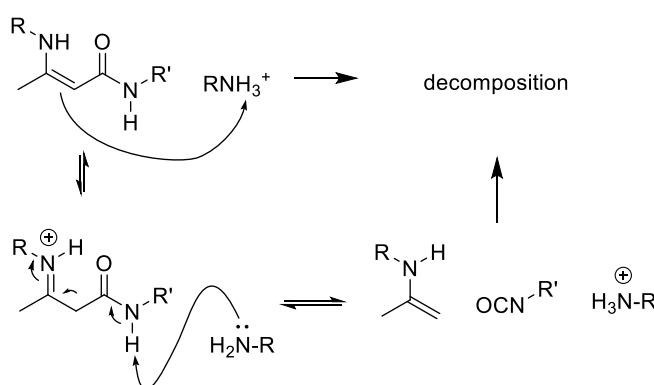


Figure 6.7: Proposed degradation mechanism of a primary Vurea.

### 6.3 Mechanical properties of Vurea-3 with and without added catalyst

The obtained Vurea-3 materials, both with and without 0.5% pTsOH added showed a similar glass-transition at  $110^\circ\text{C}$  (DSC, Figure 6.8a), a storage modulus around 2.2 GPa at room temperature, and a DMA curve that confirms the glass-transition around  $110^\circ\text{C}$ , followed by a rubbery plateau of  $\sim 8$  MPa (DMA, Figure 6.8b), which is a typical DMA-behaviour for thermosets. According to tensile

tests, the Young's modulus was  $\sim 1700$  MPa and the material yielded at a stress of  $\sim 64$  MPa and an elongation of  $\sim 6.4$  % (Figure 6.8c). Thus, significantly, addition of 0.5 mol% pTsOH did not influence the Vurea material properties as the variations are all within the measuring error (Table 6.1). The only distinct behaviour could be observed in the DMA-curve, where the catalysed sample showed a broader maximum in  $\tan \delta$  and also an increasing value at higher temperatures. This increase in  $\tan \delta$  upon heating could be the result of fast exchange reactions that increases the viscous behaviour of the material at these high temperatures.

Finally, also isothermal TGAs at  $180^\circ\text{C}$  of Vurea-3 and Vurea-3 in presence of *p*TsOH were recorded and showed a similar behaviour for both samples (Figure 6.8). Surprisingly and in contrast to the TGA-measurement shown in Figure 6.6, an initial mass loss of 4% was observed. Most likely, this initial weight loss is caused by water evaporation as the samples were not stored dry and were measured after a week. The TGA-measurement shown in Figure 6.6, which is identical during the first 18 minutes and measured straight after curing, did not show this initial weight loss.

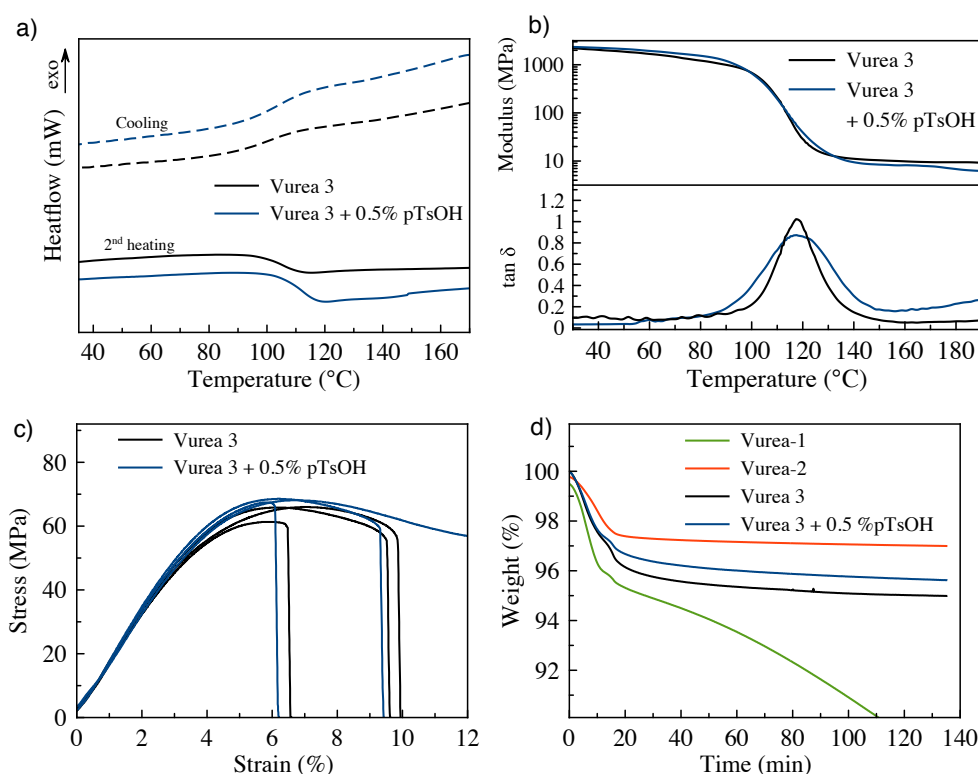


Figure 6.8: a) DSC thermogram of Vurea-3 and Vurea-3 with 0.5mol% pTsOH. b) DMA traces measured at 1 Hz in tension geometry. c) tensile tests with a cross-head speed of  $10 \text{ mm min}^{-1}$ . d) Isothermal TGA at  $180^\circ\text{C}$ .

For comparison, also isothermal TGA-measurements were performed on Vurea-1 and Vurea-2. As expected, Vurea-1 shows a strong and continuous weight loss indicating severe degradation. Vurea-2 on the other hand, did not exhibited a continuous weight loss and remained stable during the isothermal part of the measurement although the DTG curve hinted that degradation could be already possible at 180°C (Figure 6.6b).

Table 6.1: Measured properties of Vurea-3 and Vurea-3 with 0.5 mol% pTsOH.

	$T_g$ (°C)	$E'$ (MPa) <sup>a</sup>	Young modulus $E$ (MPa) <sup>b</sup>	Yield Elongation (%) <sup>b</sup>	Yield Stress (MPa) <sup>b</sup>
Vurea 3	106	2320	1709 ± 48	6.4 ± 0.5	64 ± 3
Vurea 3 + 0.5% pTsOH	110	2210	1703 ± 71	6.3 ± 0.4	68 ± 1

a) Measured *via* DMA at 30°C. b) Measured *via* tensile testing, average of 3 measurements.

## 6.4 Frequency sweep experiments

Having established the mechanical properties of the high  $T_g$  Vurea-3 materials, their rheological behaviour was examined. Since the relaxation times were expected to be significantly shorter than those of Vurethanes, frequency sweep experiments were conducted in which the angular frequency is decreased from 100 rad.s<sup>-1</sup> to 0.001 rad.s<sup>-1</sup>. This frequency range enables to measure relaxation times from 0.01 s to 1000 s. As we previously measured relaxation times of only 17 s for catalysed Vurethane samples, frequency sweep experiments were expected to be more accurate, in particular at short relaxation times. At this point, it should be emphasized that such short relaxation times are a condition for the option to process the materials by extrusion for example.

In Figure 6.9, the results of the frequency sweep experiments of both Vurea-3 materials are presented. At high frequencies (*i.e.* short timescale), the storage modulus ( $G'$ ) dominates the loss modulus ( $G''$ ), which means that the material behaves like a solid. However, when the frequency decreases, a cross-over of  $G'$  and  $G''$  can be observed. This cross-over indicates the transition of a solid-like behaviour to a liquid-like behaviour and allows to calculate the relaxation time as

$\tau = 1/\omega(\text{cross-over})$ . As summarised in Table 6.2, the measured relaxation times of the uncatalysed Vurea-3 ranged from 132 s to 57 s. To our surprise, these relaxation times are actually higher than those measured for the catalysed Vurethanes, even though model compounds showed an intrinsically much faster exchange in Vurea (See Table 3.1, p.21 chapter 3) Quite interestingly, however, the catalysed Vurea samples showed very short relaxation times going from 13.9 s at 140°C to 2.4 s at 170°C, well below those observed in catalysed Vurethane vitrimers. As indicated in Table 2, this corresponds to viscosities in the order of  $10^6$  Pa.s.

Up to this date (Oct. 2016), such low viscosities were not reported for rigid vitrimer materials and would allow very fast processing, possibly even extrusion. The activation energies of the samples were calculated as  $(44 \pm 4)$  kJ mol<sup>-1</sup> and  $(45 \pm 8)$  kJ mol<sup>-1</sup> for the uncatalysed and catalysed Vurea respectively. These values are slightly lower than those measured for the model compounds ( $\sim 49$  kJ mol<sup>-1</sup>), which could be explained by the more polar environment of the polymer matrix compared to the apolar solvent (benzene) used in the model compound study. Similar to Vurethanes, the activation energy of both the catalysed and the uncatalysed are comparable, confirming our hypothesis that the same reaction pathway is followed.

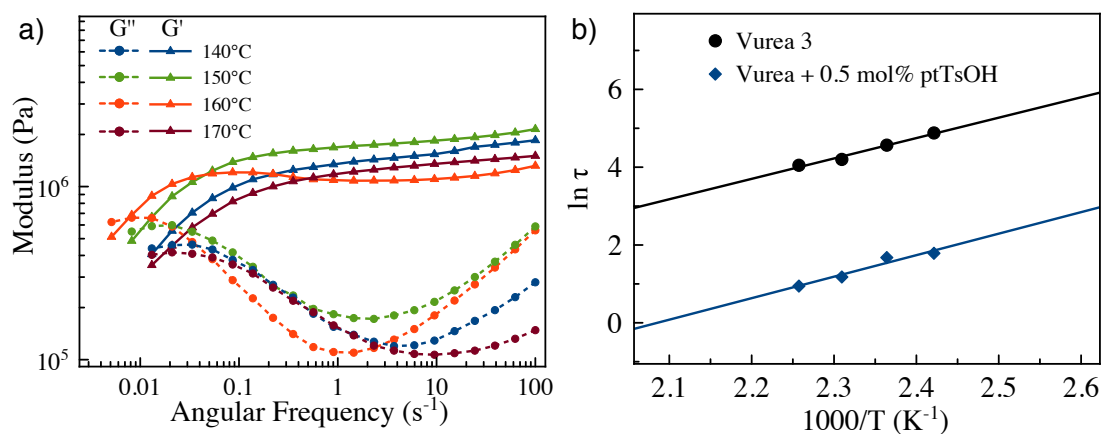


Figure 6.9: a) Frequency sweep experiments of Vurea 3 at different temperatures. b) Arrhenius plot of the measured relaxation times from the frequency sweep experiments.

Table 6.2: Cross-over frequency and corresponding relaxation times of catalyst-free Vurea 3 and Vurea 3 with 0.5 % pTsOH at different temperatures.

Composition	T (°C)	$\omega$ intersection (rad s <sup>-1</sup> )	$\tau$ (s)	$\eta$ (Pa.s)
Vurea 3	140	0.0076	132	4.0 x 10 <sup>8</sup>
	150	0.0104	96	2.9 x 10 <sup>8</sup>
	160	0.0150	67	2.0 x 10 <sup>9</sup>
	170	0.0174	57	1.7 x 10 <sup>8</sup>
Vurea 3 + 0.5% pTsOH	140	0.168	6.0	1.8 x 10 <sup>7</sup>
	150	0.187	5.3	1.6 x 10 <sup>7</sup>
	160	0.308	3.2	9.6 x 10 <sup>6</sup>
	170	0.389	2.6	7.8 x 10 <sup>6</sup>

## 6.5 Melt-flow index and extrusion

Based on the frequency sweep experiments, the viscosity of the catalysed Vurea 3 was expected to be low enough for extrusion. Before doing real extrusion experiments, the melt flow index (MFI) was measured to confirm the material's capability to flow as indicated by the frequency experiments. In this test (ISO1133), the sample is pressed with a piston of 5 kg through a die with a diameter of 2.095 mm. The weight of the polymer sample that went through the die over ten minutes is determined and is a measure of the ease in which the polymer flows. According to this test, the catalysed Vurea 3 showed a MFI of ~2.73 g at 190°C measured over 10 minutes (Figure 9a). As a reference, a catalysed Vurethane was subjected to the same test. This sample did not pass the die and remained stuck in the piston due to the high viscosity (Figure 9b).

Next, the extrudability of the catalysed Vurea 3 was examined using a mini-extruder, externally heated to 190°C (Figure 9c). It was possible to extrude little material before the motor blocked. The resulting extruded material showed a strong discoloration as it turned brown (Figure 9d), which could be caused by either degradation (*e.g.* amine oxidation) or residual dirt of the extruder. As the obtained small sample did not possess the right dimensions for DMA, the material was pressed to a film for analysis. In this manner, the mechanical properties after extrusion could be examined. As shown in Figure 10, a strong deterioration of the mechanical properties after extrusion were observed. The storage modulus as well as the  $T_g$  decreased strongly, which points to the degradation of the material.

Typically, degradation during extrusion occurs due to a combination of high temperatures and shear stresses.<sup>1</sup> In this experimental set-up, external heating to 190°C was applied. Additional shear heating could have resulted in even higher temperatures. Furthermore, due to the high viscosity of these Vurea vitrimers and an extrusion set-up designed for thermoplastic melts, shear rates are expected to be very high during extrusion, which could result in material degradation.

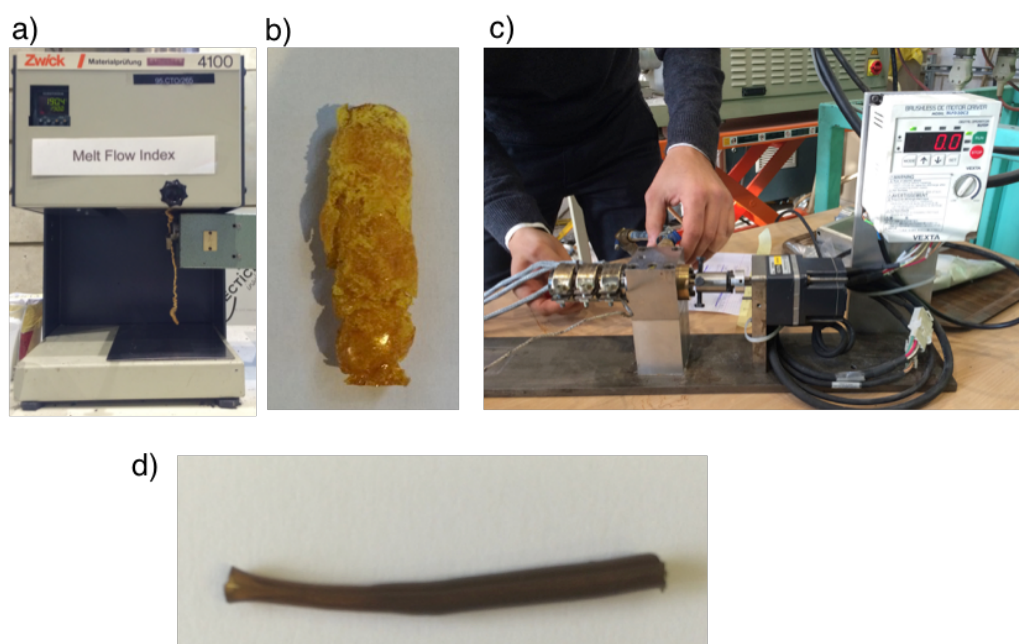


Figure 6.10: a) Melt-flow experiment of a catalysed Vurea 3 sample, showing the sample that passed the die. b) Compressed Vurethane sample that was stuck in the piston. c) Mini-extruder used for initial experiments. d) Vurea sample after extrusion.

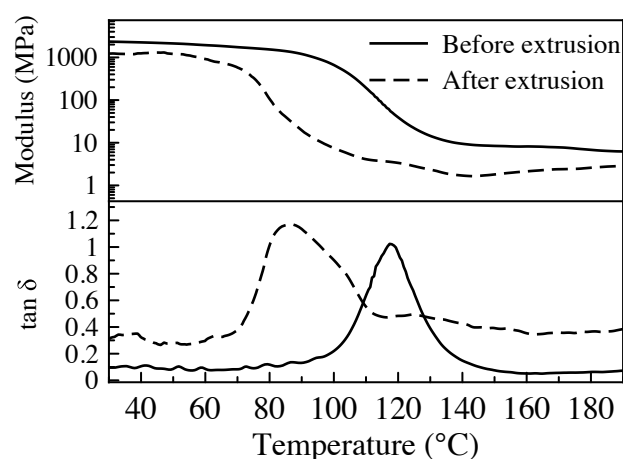


Figure 6.11: DMA-traces before and after extrusion of Vurea 3 with 0.5% pTsOH.

Normally, extrusion of thermoplastic materials is facilitated by its shear thinning behaviour. By application of high shear rates, thermoplastic melts undergo a viscosity decrease caused by the alignment of polymer chains and disentanglements.<sup>2</sup> Upon analysis of these experiments, it would be interesting to know if vitrimers undergo shear-thinning or behave like a Newtonian fluid. Drockenmoller et al. suggested a Newtonian behaviour in their work on vitrimers based on transalkylation of 1,2,3-triazoliums.<sup>3</sup> When considering a vitrimer's structure and molecular origin of its ability to flow, a Newtonian behaviour would indeed be expected as the rate of a chemical reaction is not influenced by the shear rate. Nevertheless, it would be interesting to investigate this in greater detail in the future.

This single preliminary extrusion experiment of Vurea vitrimers shows that there exist opportunities for vitrimer extrusion. Yet, to make it successful, an optimisation of the processing method should be conducted. Since extrusion is a complex process that depends on many factors, it would be an interesting separate follow-up study.

## 6.6 Vinylogous urea composites

One of the applications where the unique properties of vitrimers could be an asset, is situated in the field of composites. When the outstanding mechanical properties of composites, using a cross-linked polymer matrix, can be combined with the processability of vitrimers, new applications and production methods that replace the currently labour-intensive processes, could be aimed for.

While many procedures exist to prepare composites, one widely used method for high-end applications exploits prepregs or “pre-impregnated” fibres. These prepregs are fibres where the matrix material, usually an epoxy, is impregnated and only partially cured to the so-called B-stage. Next, several layers of these prepregs are applied in a mould and transformed to the desired multi-layer composite through combination of pressure and heat. Although this approach enables an easy one-time processing, the curing of the prepregs should be stopped and retained until final use, which results in a limited shelf-life and requires not only careful storage and transport at low temperatures but also the use of special foils as the prepregs are often tacky.

Due to the inconveniences of thermosetting matrices for prepregs, thermoplastics are more and more used as alternative since they do not show the drawbacks of thermosetting B-stage prepregs. Yet, because of the absence of cross-links, their resistance towards creep is not as good.

When this partially-cured thermoset resin or thermoplastic is replaced with a vitrimer, an enduring prepreg would be obtained that remains processable, is not tacky and does not require special storage conditions. In addition, such a vitrimer composite remains processable and even recyclable after its formation process and should have a creep-resistance comparable to thermosets. In the next part of this chapter, Vurea-based composites using a prepreg strategy will therefore be presented and a proof-of-concept of vitrimer prepregs will be demonstrated. Our strategy will thus consist of first preparing fully cured single-layer prepregs, which will be transformed to a laminate via application of heat and pressure.

### 6.1.1 Matrix adaptations and characterisation

To obtain composite materials with good properties, we first adapted slightly the composition of Vurea 3 that was studied before in this chapter. The flexible 1,6-diamino hexane **1** was replaced by the more rigid *m*-xylylene diamine **9**, which resulted in an improved material compared to Vurea-3 (Figure 6.12).

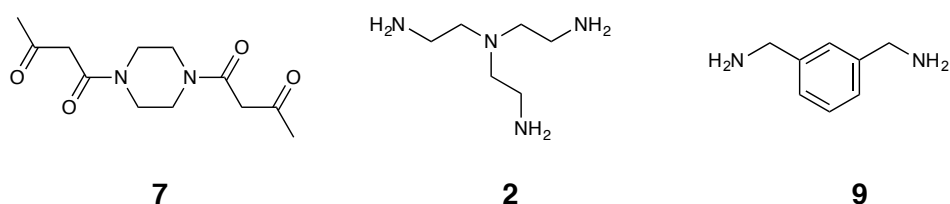


Figure 6.12: Monomers used to prepare Vurea-networks used for a composite matrix.



Table 6.3: Summary of material properties of the used Vurea matrix for composites.

	$T_g$ (°C)	Young modulus E (MPa)	Strain at failure (%)	Stress at failure (MPa)
Vurea – composite matrix	127	$2221 \pm 17$	$4.9 \pm 0.5$	$72 \pm 6$

Next, the polymerisation method was adapted to enable a good fiber-impregnation. While the Vurea networks normally were prepared in bulk, this method would not enable a good fiber impregnation. Based on our experience, the viscosity rises extremely fast and gelation occurs within a couple of minutes. Therefore, solvent was added to circumvent the fast viscosity increase and gelation. Thus, acetoacetamide monomomer **7** and the amine monomers **2** and **9** were dissolved separately in a 1/3 ratio monomers/solvent, heated until full dissolution of the acetoacetamide was achieved and only then mixed. Via this approach, gelation was delayed and the viscosity remained low enough to impregnate the fibres manually (Figure 6.13). For the complete and detailed procedure, see p.165 section 6.3.6.

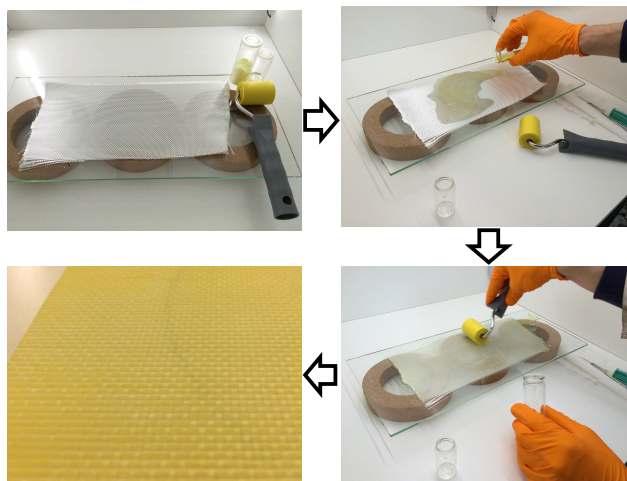


Figure 6.13: Pictures showing the manual impregnation process of glass-fiber with diluted Vurea resin. For the detailed experimental procedure, see section p.165 section 6.3.6.

Initially, ethanol was used as solvent to dilute the monomers since it proved to be a good solvent for all monomers and was expected to be removed easily. The used curing method of these prepreps consisted of a first curing during 30 min at 60°C, followed by 30 min at 90°C and finished by a post-cure from room temperature to 150°C for 3h in the vacuum oven. In this way, the solvent was first gently removed

to avoid excessive bubble-formation, followed by harsher drying to completely remove the solvent. Nevertheless, TGA-measurements (measured at  $1^{\circ}\text{C min}^{-1}$ ) showed a mass loss of approximately 5% between  $150^{\circ}\text{C}$  and  $200^{\circ}\text{C}$ , which was assigned to residual ethanol as the samples prepared in bulk did not show this mass loss (Figure 6.14). As an alternative for ethanol, methanol together with a shorter curing at higher temperature was examined. TGA-measurements of samples prepared with the same procedure but a post-cure of 30 min at  $170^{\circ}\text{C}$  under vacuum showed already an improvement but a small amount of solvent remained, while increasing the time at  $170^{\circ}\text{C}$  under vacuum to 1h resulted in solvent-free samples.

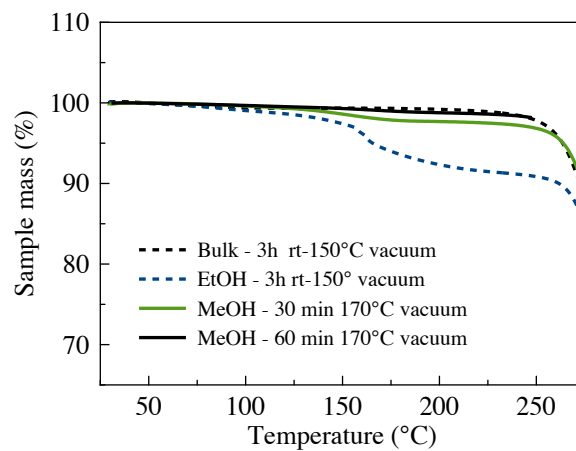


Figure 6.14: TGA-thermograms of Vurea networks prepared with solvent and different curing methods.

### 6.1.2 Multi-layer composite preparation and characterisation

With the optimised procedure that allowed good fiber impregnation and completely solvent-free samples, our strategy existed in the preparation of single layer glass-fiber sheets, which were cured completely and used as alternative to prepregs. Multi-layer composites were prepared by stacking six single-layer Vurea composite sheets with their fiber-alignment in the same direction (hereinafter denoted as  $[0^{\circ}]_6$ ) and pressing them together using a heated hydrolytic press. In a first trial, completely unidirectional fibres were used and the layers were pressed together for 30 minutes at  $150^{\circ}\text{C}$  with a pressure of approximately 100 and 200 bar (3 and 6 metric tons on  $28\text{ cm}^3$ ). In the samples compressed at 100 bar, the six layers are still clearly distinguishable with some porosities in between the layers (Figure 6.15a). Such voids are strongly undesired as they have a detrimental effect on mechanical properties of composite laminates.<sup>4</sup> When looking more

closely, it can be observed that the impregnation itself was successful as all fibres are nicely surrounded by matrix (Figure 6.15b). In the composite sample compressed at 200 bar, the different layers are less distinguishable and also less porosities remain (Figure 6.15c). On the other hand, the close-up shows that the fibres are compressed so strongly that they are in contact with each other. This fiber contact inhibits good load transfer from the matrix to the reinforcing fibres and is thus also unwanted (Figure 6.15d).

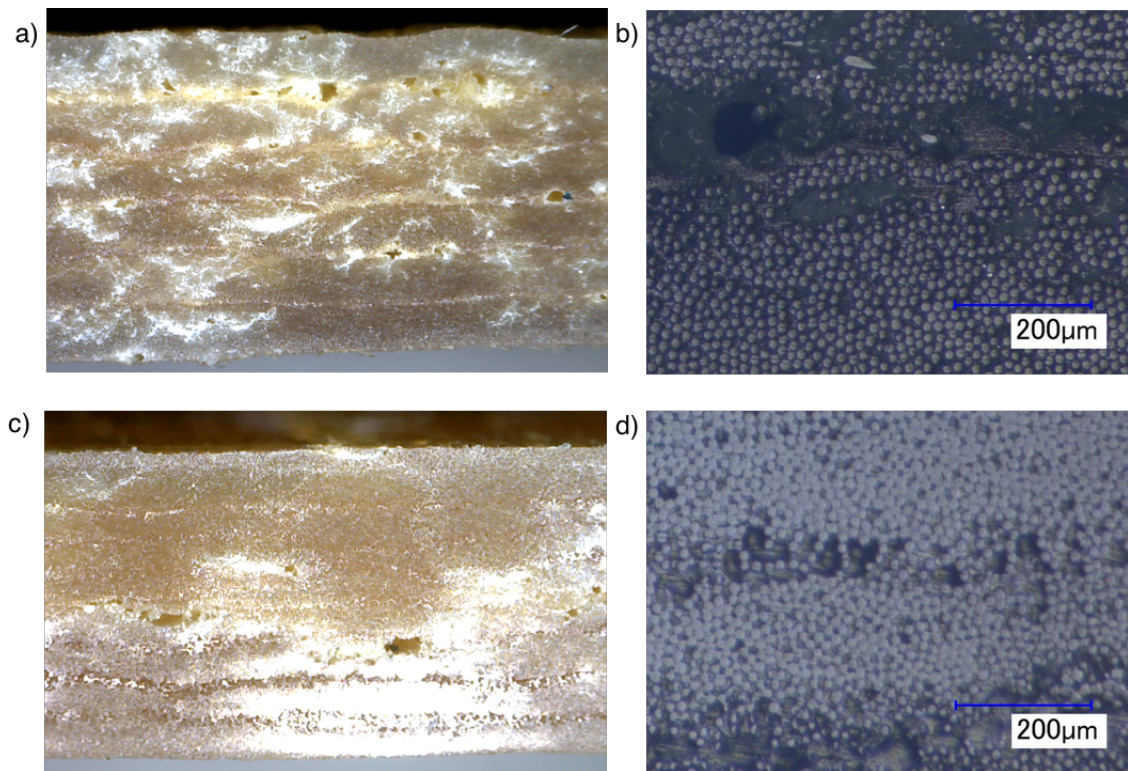


Figure 6.15: Microscope pictures of a six layer composite compressed together for: a and b) 100 bar, 30 min, 150°C and c and d) 200 bar, 30 min, 150°C.

Furthermore, it was observed that the composite-samples were pushed slightly open when applying pressure. Therefore, the completely unidirectional fiber was changed to a partially unidirectional fabric (Warp/Weft 90/10). In addition, this fabric proved to be more resistant to fiber misalignment during the manual impregnation process. With the knowledge of previous experiments, samples were compressed using a pressure of 150 bar and the temperature and pressing time were increased to 170°C and 1h to ensure full interlayer adhesion. These pressing conditions resulted in samples without any porosities and the different layers are only observable because of the tranverse fibres (Figure 6.16a and b). Moreover, no defects or delamination could be observed visibly.

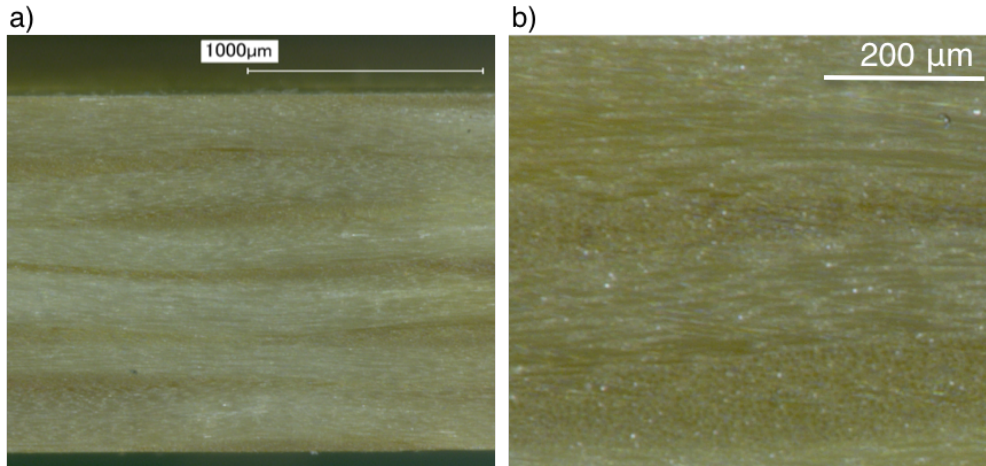


Figure 6.16: Microscope picture of a woven-fibre composite via the compression of six completely cured preregs (170°C, 1h, 150 bar).

Based on TGA-measurements of both the composite and matrix (*i.e.* resin burning-off method), a fiber volume fraction of 57% was calculated, which was slightly above the aimed 50% (Figure 6.17). This fiber volume fraction approaches those used for more demanding applications (60-70%). Probably, the fiber volume content can easily be increased without losing good impregnation by changing the monomer concentration or by simply using a smaller amount of matrix-solution.

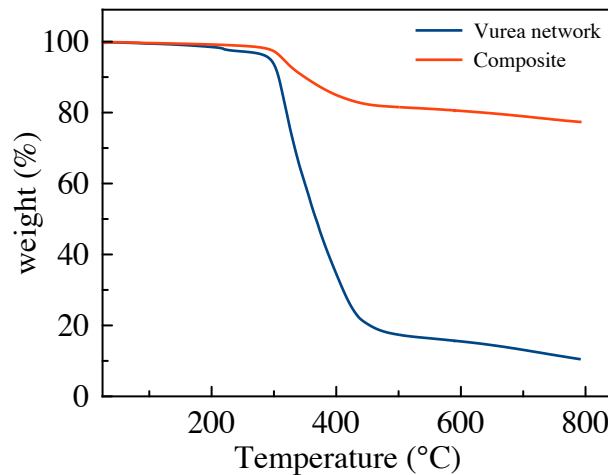


Figure 6.17: TGA-thermograms of the Vurea network and composite.

Mechanical properties were determined through tensile tests, in which three samples were loaded until failure in the direction of the fibres (0°). As depicted in Figure 6.18, a good reproducibility was achieved among these three samples, with sample two and three that were slightly less stiff and showed a higher strain and strength to failure than sample one, which besides batch-to-batch differences could also be caused by a slight difference in stacking orientation. Since the samples



consisted of six layers with a size of  $(20 \times 3)$  cm<sup>2</sup>, they were cut out from different batches of prepregs. These results thus indicate that the process of impregnation followed by the compression to a laminate, yields reproducible samples.

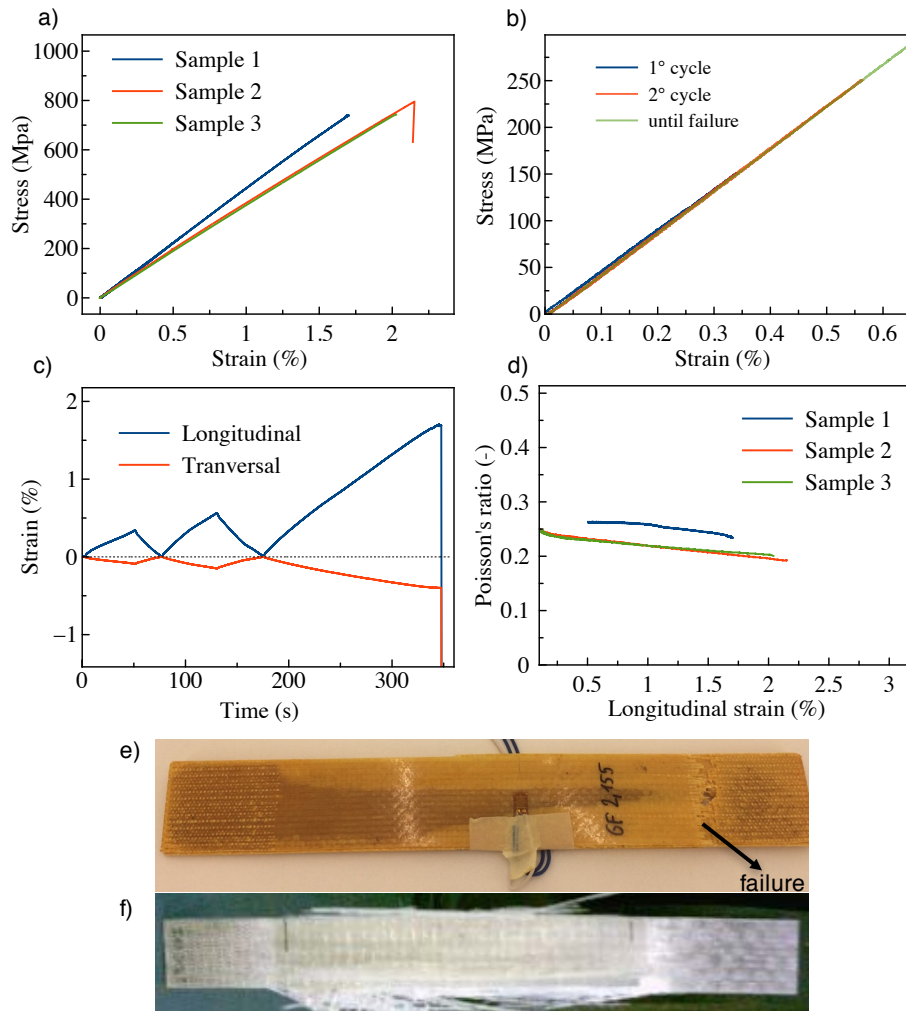


Figure 6.18: a) Stress-strain curves of Vurea composites; b) Zoom-in on the two loading-unloading cycles of sample 1. c) Strain as a function of time for two loading-unloading cycles followed by loading until failure. d) Poisson's ratio as a function of strain. e) The Vurea composite after tensile test shows that the break occurred near the grips. f) Reference UD glass fabric reinforced epoxy  $[0^\circ]_8$  after failure.

The mechanical properties are listed in Table 6.4 and are comparable to those of a similar epoxy-laminate,<sup>5</sup> which is very satisfactory and promising as the epoxy-matrix is already completely optimised. Furthermore, the examined samples failed near the grips (Figure 6.18e), which means that the measured stress and strain at failure are underestimated. Interestingly, it was also observed that the samples showed no visual damage before failure as the sample did not turned opaque, which is a clearly different behaviour compared to the epoxy-reference (Figure

6.18e and f). Moreover, no audible damage was observed until failure, which occurs normally due to the failure of part of the fibres.

For sample one, two consecutive loading-unloading cycles were applied before loading until failure. As can be seen in Figure 6.18b and c, almost no hysteresis occurs as the laminate goes almost entirely back to its initial position after being strained and shows no visible deterioration of its stiffness. Congruent with the absence of opacity, this indicates that the laminate shows no measurable damage during these two loading cycles although small ruptures are expected.

Table 6.4: Measured mechanical properties of a Vurea-based composite. For comparison, also the values of a similar epoxy lamina are shown.<sup>6</sup>

	Young modulus $E_{11}$ (GPa)	Stress at failure $X_t$ (GPa)	Strain at failure $\epsilon_{11}$ (%)	Poisson's ratio $\nu_{12}$ (-)
Vurea composite $[0^\circ]_6$	$40.2 \pm 3.0$	$791 \pm 49$	$1.9 \pm 0.2$	$0.249 \pm 0.015$
UD glass fabric reinforced epoxy $[0^\circ]_8$	42	939	2.5	0.259

A thorough investigation and optimisation of the matrix, impregnation process and laminate-formation is ongoing. This research will most probably enhance the mechanical properties even further and elaborate more on the above observations.

### 6.1.3 Proof of concept – composite processing and fiber recuperation

To demonstrate the post-curing processability of Vurea vitrimer composites, a 2-layer composite ( $([0^\circ]_2)$ ) was prepared according to the previously described method. This flat composite was thermo-formed using a pre-heated mould at  $150^\circ\text{C}$  (Figure 6.19).

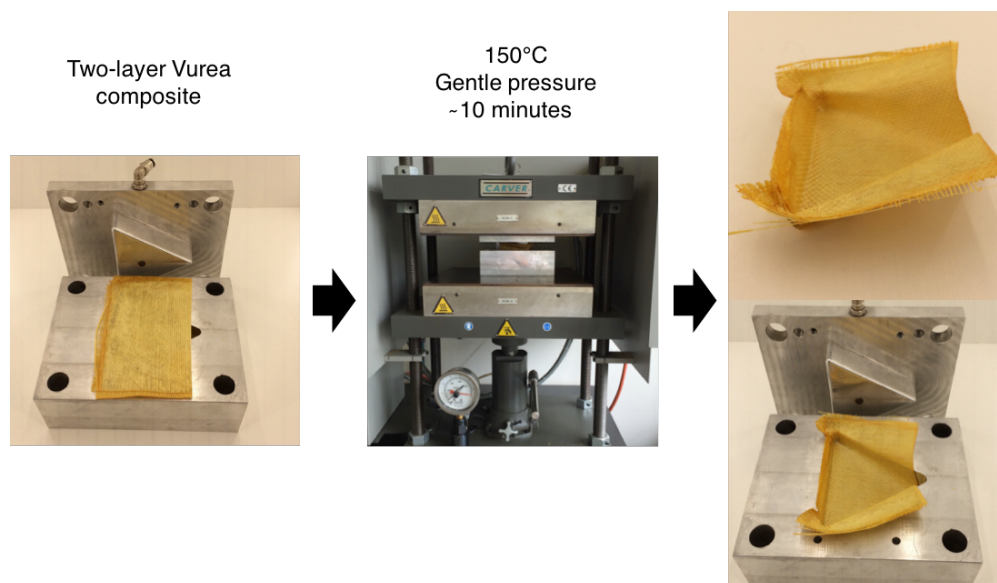


Figure 6.19: Thermoforming of a flat Vurea composite to a triangular shape.

First, the composite was positioned in the pre-heated mould and thermally equilibrated for several minutes to ensure that the composite is at the desired temperature. Next, the pressure was increased gradually to push the die in the composite without damaging the fibres, after which the composite was kept for about five minutes in this shape to allow for the reorganisation of the vitrimer matrix. Finally, the upper part of the die was removed and the composite retained its shape, even when it was still well above its  $T_g$ . After cooling, a shaped composite was obtained without visual defects besides those in the corners of the triangle due to excessive deformation of the fibres.

Also the ability to chemically recuperate the fibres was tested. Therefore, a single-layer Vurea composite was partially immersed in N-methylpyrrolidone (NMP) or a solution of NMP with a primary amine (Figure 6.20a). As the amine can induce exchange reactions that break down the network, the matrix should be easily removed from the glass-fiber fabric (Figure 6.20b). Indeed, only 15 minutes at 100°C resulted in complete removal of the matrix (Figure 6.20c). On the other hand, the reference without amine did not dissolve, even after 20 h at 100°C. At room temperature, the same results were achieved after 6h. This feature enables thus easy recuperation of the fibres.

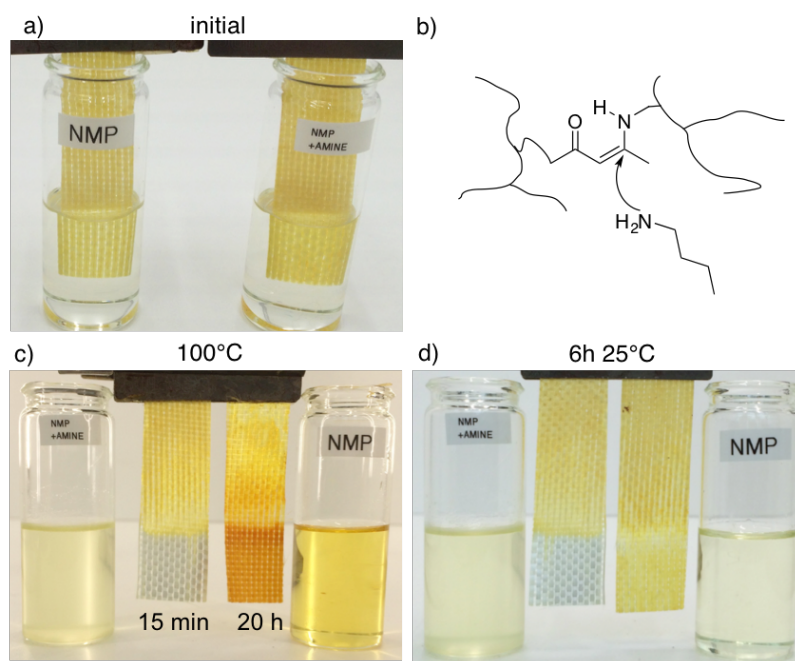


Figure 6.20: a) Immersion of a Vurea composite in NMP with (right) and without amine (left). b) Chemical origin for the recuperation of the fibres of a Vurea composite. c) Complete removal of the Vurea matrix after 15 minutes at 100°C in presence of amine. d) 6h at 25°C resulted also in completely removal of the matrix from the glass-fibres.

## 6.2 Conclusions and perspectives

In this chapter, Vurea were examined for their potential in vitrimer materials. First, Vurea networks were prepared through combination of (ethylenediamine)bis(acetoacetamide) **3** with multi-amines. Comparison of these Vurea networks with Vurethane vitrimers revealed their limited stability. Consequently, the thermal stability of networks based on different acetoacetamides was examined through TGA-measurements, which showed superior thermal stability for the Vurea-networks based on piperazine acetoacetamide **7**.

The Vurea network, prepared by mixing piperazine acetoacetamide **7**, 1,6-hexane diamine and TREN, was characterised in detail. Simultaneously, the effect of an acid catalyst (0.5 mol% pTsOH) was evaluated. The properties of both networks proved to be good with a  $T_g$  of 110°C, storage modulus of 2.2 GPa and a rubbery plateau at 8 MPa. Frequency sweep experiments were conducted to evaluate its viscoelastic behaviour, yielding relaxation times for the uncatalysed Vurea similar to those of the catalysed Vurethanes. Interestingly, the catalysed Vurea exhibited very short relaxation-times in the order of seconds only, which is the fastest



measured for rigid vitrimer networks to the best of our knowledge. Due to this fast relaxation behaviour, its ability to be processed through extrusion was evaluated but showed severe degradation of the material. Nevertheless, this initial experiment showed potential for processing through extrusion, provided that the right extrusion set-up and conditions are found in an ongoing follow-up study.

In a final part of this chapter, Vurea based composites were prepared and examined if they could serve as enduring preregs. After adapting the network composition and polymerisation method for good fiber impregnation, single-layer enduring preregs were prepared. These single-layer preregs could be transformed using a heated hydrolytic press to a 6-layer laminate. Initial assessment of its mechanical properties through tensile test revealed properties similar to those of an epoxy-composite. Furthermore, also a proof-of-concept of thermoforming and fibre-recuperation was provided.

## 6.3 Experimental

### 6.3.1 Materials

Tris(2-aminoethyl)amine (96%), butylamine ( $\geq 99\%$ ), *m*-xylylene diamine ( $\geq 99\%$ ), 2,2,6-trimethyl-4H-1,3-dioxin-4-one (95%), 1,6-diaminohexane (98%), ethylenediamine-N,N'-bis(acetoacetamide) and *tert*-butyl acetoacetate ( $\geq 98\%$ ) were purchased from Sigma Aldrich. Piperazine ( $>98\%$ ) and 1,4-phenylenediamine ( $>98\%$ ) were purchased from TCI chemicals. Glass-fiber fabric style 3025 was purchased from Porcher industries. Ethane-1,2-diyl bis(3-oxobutanoate) **5** was prepared as described by Clemens et al.<sup>7</sup>

### 6.3.2 Instrumentation

Nuclear magnetic resonance spectra were recorded on a Bruker Avance 300 or a Bruker Avance II 700 spectrometer at room temperature. IR spectra were collected using a Perkin-Elmer Spectrum1000 FTIR infrared spectrometer with a diamond ATR probe. Thermogravimetric analyses were performed with a Mettler Toledo TGA/SDTA851e instrument under air or nitrogen atmosphere. Differential scanning calorimetry (DSC) analyses were performed with a Mettler Toledo instrument 1/700 under nitrogen atmosphere at a heating rate of  $10^{\circ}\text{C min}^{-1}$ .

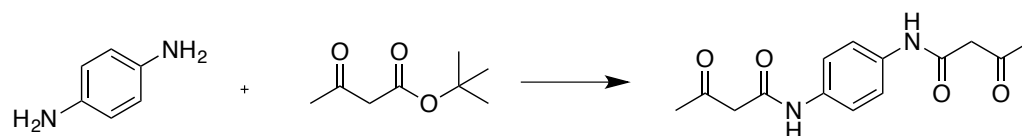
Dynamic mechanical analysis (DMA) was performed on a SDTA861e DMA from Mettler Toledo. Samples were processed using a custom-made mould and a Carver manual press model 4122.

Frequency sweep experiments were performed on an Anton-Paar physica MRC 301 rheometer with a plate geometry of 25 mm, an amplitude of 0.1%, which is within the linear viscoelastic region according to an amplitude sweep experiment, the frequency was changed from 100 rad s<sup>-1</sup> to 2.10<sup>-3</sup> rad s<sup>-1</sup> and a normal force of 10N was used.

Tensile testing of polymer samples was performed on a Tinius-Olsen H10KT tensile tester, equipped with a 100 N load cell, using a flat dog bone type specimen with an effective gauge length of 13 mm, a width of 2 mm, and a thickness of 1.3 mm. The samples were cut out using a Ray-Ran dog bone cutter. The tensile tests were run at a speed of 10 mm/min. The tensile tests of composites were performed on a servo-hydraulic INSTRON 8801 tensile testing machine with a FastTrack 8800 digital controller and a load cell of  $\pm 100$  kN (Department of Materials Science and Engineering, UGhent). The quasi-static tests were displacement-controlled with a speed of 2 mm/min. A special fixture is mounted on the tensile machine to prevent relative rotation of the grips, causing torsion of the specimen. Alignment of the grips was established using an INSTRON alignment kit. For the registration of the tensile data, a National Instruments C-series data acquisition card was used. The load, displacement and strain, given by the FastTrack controller as well as the extra signals from strain gauges were sampled on the same time basis. The used samples got a rectangular shape of (3 x 20) cm<sup>2</sup>.

Microscope pictures of the composites were obtained using a Dinolite AM411 or Keyence VHX-200 HDR microscope.

### 6.3.3 Synthesis of N,N'-(1,4-phenylene)bis(3-oxobutanamide) 6

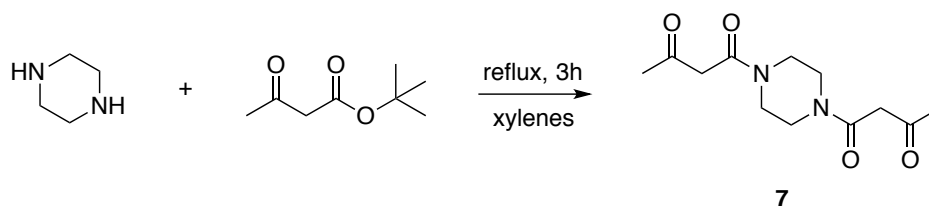


A solution of *tert*-butyl acetoacetate (21.0 mmol, 3.38 g) in xylene (50 mL) was heated to 140°C (internal temperature) with magnetically stirring. After 10

minutes, a solution of 1,4 phenylene diamine (10 mmol) in xylene (100 mL) was added dropwise using an addition funnel over a time course of 10 min. After addition, stirring was continued for 1 hour at 140°C (internal temperature). Afterwards, xylenes was removed *in vacuo* affording a pale yellow precipitate. The solids were then redissolved in ethyl acetate (50 mL) to which hexane was added dropwise until the solution started to become cloudy. At this point, the solution was left at room temperature for a minimum of 12 hours. The obtained white solids were filtered off and dried *in vacuo* (40°C), yielding the pure bisacetoacetamide 6.

Yield: 50%.  $^1\text{H}$  NMR ((DMSO- $d_6$ ), 300 MHz)  $\delta$ (ppm): 10.80 (s, 2H,  $\text{N}_\text{H}$ ), 7.50 (s, 4H,  $\text{CH}_\text{ar}$ ), 3.55 (s, 4H,  $\text{COCH}_2\text{CO}$ ), 2.22 (s, 6H,  $\text{COCH}_3$ ).

#### 6.3.4 Synthesis of 1,4-(piperazine)bis(acetoacetamide) **7**



This compound was prepared as described by Trumbo et al.<sup>8</sup> Piperazine (100 g, 1.16 mol) and tert-butyl acetoacetate (385 g, 2.44 mol) were refluxed in xylenes (300 mL) for 3h with distillative removal of tert-butanol. The xylenes was removed in vacuo yielding an orange oil that crystallised upon standing. The obtained orange solid was redissolved in boiling acetone, cooled to room temperature and diethyl ether was added until a haziness was observed. This solution was stored overnight at 0°C resulting in the formation of white crystals, which were filtered and washed with cold diethyl ether yielding **7** as a white powder.

yield: 61%.  $^1\text{H}$  NMR ((DMSO- $d_6$ ), 500 MHz)  $\delta$ (ppm): 3.68 (ss, 4H,  $-\text{C}(=\text{O})-\text{CH}_2-$  C(=O)-), 3.47-3.42 (m, 4H,  $\text{CH}_{\text{ring}}$ ), 3.35 -3.31 (m, 4H,  $\text{CH}_{\text{ring}}$ ), 2.16 (s, 6H,  $\text{CH}_3\text{C}(=\text{O})-$ ).

### 6.3.5 Representative synthesis of the Vurea networks

1,6-Hexane diamine (1.824 g, 16.6 mmol) and TREN (2.241 g; 16.6 mmol,) were weighed in a vial, heated in an oil bath to 80°C and 1,1'-(piperazine-1,4-diyl)bis(butane-1,3-dione)) (Piperazine Aam) (10.0 g; 39,3 mmol) was added in bulk while manually stirring. When a fully homogenous mixture was obtained, the mixture was poured on a Teflon sheet and cured for 3h *in vacuo* at 150°C yielding a hard glassy yellowish polymer. The conversion of acetoacetamide groups to the corresponding vinylogous urea was confirmed via ATR-IR by the disappearance of the C=O signal at 1711  $\text{cm}^{-1}$  and the good agreement with the IR spectrum of the corresponding model compound, *i.e.* 3-(butylamino)-1-(piperidin-1-yl)but-2-en-1-one. The obtained, fully cured network was ground to a fine powder and mould pressed for 30 min at 150°C after which a homogeneous, defect-free sample was obtained that was used for further characterization.

The other polymer networks were prepared in the same fashion using the amounts shown in Table 6.5.

Table 6.5: Used stoichiometry and amounts for the preparation of different polymer networks.

Network	Reagent	Eq	n (mmol)	Mass (g)
Vurea 1	Bis acetoacetamide <b>3</b>	0.95	43.8	10.000
	TREN <b>2</b>	0.42	19.4	2.833
	1,6-hexane diamine <b>1</b>	0.39	17.5	2.036
	water			3.5
Vurethane fig 1b	Bis acetoacetate <b>5</b>	0.95	11.3	10.000
	TREN <b>2</b>	0.42	19.4	2.808
	<i>m</i> -xylylene diamine <b>4</b>	0.39	17.5	2.366
Vurea 2	Acetoacetamide <b>6</b>	0.95	11.3	4.500
	TREN <b>2</b>	0.40	6.9	1.003
	<i>m</i> -xylylene diamine <b>4</b>	0.40	6.9	0.797
	DMF			4.0
Vurea 3	Acetoacetamide <b>7</b>	0.95	39.4	10.000
	TREN <b>2</b>	0.40	16.6	2.421
	1,6-hexane diamine <b>1</b>	0.40	16.6	1.924

### 6.3.6 Preparation of a single-layer Vurea composite

One layer of glass-fiber (24.5 g) was taped on a glass-plate (no releasing agent was used) and heated to 50°C in an oven. 1,4-(piperazine)bis(acetoacetamide) (7 g, 27.5 mmol) was dissolved in 10 mL methanol in an oil-bath thermostated at 90°C until a homogeneous solution was obtained. TREN (1.965 g, 11.6 mmol), *m*-xylylene diamine (1.579 g, 11.6 mmol) and *para*-toluene sulfonic acid (25 mg, 0.13 mmol) were mixed in a vial and ultrasoned until the acid completely dissolved in the amines. To this mixture, 5 mL methanol was added, mixed until a homogeneous mixture was obtained and added to the acetoacetamide solution. After stirring, this solution was gently poured over the pre-heated glass-fiber and manually spread using a pressure roller until all fibres were impregnated. The glass-plate with the composite was put in a pre-heated oven at 60°C for 30 minutes after which the sample could be removed from the glass-plate. The composite was further cured for 30 minutes at 90°C followed by 1h at 170°C *in vacuo* yielding a completely cured single-layer enduring prepreg.

## 6.4 References

- (1) Capone, C.; Di Landro, L.; Inzoli, F.; Penco, M.; Sartore, L. *Polym. Eng. Sci.* **2007**, *47*, 1813.
- (2) Sperling, L. H. *Introduction to Physical Polymer Science*; 4 ed.; Wiley-Interscience, 2005.
- (3) Obadia, M. M.; Mudraboyina, B. P.; Serghei, A.; Montarnal, D.; Drockenmuller, E. *J. Am. Chem. Soc.* **2015**, *137*, 6078.
- (4) de Almeida, S. F. M.; Neto, Z. d. S. N. *Composite Structures* **1994**, *28*, 139.
- (5) De Baere, I. Studie van Ahet afschuivingsgedrag van composieten, 2004.
- (6) De Baere, I. Studie van afschuivingsgedrag van composieten, Master, Universiteit Gent, 2004.
- (7) Clemens, R. J.; Hyatt, J. A. *The Journal of Organic Chemistry* **1985**, *50*, 2431.
- (8) Trumbo, D. L. *Polym. Bull. (Berlin)* **1991**, *26*, 481.

## Chapter 7

### Conclusion and perspectives

#### 7.1 Aim of the work

This doctoral work aimed to explore the amine exchange of enaminones as a new dynamic bond for the synthesis of vitrimers. Vitrimers, only reported for the first time in 2011,<sup>1</sup> show quite interesting features as they combine mechanical properties of thermosets with a glass-like malleability at elevated temperatures. This combination of properties was achieved through incorporation of thermally triggered exchangeable bonds that follow an associative exchange process, *i.e.* bonds are only broken after new bonds are formed (Figure 7.1). Because of this particular exchange mechanism, vitrimers are characterised by a constant cross-link density. This property also gives rise to a unique viscosity decrease upon heating, reminiscent of glass. As vitrimers combine highly desired properties that are not found back in other organic materials, they show great promise to have a considerable impact on industries that rely on cross-linked polymers.

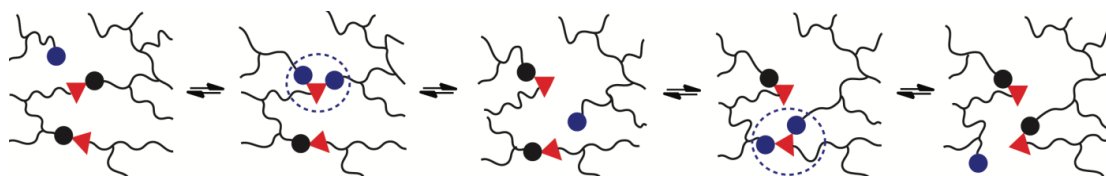


Figure 7.1: Associative exchange reactions enable network reorganisation without losing connectivity during exchange.

The pioneering work relied on catalysed transesterification reactions in epoxy materials.<sup>1-5</sup> Although transesterification was the first exchange chemistry used to demonstrate the concept of vitrimers, it provided already a high-level benchmark. Transesterification is a very simple and well-understood chemistry<sup>6</sup> that can be easily implemented in materials with good properties, via the addition of a transesterification catalyst to known epoxy-acid and epoxy-anhydride formulations. Nevertheless, the system also showed limitations as high catalyst loadings are required, transesterification is intrinsically slow and the catalyst-solubility impedes high- $T_g$  materials.

In this thesis, the amine exchange of vinylogous acyls, also referred to as enaminones, was examined as alternative exchangeable bond that would enhance vitrimer's processability and resolve the limitations in glass-transition temperature. The amine exchange on these enaminone moieties was already reported in various reports for the synthesis of small molecules.<sup>7-10</sup> Also in polymer science, enaminones and more precisely vinylogous urethanes (Vurethanes) were used in the field of water-borne coatings<sup>11</sup> and adhesives<sup>12</sup> due to their straightforward synthesis from amines and acetoacetates. Nevertheless, not one report in literature designed these enaminone containing networks to exploit its dynamic nature in bulk materials. Thus, in this PhD research, the different enaminone moieties were systematically researched for their potential in vitrimer materials (Figure 7.2).

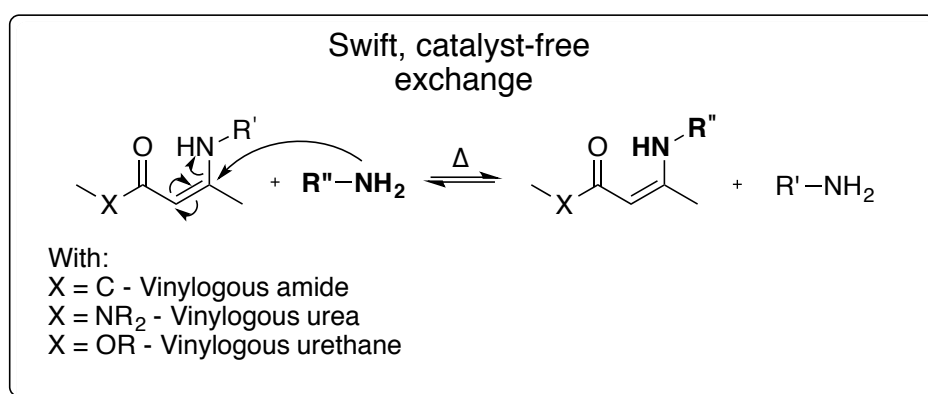


Figure 7.2: Amine exchange of enaminones was explored for new vitrimer materials.

Simultaneous with this research, that spanned from 2012 to 2016, other academic contributions were made as well to this quickly emerging field of vitrimer materials. An overview is presented in Chapter 2 and also published as a mini-review.<sup>13</sup>

## 7.2 Overview of the results

In the first part of this research, presented in chapter 3, a systematic study on low-molecular-weight compounds was conducted to assess the kinetics of the amine exchange on enaminones. This study showed that the vinylogous transamination of enaminones spans over a very wide practical temperature window, ranging from room temperature for vinylogous urea (Vurea) to temperatures as high as 170°C for substituted vinylogous amides (Vamides), the relative order of enaminones is depicted in Figure 7.3. Furthermore, two possible



exchange mechanisms were provided and it was rationalised that proton exchanges are crucial. Consequently, it was also demonstrated that the addition of a protic acid increased the exchange rate. Based on these results, Vurethanes and Vurea were selected as most promising enaminones for vitrimers as they exhibit the fastest exchange kinetics and a straightforward monomer synthesis.

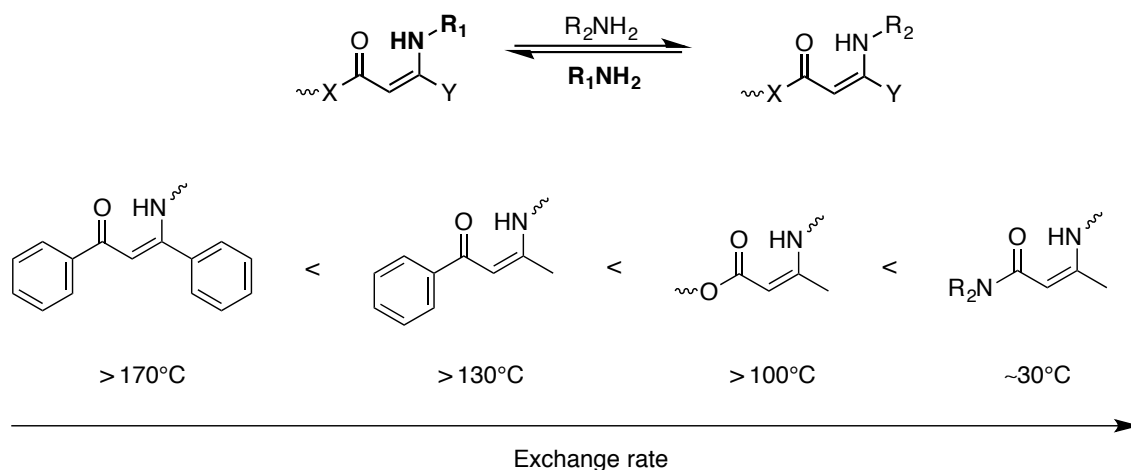


Figure 7.3: Relative order of the amine exchange of enaminones, with an indicative temperature when the exchange reaction starts to become reasonable fast.

In Chapter 4, different approaches were examined to prepare Vurethane vitrimers. The first strategy relied on amine-functional prepolymers, which would be cross-linked with bis-acetoacetates. Yet, this strategy was abandoned as side-reactions complicated the preparation of amine-functional prepolymers. The second approach, starting from low-MW amine and acetoacetate monomers, demonstrated the first proof-of-concept vitrimers based on vinylogous transamination (Figure 7.4). Poly(vinylogous urethane) networks with a glass transition temperature of 87°C and a storage modulus of ~2.4 GPa were obtained. As expected for a polymer network, the samples were insoluble even at elevated temperature and a rubbery plateau was observed by DMA. Stress-relaxation and creep experiments showed a viscoelastic liquid behaviour. Due to the fast exchange reactions and high density of exchangeable bonds throughout the network, relaxation times as short as 85 s at 170°C were achieved without the use of any catalyst. Moreover, the poly(vinylogous urethane) networks can be recycled without loss of mechanical properties. These properties position these materials among the top-performing vitrimers currently known. Furthermore, a monomer screening showed that materials with a glass-transition up to 145°C and good mechanical properties are feasible.

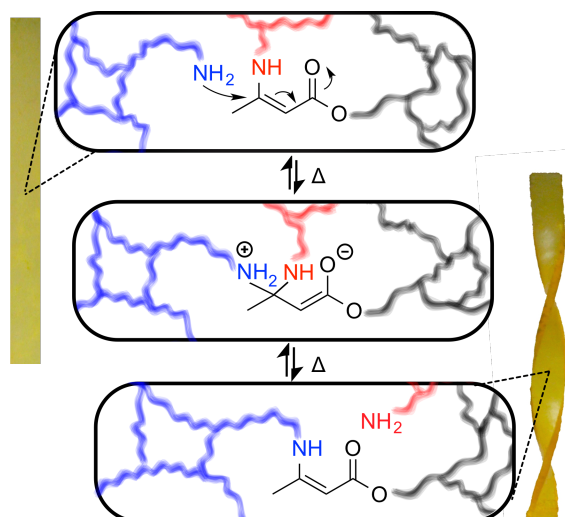


Figure 7.4: Representation of a poly(vinyllogous urethane) vitrimer, showing the molecular origins of its macroscopic vitrimer nature.

In our quest to improve the processability even more, the influence of catalyst on the amine exchange of Vurethanes was examined both in a low-MW model study as an elastomeric vitrimer (Chapter 5). Although working catalyst-free was an initial target, it was realised that addition of small amounts of additives provides a way to control the exchange kinetics. Indeed, this study showed that the amine exchange Vurethanes can easily be controlled and a good correlation between model reactions and mechanical relaxation times was observed. Addition of acids increased the exchange rate and allowed faster processing while a strong base such as TBD strongly decelerate exchange reactions, which could be interesting when a good creep resistance is aimed for. Moreover, using acid catalyst, relaxation times of the hard Vurethane vitrimers presented in chapter 4 could be reduced to 10 s, which significantly improves the processability of these materials.

In the last part of this thesis (Chapter 6), Vinyllogous urea were exploited for vitrimer materials as they showed the fastest exchange kinetics of all enaminones. Although an initial study hinted to a limited thermal stability, varying slightly the Vurea structure resulted in materials with a satisfactory thermostability. Networks were prepared by combination of 1,4-(piperazine)bis(acetoacetamide), 1,6-hexane diamine and tris(2-aminoethyl)amine. Simultaneously, also the same network catalysed with acid was investigated to find the boundaries for processability. Vitrimers with a glass transition of 110°C and a storage modulus of 2.2 GPa at room temperature were obtained. Although no significant differences were observed in material properties of the catalysed and uncatalysed samples, frequency sweep experiments indicated strongly reduced relaxation times for the acid catalysed networks. While the uncatalysed samples showed relaxation times

in the order of minutes (130 s to 60 s from 140 to 170°C), the acid catalysed samples showed relaxation times in the order of seconds (6 to 3 s from 140 to 170°C). To the best of our knowledge, these catalysed Vurea vitrimers exhibit the shortest relaxation times reported up-to-date.

Finally, Vurea vitrimers were explored as matrix for composites. After some adaptations of the matrix to enhance the glass-transition and allow for easy fiber impregnation, one-layer glass-fiber sheets were prepared that could serve as an alternative for preregs. While normal preregs require special storage conditions and anti-adhesive layers due to its partial cured matrix, the vitrimer preregs do not require special storage and anti-adhesive layers and remain processable because of its vitrimer nature. Indeed, multilayer composites could be prepared through compression of stacked preregs. The mechanical properties of the obtained materials were comparable to those of epoxy networks prepared via reaction injection moulding. Finally, a proof-of-concept of composite processing was presented through thermoforming a two-layer vitrimer composite (Figure 7.5).

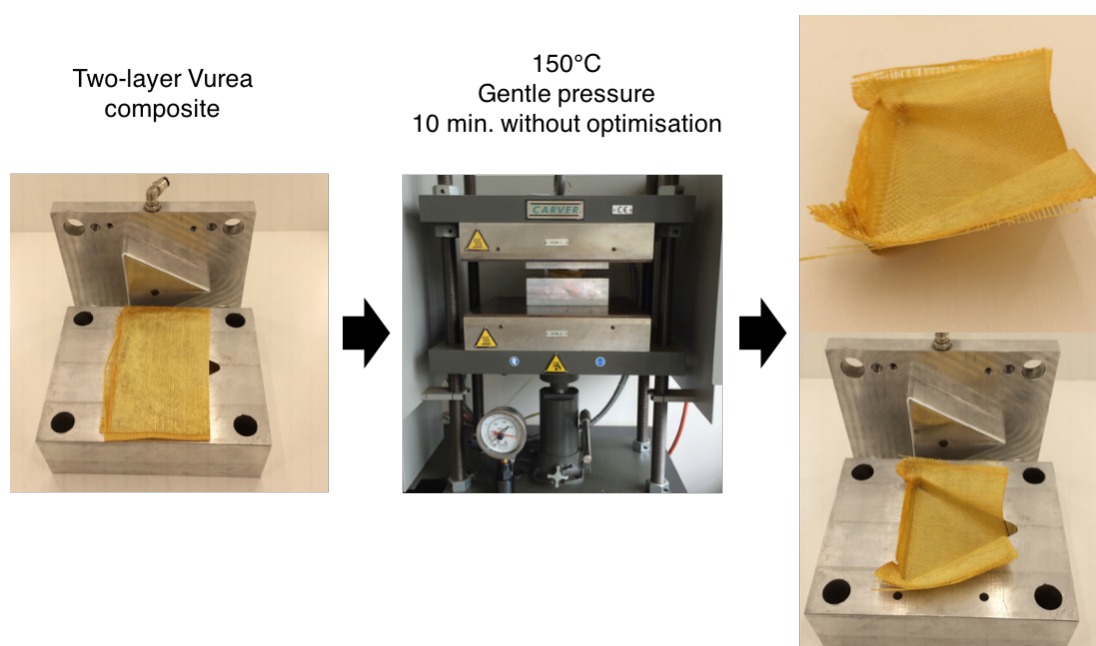


Figure 7.5: Proof-of-concept of vitrimer composite processing.

## 7.3 Perspectives

In this project, an underexplored exchange reaction in polymer chemistry was researched for its potential in the application for vitrimers, a brand new class of materials that were only reported for the first time in 2011. Consequently, many challenges and opportunities remain. As mentioned before, one of the most promising applications of vitrimers would be composites. At the end of chapter 6, a proof-of-concept for Vurea composites was reported together with initial characterisation. While these initial efforts showed already potential, a more extensive assessment of the properties and the assets of its vitrimer matrix will be required to launch industrial projects. Moreover, academic research including this work often aims to demonstrate virtues of its research, which is essential to publish, intrigue industrial researchers and initiate industrial projects. Yet, knowing limitations is at least as important. Therefore, additional research on its limitations such as aging, UV/water-resistance and amine leaching will be indispensable.

Besides composites, we presented an approach relying on the cross-linking of amine-functionalised prepolymers. Since this thesis focused mainly on materials with a high  $T_g$ , PDMS-based materials were not evaluated. Nevertheless, amine-functionalised PDMS is commercially available and could be readily used to prepare enaminone-based vitrimers. In addition, as demonstrated in chapter 3 on model compounds, the useful temperature range could be shifted by choosing the different enaminone moieties. Also the use of a photobase to inhibit transamination and unwanted creep after processing, would be feasible on such matrices. Finally, the use of fillers, which is a common practice to enhance mechanical properties in elastomers, is an interesting factor to consider in vitrimeric elastomers as already demonstrated by Leibler et al.<sup>1</sup> These various possibilities on PDMS-based enaminone vitrimers will be a part of the PhD-thesis of Yann Spieschaert.

Finally, other parts of this doctoral thesis could be subject of further improvements. For example, other ways of vitrimer processing could be interesting as this work mainly made use of compression moulding. The initial extrusion experiments of Vurea showed already some potential but require considerable efforts to avoid material degradation. Next, the used cross-link densities and excess of amines - obligatory to enable amine exchange - were often chosen based on an educated guess. Probably, there is a firm margin of improvement possible,

yet these optimisations would become only very interesting when real applications are considered in order to have a target.

## 7.4 References

- (1) Montarnal, D.; Capelot, M.; Tournilhac, F.; Leibler, L. *Science* **2011**, *334*, 965.
- (2) Capelot, M. Chimie de polycondensation, Polymères Supramoléculaires et vitrimères, PhD Thesis, Université Pierre et Marie Curie, 2013.
- (3) Capelot, M.; Montarnal, D.; Tournilhac, F.; Leibler, L. *J. Am. Chem. Soc.* **2012**, *134*, 7664.
- (4) Capelot, M.; Unterlass, M. M.; Tournilhac, F.; Leibler, L. *ACS Macro Lett.* **2012**, *1*, 789.
- (5) Montarnal, D. Use of reversible covalent and non-covalent bonds in new recyclable and reprocessable polymer materials, PhD Thesis, Université Pierre et Marie Curie, 2011.
- (6) Otera, J. *Chem. Rev. (Washington, DC, U. S.)* **1993**, *93*, 1449.
- (7) Al-Saleh, B.; Al-Awadi, N.; Al-kandari, H.; Abdel-Khalik, M. M.; Elnagdi, M. H. *J. Chem. Res.* **2000**, 16.
- (8) Abdulla, R. F.; Emmick, T. L.; Taylor, H. M. *Synth. Commun.* **1977**, *7*, 305.
- (9) Ostrowska, K.; Ciechanowicz-Rutkowska, M.; Pilati, T.; Zzuchowski, G. *Monatshefte für Chemie/Chemical Monthly* **1999**, *130*, 555.
- (10) Friary, R. J.; Seidl, V.; Schwerdt, J. H.; Chan, T. M.; Cohen, M. P.; Conklin, E. R.; Duelfer, T.; Hou, D.; Nafissi, M.; Runkle, R. L. *Tetrahedron* **1993**, *49*, 7179.
- (11) Mori, A.; Kitayama, T.; Takatani, M.; Okamoto, T. *J. Appl. Polym. Sci.* **2004**, *91*, 2966.
- (12) Lu, J.; Easteal, A. J.; Edmonds, N. R. *Pigm. Resin Technol.* **2011**, *40*, 161.
- (13) Denissen, W.; Winne, J. M.; Du Prez, F. E. *Chem. Sci* **2016**, *7*, 30.



## Chapter 8

### Nederlandstalige samenvatting

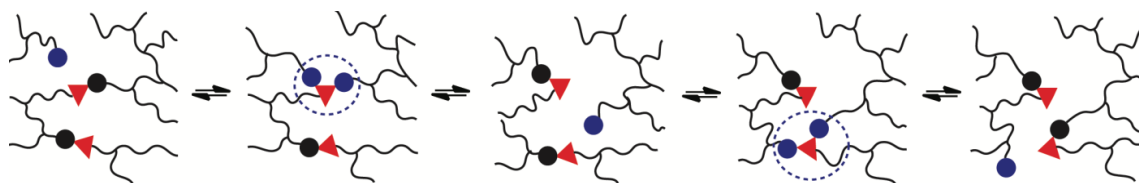
#### 8.1 Inleiding

Vandaag worden metalen in verschillende hoogwaardige toepassingen vervangen door kunststoffen die lichter zijn, maar toch gelijkwaardige mechanische eigenschappen bezitten. Composietmaterialen, gebaseerd op thermohardende harsen, zijn door hun uitstekende mechanische, thermische en chemische weerstand het meest geschikt om deze rol op zich te nemen. Echter, zulke harsen moeten meteen uitgehard worden in de definitieve vorm van het gewenste onderdeel. Bovendien is de vorm na uitharding permanent en zijn aanpassingen of herstellingen niet mogelijk. Zelfs door middel van opwarming is het uitgesloten om de onderdelen te bewerken of te herstellen zoals bijvoorbeeld een glasblazer dat kan.

Glas is dan ook een materiaal met unieke eigenschappen. Onder invloed van warmte gaat het in een zeer progressieve manier over van een vaste naar vloeibare toestand waardoor men glas, zonder het gebruik van een matrijs, complexe vormen kan doen aannemen. De ontwikkeling van materialen die uitstekende materiaaleigenschappen combineren met een verwerkbaarheid zoals die van glas zou dan ook een geweldige vooruitgang betekenen op zowel economisch als ecologisch vlak.

Een eerste grote stap in de richting van dergelijke materialen werd in 2011 gezet door Leibler, Tournilhac en medewerkers.<sup>1-3</sup> Op basis van klassieke epoxychemie werd een nieuw polymeernetwerk ontwikkeld dat zeer bijzondere eigenschappen bezit door de aanwezigheid van thermisch uitwisselbare esterbindingen in combinatie met katalysatoren in het netwerk. Onder invloed van warmte is het netwerk immers in staat zichzelf te reorganiseren. Gedurende dit proces blijft het totaal aantal knooppunten (vernettingsdichtheid) constant (Figuur 8.1). Hierdoor kan het materiaal op dezelfde progressieve wijze als glas overgaan van vast naar (taai-)vloeibaar. Tot nu toe was dit specifieke gedrag enkel gekend bij glas; bijgevolg kregen deze nieuwe polymeermaterialen de naam ‘vitrimeren’ (vitreous + polymeren). Opmerkelijk genoeg vertonen vitrimeren gelijktijdig dezelfde

kenmerken als klassieke thermoharders die gebruikt worden in industriële context: het materiaal is onoplosbaar, licht en vertoont uitstekende mechanische eigenschappen die voor composieten vereist zijn. In tegenstelling tot klassieke thermoharders hebben ze dus het voordeel dat ze onder invloed van warmte verwerkbaar worden. Door deze eigenschap kan dit materiaal naar wens vervormd worden met technieken die niet bruikbaar zijn voor thermoharders of zelfs thermoplasten. Hierdoor kunnen vormen gegenereerd worden die onmogelijk via een matrijs te maken zijn of met deze methode te duur zouden uitvallen.



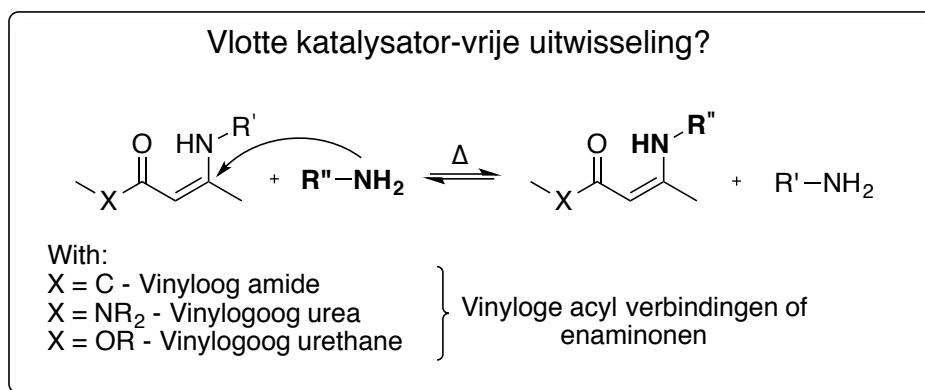
Figuur 8.1: Associatieve uitwisselingsreacties maken de reorganisatie van het netwerk mogelijk.

Hoewel deze eerste generatie vitrimeren reeds goede eigenschappen vertoonde omdat ze gebruik maken van gekende epoxy-formulaties, hebben ze ook nog enkele nadelen. Zo is transesterificatie intrinsiek traag en vereisen deze vitrimeren een combinatie van een hoge concentratie aan katalysatoren en zeer hoge temperaturen om een goede verwerkbaarheid te krijgen. Bovendien zijn materialen met een hoge glastransitietemperatuur( $T_g$ ), die net zeer interessant zijn voor composieten, niet mogelijk omwille van een beperkte oplosbaarheid van de katalysatoren.

## 8.2 Doelstelling

De uitdaging van dit project bestond erin om nieuwe, als glas verwerkbare polymeernetwerken, *i.e.* vitrimeren, te ontwikkelen op basis van een alternatieve uitwisselingsreactie. Zoals in de inleiding is aangegeven, is de toepasbaarheid van de eerste generatie vitrimeren beperkt door een lage  $T_g$  en de noodzaak aan een hoge concentratie katalysatoren. Om aan deze problemen tegemoet te komen, werd een alternatieve uitwisselingsreactie onderzocht, met name de amine uitwisseling van enaminones (Figuur 8.2). Hiermee werden vitrimeren beoogd die geen katalysator vereisen voor snelle verwerking en die een hoge  $T_g$  vertonen.





Figuur 8.2: Schematische voorstelling van de amine-uitwisseling van enaminonen.

De amine uitwisselingen van vinyloge acyl-verbindingen of enaminonen is reeds veelvuldig gebruikt in de organische chemie voor de synthese van kleine moleculen.<sup>4</sup> Ook in de polymeerchemie werden enaminonen, of meer precies vinyloge urethanen (X=O, figuur 2), onderzocht voor de synthese van watergebaseerde coatings<sup>5</sup> en adhesieven<sup>6</sup> omwille van hun eenvoudige synthese. Echter, geen enkel onderzoek heeft deze polymeernetwerken zodanig ontworpen om het dynamisch karakter van deze bouwstenen te benutten. In deze thesis werden daarom de verschillende enaminone verbindingen systematisch onderzocht voor hun potentieel als uitwisselbare binding voor vitrimeren.

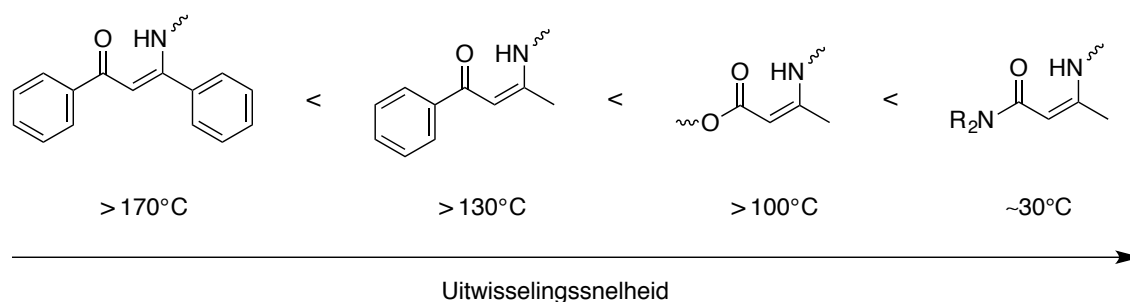
Gelijktijdig met dit onderzoek, dat liep van 2012 tot 2016, werden wereldwijd ook andere uitwisselbare bindingen geëvalueerd voor de synthese van vitrimeren. Een overzicht van de recente literatuur van dit snel uitbreidend veld van vitrimeeronderzoek is gegeven in Hoofdstuk 2 en werd ook gepubliceerd als mini-review in Chemical Science.<sup>7</sup>

### 8.3 Overzicht van de resultaten

In het eerste deel van dit onderzoek, gepresenteerd in hoofdstuk 3, werd er een systematische studie van laagmoleculaire modelcomponenten uitgevoerd ter evaluatie van de uitwisselingssnelheid van amines op de verschillende enaminone kernen. Dit kwantitatief en kwalitatief onderzoek toonde aan dat de amine uitwisseling van enaminonen reikt over een breed temperatuurbereik en sterk afhangt van het hetero-atoom naast de carbonyl functie (Figuur 8.3). Zo wisselen vinyloge urea (X=N) reeds snel uit bij kamertemperatuur, terwijl gesubstitueerde vinyloge amiden (X=C) pas vlot uitwisselen rond 170°C. De relatieve orde van de kinetische uitwisseling van de verschillende enaminone-bouwstenen is weergegeven

in. Verder werden twee mogelijke mechanismen besproken en werd er gerealiseerd dat protontransfers een essentiële stap vormen. Deze hypothese werd bevestigd doordat toevoeging van een zuur de reactie sterk versnelde.

Gebaseerd op deze studie met modelcomponenten werden vinyloge urethanen en vinyloge urea geselecteerd als meest interessante bouwstenen voor vitrimeren, omwille van hun snelle uitwisselingssnelheid en de eenvoudige synthese van precursoren.



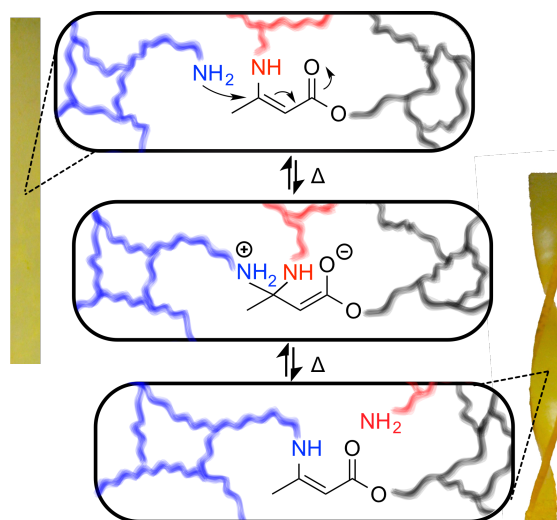
Figuur 8.3: Relatieve orde van de uitwisselingssnelheid voor enaminonen met een indicatieve temperatuur voor vlotte uitwisseling.

Als eerste dynamische binding werden vinyloge urethanen onderzocht, wat gepresenteerd is in hoofdstuk 4. Verschillende manieren om vitrimeren te maken werden geëvalueerd. De eerste strategie beoogde het vernetten van amine-gefunctionaliseerde prepolymeren. Echter, deze strategie werd vroegtijdig gestopt omwille van nevenreacties bij de synthese van deze amine-gefunctionaliseerde prepolymeren.

De tweede benadering ging uit van laagmoleculaire amine en acetoacetaat monomeren en leidde tot een ‘proof-of-concept’ van vinyloog urethaan gebaseerde vitrimeren (Figuur 8.4). Poly(vinyloog urethaan) netwerken met een glastransitietemperatuur van 87°C en een modulus van 2.4 GPa werden verkregen en vertoonden eigenschappen gelijkaardig aan deze van commerciële thermoharders. Zoals verwacht voor een polymeernetwerk, waren de vinyloge urethaan vitrimeren onoplosbaar, zelfs na langdurig verwarmen in een goed solvent. Verder toonde dynamische mechanische analyse (DMA) een typisch thermoharder gedrag op korte tijdschaal aan, met een rubber plateau karakteristiek voor materialen die vernet zijn.

Het dynamische gedrag werd vervolgens bewezen door middel van stressrelaxatie en kruipexperimenten en toonde aan dat de poly(vinyl-urethaan) netwerken

zich gedragen als een visco-elastische vloeistof. Door een combinatie van een snelle kinetische uitwisseling en hoge dichtheid van uitwisselbare bindingen doorheen het netwerk werd er zeer snelle stress-relaxatie waargenomen, met relaxatietijden tot 85s bij 170°C zonder het gebruik van een katalysator. Daarnaast werden de netwerken vier keer gerecycleerd met behoud van mechanische eigenschappen. Bovengenoemde resultaten maakten deel uit van een publicatie in *Advanced Functional Materials*.<sup>8</sup> Tot slot werd in dit deel nog een screening van rigidere monomeren uitgevoerd, wat uiteindelijk leidde tot netwerken met een hoge  $T_g$  tot 145°C.



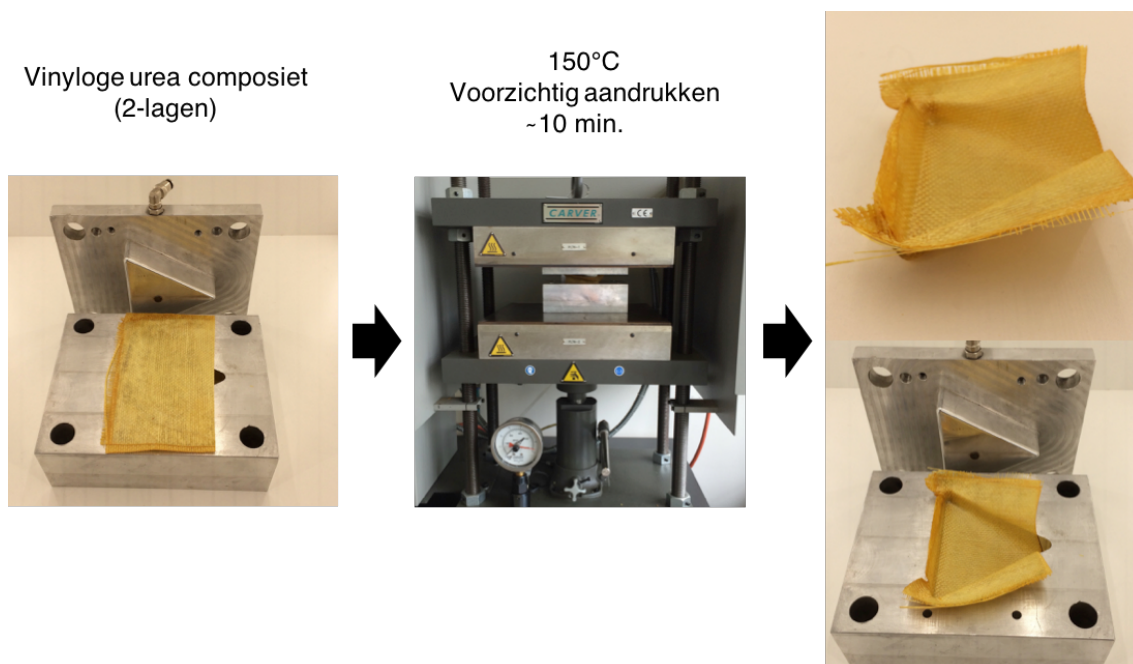
Figuur 8.4: Chemische oorsprong van de verwerkbaarheid van vinyloge urethaan vitrimeren.

Met de bedoeling om de verwerkbaarheid nog verder op te drijven, werd de invloed van katalysatoren getest op de vinyloge transaminatie, zowel in modelcomponenten als in rubberachtige vitrimeren, wat uitgebreid besproken is in hoofdstuk 5. Hoewel het doel bestond om zonder katalysator te werken, werd er gerealiseerd dat kleine hoeveelheden katalysator reeds een groot effect kunnen hebben op de verwerkbaarheid. Zo toonde deze studie aan dat de amine uitwisseling goed gecontroleerd kan worden door toevoeging van zuren en basen en dat er een goede correlatie is tussen de uitwisseling van modelcomponenten en stress-relaxatie van de vinyloog urethaan netwerken. Zoals verwacht vanuit hoofdstuk 2 zorgde de toevoeging van zuren voor een sterke toename van de uitwisselingsreactie, wat ook snellere stress-relaxatie tot gevolg had terwijl de aanwezigheid van base de reactie anderzijds vertraagde. Ten slotte werd de beste katalysator toegepast op de rigide vinyloog urethaan netwerken van hoofdstuk 4, waarmee de relaxatietijden verder gereduceerd werden tot 10 s, wat de verwerkbaarheid van deze materialen significant verbeterde.

In hoofdstuk 6, het laatste deel van deze thesis, werden vinyloge urea onderzocht als dynamische bouwstenen. De modelcomponentenstudie toonde immers aan dat deze bouwstenen enorm snel uitwisselen, zelfs bij kamertemperatuur. Hoewel een verkennende studie aantoonde dat de thermische stabiliteit voor de eerst onderzochte componenten beperkt was, werd er een thermisch stabiele vinyloge urea bouwsteen gevonden vertrekkende vanuit 1,4-(piperazine)bis(acetoacetamide). Hiervan werden vervolgens netwerken gemaakt door combinatie met 1,6-hexaan diamine en tris(2-aminoethyl)amine. Gelijktijdig werd hetzelfde netwerk ook met een zure katalysator onderzocht om de grenzen van de verwerkbaarheid van deze netwerken te testen. Vinyloge urea netwerken met een  $T_g$  van 110°C en een modulus van 2.2 GPa werden verkregen. Op het vlak van mechanische eigenschappen was er geen verschil waarneembaar tussen de katalysator-vrije en gekatalyseerde vitrimeren. Zoals geanticipeerd verschilde het dynamische gedrag wel sterk met relaxatietijden in de orde van slechts seconden voor de gekatalyseerde vinyloge urea netwerken. Naar ons weten zijn dit dan ook de best verwerkbare rigide vitrimeren die tot nu toe gekend zijn.

Tenslotte werden deze vinyloge urea vitrimeren ook nog uitgetest als matrix voor composietmaterialen. Eerst werden er nog enkele optimalisaties uitgevoerd, enerzijds om de glastransitie en mechanische eigenschappen nog verder te verbeteren en anderzijds om de bulkpolymerisatie te wijzigen naar een solvent-gebaseerde polymerisatie zodat de vezels goed geïmpregneerd kunnen worden. Op basis van dit proces werden éénlagige glasvezel composietvellen bereid die als alternatief voor prepregs kunnen dienen. Klassieke prepregs vereisen normaal speciale condities zoals gekoelde bewaring en anti-adhesie folies omwille van hun plakkerigheid. Deze vitrimeer-gebaseerde prepregs hebben in principe een oneindige houdbaarheid, omdat ze al volledig uitgehard zijn, maar ze blijven toch nog verwerkbaar door hun vitrimeer-eigenschappen. Dit werd aangetoond door deze vitrimeer prepregs om te vormen tot een 6-lagige composiet door middel van druk bij een verhoogde temperatuur. De vinyloge ureacomposieten vertoonden gelijkaardige eigenschappen als deze gebaseerd op epoxy-formulaties.

Tot slot werd er nog het concept van thermovorming aangetoond door een vlakke composiet bestaande uit twee lagen te verwerken tot een nieuwe vorm met behulp van een matrijs en een verwarmde pers (Figuur 8.5).



Figuur 8.5: Demonstratie van de verwerkbaarheid van vitrimeer-gebaseerde composieten.

## 8.4 Perspectieven

In dit project werd een vergeten dynamische binding in de polymeerchemie onderzocht voor zijn potentieel in vitrimeren, een nieuwe klasse polymeermaterialen met een sterke industriële relevantie waarvan de eerste publicatie pas in 2011 verscheen. Bijgevolg zijn er op het einde van dit onderzoek nog steeds vragen en onderzoekpistes die het waard zijn om verder onderzocht te worden.

Zoals reeds vermeld en hierboven besproken zijn composieten één van de domeinen waar het meeste potentieel in gezien wordt. Aan het einde van hoofdstuk 6 werd er reeds een demonstratie gegeven van zulke materialen met een korte evaluatie van de eigenschappen. Hoewel deze experimenten reeds het potentieel blootleggen, is er een meer uitgebreid onderzoek nodig naar de eigenschappen en voordelen die vitrimeer-gebaseerde composieten kunnen bieden. Een uitgebreidere studie is reeds gestart in samenwerking met de MMS-onderzoeksgroep van Universiteit Gent. Daarbovenop is academisch onderzoek vaak toegespitst op het aantonen van goede/nieuwe eigenschappen met het doel te publiceren en industriële partners enthousiast te krijgen. Ook dit werk is daar een voorbeeld van. Echter, de beperkingen zijn vaak minstens even belangrijk. Daarom zijn extra testen

aangewezen om de limieten van deze materialen te verkennen zoals bijvoorbeeld langdurige blootstelling aan UV-licht of water.

Naast composieten werd er in hoofdstuk 4 ook een strategie besproken die uitging van amine-gefunctionaliseerde prepolymeren. Aangezien dit project toegespitst was op materialen met een hoge  $T_g$ , werden silicone materialen (PDMS) niet onderzocht. Niettemin, amine-gefunctionaliseerd PDMS is commercieel beschikbaar en zou rechtstreeks gebruikt kunnen worden voor de bereiding van vitrimeren. Daarbovenop zou de verwerkbaarheid gemakkelijk gevarieerd kunnen worden door de keuze van de juiste dynamische bouwsteen. Hierop zijn tenslotte ook nog enkele variaties mogelijk zoals een latente base en het gebruik van vulstoffen. Deze mogelijkheden zullen verder onderzocht worden in de doctoraatsthesis van Yann Spiesschaert.

Tot slot zijn nog andere delen van dit doctoraatswerk vatbaar voor verbetering en mogelijk interessant om verder onderzocht te worden. Bijvoorbeeld, in dit werk werden de vitrimeren steeds verwerkt door compressie in een matrix. Extrusie zou echter een interessant alternatief vormen. Initiële experimenten toonden reeds potentieel aan, maar vereisen nog aanzienlijke optimalisaties om materiaaldegradatie te voorkomen. Daarnaast werden op basis van gefundeerde inschattingen vaak verhoudingen gekozen zoals de gebruikte overmaat amines (nodig voor uitwisseling) en de vernettingsgraden van de polymeernetwerken. Hier is waarschijnlijk nog veel marge voor verbetering, maar dit zou pas echt interessant worden wanneer er concrete toepassingen voor ogen zijn, zodat er doelgericht naartoe gewerkt kan worden.

## 8.5 Referenties

- (1) Capelot, M.; Montarnal, D.; Tournilhac, F.; Leibler, L. *J. Am. Chem. Soc.* **2012**, *134*, 7664.
- (2) Capelot, M.; Unterlass, M. M.; Tournilhac, F.; Leibler, L. *ACS Macro Lett.* **2012**, *1*, 789.
- (3) Montarnal, D.; Capelot, M.; Tournilhac, F.; Leibler, L. *Science* **2011**, *334*, 965.
- (4) Michael, J. P.; De Koning, C. B.; Gravestock, D.; Hosken, G. D.; Howard, A. S.; Jungmann, C. M.; Krause, R. W. M.; Parsons, A. S.; Pelly, S. C.; Stanbury, T. V. *Pure Appl. Chem.* **1999**, *71*, 979.
- (5) Mori, A.; Kitayama, T.; Takatani, M.; Okamoto, T. *J. Appl. Polym. Sci.* **2004**, *91*, 2966.
- (6) Lu, J.; Easteal, A. J.; Edmonds, N. R. *Pigm. Resin Technol.* **2011**, *40*, 161.
- (7) Denissen, W.; Winne, J. M.; Du Prez, F. E. *Chem. Sci* **2016**, *7*, 30.

- (8) Denissen, W.; Rivero, G.; Nicolaÿ, R.; Leibler, L.; Winne, J. M.; Du Prez, F. E. *Adv. Funct. Mater.* **2015**, *25*, 2451.